PARTICLE-WATER INTERACTIONS OF HYDROPHOBIC ORGANIC MICROPOLLUTANTS IN MARINE SYSTEMS

UNIVERSITY OF PLYMOUTH

M. C. RAWLING

Ph. D. 1998

DEDICATION

For my parents

and

in loving memory of

Dr. Hilary Phillip
(1956-1993)

and all those who have or will die through no fault of their own.

'Mr Rawling, you've not been introduced to your colleagues yet.
Allow me. This is...

...and I am Doctor Hilary Phillip!'

Sept. 1991

Copyright statement

Signed M. C. Rawlings

Date 10/09/98

PARTICLE-WATER INTERACTIONS OF HYDROPHOBIC ORGANIC MICROPOLLUTANTS IN MARINE SYSTEMS

by

M. CARL RAWLING B. Sc. (Hons), M. Sc.

A thesis submitted to the University of Plymouth
in partial fulfilment for the degree of

Doctor of Philosophy

Department of Environmental Sciences
Faculty of Science
University of Plymouth

In collaboration with
BMT Marine Information Systems Limited
Southampton

Submitted September 1998

PARTICLE-WATER INTERACTIONS OF HYDROPHOBIC ORGANIC MICROPOLLUTANTS IN MARINE SYSTEMS

M. Carl Rawling

Abstract

An understanding of the reactivity of hydrophobic organic micropollutants (HOMs) is of paramount importance to water quality managers because of their toxicity, persistence, and liability to bioaccumulate. In this study, the role played by the main estuarine variables (organic matter, suspended particulate matter [SPM], particle type and salinity) on HOM behaviour was investigated by employing samples from estuaries with different geochemical signatures (Chupa, Russia, and the Dart, Plym, Beaulieu and Carnon, UK). A laboratory-based technique was developed for the determination of the solubility and sorptive behaviour of HOMs using ^{14}C-labelled, beta-emitting organic compounds (2,2',5,5'-tetrachlorobiphenyl (2,2',5,5'-TCB), bis(2-ethylhexyl)phthalate ester (DEHP), and benzo[a]pyrene (BaP)) coupled with liquid scintillation counting. The results indicate that relative solubility is mainly dependent upon the type of dissolved organic carbon (DOC) present, not its concentration, and is reduced with increasing salinity. The uptake of 2,2',5,5'-TCB and BaP by particles is time dependent with a system response time (the time required to achieve 63% of the new equilibrium) of about 0.37 hours for 2,2',5,5'-TCB and 0.02 hours for BaP. The adsorption, expressed as particle-water partition coefficients, K_Ds, is to a varying extent dependent on DOC, salinity and particle characteristics (iron/manganese hydroxides, particulate carbon and specific surface area). Adsorption is best defined by a linear isotherm and is enhanced in sea water compared with river water owing to a reduction in charge on particle surfaces at high ionic strengths. This effect has been quantified using an adsorption salting constant, σ_p, whose values are typically in the range 0.4-2 L mol^{-1}. The inverse relationship between K_D and SPM concentration, an effect well documented in the literature, has been defined by a simple power law ($K_D = a.SPM^{-b}$; where a and b are site and compound-specific constants). Typical values for a and b are approximately $4x10^5$ and 0.6 for 2,2',5,5'-TCB, $50x10^5$ and 1.0 for DEHP, and $2x10^5$ and 0.5 for BaP, respectively. Empirical parameterisation of these effects are extremely useful for encoding into numerical transport and distribution models, and their application is demonstrated in this thesis by calculating the retention of HOMs by estuaries.

Author's declaration

At no time during the registration for the degree of Doctor of Philosophy has the author been registered for any other University award.

This study was financed with the aid of a studentship from the Natural Environment Research Council and carried out in collaboration with BMT Marine Information Systems Limited.

A programme of advanced study was undertaken which included guided reading in topics relating to environmental and estuarine organic chemistry. Training was given in the safe use of radioactive isotopes and the analysis of ^{14}C radiotracers using scintillation counting. Instruction was also given in a wide-range of analytical methodologies including radio-GC, flame atomic absorption spectrophotometry, organic carbon analysis, and multi-point BET nitrogen gas adsorption.

Relevant scientific seminars and conferences were regularly attended at which work was often presented; external institutions were visited for consultation purposes and scientific papers were prepared for publication.

Publications

M. C. Rawling, A. Turner & A. O. Tyler (1998) Particle-water interactions of 2,2',5,5'-Tetrachlorobiphenyl under simulated estuarine conditions. *Marine Chemistry*, **61**, 115-126.*

A. Turner & M. C. Rawling (1998) The behaviour of di-ethylhexyl phthalate in estuaries. *Marine Chemistry*, submitted.

* See Appendix C.

Conferences and presentations

Oral presentation entitled "*The partitioning of 2,2',5,5'-TCB in estuaries*" at a **Workshop on Contaminant Geochemistry**, held at BMT Marine Information Systems Limited, Southampton, UK, 13th February 1995.

Oral presentation entitled "*The partitioning of 2,2',5,5'-TCB in estuaries*" at the **Marine Postgraduates in the Geosciences**, Conference, held at the Department of Earth Sciences, Cardiff University, UK, 15th-16th February 1995.

Oral presentation entitled "*The solid-solution partitioning of hydrophobic organic micropollutants in estuarine waters*" at the SETAC-Europe (UK Branch), 6th Annual Meeting, **Unifying Themes in Environmental Chemistry and Toxicology**, held at the Plymouth Pavilions, UK, 4th-6th September 1995.

Poster presentation entitled "*Laboratory studies of hydrophobic organic micropollutants in natural waters*" at the 2nd International Symposium on, **Dioxins and Related Compounds**, held at the Netherwood Hotel, Grange-Over-Sands, UK, 24th-25th April 1996.

Oral presentation entitled "*Sediment-water interactions of hydrophobic organic micropollutants in rivers and estuaries*" at the 7th International Symposium on the, **Interactions Between Sediments and Waters**, Baveno, Italy, 22nd-25th September 1996.

Three oral presentations of current work in seminar series of the Department of Environmental Sciences, University of Plymouth, April 1996 to January 1997.

Courses and external visits

Regular meetings were held with colleagues at BMT Marine Information Systems Limited, Southampton, to discuss data and plan future work.

An EPSRC Graduate School was attended at Doncaster College Conference Centre, High Melton, 29th July to 4th August 1996.

Signed M. C. Kay

Date 10/09/98

Acknowledgements

The contributions of the following are acknowledged. First and foremost I would like to thank Dr. Andrew Turner, Director of Studies, for his immense patience, faith, encouragement and guidance during the laboratory work and compilation of this thesis. Also for his help and instruction in the use of the multi-point BET nitrogen gas adsorption equipment.

Also I would like to thank the following:

Professor G. E. Millward, for his invaluable help and guidance in the planning and writing of this project.

Dr. M. Rhead, for his help and advice during the project.

Mr A. O. Tyler, of BMT Marine Information Systems Limited, Southampton, for his continual interest and advice during the practical phase of this project.

Mr N. Crocker, Department of Biological Sciences, for his help and instruction in the safe use of ^{14}C-radiotracers and the scintillation counter.

Mr K. Solman, Geographical Sciences, for his help and instruction in the use of the Schimadzu TOC-5000 total carbon analyser, and Mr D. Henon, Environmental Sciences for his help in analysing the estuarine sediments for organic carbon.

Dr. J. Zhou, formerly of PML (now UCNW, Bangor), for the determination of the purity of the compounds by GC-MS.

Dr. R. D. Pemberton for his help and instruction in the use of the Radio-GC, and Ms T. Hyde for assistance during the assessment of the radiochemical purity of the compounds.

Friends and colleagues at the University of Plymouth for their continuous support, help and friendship.

Finally I would like to thank my Parents, my brothers and their families, Andrew, Mark, Marie-Claire and my numerous 'drinking partners' for their continuous support, help, and friendship over the last few years. Much appreciated...thank you.

CONTENTS

LIST OF FIGURES

LIST OF SCHEMES

LIST OF TABLES

CHAPTER 1: INTRODUCTION

1.1. Hydrophobic Organic Micropollutants

Of the 1.8 million organic compounds that have been synthesised by humans, over 60000 are presently in use (Ernst *et al.*, 1988). It is estimated that, on a global scale, up to one third of organic compounds produced (~ 30-60 million t a^{-1}) enters the environment (Stumm & Morgan, 1996). The environmental behaviour, transport and fate of many of these ubiquitous organic micropollutants are of major concern to water quality managers, owing to their toxicity, persistence, and liability to bioaccumulate. This is especially true for compounds which are hydrophobic, including polychlorinated biphenyls (PCBs), phthalate esters (PEs), polycyclic aromatic hydrocarbons (PAHs), and polychlorinated dibenzodioxins and dibenzofurans. Although these primarily commercially produced compounds were once thought to be exclusively anthropogenic in origin, being manufactured by or as by-products of industry, it is now being recognised that some hydrophobic organic micropollutants (HOMs; see glossary for definitions of scientific terms and abbreviations used in this thesis) such as polychlorinated dibenzodioxins and dibenzofurans are natural products and ubiquitous throughout the environment (Gribble, 1994). Natural sources of PAHs have been identified including wood and fossil fuel combustion, and the early diagenesis of natural organic matter (Simcik *et al.*, 1996). It has also been suggested that high concentration levels of PEs found in a range of biota were of biogenic origin (Giam *et al.*, 1984), although contamination of samples could not be ruled out.

Estuaries are potentially a significant reservoir for these compounds, as HOMs are discharged directly into estuaries from a variety of anthropogenic sources including, arable, domestic, and industrial. Given the long residence time of sediments in estuaries (typically decades; Dyer, 1989), and the fact that these compounds are resistant to degradation (Lang, 1992; Ejlertsson *et al.*, 1997), HOMs are highly persistent in the marine environment. Thus the large reservoir of HOMs in aquatic systems, coupled with the high lipid content of aquatic organisms, provides a great potential for HOMs to enter the aquatic food chain in which they may be highly toxic at relatively low levels.

The large range of individual HOMs present in the environment, renders it impossible to investigate all such compounds. Therefore, this thesis will primarily investigate a PCB, a PE, and a PAH (Section 1.2.1.). As such this introduction will concentrate on these three classes of HOMs.

1.2. General Properties of HOMs

General properties of HOMs include their low aqueous solubility and their lipophilicity. The tendency of a HOM to partition between water and either sediment, organic matter, or animal lipids (*i.e.* their liability to bioaccumulate), can be predicted from the laboratory-derived *n*-octanol-water partition coefficient, K_{ow} (Karickhoff, 1984; Brownawell & Farrington, 1985; Gobas *et al.*, 1991). That is, the equilibrium distribution of an organic compound between *n*-octanol and water; *n*-octanol was selected as the solvent because it displays many of the characteristics associated with natural organic matter, and can be derived from (Hawker & Connell, 1988):

$$K_{ow} = \frac{C_o}{C_w} \qquad (1.1)$$

where C_o is the concentration of the compound in *n*-octanol (w/v), and C_w is the concentration of the compound in the water or aqueous phase (w/v). Values of log K_{ow} and aqueous solubilities for selected HOMs, are given in Table 1.1. For non-polar organic compounds the relatively high log K_{ow} values (Table 1.1.) are primarily due to their incompatibility with water (*i.e.* low solubility).

1.2.1. Selected compounds

Initially this study was to concentrate on several PCB congeners in order to encompass the range of physicochemical properties displayed within this class of compound (Section 1.2.2; Table 1.2.), however, changes in shipment and import legislation prevented this, and resulted in a limited number of ^{14}C-labelled HOMs available. Therefore, the testbed HOMs under study in this work are an abundant PCB of moderate toxicity, 2,2',5,5'-tetrachlorobiphenyl (2,2',5,5'-TCB; IUPAC 52), a mass produced PE, bis(2-

ethylhexyl)phthalate ester (DEHP), and a persistent and carcinogenic PAH, benzo[a]pyrene (BaP). Their chemical structures are shown in Figure 1.1. and Table 1.2. summarises the general physicochemical properties of these compounds which are important in the understanding of their environmental fate and behaviour.

The next three sections discuss the general chemical properties associated with the individual classes of compounds which are the subject of this study: namely, PCBs, PEs, and PAHs.

Table 1.1: Aqueous solubility and log K_{ow} values for selected HOMs.

HOM	Aqueous solubility @ 20°C ($\mu g\ L^{-1}$)	Log K_{ow}
PCBs		
2-CB	237 [a]	4.46 [b]
2,2',5,5'-TCB	25 [a]	6.18 [a]
Decachlorobiphenyl	0.014 [a]	8.18 [b]
PEs		
Dimethyl phthalate (DMP)	$4.2x10^{6}$ [c]	1.61 [c]
Di-n-butyl phthalate (DnBP)	11200 [c]	4.45 [c]
Bis(2-ethyl-hexyl)phthalate (DEHP)	3.0 [c]-400 [d]	4.88 [e]-9.64 [d]
PAHs		
Phenanthrene	1100 [a]	4.57 [a]
Pyrene	904 [a]	5.13 [a]
Benzo[a]pyrene (BaP)	0.11 [f]-1.52 [a]	5.98 [g]
Polychlorinated dibenzodioxins		
2,3,7,8-TCDD	0.16 [a]	6.64 [a]
1,2,3,4,7,8-HxCDD	0.0044 [h]	7.80 [h]
1,2,3,4,6,7,8-HpCDD	0.0024 [h]	8.00 [h]
Polychlorinated dibenzofurans		
1,2,4,6,8-PCDF	0.236 [h]	6.50 [h]
1,2,3,4,6,7,8-HpCDF	0.0014 [h]	8.10 [h]

Sources: [a] Schwarzenbach *et al.*, 1993; [b] Hawker & Connell, 1988; [c] Staples *et al.*, 1997; [d] Giam *et al.*, 1984; [e] Fatoki & Vernon, 1990; [f] Karcher *et al.*, 1983; [g] Karcher *et al.*, 1988; [h] Adriaens *et al.*, 1995.

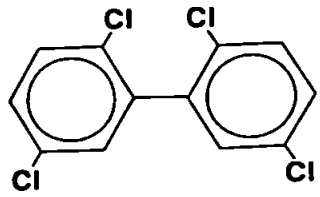

(i) 2,2',5,5'-TCB

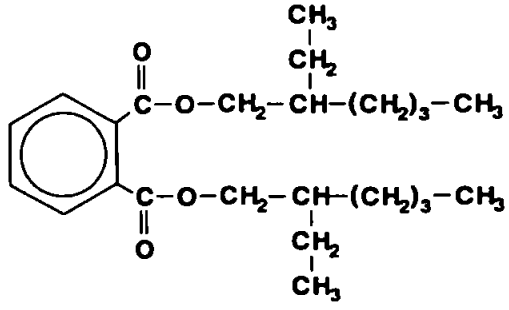

(ii) DEHP

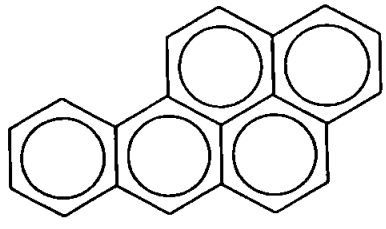

(iii) BaP

Figure 1.1: Chemical structures of the HOMs under study: (i) 2,2',5,5'-tetrachlorobiphenyl (2,2',5,5'-TCB), (ii) bis(2-ethylhexyl)phthalate ester (DEHP), and (iii) benzo[a]pyrene (BaP).

Table 1.2: Physicochemical properties important in the environmental fate of the HOMs under study, and their toxicity, where LD_{50} is the lowest lethal dose and rmm is the relative molecular mass.

	Compound		
Property	**2,2',5,5'-TCB**	**DEHP**	**BaP**
Molecular Formulae	$C_{12}H_6Cl_4$	$C_{24}H_{38}O_4$	$C_{20}H_{12}$
Average rmm (g mol^{-1})	292.0	390.6	252.3
Vapour pressure (mm Hg)	$2.5x10^{-8}$ [a]	$1.0x10^{-7}$ [b]	$7.24x10^{-12}$ [a]
Melting point (°C)	86.5-89.0 [c]	-47 [b]	176.5 [a]
Aqueous solubility @ 20°C (μg L^{-1})	25 [a]	3.0 [b]-400 [d]	0.11-12 [c]
Log K_{ow}	6.18 [a]	4.88 [f]-7.50 [b]	5.98 [g]
Toxicity:			
Mammalian LD_{50} (g kg^{-1} body wt)	1 [c]	14-30 [d]	0.2 [c]

Sources: [a] Schwarzenbach *et al.*, 1993; [b] Staples *et al.*, 1997; [c] Hutzinger *et al.*, 1974; [d]Giam *et al.*, 1984; [e] Karcher *et al.*, 1983; [f] Fatoki & Vernon, 1990; [g] Karcher *et al.*, 1988.

1.2.2. Polychlorinated biphenyls

The general chemical structure for polychlorinated biphenyls (PCBs) is shown in Figure 1.2., which also indicates the numbered biphenyl ring system used to identify individual congeners.

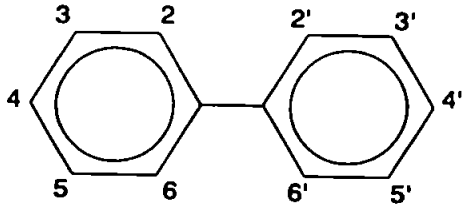

Figure 1.2: The general chemical structure for PCBs, showing possible unprimed and primed chlorine positions.

PCBs are a class of aromatic compounds once commercially produced on a large scale by the direct chlorination of biphenyl, and sold as complex mixtures differing in their average chlorination level under various trade names (e.g. Aroclor®, Phenoclor®,

Pyralene®, Clophen®, Kanechlor®, Santotherm®, and Fenclor®; Hutzinger *et al.*, 1974). PCBs are generally stable, inert, colourless, flame resistant, and electrically insulating. They are used in a wide variety of industrial processes including heat-transfer fluids, hydraulic fluids, solvent extenders, plasticizers, flame retardants, organic diluents, and dielectric fluids (Abramowicz *et al.*, 1993). They occur as a series of 209 chlorinated compounds, or congeners, with distinct physicochemical properties (Bergen *et al.*, 1993). The degree of chlorination also gives rise to distinct biological and toxicological properties. For example, the aqueous solubility of PCB decreases with increasing chlorine content (Table 1.1.), whilst highly chlorinated PCBs are less likely to be hydroxylated and excreted from biotic tissues (Hutzinger *et al.*, 1974).

Although world-wide commercial production of PCBs began in 1929 (Bruckmeier *et al.*, 1997), it was not until 1966 that they achieved world-wide recognition as significant ubiquitous environmental contaminants (Hutzinger *et al.*, 1974). At this stage the human toxicity of the commercially produced PCB mixtures had long been established as causing yellow atrophy of the liver in fatal cases, whilst chronic exposure leads to dermatitis and fatty degeneration of the liver. However, the toxicity of individual PCBs in both humans and ecological food chains had still to be established. Since that time their ubiquitous presence in biotic adipose tissues has been established (Niimi, 1996). From Table 1.3. it is clear that fish are the main source of PCBs in the human diet. Fish by-products are used as poultry feed and therefore account for the high PCB levels in eggs (Hutzinger *et al.*, 1974).

Monsanto, the sole manufacturer of PCBs in the USA, voluntarily cut production from 33000 t a^{-1}(1970) to 13000 t a^{-1}(1971) (Hutzinger *et al.*, 1974). World-wide production declined further in the 1980s through both unilateral and international legislation. Recycling was encouraged through such restrictions in the production, availability and use of PCBs. Of the total world production of PCBs it is estimated that approximately 31% has entered the terrestrial and aquatic environment, 4% has degraded or been incinerated, whilst the remaining 65% are still in use in industrial and domestic electrical equipment, or deposited in landfills and dumps (Tanabe, 1988). The potential for further environmental contamination is therefore significant.

Table 1.3: PCB levels in humans and food goods.

Environmental Compartment	2,2',5,5'-TCB	Total PCB
Humans ($\mu g\ kg^{-1}$)		
UK adipose tissue	1.8 [a]	930 [a]
Inuit blood plasma	30 [b]	4080 [b]
Food Goods ($\mu g\ kg^{-1}$)		
Chicken eggs		500 [c]
UK apples	0.24 [d]	19 [d]
UK mean vegetation	2.8 [a]	28 [a]
Herring		2700-11000 [e]

Sources: [a] Harrad *et al.*, 1994; [b] Ayotte *et al.*, 1997; [c] Hutzinger *et al.*, 1974; [d] Lovett *et al.*, 1997; [e] Järnberg *et al.*, 1993.

1.2.3. Phthalate esters

The general structure of phthalate esters (PEs) is shown in Figure 1.3. where R and R' denote hydrocarbon groups, usually alkyl chains consisting of between 1 and 13 carbon atoms in length. PEs are the diesters of phthalic acid. It is important to note that the polar carboxyl group is situated in the middle of the molecule and will, therefore, have a minimal effect upon their physical properties, and hence their environmental behaviour (Giam *et al.*, 1984).

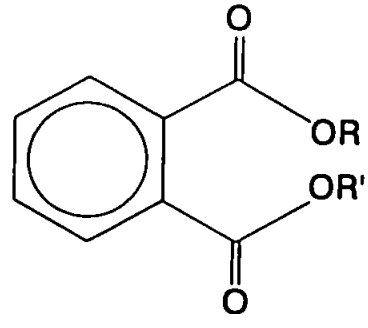

Figure 1.3: The general structure for PEs, where R and R' denote hydrocarbon groups.

PEs are amongst the most common industrial chemicals. The annual production of PEs in 1994 was estimated at 4.2 million tonnes (Ejlertsson *et al.*, 1997). However, this seems a rather conservative estimate given that the annual production of bis(2-

ethylhexyl)phthalate (DEHP) alone, which accounts for ~50% of the total global PE production, was estimated at 3-4 million tonnes in 1986 (Wams, 1987). PEs are mainly used as plasticizers in the production of a range of plastics, including PVC, constituting up to 67% of their total weight (Giam *et al.*, 1984). They are also used in a variety of other commercial products such as insect repellents, cosmetics, decorative inks, munitions, industrial lubricating oils, and to a limited extent in food packaging (Fatoki & Vernon, 1990). This broad range of applications, high production levels, and the fact that these compounds are not chemically bonded to the plastic matrices has ensured that PEs have become ubiquitous environmental pollutants.

PEs are liquids at ambient temperatures, thus the associated low melting and high boiling points of PEs contribute to their usefulness as plasticizers (Brooke *et al.*, 1991). The water solubility of PEs decreases as their molecular weight and alkyl chain length increases. However, there has recently been intense speculation that the majority of published water solubilities for the higher molecular weight PEs are incorrect and have been overestimated (Staples *et al.*, 1997). This may be due to a variety of experimental artefacts:

(i) contamination from plastic laboratory equipment (Giam *et al.*, 1984);

(ii) the ability of PEs to form stable, homogenous dispersions, or micelles, of undissolved chemical which is inseparable from the aqueous phase (Brown *et al.*, 1996);

(iii) high molecular weight PEs are slightly less dense liquids than water at ambient temperatures and thereby form surface films at the air-water interface, leading to errors when water samples for analysis are withdrawn through this surface film (Staples *et al.*, 1997).

Accordingly, published saturated water solubilities for the higher molecular weight PEs can vary by several orders of magnitude. For example, the published water solubility for DEHP ranges from 3.0 $\mu g\ L^{-1}$ (Staples *et al.*, 1997) to 400 $\mu g\ L^{-1}$ (Giam *et al.*, 1984). Sea water solubilities would be expected to be even lower through salting out (Means, 1995). This overestimation of PE water solubility is reflected in the range of K_{ow} values shown in Table 1.1. for DEHP. PEs also hydrolyse in water to form an acid and alcohol (Schwarzenbach *et al.*, 1993). However, due to their low water solubility hydrolysis is slow, with half lives ranging from 3 years for dimethyl phthalate ester (Giam *et al.*, 1984), the fastest phthalate to hydrolyse, to 2000 years for DEHP (Staples *et al.*, 1997).

1.2.4. Polycyclic aromatic hydrocarbons

Polycyclic aromatic hydrocarbons (PAHs) are compounds containing typically two to eight aromatic rings that are produced during the incomplete combustion of petroleum products, wood, and coal. The chemical structure of phenanthrene is given as an example in Figure 1.4., and the structure of BaP is shown in Figure 1.1.

Major anthropogenic PAH emissions include automobile exhaust, coke and steel production, whilst natural PAH emissions include forest fires and volcanic eruptions (Sheu *et al.*, 1997). The anthropogenic contribution to the environment outweighs PAH input from other sources (Simcik *et al.*, 1996), rendering PAHs environmental micropollutants (D'Adamo *et al.*, 1997). PAHs exhibit a wide range of physico-chemical properties (e.g. vapour pressure, aqueous solubility) (Karcher *et al.*, 1983; Karcher *et al.*, 1988) that demonstrate their hydrophobic character and influence their environmental fate (Table 1.1.). The aqueous solubility and volatility of PAHs decrease as the number of aromatic rings increases (Futoma *et al.*, 1981).

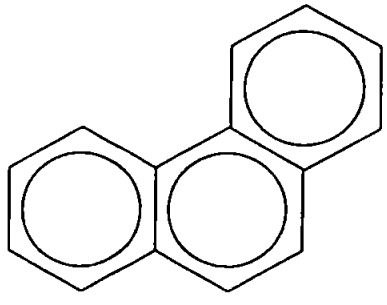

Figure 1.4: The chemical structure of the PAH, phenanthrene.

The carcinogenic nature of PAHs was first deduced in the early 20th century, but like PCBs, research into their environmental impact did not begin until the late 1960s (Futoma *et al.*, 1981). PAHs have the ability to be transported long distances as gases or aerosols due to their apparent resistance to degradation on atmospheric particles (Simcik *et al.*, 1996). The fact that PAHs are known carcinogens (Karcher *et al.*, 1983; Karcher *et al.*, 1988) coupled with their transport on such small air-borne particulate matter (< 2.5 μm) increases their potential carcinogenic effect due to easy inhalation through the upper respiratory tract into the bronchioles and alveoli of the lungs (Sheu *et al.*, 1997).

Several PAHs, which closely resemble steroid hormones, have recently been identified as environmental oestrogens (Santodonato, 1997). PAHs have been shown to disrupt endocrine function in rats. However, there is no evidence to support similar oestrogenic or antioestrogenic effects of PAHs in humans (Santodonato, 1997).

1.3. Reactivity of HOMs in the Aquatic Environment

1.3.1. Partitioning, fate, and transport of HOMs in aquatic systems

The partitioning, fate, and transport of HOMs in aquatic systems is conceptualised in Figure 1.5. Such chemical modelling approaches and their interfacing with water dynamics are well-defined for trace metals (Huthnance *et al.*, 1993; Turner *et al.*, 1993; Ng *et al.*, 1996) but less so for trace organics (Landrum, 1989; Morrison *et al.*, 1996; Turner & Tyler, 1997) with many of the pathways still to be confirmed and quantified.

The limited database on HOM environmental distribution and reactivity has resulted in the development of HOM transport and distribution models based upon the physicochemical properties of the HOM rather than in-situ distribution data. This is exemplified by HOM distribution models based upon the fugacity concept (see glossary). Fugacity models provide information on the environmental behaviour of HOMs, on both a global and regional scale, between at least four bulk compartments; air, water, soil, and sediment (Mackay & Paterson, 1991). Although each bulk compartment may consist of sub-compartments, (such as gas, liquid, solid, and biota), the model assumes equilibrium exists between these sub-compartments, but not between the bulk compartments. However, the use of equilibrium conditions for all sub-compartments may not be appropriate, as a non-steady state may apply in some instances, for example, in estuaries. Transport processes between the bulk compartments are summarised in Figure 1.6., and are derived either directly or via established trends relating to the physicochemical properties of the HOM. Similarly, localised HOM transport and distribution models, such as ECoS (Estuarine Contaminant Simulator; Harris *et al.*, 1993; Liu, 1996) and PISCES (Pollution Information for Contaminants in Estuaries and Seas; Ng *et al.*, 1996) remain intrinsically dependent upon the physicochemical properties of the HOM. The development of HOM transport and distribution models based upon the partitioning,

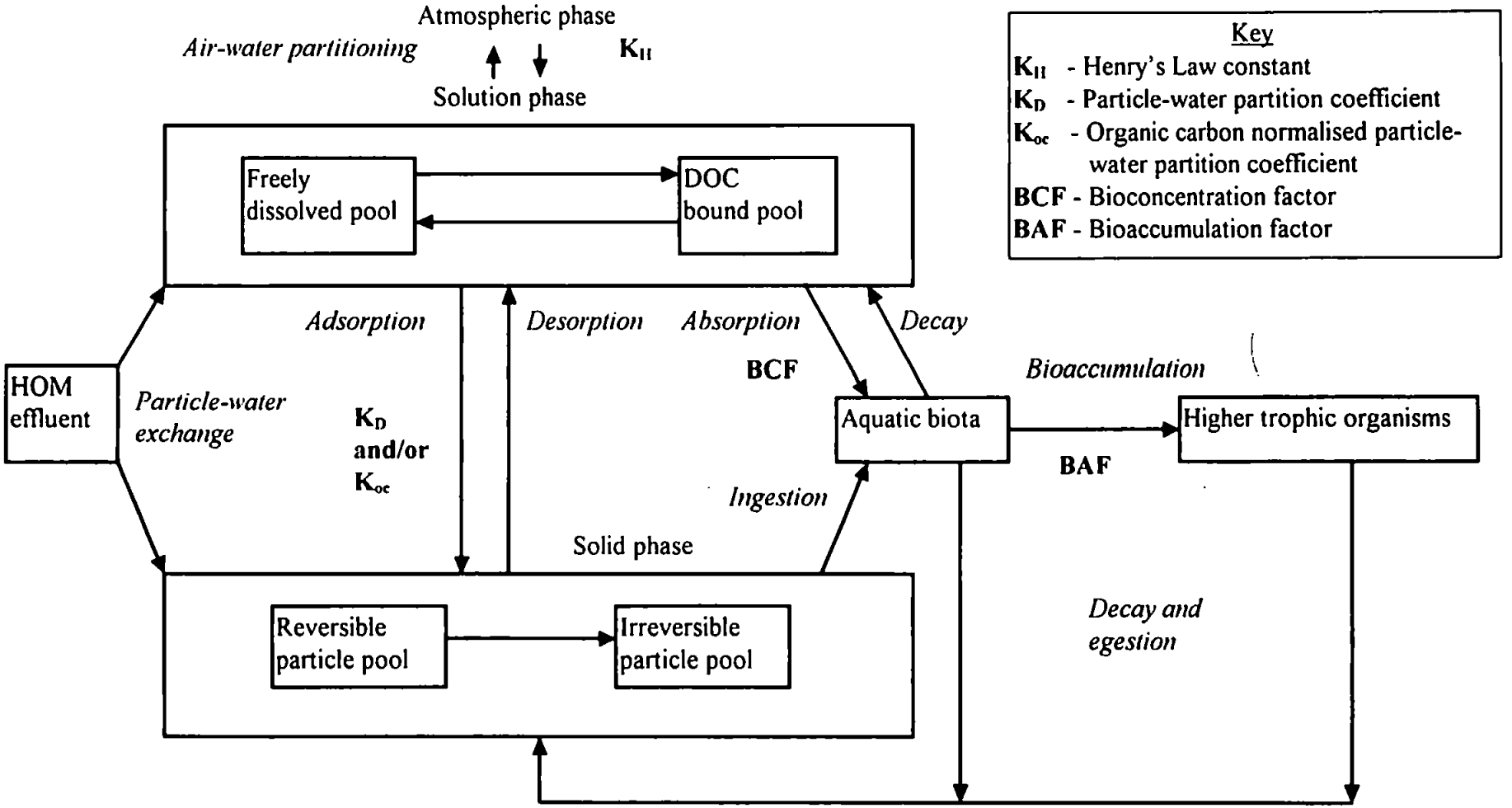

Figure 1.5: Aquatic environmental partitioning, fate and transport model for HOMs (adapted from Landrum, 1989).

fate, and transport data of HOMs measured directly from the environment is essential to assess the validity of existing transport and distribution models.

The aquatic environmental partitioning, fate, and transport of HOMs relating to Figure 1.5. are discussed in more detail in the following four sections.

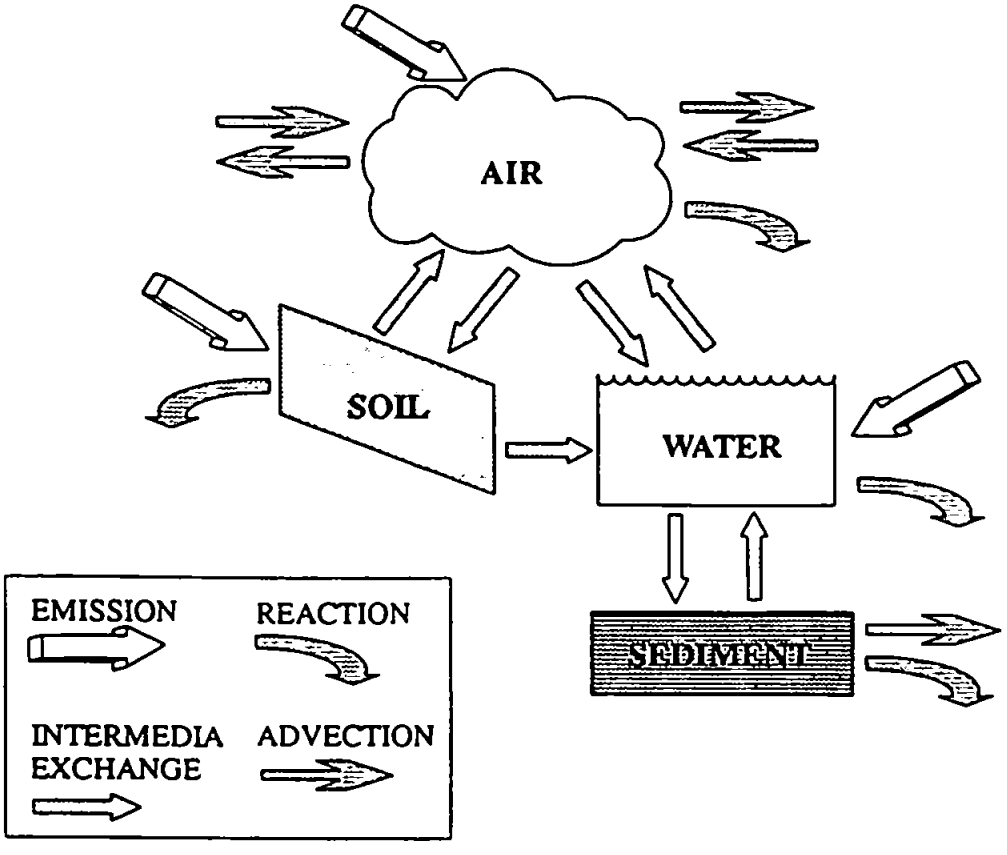

Figure 1.6: Summary of the distribution processes occurring between the bulk compartments represented in Fugacity models (adapted from Mackay & Paterson, 1991).

1.3.1.1. Air-water partitioning

Volatilisation of HOMs into the atmosphere from the dissolved phase can arise, leading to the long distance transport and distribution of HOMs as gases or adsorbed to atmospheric particles. These aerosol-adsorbed HOMs are then removed from the atmosphere (and hence back into the aquatic environment) via dry deposition or rain washout ultimately accumulating in sink areas such as aquatic sediments (Sheu *et al.*, 1997). The tendency of a chemical to escape from an aqueous phase into the air is

quantified by an equilibrium distribution coefficient known as the Henry's Law constant, K_H, atm m^3 mol^{-1} (Schwarzenbach *et al.*, 1993). This is the ratio of the vapour pressure, V, to the molar water saturated solubility, S_{sat}, at a stated temperature, commonly 25°C:

$$K_H = \frac{V M_r}{S_{sat}} \qquad (1.2)$$

where M_r is the relative molecular mass of the HOM. Values of K_H shown in Table 1.4. indicate that the selected HOMs have negligible volatility. However, there is growing concern that some HOMs of relatively low molecular mass (e.g. naphthalene and monochlorinated biphenyls) are volatile enough at normal environmental temperatures to cycle among air, water, and soil, as outlined above, on a global scale (Wania & MacKay, 1996). In general, such HOMs volatilise in the warm low latitude regions, eventually being deposited in the cold high latitude polar regions, whilst the less volatile HOMs remain close to their point of release, and are retained in the sediment (Law *et al.*, 1991a).

Table 1.4: Henry's Law constant, K_H, for selected HOMs.

HOM	K_H @ 25°C (atm m^3 mol^{-1})
2,2',5,5'-TCB	0.288 [a]
DEHP	1.7×10^{-5} [b]
BaP	1.2×10^{-3} [a]

Sources: [a] Schwarzenbach *et al.*, 1993; [b] Staples *et al.*, 1997.

1.3.1.2. Particle-water interactions

On release, for example as an industrial effluent, into the aquatic environment adsorption of the HOM, primarily due to hydrophobic bonding, on to the particles will occur. The partitioning between particles and water can be defined by the partition coefficient, K_D, mL g^{-1} (Karickhoff, 1984):

$$K_D = \frac{P}{C} \qquad (1.3)$$

where P is the compound concentration in the particulate phase (w/w) and C is the compound concentration in the dissolved phase (w/v).

The dissolved phase comprises two main pools, that of the freely dissolved, unassociated compound, and that of the compound associated with the dissolved organic carbon (DOC). Natural DOC comprises a heterogeneous mixture of organic compounds, approximately 50% of which is comprised of humic and fulvic acids (Hunchak-Kariouk *et al.*, 1997). The amount of DOC present in the aqueous phase and its forms influences the biodegradation, bioaccumulation, and toxicity of a HOM. It is therefore a major factor in determining the environmental distribution of such compounds.

The solid phase of the aquatic environment comprises HOMs either reversibly, or irreversibly, adsorbed by sediment and/or suspended particulate matter, SPM. Recycling of HOMs from these sediments back into the water column can therefore occur (Sanders *et al.*, 1996). Adsorption of HOMs onto the solid phase is controlled by the relative hydrophobicity of the compound. HOMs and other nonreactive, neutral chemicals tend to adsorb predominately to the organic matter associated with the solid. This natural organic material is believed to exist as globular units of coiled organic chains as the organic material attempts to minimise its hydrophobic surface area exposed to the aqueous solution. Nonpolar organic compounds, such as HOMs, become 'dissolved' into these macromolecules, *i.e.* physically penetrate between the coiled organic chains (Schwarzenbach *et al.*, 1993). The partitioning of HOMs between the organic coating of particles and the aqueous phase is defined by the organic carbon normalised partition coefficient, K_{oc}, mL g^{-1} (Gawlik *et al.*, 1997):

$$K_{oc} = \frac{K_D.100}{POC} \qquad (1.4)$$

where POC is the percentage particulate organic carbon in the sediment. The range of published log K_D and log K_{oc} values, for the selected compounds, is shown in Table 1.5.

Table 1.5: Range in published partition coefficients, log K_D and log K_{oc}, for the selected HOMs.

HOM	Log K_D (mL g^{-1})	Log K_{oc} (mL g^{-1})
2,2',5,5'-TCB	4.87 [a] -5.07 [b]	5.35 [a] -5.83 [c]
DEHP	2.66 [d] -5.40 [e]	4.85 [f] -6.12 [g]
BaP	5.78 [c] -7.70 [h]	6.66 [c] -8.30 [h]

Sources: [a] Baker *et al.*, 1986; [b] Bergen *et al.*, 1993; [c] Eadie *et al.*, 1990; [d] Williams *et al.*, 1995; [e] Ritsema *et al.*, 1989; [f] Preston & Al-Omran, 1989; [g] Zhou & Rowland, 1997; [h]Broman *et al*, 1991.

1.3.1.3. Aquatic toxicity, bioaccumulation, and bioconcentration

Uptake by aquatic organisms may occur in several ways, either via ingestion of sediments during feeding, causing absorption of HOM from the sediments across the gut membrane, or via absorption of the truly dissolved HOM across the gill membrane. The pathways by which HOMs are transferred from the sediment and/or water to benthic and pelagic food webs remain poorly understood (Muir *et al.*, 1992). Once HOMs have entered the food chain it is still unclear as to how much is bioaccumulated by higher trophic organisms and how much returns to the solid and solution phases of the aquatic system via decay and egestion. Further work is needed to determine the extent to which these compounds can be passed up the marine food chain to commercially important species (Rubinstein *et al.*, 1990). Bioaccumulation (*i.e.* the accumulation of contaminants in biotic tissues via all exposure routes including diet and water) and bioconcentration (*i.e.* the accumulation of contaminants due to aqueous exposure only) are quantified by the bioaccumulation and bioconcentration factors, respectively (BAF and BCF, respectively). The BAF and BCF are defined by the ratio of contaminant concentration in the biotic tissues to that in the water (mL g^{-1} dry, wet, or lipid body weight; Staples *et al.*, 1997).

Marine organisms have been shown to bioaccumulate PCBs (Rubinstein *et al.*, 1990). Three marine benthos organisms, sandworms (*Nereis virens*), clams (*Macoma nasuta*) and shrimp (*Palaemonetes pugio*) were exposed to PCB contaminated river sediment. All three species accumulated PCBs over the 120 day period of the laboratory based experiment and did not depurate these compounds once removed from contaminated to uncontaminated sediments. Due to the lipophilic nature of these compounds, higher concentrations of PCBs are found in aquatic organisms and tissues

with a high lipid content, such as marine mammals. The pattern of PCB congeners and concentrations in such biotic tissues tends to resemble that of the commercially produced PCB mixtures (Mössner & Ballschmiter, 1997). The PCB concentrations found in the blubber of marine mammals taken from Cardigan Bay, UK, were higher than expected and did not come from localised pollution (Morris *et al.*, 1989). It was suggested that PCBs were bioaccumulated from their diet (mainly pelagic fish such as mackerel, herring, and monkfish) despite these organisms not showing elevated PCB levels. These high values have been linked with reproductive disorders observed in marine mammal populations. Coupled with the fact that between 15% and 90% of bioaccumulated PCBs in female marine mammals are excreted whilst lactating (Tanabe, 1988), there is cause for concern, both on the possible biological effects on future generations and the potential for the persistency of these compounds in marine organisms despite reductions in PCB discharge.

PEs have a subtle toxicity which generally decreases with increasing alkyl chain length (Giam *et al.*, 1984). DeFoe *et al.* (1990) found that DEHP was not acutely toxic to fathead minnows (*Pimephales promelas*), even at the highest concentration tested (121 mg L^{-1}). However, this could be due to the true aqueous solubility of high molecular weight PEs being too low to allow the test organisms to reach a critical body burden that would cause adverse effects. DEHP BCFs for the fathead minnow (*Pimephales promelas*) range from 155±36 mL g^{-1} wet wt to 900±69 mL g^{-1} wet wt. However, the bioaccumulation of PEs through aquatic food chains is believed to be limited owing to the ability of higher trophic organisms to biotransform and remove these compounds from their tissues (Staples *et al.*, 1997).

Experiments in rats and hamster embryos, however, have shown carcinogenic and mutagenic effects (Giam *et al.*, 1984), but acute toxicity remains low. It was suggested that present day applications and emissions of DEHP pose no serious threat to humans or the environment (Wams, 1987); however, this is no longer believed to be the case as PEs are suspected of mimicking oestrogen (Jobling *et al.*, 1995). This has recently been highlighted in a spate of articles published by the national media.

The tendency of HOMs to bioaccumulate, coupled with the carcinogenic nature of compounds such as PAHs is cause for concern, especially within commercially important food stocks and their related food chains. A study by D'Adamo *et al.* (1997) into the bioaccumulation of PAHs through the marine food chain of microalgae (*Dunaleilla tertiolecta*), mussel (*Mytilus galloprovincialis*), and seabass (*Dicentrarchus*

labrax) showed that although the PAHs, BaP, and 7,12-dimethylbenz(a)anthracene were bioaccumulated in the mussel population, the seabass were able to metabolise and remove the PAHs through an efficient detoxification enzymatic system located in the liver. This suggests that although PAH bioaccumulation is cause for concern in lower trophic organisms, they are not necessarily bioaccumulated in higher trophic organisms.

Research has, therefore, shown that bioaccumulation of both PEs and PAHs may not occur in higher trophic organisms, as a result of increased biotransformation owing to the more developed and efficient detoxification enzymatic systems of such organisms (D'Adamo *et al.*, 1997). However, bioaccumulation remains a major concern in the case of PCBs and other chlorinated HOMs (Rubinstein *et al.*, 1990; Law *et al.*, 1991a).

1.3.1.4. Degradation

Removal of HOMs from aquatic sediments via degradation is a slow process and has recently been the focus of considerable research (Rhee *et al.*, 1993; Ye *et al.*, 1996; Ejlertsson *et al.*, 1997). HOM removal is primarily via microbial degradation, which is dependent upon the anaerobic/aerobic sediment conditions and the microbial population present (Lang, 1992; Li *et al.*, 1996).

Removal of PCBs from the environment can be via several processes of degradation: (i) combustion, (ii) photolysis or (iii) biodegradation. The first two processes are extremely rare and slow, respectively. Therefore, microbial degradation is the main natural removal process of PCBs from the environment with aerobic degradation affecting the less chlorinated PCBs, whilst anaerobic degradation causes the reductive dechlorination of the higher chlorinated PCBs (Lang, 1992). This selective degradation of the less chlorinated PCB congeners, under aerobic conditions, was reflected in the PCB distribution associated with the surface layer of bed sediment in the Mediterranean Sea (Dachs *et al.*, 1997a). Reductive dechlorination of PCBs in Hudson River sediment by anaerobic microbes was found to be dependent upon the chlorine pattern of the congener (Rhee *et al.*, 1993). However, these removal processes only occur under specific conditions on specific congeners at specific PCB concentration levels above that usually found in the environment (Lang, 1992). Therefore, the potential for PCBs to be long-term environmental contaminants remains.

The stability of PEs is less than that of the more persistent PCBs. Photodegradation and hydrolysis of PEs in the aqueous environment are slow processes

and play a minor role in the degradation of these compounds. The main removal process is by microbial degradation. For example, DEHP biodegradation occurs under aerobic conditions, but not under anaerobic conditions (Wams, 1987), and its rate is dependent upon the microbial population present. The water solubility of PEs was found to be a controlling factor in their microbial degradation (Ejlertsson *et al.*, 1997), with highly soluble PEs such as dibutyl phthalate being degraded, while PEs with low solubility, such as DEHP, did not degrade. The half-life of DEHP in aerobic sediment is approximately 90 days, longer than that for freely dissolved DEHP (2-15 days), suggesting that these compounds are less persistent in the aquatic environment than other HOMs (Staples *et al.*, 1997).

Microbial degradation of particulate bound PAHs, to less toxic products, has been demonstrated in the laboratory under artificial conditions (Ye *et al.*, 1996) as well as for pyrene in natural marine sediments (Li *et al.*, 1996). However, these biotransformations and the conditions under which they occur remain poorly understood. The PAHs, naphthalene and BaP, were found to have higher degradation rates in the water column of the Tamar Estuary, UK (72% and 0.035% d^{-1}, respectively), compared to marine waters (3% and 0.011% d^{-1}, respectively) (Readman *et al.*, 1982). Microbial degradation rates for naphthalene (turnover rate of 1-2 days) are less than the flushing times of the Tamar Estuary (up to 21 days), suggesting that microbial degradation is the principal removal mechanism for naphthalene in this environment. However, the slow degradation rates for BaP (turnover rate of 2000-9000 days) indicate that the sediments of the Tamar Estuary ultimately act as a sink for this compound in the short to medium term. Thus, sediments are an important sink for the more persistent PAHs (Futoma *et al.*, 1981).

1.4. Concentrations and Distribution of HOMs in the Aquatic Environment

The following sections summarise the known aquatic concentrations and distributions of the selected classes of HOMs.

1.4.1. Polychlorinated biphenyls

Examples of concentrations of PCBs in the aquatic environment are given in Table 1.6. A survey of the distribution of dissolved PCBs in the North Sea by Schulz-Bull *et al.* (1991), showed that for the sum total of PCBs, dissolved concentrations were highest at the low salinity stations (salinity range; $31x10^{-3}$-$33x10^{-3}$) in the coastal waters of the German Bight, and the lowest concentrations were found at the higher salinity stations (salinity > $35x10^{-3}$) in the north-western part of the North Sea. The higher dissolved PCB concentrations found in the summer (Table 1.6.) reflect the lower salinities encountered in the North Sea during that period. This inverse relationship with salinity indicates a predominantly fluvial source. Conservative behaviour of dissolved PCBs, with concentrations greatest in rivers has been reported in the Elbe (Duinker *et al.*, 1982) and Rhine (Klamer *et al.*, 1994) estuaries. The dissolved concentrations of the PCBs 2,4,4'-trichlorobiphenyl (IUPAC 28) and 2,2',3,4,4',5'-hexachlorobiphenyl (IUPAC 138) versus salinity in the Rhine Estuary are shown in Figure 1.7.

PCBs associated with suspended particulate matter (SPM) tend to be the more volatile, less chlorinated congeners, possibly due to the selective recycling of these congeners from the bed sediment (Dachs *et al.*, 1997a). Particulate PCB concentrations in the Rhine Estuary were seen to decrease seaward (Figure 1.8.) suggesting a fluvial source of particulate PCBs that are deposited in the sediments close to the landward source (Klamer *et al.*, 1994).

PCB concentrations in Humber Plume surface sediments were found to be lower than that for sediments in other areas of the North Sea (Klamer & Fomsgaard, 1993), suggesting that this estuary is not a major source of PCBs to the North Sea. A study by Law *et al.* (1991a), on the leaching of PCBs from a contaminated industrial estate into the River Dee, UK, showed that the PCBs remained trapped in the river sediments close to the site of release, and that the quantities reaching the Irish Sea sediments were minimal. This also explains the very high PCB levels encountered in sediments of the Hornsmill Brook, Mersey Estuary, located close to a landfill site (Johnston *et al.*, 1991). On a larger scale, a similar trend was noticed for PCB concentrations in the surface waters and marine mammal tissues in the Pacific Ocean. PCB concentrations were highest in the mid-latitudes of the northern hemisphere, decreasing north and southwards away from the main industrial regions. It is believed that this pattern reflects the extensive production and use of PCBs in the industrialised countries mainly

Table 1.6: Aquatic concentrations for total PCBs and the congener, 2,2',5,5'-TCB, where SPM is the suspended particulate matter.

Environmental Compartment	2,2',5,5'-TCB	Total PCB
Solution phase (pg L^{-1})		
River water		
UK average	69 [a]	1200 [a]
Estuarine and sea water		
Rhine, Netherlands	85-409 [b]	420-2450 [b]
North Sea: Winter	1.0-9.7 [c]	13.7-133.7 [c]
Summer	1.8-28 [c]	28.1-415.0 [c]
Mediterranean Sea	8.5 [d]	59.7 [d]
Solid phase (μg g^{-1})		
SPM		
Mediterranean Sea	1.0 [d]	1.62 [d]
Scheldt Estuary, Netherlands	0.016-0.073 [b]	0.22-1.1 [b]
Rhine Estuary, Netherlands	0.003-0.027 [b]	0.061-0.22 [b]
Haringvliet Estuary, Netherlands	0.009 [e]	0.095 [e]
River and Lake sediment		
Dee Estuary, UK		45 [f]
Hornsmill Brook, UK		280 [g]
Großer Arbersse (lake), Germany	1.1 [h]	1.26 [h]
Estuarine and Marine sediment		
Dee Estuary, UK		0.09 [f]
Humber Plume, UK	0.0003-0.0021 [i]	0.003-0.019 [i]
New Bedford Harbour, USA	177 [j]	2167 [j]
Aquatic Organisms (μg g^{-1})		
Marine fish		
Herring (*Clupea harengus*)	<0.001 [e] (UK)	0.039 [e] (UK)
		2.7-11 [k] (Baltic)
Mackerel (*Scomber scombrus*)	<0.001 [e] (UK)	0.16 [e] (UK)
Monkfish (*Squantina squantina*)	0.016 [e] (UK)	4.2 [e] (UK)
Marine mammals		
Grey Seal (*Halichoerus grypus*)		66 [k] (Baltic)
	0.064 [e] (UK)	17 [e] - 44 [g] (UK)
Harbour Porpoise (*Phocoena phocoena*)		11-13 [k] (Baltic)
	0.45-1.3 [e] (UK)	23-93 [e] (UK)
Common Dolphin (*Delphinus delphinus*)	1.27 [l] (N. Atlantic)	78 [l] (N Atlantic)
Striped Dolphin (*Stenella coeruleoalba*)	0.50-0.55 [e] (UK)	20-23 [e] (UK)
Pilot Whale (*Globicephala melaena*)	0.15 [l] (N. Atlantic)	10 [l] (N Atlantic)

Sources: [a] Harrad *et al.*, 1994; [b] Klamer *et al.*, 1994; [c] Morris *et al.*, 1989; [d] Dachs *et al.*, 1997a; [e] Van Eck *et al.*, 1997; [f] Law *et al.*, 1991a; [g] Johnston *et al.*, 1991; [h] Bruckmeier *et al.*, 1997; [i] Klamer & Fomsgaard, 1993; [j] Brannon *et al.*, 1991; [k] Järnberg *et al.*, 1993; [l] Mössner & Ballschmiter, 1997.

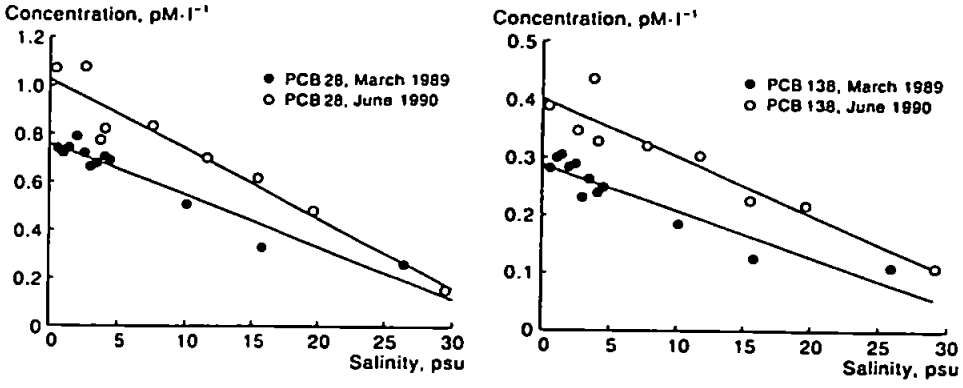

Figure 1.7: The dissolved concentrations of 2,4,4'-TCB (IUPAC 28) and 2,2',3,4,4',5'-HCB (IUPAC 138) versus salinity in the Rhine Estuary for both March 1989 and June 1990 (source: Klamer *et al.*, 1994).

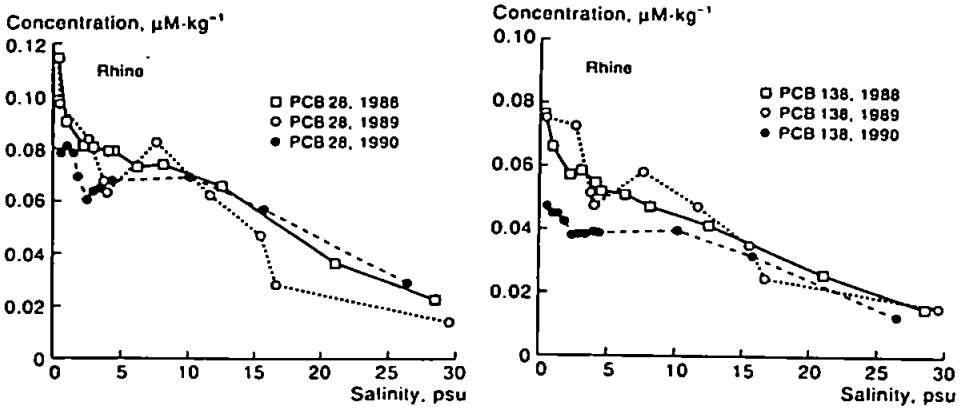

Figure 1.8: The particulate concentrations of 2,4,4'-TCB (IUPAC 28) and 2,2',3,4,4',5'-HCB (IUPAC 138) versus salinity in the Rhine Estuary for three consecutive years, 1988-1990 (source: Klamer *et al.*, 1994).

located at these latitudes (Tanabe, 1988). The PCB production history is often reflected in the pattern of PCB congener concentrations found in aquatic sediment cores (Figure 1.9.) resembling that of the commercially produced PCB mixtures (Van Zoest & Van Eck, 1993; Bruckmeier *et al.*, 1997). Present day PCB inputs to surface sediments, which may influence core profiles, include postdepositional mixing, continued atmospheric and fluvial sediment inputs (Van Metre *et al.*, 1998), and must be taken into account when predicting the persistence of HOMs in estuarine systems. In addition to this large reservoir of PCBs already present and circulating throughout the

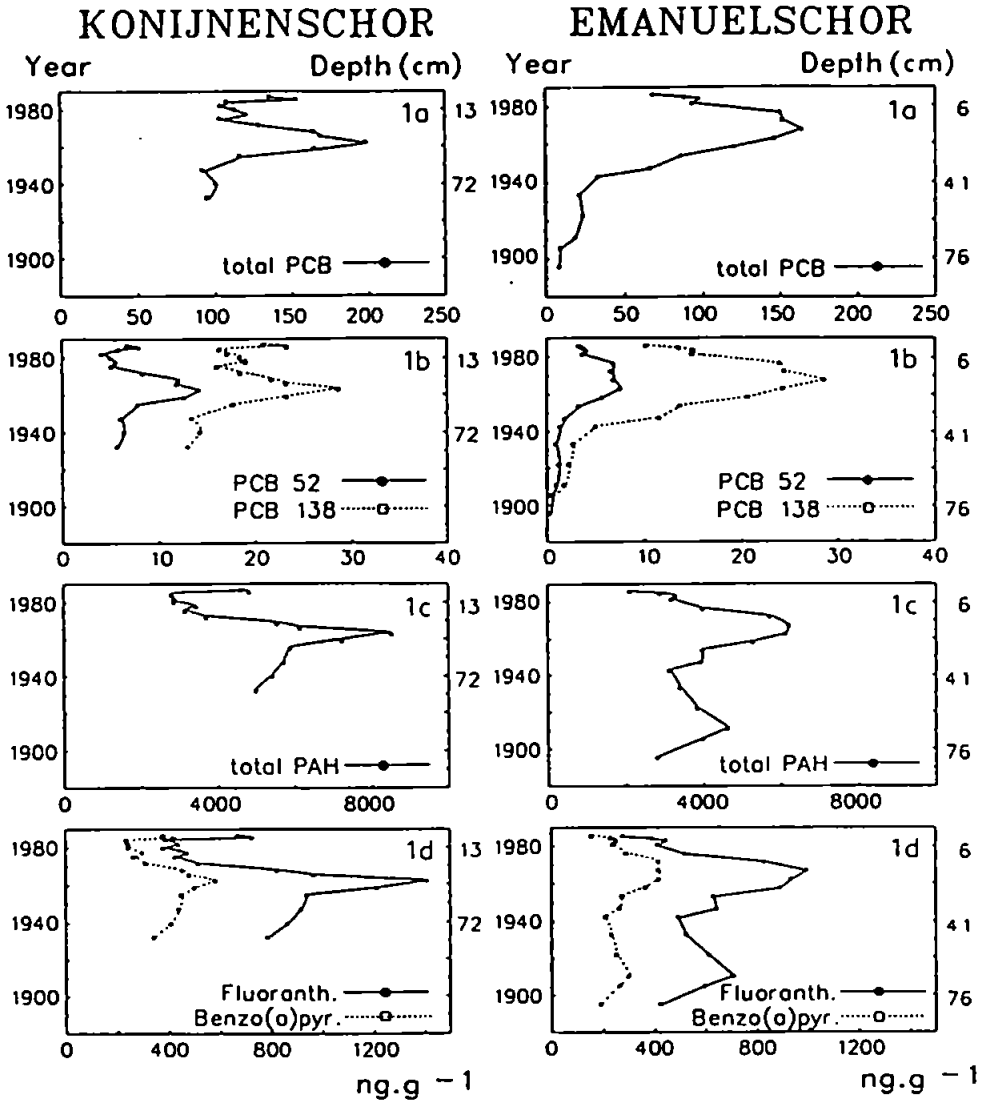

Figure 1.9: (a) Total PCB, (b) 2,2',5,5'-TCB (IUPAC 52) and 2,2',3,4,4',5'-HCB (IUPAC 138), (c) Total PAH and (d) Fluoranthene and BaP concentration (ng g^{-1}) in two sediment cores from the Scheldt Estuary salt marshes, as a function of sediment depth and age (source: Van Zoest & Van Eck, 1993).

environment, the potential for further PCB contamination remains owing to the considerable quantities of PCBs stockpiled and remaining in old industrial and domestic appliances (Bruckmeier *et al.*, 1997).

1.4.2. Phthalate esters

Similar to that for the dissolved PCBs in the Elbe and Rhine estuaries, dissolved PEs were found to behave conservatively, with concentrations decreasing with increasing salinity, in the Mersey Estuary (Preston & Al-Omran, 1986). The large range of dissolved PE concentrations is highlighted in Table 1.7. In some cases dissolved DEHP concentrations are higher than its solubility due to two reasons: (i) the difficulty in accurately determining these compounds in water as mentioned earlier (Section 1.2.3.), and/or (ii) the different methods of water sample collection, in some cases 'whole', unfiltered, water samples were analysed (Law *et al.*, 1991b). The variability associated in determining the concentrations of these compounds is exemplified in a study by Fatoki & Vernon (1990) of the river systems and a sewage treatment plant of Manchester, UK. PEs were found at a concentration of 6.39±10.72 $\mu g\ L^{-1}$; a possible source here was leaching from disposed plastic wastes.

DEHP and total PE concentrations in both the marine and riverine Mersey sediments are similar (Preston & Al-Omran, 1989), suggesting little release of these compounds from the estuarine sediments, or effective mixing of different source materials. Nevertheless, aquatic sediments represent an important sink for PEs. The production levels of individual plasticizers, like those of PCBs, are often reflected in the PE concentrations of aquatic sediment cores (Peterson & Freeman, 1982). However, environmental distributions for these compounds remain limited.

1.4.3. Polycyclic aromatic hydrocarbons

Examples of concentrations of PAHs in the aquatic environment are given in Table 1.8. Estuarine water column concentrations of BaP, and the higher molecular weight PAHs, were found to be highly correlated with suspended particulate material in the Tamar Estuary, UK. The highest PAH concentrations occurred at the turbidity maximum, as well as a lower localised peak in the industrialised part of the estuary associated with anthropogenic inputs (Readman *et al.*, 1982). However, no correlation was found with

Table 1.7: Aquatic concentrations for DEHP and total PEs, where SPM is the suspended particulate matter.

Environmental Compartment	DEHP	Total PE
Solution phase (ng L^{-1})		
River water		
Tees Bay, UK	980-2200 [a]	2171-4280 [a]
River Ouse, UK	740-21000 [b]	
River Trent, UK	740-18000 [b]	
River Mersey, UK	251 [c]	2925 [d]
Estuarine and sea water		
Mersey Estuary, UK	125 [d]	
Irish Sea	33 [c]-1500 [a]	626-5840 [a]
Plymouth Sound, UK	70-8400 [a]	130-8617 [a]
Solid phase (μg g^{-1})		
SPM		
River Ouse, UK	3.81-22.8 [b]	
River Trent, UK	7.78-31.1 [b]	
Mersey Estuary, UK	0.51 [d]	0.73 [d]
River sediment		
River Ouse, UK	2.30-6.49 [b]	
River Trent, UK	0.84-12.0 [b]	
River Mersey, UK	0.56 [c]-1.22 [d]	1.64 [d]
Estuarine and sea sediment		
Mersey Estuary, UK	0.41 [c]-1.20 [d]	1.69 [d]
Aquatic Organisms (μg g^{-1})		
Marine fish		
Herring (*Clupea harengus*)	4.71 [e] (Canada)	17 [e] (Canada)
Mackerel (*Scomber scombrus*)	6.5 [e] (Canada)	27 [e] (Canada)
Marine mammals		
Seal (*Phoca vitulina*)	10.6 [e] (Canada)	

Sources: [a] Law *et al.*, 1991b; [b] Long *et al.*, 1998; [c] Preston & Al-Omran, 1986; [d] Preston & Al-Omran, 1989; [e] Giam *et al.*, 1984.

salinity. Seasonal monitoring of the PAHs, fluoranthene and pyrene, in the Humber Estuary, UK, showed that the highest dissolved concentrations were detected in September and the lowest in June (Zhou *et al.*, 1996). In general these compounds decreased seaward. Dilution and rapid partition to suspended particulates were suggested to explain this trend.

A similar trend was observed in the Humber Plume region with PAH sediment concentrations decreasing seaward (Figure 1.10; Klamer & Fomsgaard, 1993). In contrast, there were no changes in PAH concentrations in sediments along the Gironde

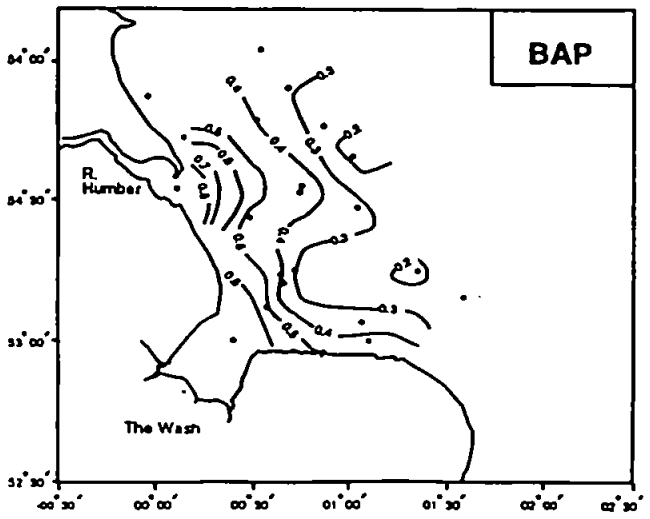

Figure 1.10: Concentration profiles (nM kg^{-1} dry wt) for BaP in Humber Plume surface sediments (< 63 μm) in July/August 1990 (source: Klamer & Fomsgaard, 1993).

Table 1.8: Aquatic concentrations for BaP and total PAHs, where SPM is the suspended particulate matter.

Environmental Compartment	BaP	Total PAH
Solution phase ($ng\ L^{-1}$)		
River water		
Lincoln Creek, USA	3-65 [a]	649 [a]
Estuarine and sea water		
Tamar Estuary, UK	9.1 [b]	97.3 [b]
Baltic Sea	1.0-5.7 [c]	300-744 [c]
Mediterranean Sea	0.09 [d]	1.8 [d]
Solid phase ($\mu g\ g^{-1}$)		
SPM		
Tamar Estuary, UK	0.741 [b]	9.963 [b]
River sediment		
Dordogne River, France	0.097 [e]	1.416 [e]
Estuarine and sea sediment		
Gironde Estuary, France	0.059 [e]	0.871 [e]
Tamar Estuary, UK	0.724 [b]	4.894 [b]
Scheldt Estuary, Netherlands	0.180-0.33 [f]	2.0-4.4 [f]
Humber Plume, UK,	0.00003-0.00017 [g]	0.0007-0.0027 [g]

Sources: [a] Crunkilton & DeVita, 1997; [b] Readman *et al.*, 1982; [c] Broman *et al.*, 1991; [d]Dachs *et al.*, 1997b; [e] Budzinski *et al.*, 1997; [f] Van Zoest & Van Eck, 1993; [g] Klamer & Fomsgaard, 1993.

Estuary (Budzinski *et al.*, 1997) either spatially or seasonally, suggesting that fine suspended particles have a similar affinity for PAHs as coarse bed sediment in this environment. In general, individual PAH concentrations in the Tamar surface sediments were similar to those found in the SPM (Readman *et al.*, 1982) as shown for BaP in Table 1.8.

Scheldt Estuary sediment cores peaked in the mid 1960s (Figure 1.9.) possibly reflecting the decrease in the use of coal as a domestic heating fuel (Van Zoest & Van Eck, 1993). The PAH environmental input is more complicated than that for PCBs and PEs, which reflect anthropogenic production levels, owing to the possible significant natural input of PAHs on a regional level from forest fires and volcanic eruptions.

1.5. The Estuarine Environment

The present research focuses on the reactivity of HOMs in estuaries. The physical and chemical complexities and economic importance of estuaries are now therefore discussed.

Estuaries are areas where sea water mixes with river water. The interaction between the two water types provides a circulation of water and mixing processes that are driven by the density difference between the water types (Dyer, 1997). Owing to the contrasting composition of these two water types, and their particle populations, a variety of physical, chemical, and biological processes will act upon any dissolved or particulate material, such as HOMs, throughout this estuarine mixing zone (Chester, 1990). Hence, sorption-controlling parameters, such as dissolved and particulate organic matter and salinity, tend to be highly variable, both spatially and temporally within this environment, ensuring that identification and investigation of these processes remains difficult.

Estuaries, owing to their fertile waters, sheltered anchorages, and navigational access have become the centre of anthropogenic development. This increases the potential for industrial and domestic effluent discharge direct into the estuary, with the organic-rich estuarine sediment as a possible sink for micro-contaminants such as HOMs. This possible reservoir of highly toxic chemicals in close proximity to urban settlements could pose a serious threat to the health of these communities and that of the estuarine ecosystem itself. Insufficient regulation and poor understanding of the various forms and

sources of effluent into estuaries exemplifies the problem (Johnston *et al.*, 1991). Therefore, the environmental significance of the fate of HOMs and similar compounds in estuaries should not be underestimated. It must, however, be remembered that trends in data derived from one estuary do not imply a global or inter-estuarine trend, owing to the infinite number of contrasting interactions caused by the numerous variables, rendering no two estuaries alike (Dyer, 1997). Published data on the behaviour of HOMs in this complex environment remains sparse (Preston & Al-Omran, 1989; Tyler & Millward, 1996), hence the estuarine environment was chosen as the focus for this investigation.

1.6. Research Aim and Objectives

The behaviour of HOMs in aquatic systems is clearly complex and remains poorly understood. Information on their behaviour in aquatic systems has been lacking because of the difficulty involved in the determination and analysis of such microcontaminants in natural waters. The extremely low environmental levels usually encountered for HOMs (Tables 1.6.-1.8.) requires the use of a multi-staged analytical procedure. This involves several preconcentration steps, following the extraction and clean-up stages of voluminous environmental samples, before determination and evaluation by gas-chromatography coupled with an identification system (e.g. a mass spectrometer) (Futoma *et al.*, 1981; Giam *et al.*, 1984; Lang, 1992). The potential for alaising results, arising from sample contamination and/or loss via adsorption onto laboratory-ware, is relatively high.

The majority of prior investigations into the behaviour and fate of HOMs in the aquatic environment which have been laboratory based have employed artificial sediments, such as kaolinite and montmorillonite (Sullivan *et al.*, 1982; Horzempa & Di Toro, 1983; Murphy *et al.*, 1990; Williams *et al.*, 1995; Hunter *et al.*, 1996; Mader *et al.*, 1997; Zhou & Rowland, 1997), or artificial waters (Means *et al.*, 1980; Al-Omran & Preston, 1987; Hegeman *et al.*, 1995), and/or the use of K_{ow} as a predictive measure (Karickhoff, 1984; Brownawell & Farrington, 1985; Voice & Weber, 1985; Bergen *et al.*, 1993). Although, these data are important in providing information on defining the environmental partitioning of HOMs, it remains difficult to extrapolate such information to the highly variable conditions of estuaries.

This study therefore aims to investigate the role played by the main estuarine variables (organic matter, SPM, particle type, and salinity) on HOM behaviour, by employing natural sediments suspended in their native waters under realistic estuarine conditions. To this end, this thesis describes a laboratory based technique which determines the solubility and adsorptive behaviour of HOMs using ^{14}C-labelled, beta-emitting compounds coupled with liquid scintillation counting, using natural water and sediment samples from estuaries. Results are presented for the selected compounds monitored under a variety of environmental conditions using samples collected from several contrasting estuaries (Sections 3.2., 4.3. & 4.4.).

Hence, the overall research aim of this project is to improve the understanding of the partitioning, fate, and transport of HOMs in estuaries. Specifically this will involve the completion of the following objectives:

(i) Developing a suitable method to determine the aqueous behaviour and particle-water partitioning of HOMs over a range of simulated estuarine conditions using natural samples;

(ii) determining the extent to which estuarine physico-chemical conditions control HOM solubility and the adsorption of HOMs to estuarine sediments; and

(iii) formulating empirical partitioning codes that will be available for incorporation into established aquatic pollutant transport models such as the Estuarine Contaminant Simulator, ECoS (Harris *et al.*, 1993; Liu, 1996), and Pollution Information for Contaminants in Estuaries and Seas, PISCES (Ng *et al.*, 1996).

CHAPTER 2: SAMPLING AND METHODOLOGY

2.1. Introduction

Conventional techniques for the determination and analysis of hydrophobic organic micropollutants (HOMs) in the environment include gas chromatography-mass spectrometry (Futoma *et al.*, 1981; Giam *et al.*, 1984; Lang, 1992). Such techniques are relatively complex and time consuming, involving numerous stages (including; preconcentration and clean-up stages of voluminous samples), which increase the potential for sample contamination and/or loss via adsorption (Bruckmeier *et al.*, 1997).

In this work, an efficient, routine method was developed to investigate the effects of different variables on the solubility and particle-water partitioning of HOMs. These variables include salinity, dissolved organic carbon (DOC) content, and particulate organic carbon (POC) content. The approach was designed to reproduce environmental behaviour, employing the use of 'natural' water and sediment samples under controlled laboratory conditions. Despite extensive investigation of HOM behaviour in freshwater lakes, especially the Great Lakes of North America (Voice & Weber, 1985; Baker *et al.*, 1986; Eadie *et al.*, 1990), little data are available on HOM behaviour in estuarine (Turner & Tyler, 1997) and marine environments (Ernst *et al.*, 1988; Bergen *et al.*, 1993). Hence the highly variable river-estuary environment was chosen as the site of sample collection and HOM particle-water interaction investigations in this project.

The method used to investigate the relative solubility and particle-water partitioning of HOMs in estuaries is based on the addition and equilibration of a ^{14}C-radiolabelled organic compound to filtered river or sea water samples turbidised with estuarine sediment. This is followed by determination of the radioactivity on the solid and in solution using liquid scintillation counting after phase separation by centrifugation (Zhou *et al.*, 1995; Turner & Tyler, 1997). This approach is described in detail (Section 2.7.) with reference to method evaluation and development.

Estuarine water and sediment samples for investigation were collected from one Russian and four British estuaries, shown in Figure 2.1. and described below. These estuaries were chosen for their contrasting water and sediment characteristics.

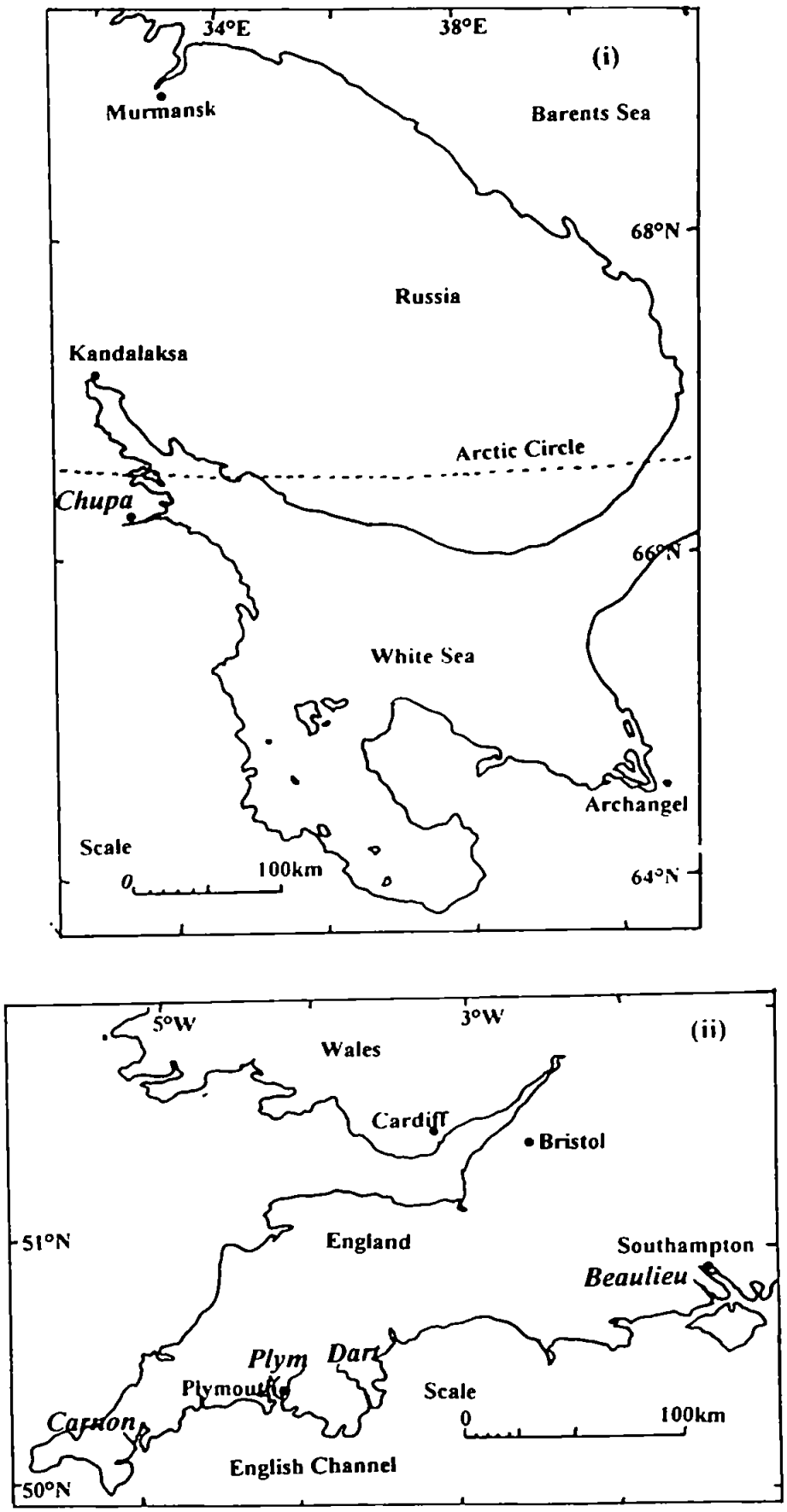

Figure 2.1: Maps of (i) Northern Russia and (ii) Southern England showing sites of the estuaries studied.

2.2. Site Descriptions

(i) The Chupa Estuary (66°20'09N 33°42'29E), Russia, is situated in the White Sea, just south of the Arctic circle. This highly stratified salt wedge estuary (Rawling, 1994) is 30 km long with a tidal range of 1-2 m and is ice covered between October and April. Successive freeze and thaws results in the production of fine fluvial sediments which become organic rich during the productive summer months. Drainage into the estuary is mainly from the surrounding 'Taiga', or forests of conifers, ash, and birch. Anthropogenic input is limited and the Chupa Estuary remains relatively pristine with only pockets of localised pollution (Rawling, 1994). Water and sediment samples were collected from the Chupa Estuary during the Anglo-Russian Interdisciplinary Estuarine Study (ARIES) survey of July 1994.

(ii) The River Dart (50°26'55N 03°34'50W), Devon, is a well-mixed estuary 20 km long with a tidal range of 2-3 m. Draining the peaty catchment area of the Dartmoor National Park and Forest this estuary was chosen for its relatively high organic carbon content, comprising both dissolved and particulate matter. Water and sediment samples were collected in January 1995. Supplementary samples of river water were collected in September 1995.

(iii) The Plym Estuary (52°07'50N 04°07'75W), Plymouth, Devon, is 7 km long and well-mixed with a tidal range of 2-3 m. The catchment area of the River Plym encompasses the Dartmoor National Park and coniferous and deciduous woodland. This industrialised estuary is lined with various industries including a large sewage works, a landfill site, and a china-clay works. The Plym was chosen because of the composition of the sediments from its extensive intertidal mudflats. These sediments contain a high proportion of china-clay derived from the upriver workings (Gibbs, 1984). Both water and sediment samples were collected from the Plym Estuary in February 1996. Additional river water samples were collected in September and November 1996.

(iv) The River Beaulieu (50°47'00N 01°21'76W), Hampshire, is 20 km in length and the estuary is well-mixed, with a tidal range of 2-3 m exposing mudflats at low water. The catchment area of the Beaulieu encompasses the heathland and bogs of the New Forest National Park. The river water contains high levels of dissolved organic matter and dissolved iron (Hunter & Liss, 1979). Water and sediment samples were collected in June 1996.

(v) The Carnon River and its estuary Restronguet Creek (50°11'25N 05°04'25W), Cornwall, is 15 km in length with a well-mixed estuary, a tidal range of 2-3 m, and intertidal mudflats. The Carnon River catchment area is littered with disused tin mines, most noticeably the Wheal Jane Tin Mine, which produce acidic, iron-rich effluent (Johnson & Thornton, 1987; Newton & Liss, 1987). River water and sediment samples were collected from the Carnon River and sea water samples from the outer creek in March 1997.

2.3. Sample Collection and Storage

2.3.1. Riverine and marine water samples

The Chupa Estuary water samples were collected from the Russian research vessel *Professor Vladimir Kuznetzov* into Decon®-cleaned plastic bottles, chosen in preference to glass pyrex bottles due to the extensive travelling involved during this survey. However, for the remaining work, water samples were collected by hand into Decon®-cleaned and ashed glass pyrex bottles, in order to minimise contamination by synthetic organic material. River end member water samples were collected from above the furthest point of saline water intrusion into the estuary, whilst the marine end members or sea water samples were collected from the mouth of the estuary, at a salinity of 21.3-33.8x10^{-3}. On return to the laboratory the water samples were filtered through pre-ashed 47 mm diameter Whatman GF/F filters (pore size 0.7 μm) and stored in clean ashed glass pyrex bottles in the dark at 4°C until required.

2.3.2. Estuarine sediment samples

Subtidal (Chupa and Dart) or intertidal mudflat (Plym, Beaulieu, and Carnon) estuarine sediment samples were collected and stored frozen in clean glass jars until needed, with the exception of the Chupa sediment sample which was stored frozen in a clean plastic container to reduce the risk of breakage during transit.

2.4. Sample Characterisation

2.4.1. Water characterisation

A calibrated MC5 Salinometer T/S Bridge and calibrated Hanna pH meter were used to determine the physicochemical properties of the water samples *in situ*. On return to the laboratory chlorinity, alkalinity, calcium, and dissolved organic carbon (DOC) of the water samples were determined in triplicate.

For river and sea water samples the chlorinity was determined by silver nitrate-thiocyanate titration using a ferric alum indicator (Jeffery *et al.*, 1989) and the alkalinity determined by sulphuric acid titration using a calibrated Hanna pH meter (O'Neill, 1993). For calcium analysis, 3 mL of river water sample were diluted into 22 mL 0.2% w/w KCl and then determined on a GBC double beam atomic absorption spectrophotometer (AAS) in the flame mode with a nitrous oxide-acetylene flame, calibrated using Ca standards diluted in KCl (DeVargas *et al.*, 1994) at a wavelength of 422.7 nm.

For DOC analysis, 100 mL water samples were filtered through pre-ashed 47 mm diameter Whatman GF/F filters (pore size 0.7 μm). The filtrate was placed in ashed pyrex glass bottles, and acidified with 1% phosphoric acid (AristaR) (Statham & Williams, 1983) before being tightly sealed with a glass stopper, ensuring no air bubbles were trapped. Samples were stored in the dark at 4°C until DOC was determined using a Schimadzu TOC-5000 total organic carbon analyser. The limit of detection was ~0.001 mg L^{-1}. Procedural blanks, using Milli-Q water, were within the range, 0.27-0.66 mg L^{-1}.

2.4.2. Sediment characterisation

To determine the concentration of Fe, Mn, and Ca in the < 63 μm estuarine sediment fraction, approximately 200 mg of freeze-dried sediment was extracted with a mixture of 0.05M hydroxylamine hydrochloride in 25% v/v acetic acid (BDH AristaR) for 16 h, at room temperature (Chester & Hughes, 1967). Analysis of Fe and Mn was performed in triplicate on an Instrumental Laboratory 1L AAS, calibrated using acidified standards. The digests were diluted into 0.2% w/w KCl solution before calcium analysis (also carried out in triplicate) was performed on a GBC double beam AAS as outlined in Section 2.4.1. A summary of analytical conditions for the AAS are shown in Table 2.1. Procedural blanks, carried out in the absence of sediment, were below the limit of detection for each of the metals determined.

Percentage total organic matter was estimated as loss on ignition (LOI). Sediment was collected on a pre-weighed, pre-ashed 47 mm diameter Whatman GF/F filter (pore size 0.7 μm), dried, re-weighed, then placed in a Carbolite ESF3 Muffle Furnace at 550°C for 5 hours and re-weighed (Williams, 1985; Section 4.1.1.). Particulate organic carbon (POC) was measured using a Schimadzu TOC-5000 total organic carbon analyser after digestion in 40% v/v phosphoric acid (AristaR). The specific surface area (SSA) of the freeze-dried sediment was determined by a multi-point BET nitrogen gas adsorption technique (Millward *et al.*, 1990).

Table 2.1: Analytical conditions for atomic absorption spectrophotometry.

Metal	Wavelength (nm)	Slit width (nm)	Flame	Limit of Detection ($\mu g\ mL^{-1}$)	Standard range ($\mu g\ mL^{-1}$)
Fe	386.0	0.3	air-C_2H_2	0.80	2.0-40
Mn	403.1	0.3	air-C_2H_2	0.15	0.8-16
Ca	422.7	0.3	N_2O_2-C_2H_2	0.02	0.8-16

2.5. Radiochemical Manipulations

A laboratory-based method has been used to determine the relative solubility and sorptive behaviour of HOMs using ^{14}C-labelled, beta-emitting radioisotopes coupled with liquid scintillation counting (Zhou *et al.*, 1995; Turner & Tyler, 1997). The development and subsequent evaluation of the radiotracer methods are described in detail below.

2.5.1. Radioactive compounds used in this investigation

Three radiolabelled compounds: 2,2',5,5'-tetrachlorobiphenyl-UL-^{14}C (abbreviated to 2,2',5,5'-TCB); bis(2-ethylhexyl)phthalate-UL-^{14}C (DEHP); and benzo[a]pyrene-7-^{14}C (BaP); were obtained from Sigma® Chemical Company, details of which are shown in Table 2.2. On purchase the purity of the compounds was ≥ 98%. After 12 months the purity of the compounds, was determined by GC-MS (Dr J. L. Zhou, personal communication) and the purities (Table 2.2.) were found to be ≥ 99% (11/95) and ≥ 95% (04/96) for 2,2',5,5'-TCB, and ≥ 95% (04/96) for DEHP, respectively (see Appendix A1 for relevant chromatograms).

The radiochemical purity of the compounds was also assessed by radio-GC (Tancell & Rhead, 1996) both before and after an experiment using Plym river water and sediment samples. There was no indication of any radiochemical degradation during the experimental procedure (see Table 2.2. and Appendix A2).

All compounds were diluted into a stock *n*-hexane solution to obtain a concentration of 1.85×10^6 Bq mL^{-1}. This stock solution was diluted for laboratory use by adding 80 µL of the stock solution to 4 mL of *n*-hexane, hence, obtaining an activity of 37×10^3 Bq mL^{-1} (or 925 Bq per 25 µL spike). All radioactive solutions were stored in the dark at 4°C.

2.6. Liquid Scintillation Counting

Detection and quantification of the radioactivity of a ^{14}C spiked sample was by liquid scintillation counting (LSC). Liquid scintillators find widespread employment in the measurement of pure *β-ve* emitters (Rust *et al.*, 1993; Tait & Wiechen, 1993; Barbeau & Wollast, 1994; MAFF, 1995), such as ^{14}C, ^{3}H, ^{32}P, ^{35}S, ^{89}Sr, ^{90}Sr, and ^{63}Ni, and are especially useful when the emitter particle energy is low, as in the case of ^{14}C and ^{3}H.

Scintillation counters detect radiation by measuring the scintillations (tiny flashes or photons of light) produced by radiation in certain materials (Fifield & Kealey, 1995). The radioactive sample is combined with a liquid scintillation 'cocktail' containing a solvent and one or more scintillators (solutes or fluors). Negatrons emitted by the radioactive sample ionise and excite the components of the liquid scintillation cocktail which converts this energy into photons of light. This fluorescence, or scintillation,

Table 2.2: General properties of the radioactive compounds used in this investigation

Compound	Abbreviation	Specific activity (Bq $mmol^{-1}$)	^{14}C labelling	Average rmm (g mol^{-1})	Compound purity on purchase (%)	Compound purity after twelve months (%)	Radio-chemical purity before experiment (%)	Radio-chemical purity after experiment (%)
2,2',5,5'-Tetrachlorobiphenyl	2,2',5,5'-TCB	$4.9x10^8$	UL	292.0	≥ 98	≥ 99	≥ 98	≥ 98
Bis(2-ethylhexyl)phthalate	DEHP	$3.9x10^8$	UL	390.6	≥ 98	≥ 95	≥ 95	≥ 95
Benzo[a]pyrene	BaP	$9.8x10^8$	7	252.3	≥ 98	na	100	100

where na is not analysed and UL is uniformly labelled.

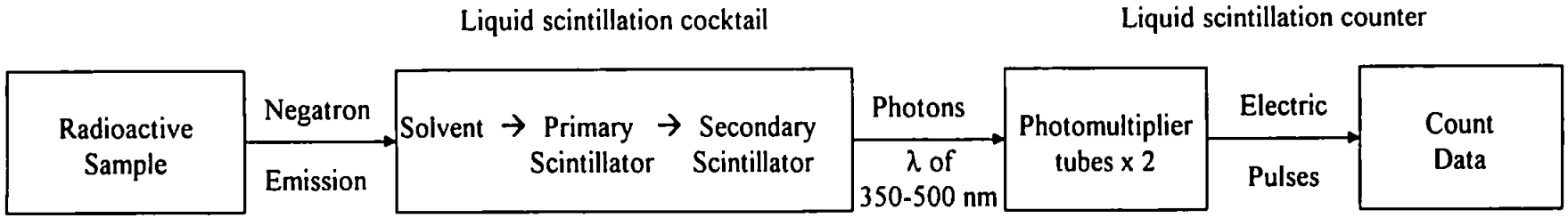

Figure 2.2: Transfer of energy from radioactive sample to liquid scintillation counter.

is then detected and quantified by the two photomultiplier tubes of the scintillation counter. Although the organic solvent of the liquid scintillation cocktail fluoresces when bombarded with radioactivity, it does so at a wavelength which is not efficiently detected by the photomultiplier tubes. Hence, the presence of primary and secondary scintillators dissolved in the organic solvent of the liquid scintillation cocktail, which in turn accept the energy from the solvent and fluoresce at longer wavelength (350-500 nm), which means the energy can be detected more efficiently. If both photomultiplier tubes are activated by one photon burst (coincidence count resolving time $\leq$ 20 nanoseconds) then one radioactive event is registered and converted into a measurable electrical pulse. All non-coincident events are presumed to be background noise and ignored by the instrument. The electric pulse is directly proportional to the energy of the original radioactive event absorbed by the scintillation cocktail. The electric pulses from the photomultiplier tubes are then analyzed and converted, via complex electronic circuitry, to a final determination of the rate (or count) of radioactive decay in the sample. This energy transfer from radioactive sample to liquid scintillation counter is summarised in Figure 2.2.

2.6.1. Advantages and limitations of liquid scintillation counting

The main advantages of LSC over other available methods for the detection and quantification of radioactive decay include: (i) higher count rates due to the rapidity of fluorescence decay (10^{-9} s); (ii) higher counting efficiencies (> 50%) for the low energy *β-ve* emitters; (iii) simple sample preparation; and (iv) the ability to count separately different isotopes in the same sample, *i.e.* dual labelling (Goulding, 1986). The major disadvantages of LSC are listed below.

2.6.1.1. Self-absorption

Self-absorption is the inability of LSC to efficiently count the radioactive decay in solid samples, such as particles and membrane filters. Radioactivity from a solid sample surface must traverse the air between the sample and vial, then between the vial and the photomultiplier tube. It is found that negatrons emitted beyond a certain minimum distance are completely absorbed and therefore never reach the counter. This is particularly a problem with low energy *β-ve* emitters such as ^{14}C. If homogeneity of the

sample is not possible then particulate samples must be digested or otherwise solubilised prior to counting (Goulding, 1986).

2.6.1.2. Quenching

Quenching occurs when the energy transfer process from radiotracer to photomultiplier tube (Section 2.6.) suffers interference, reducing the light output, therefore, decreasing the counting efficiency of the scintillation counter.

1. Chemical quenching is caused by chemicals in the sample which interfere with the energy transfer from the solvent to the primary scintillator or from the primary scintillator to the secondary scintillator of the scintillation cocktail. Such chemicals include organic halides, sulphur compounds, and oxygen compounds.
2. Colour quenching occurs if a sample is coloured. Coloured samples diminish the mean path of fluorescence photons from the vial to the photomultiplier by absorbing some of the light emitted within the scintillation cocktail.
3. Photon quenching occurs when the sample and scintillation cocktail are immiscible, resulting in a heterogeneous counting mixture. Under such conditions, the maximum interaction between the negatron and scintillation cocktail is not achieved, causing a type of self-absorption effect, resulting in variable and highly inaccurate data from the counting process. Sample conditions giving rise to photon quenching are high salt concentration and extreme pH.
4. Similar to photon quenching, optical quenching occurs if dirty scintillation vials are used. These will absorb some of the light being emitted before it reaches the photomultiplier.

2.6.1.3. Luminescence

Chemiluminescence and/or bioluminescence occurs when a chemical or biochemical reaction within the sample matrix stimulates the emission of light unrelated to excitation of the scintillation cocktail by radioactivity leading to an overestimation of the true count. Sample conditions giving rise to chemiluminescence include a high pH, the presence of oxygen, plant extracts containing chlorophyll, and contaminated scintillation cocktails.

Similarly, phospholuminescence results from the sample matrix and/or the sample vial itself, absorbing UV light and re-emitting it. Pigmented samples, and samples and/or sample vials and caps activated by the UV component of sunlight, strip-lighting, or sterilisation lamps, are most likely to phosphoresce.

2.6.2. Instrumentation

Over the experimental period two different scintillation counters were used: a Philips PW4700 Liquid Scintillator Counter, from October 1994-December 1995, and a Beckman LS6500 Multi-purpose Scintillation Counter, from January 1996-September 1997.

The liquid scintillation cocktail used throughout this investigation was Ultima Gold LSC-Cocktail (Packard Canberra), containing the solvent alkylnaphthalene, the primary scintillator, 2,5-diphenyloxazole (PPO), and the secondary scintillator, p-bis-(σ-methylstyryl)benzene (bis-MSB).

2.6.3. Determination of absolute counts

Variation in the number of recorded counts can occur due to the randomness of the radioactive decay process and not from any variation within the scintillation counter itself. This possible source of variation in the results is eliminated by counting to a preset counting precision. Both instruments were, therefore, set to a counting precision of 1% or 40000 counts per minute (CPM). This established a 95% confidence level for the count (the 2 sigma statistical value). If counts were low a 20 minutes maximum counting period was used, but a lower counting precision was achieved.

Variable data can also occur due to the quenching of individual samples (Section 2.6.1.2). Chemical and colour quenching are quenchable. That is, by determining the counting efficiency of each sample, using an appropriate quench correction (or standardisation) method, the relative sample activity (CPM) can be converted to an absolute sample activity in disintegrations per minute (DPM) by:

$$DPM = \left(\frac{CPM - BKG}{E} \right) \qquad (2.1)$$

where CPM is the counts per minute in the appropriate channel, BKG is the background count (derived from such sources as cosmic radiation, natural radioactivity in the vicinity, nearby x-ray generators, and circuit noise) in CPM for the channel, and E is the counting efficiency calculated from quench correction (Section 2.6.4).

2.6.4. Quench correction

Count calibration involves the construction of quench curves relating the counting efficiency to the amount of quenching in an unknown sample. Methods of quench correction include sample channels ratio, external standard channels ratio and automatic quench correction. The different quench correction methods used for the individual scintillation counters are discussed in Sections 2.6.4.1 and 2.6.4.2.

2.6.4.1. Quench correction for the Philips PW4700 Liquid Scintillator Counter

Chemical quenching in the sample causes a change in the observed pulse-height of the β energy spectrum, as does the addition of a quenching agent to a sample. This spectral shift is dependent upon the concentration of quenching agent used, enabling a quench correction curve to be established by counting a series of samples containing a known constant amount of radioactivity but varying concentration of quencher. If two channels of the analyser are adjusted to monitor different parts of the spectrum simultaneously, then the ratio of the counts in the channels can be used as an index for the observed sample counting efficiency. This forms the basis of two quench correction methods, sample channels ratio (SCR) and external standard channels ratio (ESR). The channels ratio method has both a longer counting time and tends to be less accurate at low sample count rates than ESR. Due to low activity of the samples the preferred method of quench correction was ESR.

In ESR a gamma (γ) emitting external standard, built into the scintillation counter, is automatically brought up close to the counting vial. The γ rays produce Compton electrons, which form a spectrum similar to that of *β-ve* particles (Figure 2.3.). This spectrum is counted in two factory set channels by the scintillation counter. The sample and external standard counts are collected by the scintillation counter for 30 seconds and stored positively. Then the sample is counted alone in the external standard

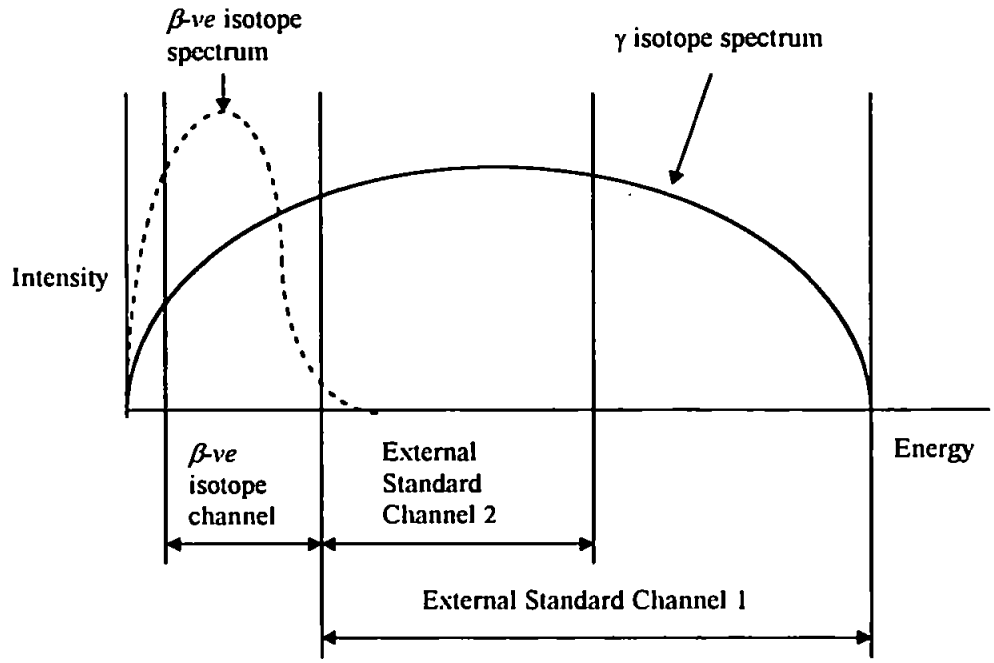

Figure 2.3: Quench correction channel settings for external standard channels ratio (adapted from Philips Operating Manual, undated).

channels for a further 30 seconds and the counts stored negatively. The ESR is then calculated from the ratio of the count rates:

$$ESR = \left[\frac{(\text{external standard and isotope counts in CH2}) - \text{isotope counts in CH2}}{(\text{external standard and isotope counts in CH1}) - \text{isotope counts in CH1}}\right] \times 2 \qquad (2.2)$$

where CH1 and CH2 are the external standard channels 1 and 2 respectively. The multiplication by 2 results in an ESR between 1 (minimum quenching) and 2 (maximum quenching). The ESR measurement precedes the sample measurement, and requires a total counting time of 1 minute, irrespective of the pre-set precision counting time (Philips Operating Manual, undated).

Quench correction curves were, therefore, established for the Philips PW4700 Liquid Scintillator Counter, as follows. A series of samples consisting of 10 mL scintillation cocktail, 2 mL sample matrix, and a 25 µL (925 Bq) spike of ^{14}C radioisotope, were prepared in glass scintillation vials and counted. The samples were then removed from the counter and any samples giving rise to 'rogue' counts (due to the

randomness of the radioactive decay) were disregarded. To the remaining samples increasing volumes of CCl_4, a quenching agent, were added (volumes: 0, 25, 50, 75, 100, 150, 200, 300, 350, 400 µL). The samples were then recounted. The counting efficiency and external standard ratio varies with the quantity of CCl_4 added. A quench correction curve is plotted and used to determine the counting efficiency of experimental samples. As the calibration curve can be specific to the type of isotope, scintillation cocktail, and sample matrix used in its preparation, individual quench correction curves were prepared for each isotope and sample matrix used. However, little, or no variation between these quench correction curves was noticeable and examples from the data set are shown in Figure 2.4. The external channel ratio for each experimental sample is determined by the counter enabling the counting efficiency to be read from the graph, from which the absolute count of the sample can then be calculated (Equation 2.1).

2.6.4.2. Quench correction for the Beckman LS6500 Multi-purpose Scintillation Counter

The Beckman LS6500 Multi-purpose Scintillation Counter has an Auto DPM mode. This mode allows the counter to automatically correct raw sample counts for quenching and convert them into absolute counts without the need for the operator to construct a quench correction curve (Beckman Operating Manual, 1993). The instrument determines the extent of quench in each sample and then using a factory installed quench correction curve, stored in the instrument's library, automatically corrects for counting efficiency and calculates the sample's absolute count in DPM. The counting precision for Auto DPM calibration is set at 1%. Stored quench curves were checked and calibrated by trained Beckman technicians during installation of the instrument and thereafter at six monthly intervals.

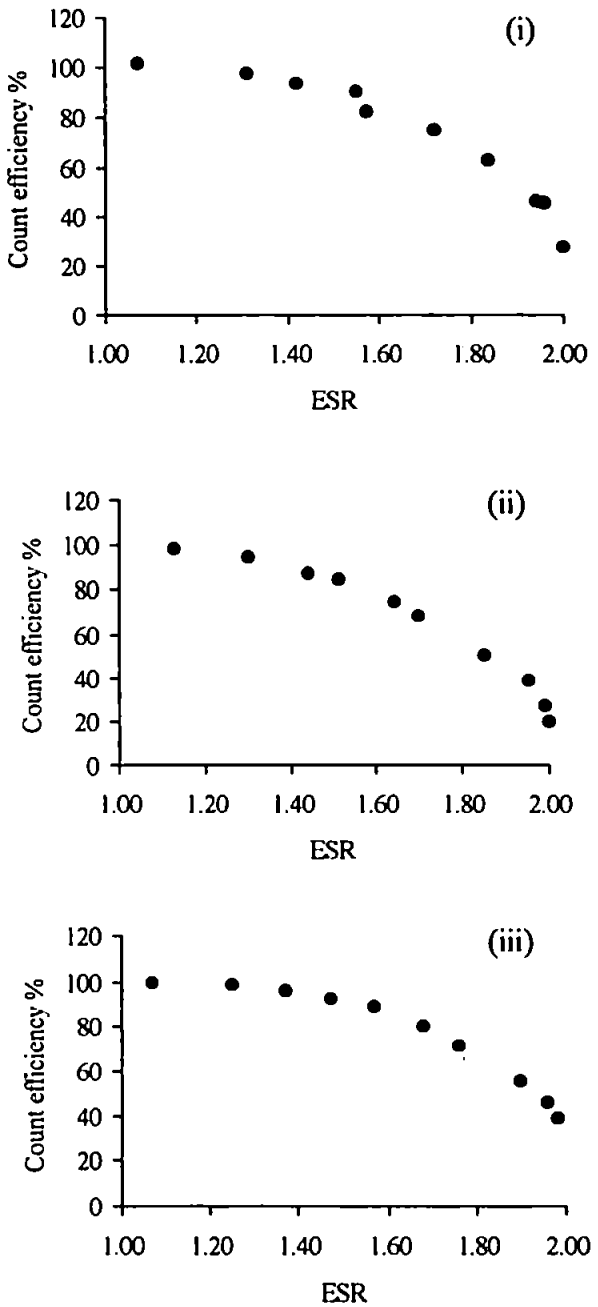

Figure 2.4: Quench correction curves for 2,2',5,5'-TCB in three different matrices: (i) river water, (ii) sea water, and (iii) *n*-hexane, where ESR is the external standard channel ratio.

2.6.5. Minimisation of unquenchable interferences

Although chemical and colour quenching can be quantified, other forms of count interference (Sections 2.6.1.1-2.6.1.3) are unquenchable, *i.e.* accurate quench monitoring is not possible. Therefore, it is imperative that such interferences are assessed and where possible removed, to avoid variability in the results of repeat counts and different samples.

2.6.5.1. Photon quenching

Preparation of sea water samples resulted in a two phase mixture that was prone to separation during long periods of sample counting. This was cause for concern as variable and inaccurate sample counts were possible due to photon quenching (Section 2.6.1.2). Ways of eliminating this phase separation problem, caused by the high salinity of the sea water samples, included using less sample, more cocktail, or switching to a cocktail with better sample holding characteristics. Ultima Gold LSC-Cocktail is designed for use with aquatic samples, therefore the volume ratio of sea water sample to cocktail was investigated. The counting efficiency of the sample was determined by increasing the quantity of filtered sea water (0.1, 0.2, 0.4, 0.7, and 1.0 mL) added to 4 mL of spiked cocktail containing a known amount of radioactive isotope. The sample became cloudy when ≥ 0.7 mL of sea water was added, but did not settle until after 24 hours (counting was usually carried out overnight over a maximum period of 16 hours). The counting efficiency for samples containing up to 1 mL was found to be ~100% (Figure 2.5.), and therefore photon quenching was not considered a problem up to this volume.

2.6.5.2. Optical quenching

Dirty scintillation counting vials giving rise to optical quenching (Section 2.7.1.2.) was considered a possible source of erratic counts in the Philips PW4700 Liquid Scintillator Counter, where recycled glass scintillation vials were used for sample counting. A stringent and rigorous vial cleaning procedure was therefore followed, which entailed: (i) *n*-hexane rinse, (ii) soak in decontaminating solvent (Decon® 90) for 24 hours, (iii) rinse with Milli-Q water, (iv) soak in Milli-Q water for 24 hours, (v) rinse with Milli-Q water several times followed by (vi) air-drying in a warming cabinet. Acid-cleaning of

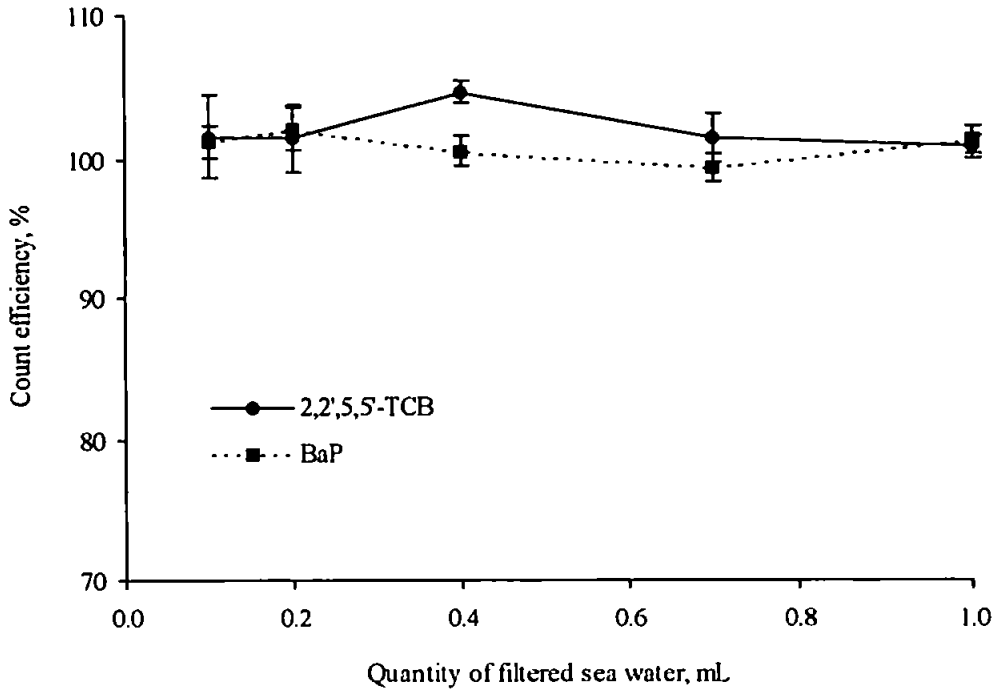

Figure 2.5: Determination of the effect of photon quenching caused by increasing the quantity of sea water sample added to 4 mL of liquid scintillation cocktail, where the mean value and standard deviations are shown (n=4).

the glass vials was avoided as this modifies the glass surface, greatly increasing the chance of sample contamination by adsorption. To ensure that the outside of the glass vials remained clean during handling, plastic gloves were worn during sample preparation. The use of disposable plastic vials in the Beckman LS6500 Multi-purpose Scintillation Counter eliminated the chances of optical quenching in this instrument.

2.6.5.3. Luminescence

Major interferences from chemiluminescence can be overcome by refrigeration of the sample to 4°C, removal of the offending chemical, acceleration of the reaction to completion by heating, or the storage of samples for a period of time before counting allowing any chemiluminescence to decay (Goulding, 1986). Phospholuminescence can similarly be reduced by a period of 'dark-adaptation' (*i.e.* storage in the absence of light), usually longer than an hour, before the sample is counted.

The proportion of the total count rate caused by luminescence, as opposed to actual radioactive disintegrations was assessed (as a percentage) for all samples by the Lum-Ex correction facility of the scintillation counter. If the Lum-Ex value of a given sample was 5-10% or greater, then luminescence was seen to be a problem and the appropriate steps were taken to eliminate the problem. A period of 'dark-adaptation' for one hour (followed by recounting) was found to be sufficient to reduce any luminescence occurring in the samples.

Part of the practical work of this project involved the use of irradiated sea water, *i.e.* sea water exposed to a UV lamp, a possible source of phospholuminescence. After irradiation for three hours the sea water was placed in the dark for 24 hours at 4°C before counting. Spiked samples had a counting efficiency of ~100% and an acceptable Lum-Ex value. Background counts, however, were found to have increased 25% compared to the background count of non-irradiated sea water, returning to a comparable level after six days of 'dark-adaptation' (Figure 2.6.). Irradiated sea water was therefore not deemed suitable for experimental work until after a period of seven days 'dark-adaptation'.

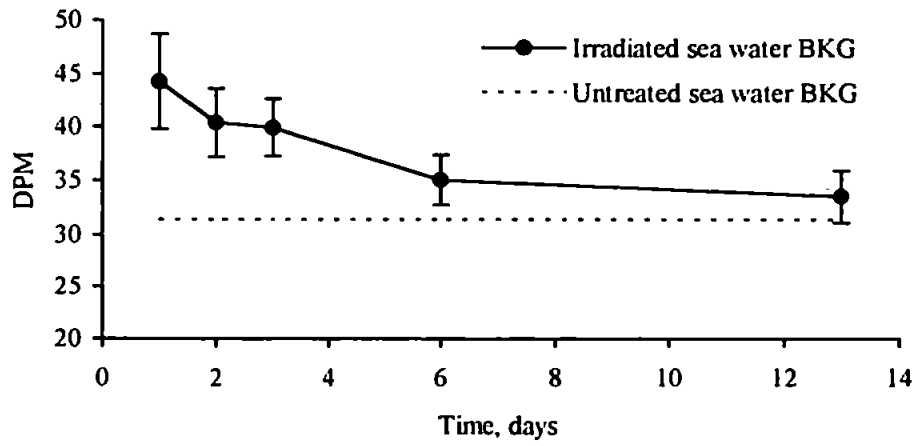

Figure 2.6: Effect of phospholuminescence on irradiated sea water background counts, where BKG is the background count, and DPM is the activity in disintegrations per minute. The mean value and standard deviations are shown (n=4).

2.7. Experimental Procedure

2.7.1. Laboratory safety

Compound toxicity coupled with their radioactivity called for extreme caution and the highest level of laboratory safety during their handling. Levels of radioactivity were kept to a minimum in the main marine chemistry laboratory during experiments. All stock solutions were stored in the designated refrigerator of the University's storage facility for radioactive compounds, and only the diluted compound (Section 2.5.2.) was kept in the laboratory. Radioactive waste was disposed of as soon as possible. All experimental work was carried out on a tray, in a fume cupboard, or on a designated work bench area which was clearly labelled using 'radioactive hazard tape'. An 'organic-fume' mask, protective clothing and plastic gloves were worn at all times.

2.7.2. Solubility and particle-water interaction experiments

To determine the relative solubility and particle-water partitioning of HOMs an experimental procedure was devised that:

1. eliminates the carrier solvent during the introduction of the HOM to an aqueous sample;
2. minimises adsorption of the HOM onto glassware during phase separation;
3. avoids radio-counting particles directly (which would result in inconsistent counts due to self-absorption); and
4. could be performed routinely in order to investigate different environmental effects.

These criteria were addressed by developing the following method (see: Lotse *et al.*, 1968; Zhou *et al.*, 1995; Turner & Tyler, 1997). A summary of this experimental procedure is shown in Figure 2.7.

To prevent the formation of an emulsion between the carrier solvent (*n*-hexane), holding the radiotracer, and the aqueous phase, the carrier solvent had to be removed before the addition of the sample. Using a *n*-hexane-rinsed glass microsyringe, a 25 µL (925 Bq) spike of the ^{14}C-labelled HOM was placed onto the side of a clean 30 mL glass centrifuge tube, and the carrier solvent removed by evaporation under a laminar flow hood. This was followed by the introduction to the glass centrifuge tube of 20 mL

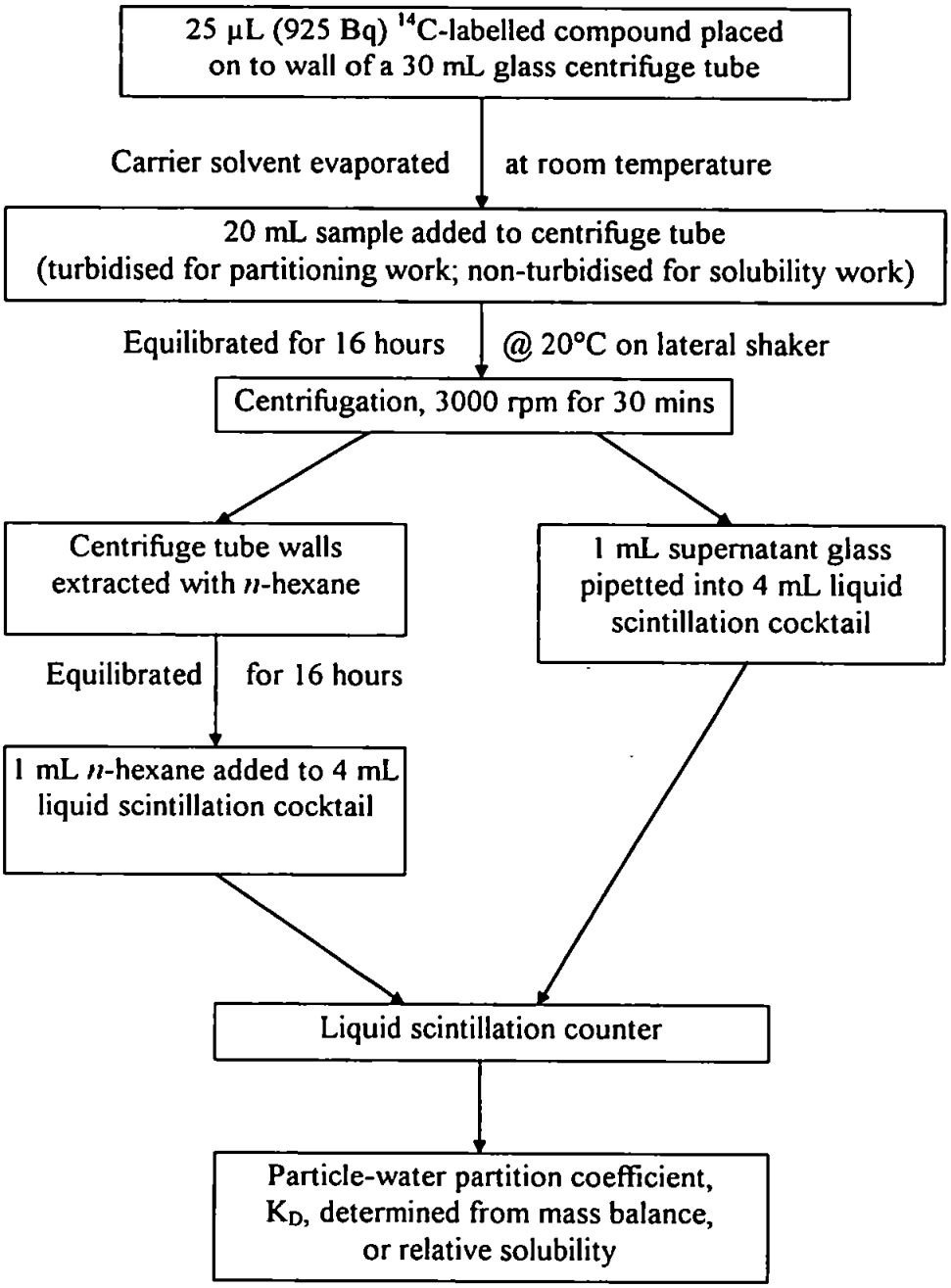

Figure 2.7: Summary of experimental procedure used to determine the relative solubility and particle-water partition coefficient of HOMs in estuarine waters.

of filtered (for relative solubility work) or turbidised (for particle-water interaction work) river or sea water. Preparation of the turbidised water samples is described in detail in Section 2.7.3.

The centrifuge tubes were then sealed, using clean ground-glass stoppers, wrapped in aluminium foil and allowed to equilibrate for 16 hours at 20°C under constant agitation on a lateral shaker.

Due to the hydrophobic nature of the compounds, contact with the large surface area of a filtration unit had to be avoided during phase separation. The solid and solution phases were therefore separated by centrifuging at 3000 rpm for 30 minutes. After centrifugation the activity of HOM in the dissolved phase was determined by glass-pipetting 1 mL of supernatant into 4 mL of Ultima Gold-LSC cocktail, ensuring that the particles at the bottom of the centrifuge tube were not disturbed. The remaining contents of the centrifuge tube were then discarded, and the residual HOM adsorbed to the centrifuge tube walls extracted using 4 mL *n*-hexane; here, the tubes are extracted for 16 hours, in the dark, at a constant temperature of 20°C under continuous agitation, and a 1 mL aliquot of the extract was then glass-pipetted into 4 mL of Ultima Gold-LSC cocktail. All experiments were undertaken in quadruplicate to determine the repeatability of the method. The relative standard deviations of the results were generally below 10% and are discussed further in Section 2.7.5.

2.7.3. Preparation of sediment slurries

Sediment preparation for the particle-water partitioning work entailed passing the sediment through a nylon mesh of 63 μm pore diameter under slight agitation with river water. This fraction (< 63 μm) of estuarine sediment represents the resuspendable particle population. The slurry of < 63 μm sediment particles in river water was collected in a clean glass jar. This stock slurry (having a particle concentration of ~15-150 g L^{-1}) was then diluted with filtered river water (Section 2.3.1.) to obtain a series of slurries whose particle concentrations are given in Table 2.3. These sediment slurries were stored at 4°C in the dark with occasional agitation, and regularly calibrated for sediment concentration by subsample filtration. When required, between 0.2 and 1.0 mL of these sediment slurries were added to filtered river or sea water to obtain a final volume of 20 mL, and a suspended particulate matter (SPM) concentration in the range 10 - 1000 mg L^{-1}. These conditions were employed for the radiotracer experiments.

Table 2.3: Concentration of suspended particulate matter [SPM] in sediment slurries and 20 mL samples used in radiotracer experiments.

Estuary	Sediment slurry [SPM] (g L^{-1})	Volume of slurry (mL)	Resulting [SPM] in 20 mL (mg L^{-1})
Chupa	1.69	1.00	85
	1.69	0.75	62
	1.69	0.50	46
	1.69	0.25	28
Dart	19.1	1.00	958
	24.0	0.50	601
	4.80	0.50	120
	0.96	1.00	48
	0.21	1.00	10
Plym	19.7	1.00	985
	19.7	0.50	493
	3.28	1.00	164
	1.16	1.00	58
	1.16	0.20	12
Beaulieu	20.3	1.00	1015
	20.3	0.50	508
	3.25	1.00	163
	1.18	1.00	59
	1.18	0.20	12
Carnon	19.7	1.00	983
	19.7	0.50	492
	3.28	1.00	164
	1.15	1.00	58
	1.15	0.20	12

2.7.4. Partitioning and relative solubility calculations

As the particulate phase could not be counted directly due to self-absorption (*i.e.* the inability of liquid scintillation counters to efficiently count the radioactive decay in solid samples; see Section 2.6.1.1.), a mass balance approach was used to derive the particle-water partition coefficient, K_D (mL g^{-1}), for the HOMs as follows:

$$K_D = \frac{P}{C} \qquad (2.3)$$

$$K_D = \left[\frac{\left(A_o - \left(A_c + A_w\right)\right)}{A_c}\right] \cdot \left[\frac{V}{m}\right] \qquad (2.4)$$

where P is the compound concentration in the particulate phase (w/w), C is the compound concentration in the dissolved phase (w/v), A_o is the activity of the original spike, A_c is the activity in the aqueous phase, A_w is the activity adsorbed onto the walls of the centrifuge tube, V is the volume of the water aliquot (mL), and m is the mass of particles (g) in the suspension.

The relative solubility of the HOMs was determined from the aqueous activity, A_c, as follows:

$$S_r = \left[\frac{A_c}{\text{Spec. Act.}}\right] . \text{rmm} \qquad (2.5)$$

where S_r is the relative solubility of the HOM (g L^{-1}), *i.e.* relative to the amount of compound added and dependent upon the sample type and temperature (20°C), A_c is the aqueous activity (Bq mL^{-1}), Spec. Act. is the specific activity of the ^{14}C-labelled HOM (Bq $mmol^{-1}$), and rmm is the relative molecular mass of the HOM (g mol^{-1}).

2.7.5. Data acceptance criteria

Determination of the absolute count (Section 2.6.3.) requires the use of a background count, BKG. A BKG was determined for all the matrices used during the investigation by counting 1 mL of the matrix in 4 mL of LSC-cocktail. As with all stages of the experimental procedure this was carried out in quadruplicate. If the relative standard deviation (RSD) was below 10% then the average BKG value was used. This was generally the case. However, if the RSD was over 10% then one of the four values was discarded to decrease the RSD value (the random nature of negatron emission causes occasional erratic counts). The limit of detection, LOD, was calculated from the sample mean, $\bar{x}$, and standard deviation, s_{n-1}, of the BKG as follows:

$$LOD = \bar{x} + (3\ s_{n-1}) \qquad (2.6)$$

The matrix BKG and LOD were determined prior to each experiment, and varied between experiments by up to 10 CPM. A small selection are shown in Table 2.4.

All relative solubility and particle-water partitioning experiments were carried out in quadruplicate and the resultant data were treated according to the same criteria laid out above, with any counts below the limit of detection being ignored. The RSDs for both 2,2',5,5'-TCB and BaP counts were on the whole below 10%. However DEHP counts were more variable and even the removal of an erratic count generally resulted in a RSD within the range 5-40% and on occasion over 50%.

As both relative solubility and K_D (calculated from mass balance) were calculated using numerous independent measurements, the data were prone to a culmination of error, or error propagation, over the various stages of the experimental procedure. The propagation of error, SD (Caulcutt & Boddy, 1983; outlined in Appendix B), was calculated for all mass balance calculations, and shown as error bars on the appropriate graphs.

Table 2.4: Background counts and limits of detection for experimental counts in various matrices

Matrix	BKG (CPM)	S_{n-1} (CPM)	LOD (CPM)	RSD (%)
Milli-Q	20	1.1	23	5.52
River Plym	31	2.4	38	7.72
Sea water	36	2.4	44	6.78
***n*-hexane**	33	1.9	38	5.86

where BKG is the mean background activity, n=4, in counts per minute (CPM), S_{n-1} is the standard deviation, LOD is the limit of detection and RSD is the relative standard deviation of the background count.

2.7.6. Evaluation of experimental procedure

An accurate measure of K_D is critically dependent on the recovery of the activity of the original compound added. However, preliminary experiments using an aqueous sample containing no particles showed that complete recovery of 2,2',5,5'-TCB was not achieved (mean recovery = 69.5±5.3% [n=6]). Ways of improving HOM recovery were therefore investigated. An exhaustive re-evaluation and development of the original experimental procedure was pursued over an initial eight month period and is described in detail below. All method evaluation data generated are summarised in Appendix B1. The improvement in HOM recovery was paramount to the success of this experimental procedure.

2.7.6.1. Volatilisation of ^{14}C-labelled compounds

Evaporation of the carrier solvent was a possible source of compound loss, via volatilisation. This was investigated by determining the percentage of radiotracer recovered following solvent evaporation over a range of time periods. A series of glass scintillation vials were spiked with a known amount of HOM, followed by carrier solvent evaporation at time intervals up to 30 minutes, before the addition of 4 mL of Ultima Gold-LSC cocktail and counting of the sample. This was repeated for all three HOMs and the results are shown in Figure 2.8. Compound loss due to volatilisation is clearly noticeable after 20 minutes for both 2,2',5,5'-TCB and DEHP, and after only 5 minutes for BaP. Loss of these compounds, via volatilisation, could therefore be minimised by ensuring that an aqueous sample had been introduced to the glass centrifuge tube within these time restraints

2.7.6.2. Solvent rinse of glass pipette

Radiotracer loss due to adsorption of the HOM on to the walls of the glass pipette during transfer of the aqueous aliquot from the centrifuge tube to the LSC-cocktail was assessed. Any of the radiotracer adhering to the glass pipette wall was accounted for by immediately rinsing the pipette with 1 mL of hexane, which was pipetted into 4 mL of LSC-cocktail. The activity in the aqueous phase, A_c (in Equation 2.5), was therefore equal to the sum of the aqueous aliquot and pipette rinse counts. The importance of the

pipette rinse is clearly illustrated in Table 2.5., accounting for up to 3.5% of the original count for 2,2',5,5'-TCB.

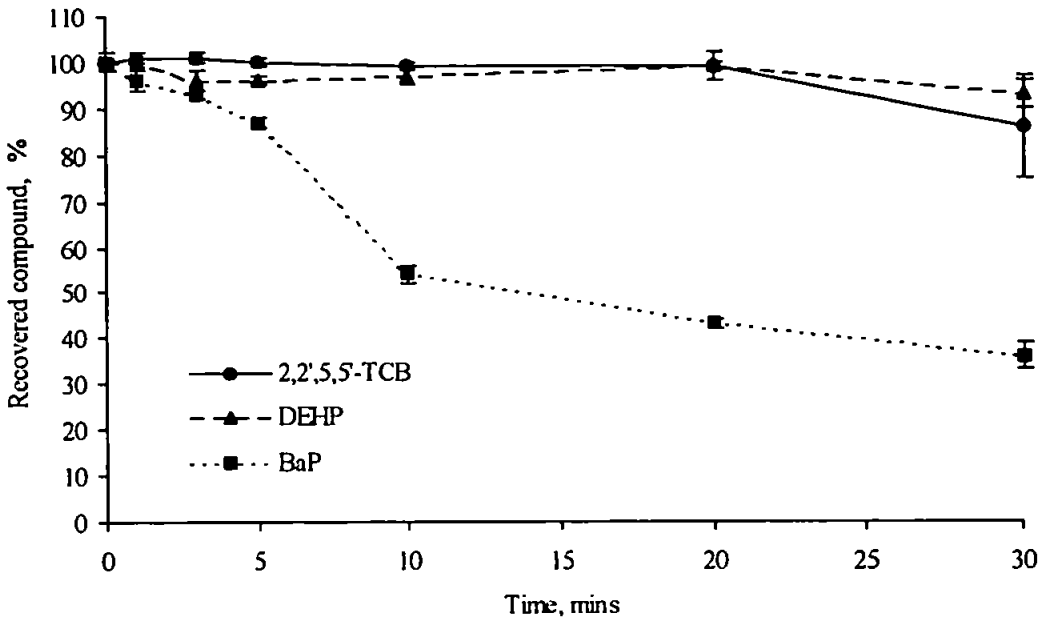

Figure 2.8: Loss of radiotracer, via volatilisation, during evaporation of the carrier solvent, where the mean value and standard deviations are shown (n=4).

Table 2.5: Percentage recovery from Milli-Q water of the original HOM activity for the four procedural stages of activity determination

^{14}C-labelled compound	% Recovery, $\bar{x}\pm s_{n-1}$				% HOM recovered $\bar{x}\pm$SD
	A_c		A_w		
	Aqueous phase	Pipette rinse	First wall extraction	Second wall extraction	
2,2',5,5'-TCB	61±7	3.5±0.9	12±3	1.7±1.5	79±8
DEHP	18±5	0.7±0.5	56±10	6.4±4.5	81±11
BaP	18±2	0.3±0.5	59±4	13±2	89±5

where $\bar{x}$ is the sample mean, s_{n-1} is the sample standard deviation, SD is the propagation of error and n=4.

2.7.6.3. Solvent rinse of glass centrifuge tubes

The efficiency of the extraction of the HOM adhered to the glass centrifuge tube walls was re-evaluated by (i) varying both the volume of solvent and solvent type used, and (ii) repeat solvent extractions.

(i) 2,2',5,5'-TCB, was used during the investigation into the effect of solvent volume (4-12 mL) and solvent type (*n*-hexane versus dichloromethane, DCM) on the extraction of HOM adhered to the glass centrifuge tube walls. Figure 2.9. shows that within analytical uncertainties, compound recovery was largely independent of both solvent volume and solvent type. *n*-hexane was chosen for subsequent investigations, using 10 mL for centrifuge tube wall extraction in relative solubility work and 6 mL in all particle-water partitioning work.

(ii) Repeating the extraction of HOM adsorbed on to the glass centrifuge tube walls resulted in a 12.8% improvement in total recovery for BaP. Improvements in recovery were also noted for the other two HOMs and are shown in Table 2.4. Therefore, A_w (in Equation 2.5) was equal to the sum of the activity of the two glass wall extractions.

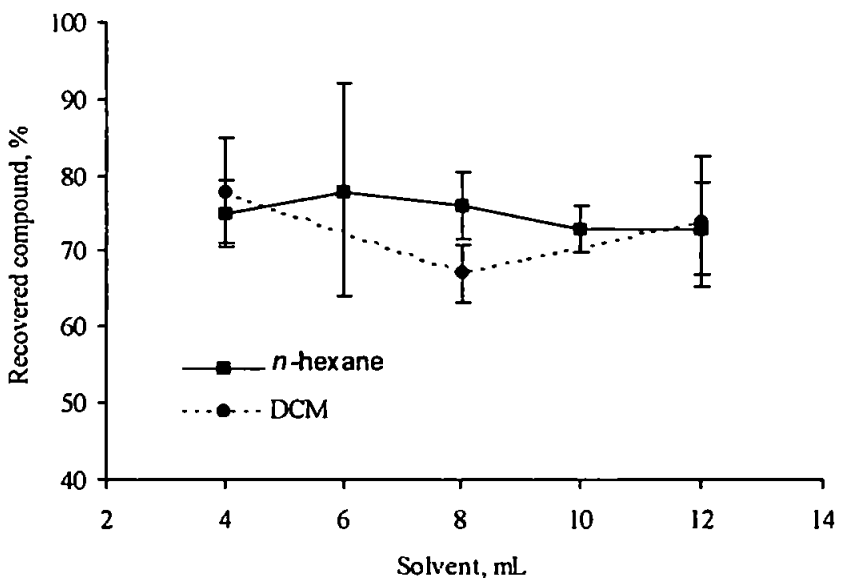

Figure 2.9: Recovery of 2,2',5,5'-TCB as a function of solvent volume and solvent type, where DCM is dichloromethane and the mean values and propagated errors are shown (n=4).

2.7.6.4. HOM activity

Varying the HOM activity, and hence mass, of the initial spike had little effect on the recovery of 2,2',5,5'-TCB (Figure 2.10.). However, recovery improved for DEHP as the spike activity increased. The reverse was true in the case of BaP, with recovery decreasing and becoming more variable as the initial spike activity increased. The 25 µL spike with an activity of 925 Bq, or 55000 DPM, gave similar recovery rates for all three radiotracers and was retained as the standard spike activity.

2.7.6.5. Irreversible adsorption

Despite an overall improvement in the HOM recovery, complete recovery was not achieved. This appears to be a common problem with such compounds studied in the laboratory (Maaret *et al.*, 1992; Zhou *et al.*, 1995). It is suspected that unrecovered HOM is irreversibly adhered on to the glassware. It is possible that the ageing of centrifuge tubes may increase the surface area of their walls, increasing the likelihood of irreversible HOM adsorption. Similar investigations have shown an increase in constituent loss by ageing of glass and plastics (Muller *et al.*, 1991). However, comparison of HOM recovery using new and aged (total extraction period > 1000 hours) glass centrifuge tubes, Table 2.6., showed no significant statistical difference in HOM recovery.

If the loss of HOM is due to irreversible adsorption on to the glass centrifuge tube walls then cross contamination between experiments was possible, if the centrifuge tube cleaning process is inadequate. The cleaning process was identical to that used for the glass vials described in Section 2.6.5.2. Procedural blanks, *i.e.* clean unspiked centrifuge tubes, *n*-hexane extracted and counted, showed that further leaching of ^{14}C from the glass walls was not significant as activity counts were below the limit of detection.

Optimum HOM recoveries are summarised in Table 2.6. for the various water matrices. Recovery was slightly lower when sea water was used, possibly due to the 'salting out effect' of saline solutions on HOMs (Means, 1995).

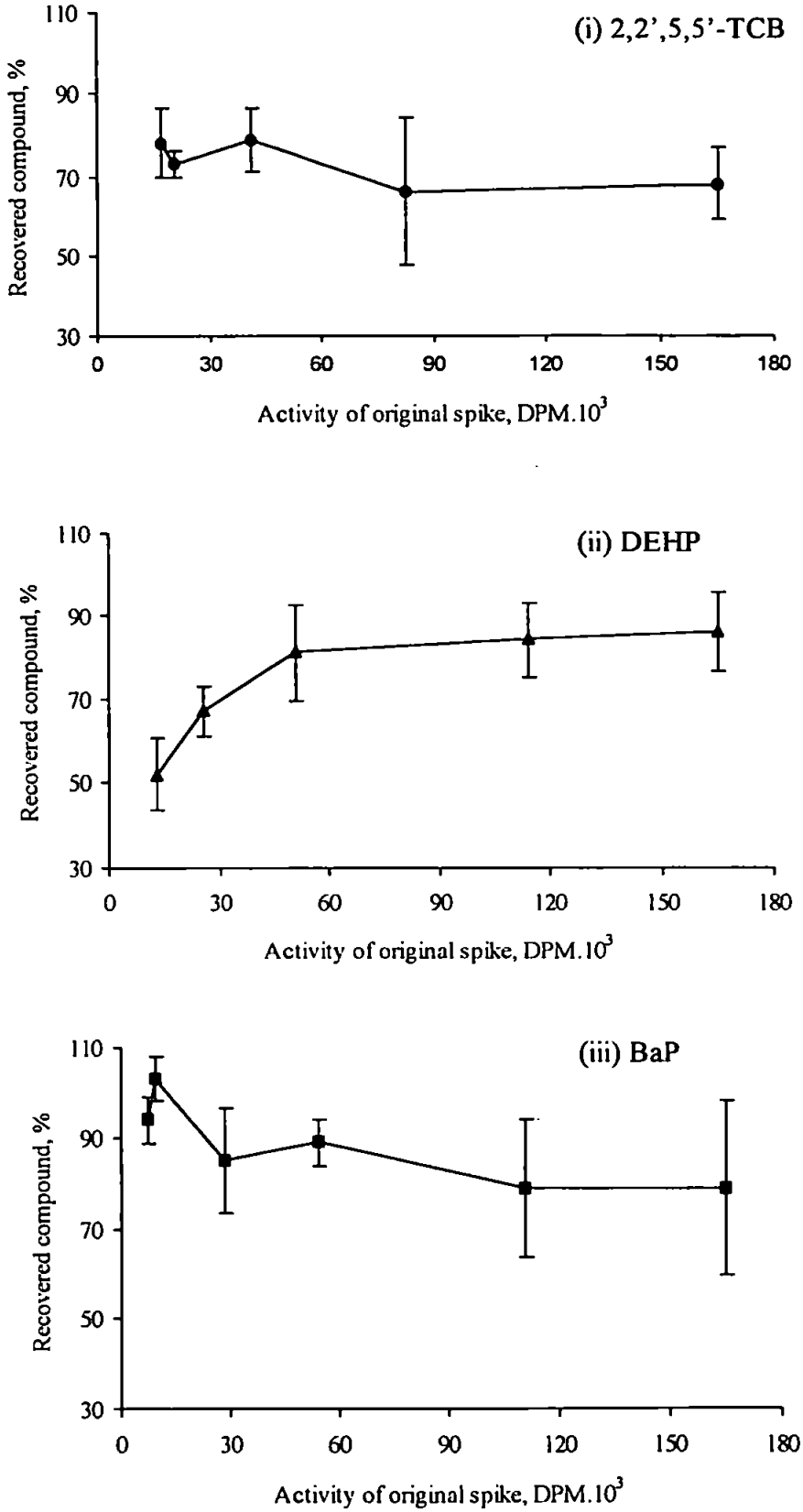

Figure 2.10: Recovery of the ^{14}C-labelled HOM as a function of original activity for: (i) 2,2',5;5'-TCB, (ii) DEHP, and (iii) BaP, where the mean values and propagated errors are shown (n=4).

Table 2.6: Recovery of original HOM activity in various water matrices

Water matrix	%	2,2',5,5'-TCB	DEHP	BaP
Milli-Q				
a. Old tubes	$\bar{x}$ ± SD	79±8	81±12	89±5
	R	71-85	80-83	87-92
b. New tubes	$\bar{x}$ ± SD	83±13	93±17	94±10
	R	78-89	78-99	89-100
River Plym	$\bar{x}$ ± SD	80±2	68±5	94±10
	R	77-84	61-72	89-96
Sea water	$\bar{x}$ ± SD	76±5	74±7	79±4
	R	71-81	70-78	73-82

where $\bar{x}$ is the sample mean, SD is the propagation of error, and R is the range (n=4).

2.7.7. Summary of experimental procedure development

Loss of HOM was reduced to ~ 20% for both 2,2',5,5'-TCB and DEHP, and ~ 10% for BaP, of the original spike activity. This was achieved after the introduction of various changes to the original experimental procedure used. In summary, these changes were:

1. the introduction of the glass pipette *n*-hexane rinse after transfer of the aqueous aliquot to the LSC-cocktail;
2. an increase in the volume of *n*-hexane used in the glass centrifuge tube wall extractions, 10 mL for relative solubility work and 6 mL for particle-water partitioning work;
3. a repeat *n*-hexane extraction of the glass centrifuge tube walls.

These changes to the experimental procedure were used in all subsequent investigations. Therefore, Equations 2.4 and 2.5, used for K_D and relative solubility calculations, respectively, became:

$$K_D = \left[\frac{\left(A_o - \left[\left(\left(A_c + A_c^{\bullet}\right) + \left(A_w + A_w^{\bullet}\right)\right)\right]\right)}{\left(A_c + A_c^{\bullet}\right)}\right]\left[\frac{V}{m}\right] \qquad (2.7)$$

and:

$$S_r = \left[\frac{\left(A_c + A_c^{\bullet}\right)}{\text{Spec. Act.}}\right] \cdot \text{rmm} \qquad (2.8)$$

where $A_c^{\bullet}$ is the activity of the pipette rinse and $A_w^{\bullet}$ is the activity of the repeated extraction of the walls of the centrifuge tube.

The unrecovered HOM will result in a systematic error of a few percent in K_D determinations. Although it is not possible to determine the loss of compound when particles are present, any loss will result in an overestimation of K_Ds derived by this approach, the significance of which is addressed in Chapter 4.

CHAPTER 3: RELATIVE SOLUBILITY OF HOMS

3.1. Introduction

The particle reactivity, transport, and fate of hydrophobic organic micropollutants (HOMs) are to some extent dependent upon the solubility of the HOM. Therefore, before the estuarine particle-water interactions of the HOMs can be fully understood the change in HOM solubility over the river-sea interface must be investigated. All generated data used in this chapter are summarised in Appendix B2.

3.1.1. Physicochemical characteristics of the water samples

The physicochemical properties of the sea, river, and Milli-Q water samples are shown in Table 3.1. along with the world average values for both high and low alkalinity river waters. The data show the contrasting properties of the estuarine environments chosen. The water samples cover a range of environmental conditions over which both the solubility and the particle-water interaction (see Chapter 4) of HOMs could be investigated.

3.1.2. Experimental strategy

The objectives of this approach were to identify the main physicochemical water properties affecting solubility and investigate these properties in detail. A summary of the experimental strategy employed is shown in Scheme 3.1. Logistically (due to the limited availability of radiotracers, apparatus and time), not all water properties were investigated. Dissolved organic carbon, DOC, and salinity were identified as being the most important physicochemical variables (Hashimoto *et al.*, 1984), and were therefore varied and investigated in artificially controlled laboratory experiments. Experiments were carried out at a constant temperature of 20°C, to correspond with published data. Although important in the seasonal behaviour of HOMs, the effect of temperature on HOM solubility was not investigated in this work, and has previously been investigated (Whitehouse, 1984). Alkalinity and pH are important indicators of any changes in the carbonate equilibrium balance (O'Neill, 1993), and can vary extensively throughout an

estuary (Chester, 1990). However, the effect of pH was not directly investigated in these experiments. Any change in pH is unlikely to have a significant effect on HOMs themselves as they are non-ionic compounds (Schwarzenbach *et al.*, 1993). Although phthalate esters (PEs) contain polar carboxyl groups, they are situated towards the centre of the compound and are thus believed to have negligible effect upon their environmental behaviour (Giam *et al.*, 1984). However, the indirect role of changes in pH, *i.e.* via modification of the physicochemical properties of dissolved organic matter, DOM, and/or estuarine particles (Wijayaratne & Means, 1984) on the solubility and adsorption of HOMs must not be ruled out. The pH of Milli-Q can fall below 7, especially when left standing in the laboratory for longer than a week. Therefore any experiments involving Milli-Q were carried out within this time scale. Similarly, for experiments involving humic acid, the pH was maintained within the extreme values of Milli-Q water and the estuarine water samples.

3.2. Relative Solubility

The relative solubility, S_r, (Equations 2.5. and 2.8.) of the ^{14}C-labelled HOMs can be defined as the activity in the aqueous phase (as a measure of solubility), relative to the total amount, or activity of compound added, the temperature (all experiments were carried out in a constant temperature room at 20±1°C), and the water matrix (*i.e.* function of salinity and DOC).

3.2.1. Relative solubility isotherms

Figures 3.1.-3.5. compare the relative solubilities of the three HOMs in different water types over dissolved compound concentration ranges typically encountered in the estuarine water column (Duinker *et al.*, 1985) and pore waters (Brownawell & Farrington, 1985). Each set of relative solubility isotherms is discussed for individual compounds.

Table 3.1: Physicochemical properties of sea, river and Milli-Q water samples

Sample	Salinity ($x10^{-3}$)	Conductivity (μS)	Chlorinity ($mg\ L^{-1}$)	pH	$[CO_3^{2-}]$ ($mg\ L^{-1}$)	$[HCO_3^-]$ ($mg\ L^{-1}$)	$[Ca^{2+}]$ ($mg\ L^{-1}$)	DOC ($mg\ L^{-1}$)
Sea water								
$\bar{x}\pm s_{n-1}$, n=4	30.1±4.81	$46\pm5x10^3$	$17.4\pm2.2x10^3$	7.96±0.50	3.94±1.53	110±21.3	na	1.41±0.15
R	21.2-33.8	$40\text{-}53x10^3$	$15.4\text{-}20.4x10^3$	7.57-8.96	2.42-6.06	90.0-139		1.30-1.51
River water								
$\bar{x}\pm s_{n-1}$, n=3								
Chupa	<0.3	na	na	9.15	na	na	na	na
Dart	<0.3	64	14±1	5.68-7.79	nd	4.93	2.08±0.10	2.08±0.07
Plym (R)	<0.3	100	13-31	6.59-7.00	nd	7.40-14.8	5.00±0.19	0.98-2.42
Beaulieu	<0.3	210	31±4	7.25	2.42	45.1	20.8±0.74	8.97±0.63
Carnon	<0.3	340	53±5	5.25	nd	3.70	20.0±1.80	0.92±0.07
World average river water								0.50-30[b]
Low alkalinity	0.041[a]	-	7.1[a]	7.30[a]	$5.6x10^{-3}$ [a]	6.1[a]	3.48[a]	
High alkalinity	0.144[a]	-	7.1[a]	8.43[a]	1.08[a]	83[a]	22.8[a]	
Milli-Q	<0.3	0.056	nd	5.00-7.00	nd	nd	nd	0.27-0.66

where $\bar{x}$ is the sample mean, s_{n-1} is the sample standard deviation, n is the number of samples, R is the range, na is not analysed and nd is not detected (sources: [a] Dyrssen & Wedbourg, 1980; [b] Mantoura & Woodward, 1983). A range of data are given for the River Plym, where possible, to incorporate the three water samples collected (Section 2.2.).

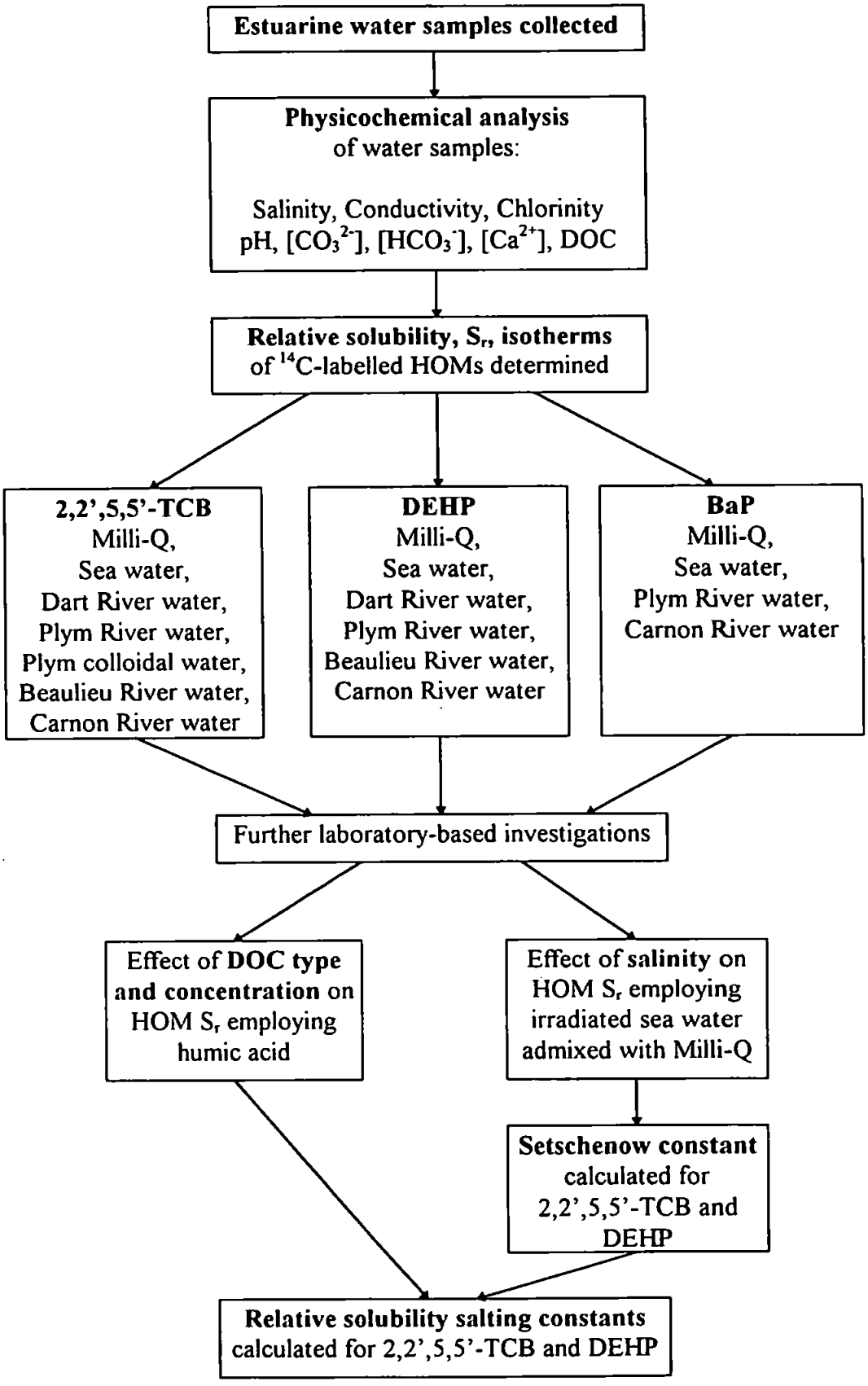

Scheme 3.1: Schematic diagram summarising the experimental strategy for the solubility of hydrophobic organic micropollutants, HOMs, where DOC is dissolved organic carbon.

3.2.1.1. 2,2',5,5'-Tetrachlorobiphenyl

The relative solubility isotherms for 2,2',5,5'-TCB in various water matrices are shown in Figures 3.1. and 3.2. The Milli-Q experiment (Figure 3.1.) was conducted over a larger range of added compound mass in order to investigate solubility more thoroughly. The linear and logarithmic isotherms are shown (Figure 3.1. and Table 3.2). The Milli-Q relative solubility isotherm is curved up to a relative solubility value of ~35 $\mu g\ L^{-1}$ as it approaches the published saturated solubility, S_{sat}, which ranges from 25.4 $\mu g\ L^{-1}$ (Schwarzenbach *et al.*, 1993) to 46.0 $\mu g\ L^{-1}$ (Hutzinger *et al.*, 1974). The expected flattening out of the isotherm as the relative solubility approached the saturated solubility occurred at the greater published saturated solubility value, followed by an increase in the isotherm between the added masses 1.65 and 2.27 µg. This suggests the formation of an emulsion, or micelles, resulting in an overestimate of the relative solubility and a larger propagated error in the relative solubility data at the larger compound masses added. This is important with regards to further investigations of this compound, in that the mass of compound added to the reaction vessel must be less than ~ 2 µg to prevent the formation of micelles in the solution phase, an artefact which would result in an underestimate of the sediment-water partition coefficient, K_D. The equations of the different fits to the data are shown in Table 3.2., along with their r^2 and p values.

The logarithmic fit of the sea water relative solubility isotherm (Figure 3.2.[i] and Table 3.2.) was similar to that of the Milli-Q isotherm (Figure 3.1.) over the first four data points. The overall relative solubility was slightly lower due to electrolytic effects on the aqueous activity coefficients of the compound or the reduction in volume of water available for dissolution through electrostriction (Means, 1995), an effect commonly described as 'salting out' (see Section 3.2.4. for further details). This may well have implications on the bioavailability and reactivity of HOMs in different water types.

In river waters, the relative solubility isotherms are best defined by a linear equation (suggested by their excellent linear regression, r^2, value, shown in Table 3.2.), suggesting that micelle formation has not occurred within the range of added compound mass. Enhanced solubility of HOMs in the presence of DOM is well documented (Landrum *et al.*, 1984; Chiou *et al.*, 1986) and can be understood from the surfactant characteristics of the natural DOM; *i.e.* the HOM binds to hydrophobic regions of DOM, such as alkyl chains, while the entire complex is held in solution or colloidal dispersion by hydrophilic sites of the DOM such as carboxylic acid or hydroxyl groups (Hassett & Anderson, 1978). Hence the HOMs exist in the aqueous phase in two forms, that is,

either freely dissolved or bound to DOM. It is believed that only the freely dissolved phase is available for adsorption onto particles (Caron *et al.*, 1985).

The gradients of the riverine isotherms are not correlated with the concentrations of DOC suggesting that while the solubility is independent of the amount of DOC, solubility may be dependent on the chemical characteristics or type of DOC. For example, in the Carnon, which shows the steepest gradient (Table 3.2.), river water DOC may be relatively non-polar (through interactions with protons in the acidic waters of the Carnon) compared with that of the Dart, which shows the shallowest gradient. The presence of colloids in the Plym river water (*i.e.* centrifuged river water in the presence of particles, Section 4.4.3.) also had little apparent effect on the relative solubility of 2,2',5,5'-TCB (cf. Figures 3.2.[iii] and 3.2.[iv]).

Table 3.2: Relative solubility isotherm equations for 2,2',5,5'-TCB in various water matrices.

Water Matrix	Equation	r^2	p
Milli-Q			
linear isotherm (first 4 points)	y = 29.34x	0.988	<0.001
linear isotherm (all points)	y = 25.19x	0.994	<0.001
logarithmic isotherm (first 5 points)	y = 13.99ln(x) + 27.98	0.979	0.001
Sea water			
linear isotherm (first 4 points)	y = 25.77x	0.982	<0.001
linear isotherm (all points)	y = 28.85x	0.998	<0.001
logarithmic isotherm (all points)	y = 15.34ln(x) + 28.46	0.964	0.003
River waters			
Dart	y = 28.87x	0.991	<0.001
Plym	y = 31.94x	0.998	<0.001
Plym colloidal	y = 34.48x	0.987	<0.001
Beaulieu	y = 33.72x	0.998	<0.001
Carnon	y = 38.25x	0.999	<0.001

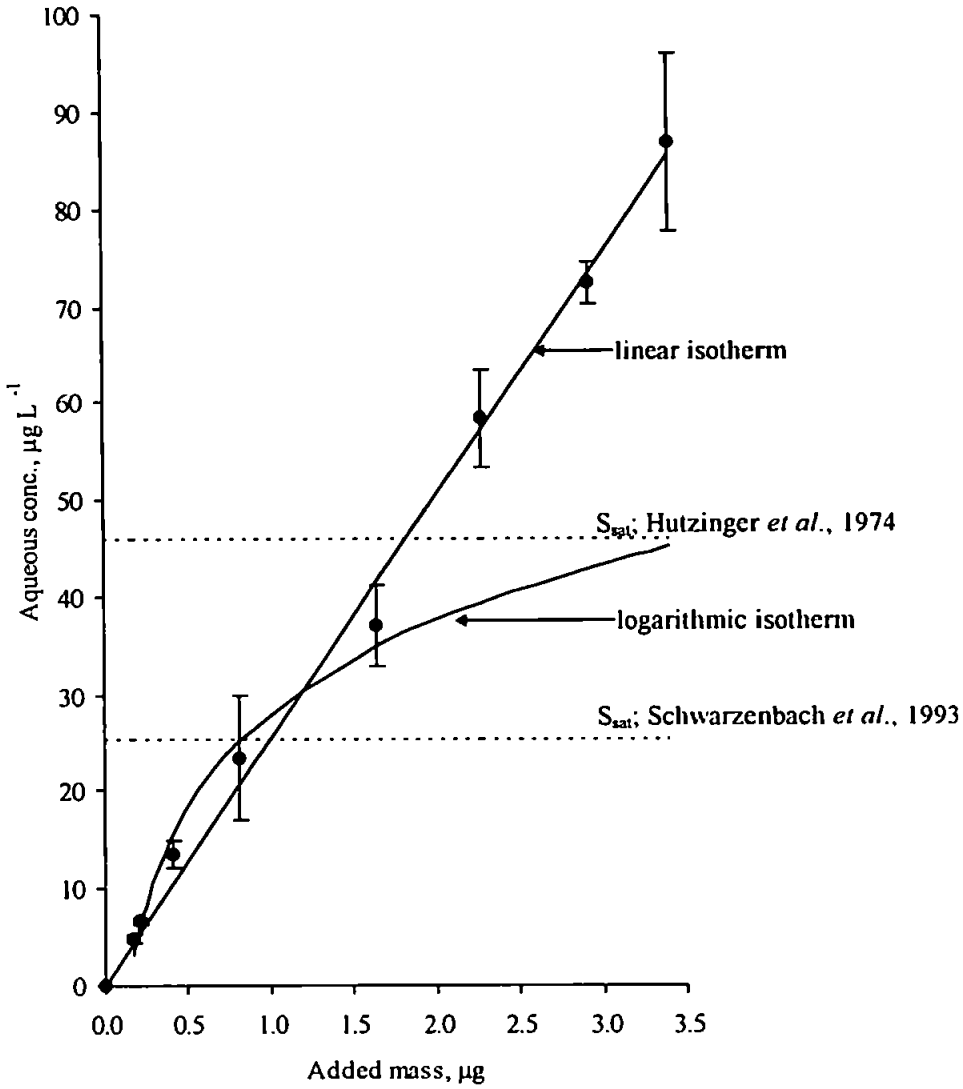

Figure 3.1: Relative solubility isotherms for 2,2',5,5'-TCB in Milli-Q, where S_{sat} is the saturated solubility and the mean value and propagated errors are shown (n=4).

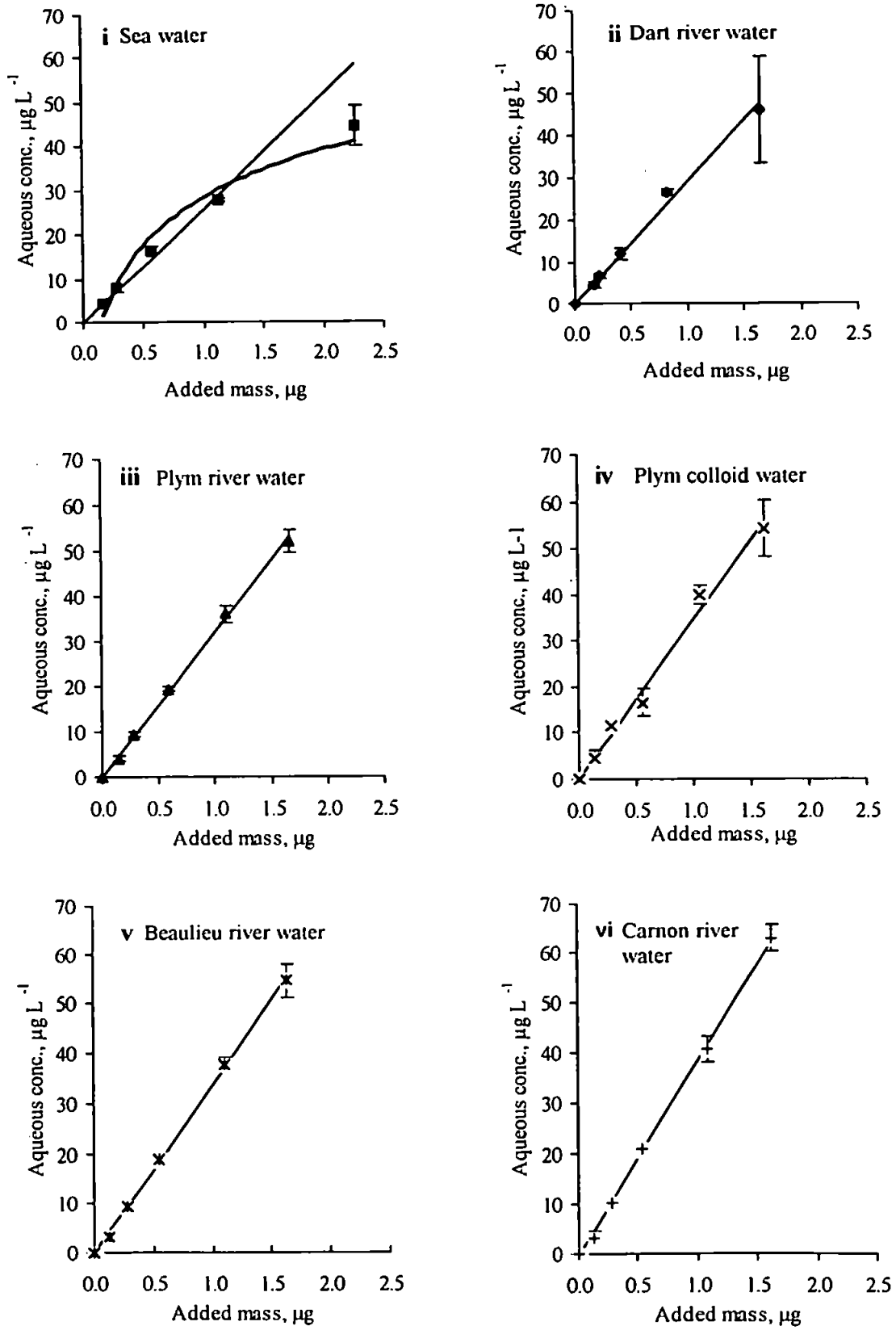

Figure 3.2: Relative solubility isotherms for 2,2',5,5'-TCB in various water matrices: (i) sea water, (ii) Dart river water, (iii) Plym river water, (iv) Plym colloid water, (v) Beaulieu river water, and (vi) Carnon river water, where the mean value and propagated errors are shown (n=4).

3.2.1.2. Bis(2-ethylhexyl)phthalate ester

Unlike the 2,2',5,5'-TCB relative solubility isotherms, no overall pattern emerges for the phthalate ester (PE). The widely varying solubility isotherms for DEHP in all the water matrices coupled with the large error bars associated with these data (Figure 3.3.) exemplifies the non-systematic behaviour of this compound in such experiments. This may be due to: contamination problems (Giam *et al.*, 1984); the ability of DEHP to form stable, homogeneous dispersions (*i.e.* micelles) in solution when mechanical energy has been applied (Brown *et al.*, 1996); or the formation of a surface layer of the PE (which is a less dense liquid than water) at the air-water interface, causing analytical errors during extraction of the water sample for counting (Staples *et al.*, 1997). Thus the published S_{sat} for DEHP varies by more than an order of magnitude between 3.0 $\mu g\ L^{-1}$ (Staples *et al.*, 1997) and 400 $\mu g\ L^{-1}$ (Giam *et al.*, 1984), although the lower S_{sat} for DEHP is probably closer to the true value and has therefore been shown in Figure 3.3. (i). This suggests that the majority of data are above the S_{sat} value of DEHP, although the presence of DOM in some of the river waters may account for enhanced solubility. The large propagated errors of the S_r values at higher added masses suggest the presence of micelles and/or a surface film. Micelles of DEHP were visible to the naked eye and seen adsorbed to the side walls of the reaction vessels during experiments involving the higher masses of added DEHP.

Despite the variable data, the relative solubility isotherms are reasonably linear, with the possible exceptions of the Plym and Beaulieu rivers where an exponential relationship could be best used to describe the isotherms. Both linear and exponential isotherms were calculated for each water type and are shown in Figure 3.3. and Table 3.3. The exponential fit of the Plym and Beaulieu data suggests that DEHP may modify or interact with the DOC in these rivers, enhancing DEHP solubility at higher masses.

The relative solubility of DEHP is augmented in Milli-Q water compared to the river waters. DEHP may already be present in Milli-Q at high concentrations due to contamination from the plastics of the Milli-Q production system (Giam *et al.*, 1984) increasing the likelihood of micelle formation which would inturn augment the S_r of DEHP in Milli-Q. PEs are known to hydrolyse in water (Giam *et al.*, 1984) to form an acid and alcohol. In the DOC-poor Milli-Q water, full hydrolysis of DEHP would increase its solubility. This is, however, unlikely to affect the results here as the hydrolysis of PEs, due to their low water solubility, is a slow process, with DEHP having a half life of over 2000 years (Staples *et al.*, 1997).

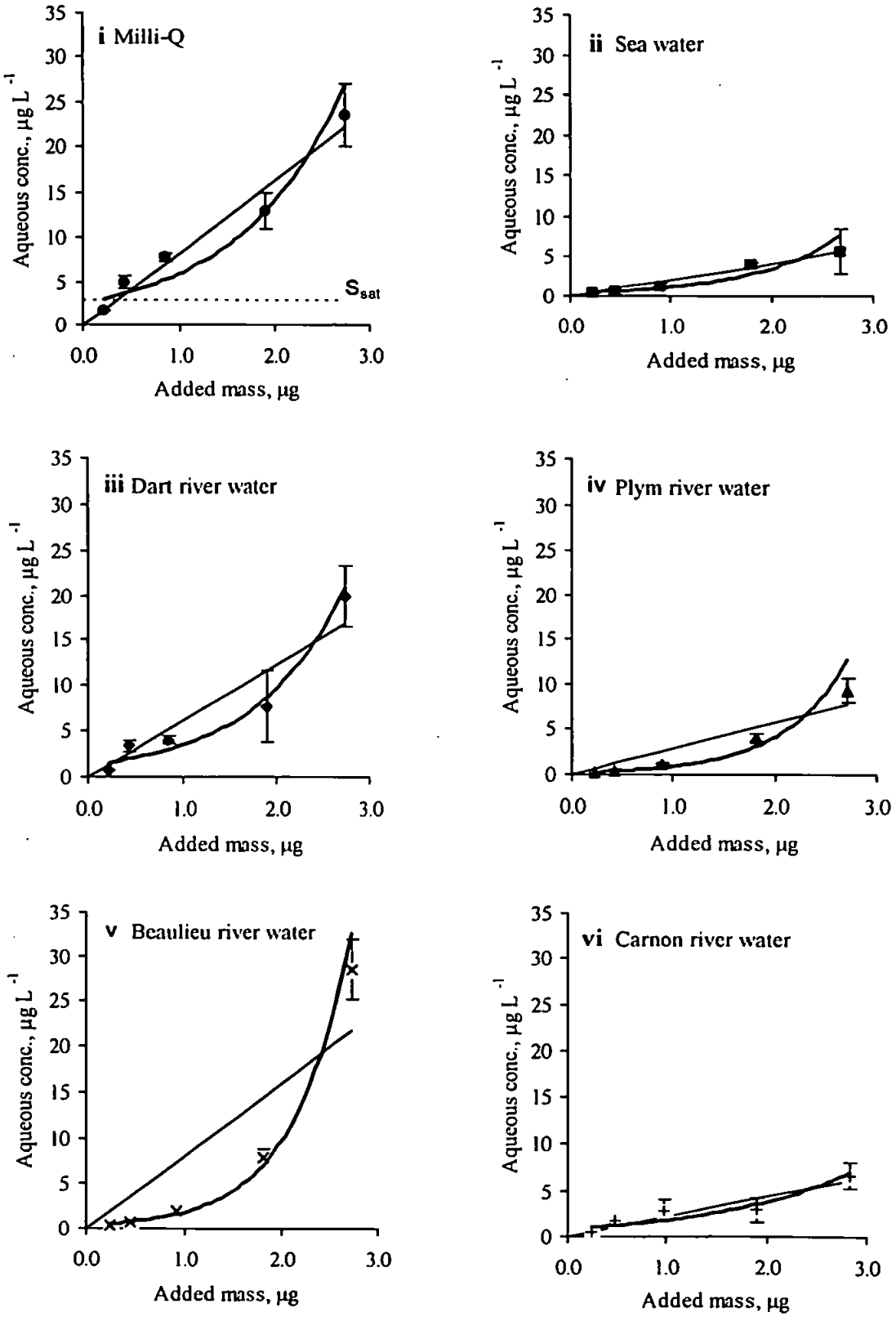

Figure 3.3: Relative solubility isotherms for DEHP in various water matrices: (i) Milli-Q, (ii) sea water, (iii) Dart river water, (iv) Plym river water, (v) Beaulieu river water, and (vi) Carnon river water, where S_{sat} is the saturated solubility (Staples *et al.*, 1997), and the mean values and the propagated errors are shown (n=4).

The relative solubility of DEHP in sea water is considerably lower than Milli-Q; the ratio of the isotherm gradients in Milli-Q water to sea water is about 4. Salting out of DEHP from pure to sea water is therefore significant. Compared with Milli-Q water, the relative solubility of DEHP in the river waters is inhibited either by the presence of small amounts of salt (salting out) or DOC. Despite the high relative solubility of DEHP in Milli-Q a relationship between the riverine linear isotherm gradients and DOC concentration exists (Figure 3.4.), suggesting that DOC concentration is a controlling factor in the relative solubility of DEHP.

Table 3.3: Relative solubility isotherm equations for DEHP in various water matrices.

Water	Linear isotherm			Exponential isotherm		
Matrix	Equation	r^2	p	Equation	r^2	p
Milli-Q	$y = 8.14x$	0.963	<0.001	$y = 2.475e^{0.871x}$	0.844	0.028
Sea water	$y = 2.09x$	0.974	<0.001	$y = 0.358e^{1.145x}$	0.935	0.007
River waters						
Dart	$y = 6.17x$	0.878	0.001	$y = 1.219e^{1.038x}$	0.829	0.032
Plym	$y = 2.88x$	0.890	0.002	$y = 0.172e^{1.585x}$	0.924	0.009
Beaulieu	$y = 8.02x$	0.779	0.008	$y = 0.354e^{1.658x}$	0.990	<0.001
Carnon	$y = 2.21x$	0.869	<0.001	$y = 0.858e^{0.746x}$	0.769	0.051

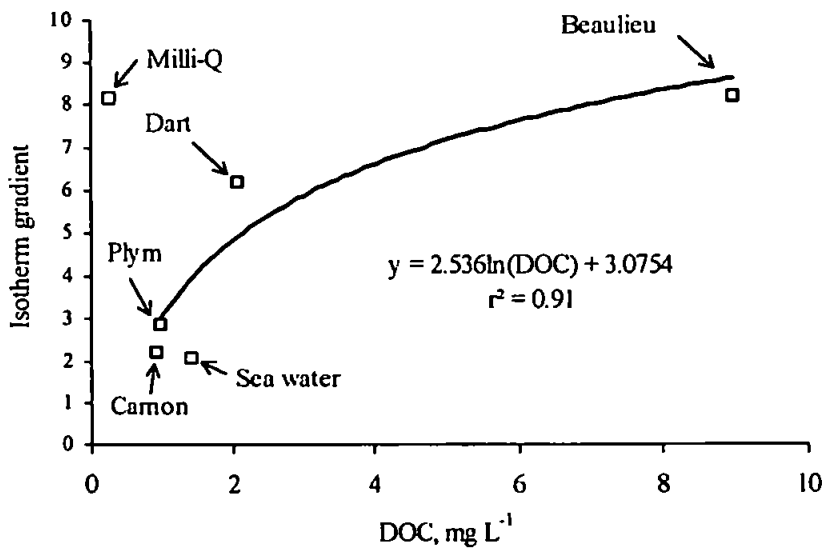

Figure 3.4: Relationship between the DEHP relative solubility isotherm gradient and riverine dissolved organic carbon concentration, DOC (closed symbols). Sea water and Milli-Q values, not used in the regression, have been shown as open symbols for reference.

3.2.1.3. Benzo[a]pyrene

The relative solubility isotherms for BaP in all waters are clearly not linear (Figure 3.5.) but logarithmic (Table 3.4.), presumably because the experiments were conducted close to the saturated solubility of BaP of 1.52 μg L^{-1} (Schwarzenbach *et al.*, 1993). The large propagated errors for the S_r of BaP at high added masses are probably due to the formation of micelles known to occur under such conditions (Futoma *et al.*, 1981).

The salting out effect is clearly evident in the case of BaP (Figure 3.5.[ii]), exemplified by the low S_r (generally < 1.5 μg L^{-1}) in sea water compared to that in Milli-Q (1.0-2.5 μg L^{-1}). Whitehouse (1984) suggested that such significant changes in the solubility of PAHs were only associated with large changes in salinity. In practice they are only important in environments where such large changes in salinity occur, *i.e.* estuaries.

DOC appears to have little effect on the relative solubilities of BaP in the different river waters, despite the different DOC concentrations and types existing in these environments. A study by DePaolis and Kukkonen (1997) showed that a pH change (5.0-8.0) had no significant effect on the binding capacity of BaP to natural DOM, and therefore, relative solubility of BaP would not be expected to be affected by the acidic mine waters of the Carnon.

Table 3.4: Relative solubility isotherm equations for BaP in various water matrices.

Water Matrix	Equation	r^2	p
Milli-Q	y = 0.52ln(x) + 2.91	0.990	<0.001
Sea water	y = 0.26ln(x) + 1.74	0.976	<0.001
River waters			
Plym	y = 0.62ln(x) + 3.07	0.937	0.002
Carnon	y = 0.41ln(x) + 2.45	0.987	<0.001

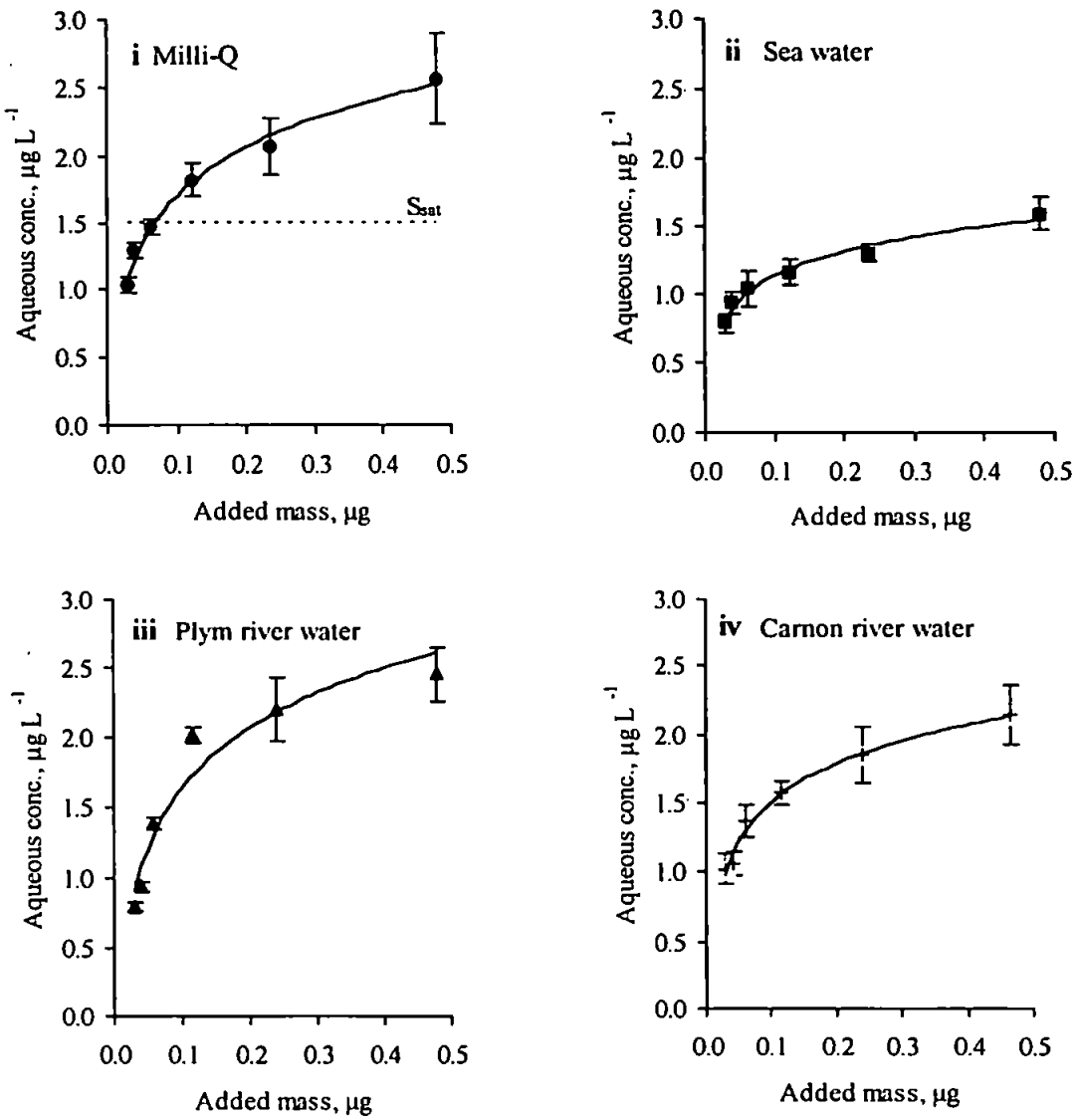

Figure 3.5: Relative solubility isotherms for BaP in various water matrices: (i) Milli-Q, (ii) sea water, (iii) Plym river water, and (iv) Carnon river water, where S_{sat} is the saturated solubility (Schwarzenbach *et al.*, 1993), and the mean values and propagated errors are shown (n = 4).

3.2.2. Glass-water partitioning

An alternative way of expressing the S_r data is as glass-water partition coefficients (Zhou *et al.*, 1995). The glass-water partition coefficient is the measure of HOM partitioning between that adsorbed to the centrifuge glass walls and that dissolved in solution. This partitioning is an artefact of the experimental design, yet essential for the understanding of the role played by the glass walls of the centrifuge tube in these experiments.

3.2.2.1. Calculation of glass-water partition coefficients

Glass-water partition coefficients were calculated as follows:

$$K_g = \left[\frac{A_w}{A_c}\right]\left[\frac{V}{SA}\right] \qquad (3.1)$$

where K_g is the glass-water partitioning coefficient (mL cm^{-2}), A_w is the activity of compound on the centrifuge tube glass walls, A_c is the activity of compound in the aqueous phase, V is the water volume (mL), and SA is the surface area (cm^2) of the centrifuge tube glass wall in contact with the aqueous phase to a volume of 20 mL.

The SA was calculated geometrically, as the sum of the surface areas of the two fractions of the centrifuge tube shown in Figure 3.6:

$$SA = \text{Area of cylinder} + \text{Area of hemisphere} \qquad (3.2)$$

$$SA = 2\pi rd + 2\pi r^2 \qquad (3.3)$$

where r is the radius (1.15 cm) and d the height (4.03 cm) of the tube filled up to a volume of 20 mL. Using these values, an SA of 37.57 cm^2 was derived.

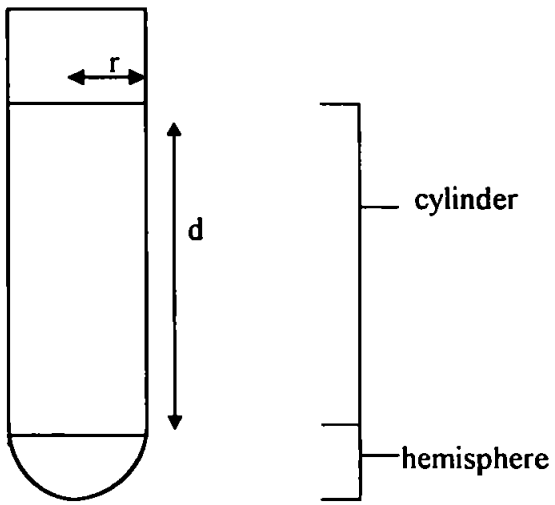

Figure 3.6: Geometrics of the centrifuge tube glass walls.

3.2.2.2. Glass-water partition coefficients for 2,2',5,5'-tetrachlorobiphenyl and bis(2-ethylhexyl)phthalate ester

Glass-water partition coefficients were calculated for 2,2',5,5'-TCB and DEHP in each of the matrices using the linear portions of the isotherms (Figure 3.7.) in two ways. Firstly, by assuming that A_w was equal to that recovered by the repeated solvent extractions, and secondly by deriving A_w from mass balance:

$$A_w = A_o - A_c \qquad (3.4)$$

where A_o is the original activity. These data are summarised in Table 3.5.

Glass-water partitioning is exemplified for 2,2',5,5'-TCB using both approaches (Figure 3.7.[i] and [ii]). The significance (r^2) of the graphs improved when the mass balance approach was adopted (Table 3.5.), suggesting a loss of original activity due to irreversible adsorption onto the centrifuge tube walls. The K_gs for 2,2',5,5'-TCB were higher in Milli-Q and sea water (assuming a mass balance) than in river water (with the exception of the River Dart compared to Milli-Q) emphasising the greater solubility of 2,2',5,5'-TCB in river water, as previously discussed.

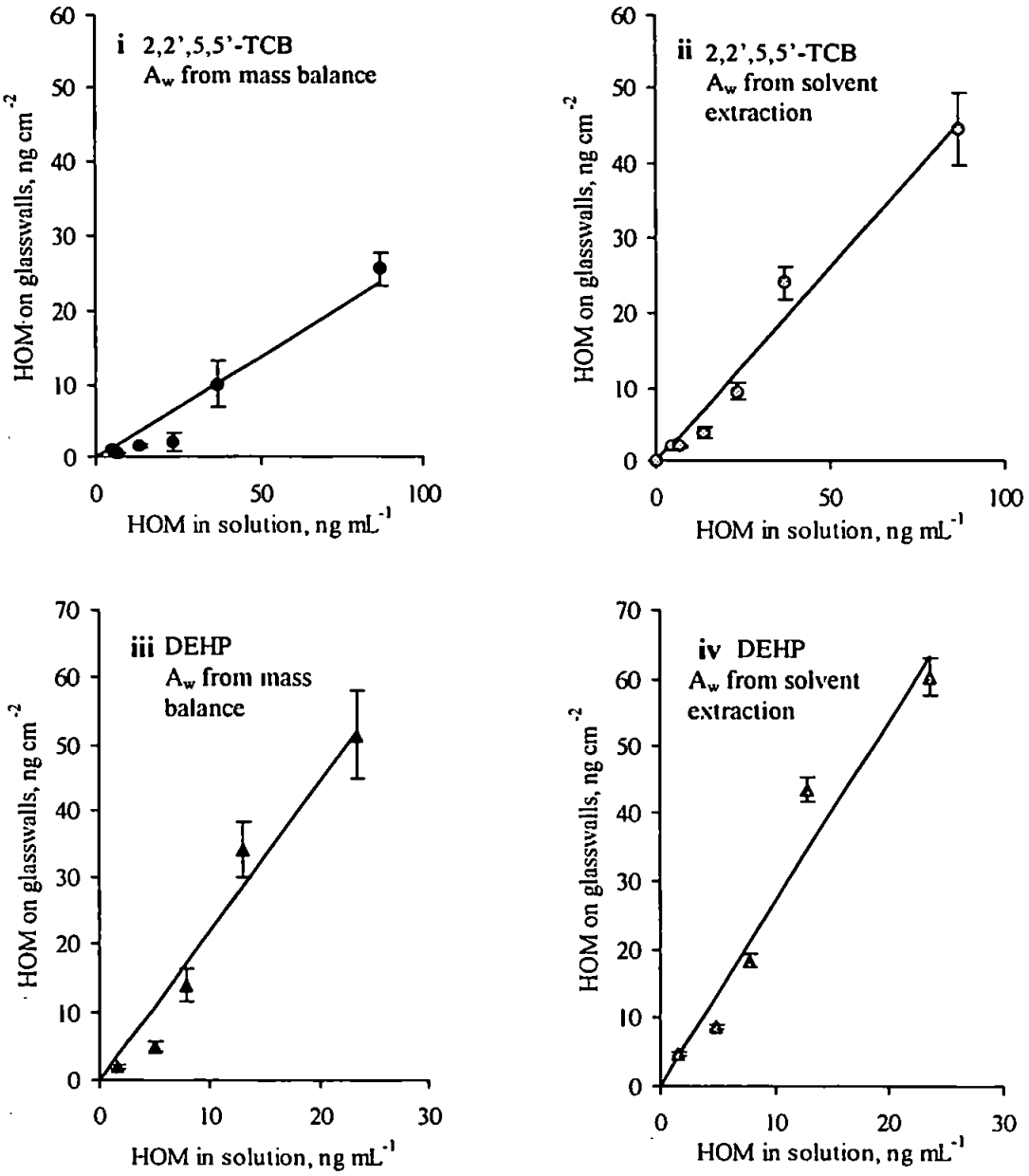

Figure 3.7: Adsorption of HOMs on to the centrifuge tube glass walls in the absence of particles for 2,2',5,5'-TCB in Milli-Q water (i) A_w from mass balance, (ii) A_w from solvent extraction, and for DEHP in Milli-Q water (iii) A_w from mass balance, (iv) A_w from solvent extraction, where the mean values and propagated errors are shown (n=4) and A_w is the activity of compound on the centrifuge tube glass walls.

Table 3.5: Summary of K_g values for 2,2',5,5'-TCB and DEHP.

HOM	Water matrix	Solvent extracted			Mass balance		
		K_g (mL cm^{-2})	r^2	p	K_g (mL cm^{-2})	r^2	p
2,2',5,5'-TCB	Milli-Q	0.28	0.942	<0.001	0.52	0.970	<0.001
	Sea water	0.44	0.930	<0.001	0.70	0.959	<0.001
	River water						
	Dart	0.32	0.943	<0.001	0.54	0.927	<0.001
	Plym	0.14	0.941	<0.001	0.30	0.977	<0.001
	Beaulieu	0.13	0.958	<0.001	0.26	0.984	<0.001
	Carnon	0.08	0.783	0.002	0.16	0.970	<0.001
DEHP	Milli-Q	2.22	0.955	<0.001	2.69	0.950	<0.001
	River water						
	Plym	5.30	0.812	0.002	7.87	0.766	0.003
	Carnon	9.65	0.871	0.001	11.07	0.871	<0.001

Glass-water partitioning for DEHP is also shown in Figure 3.7. and K_g values for the linear data are shown in Table 3.5. For DEHP the significance is similar for both the solvent extraction and mass balance approaches. The K_g values indicate that DEHP has a greater affinity for the glass than 2,2',5,5'-TCB.

Glass-water partitioning values for BaP have not been derived because the relative solubility isotherms were non-linear (*i.e.* K_g would vary as a function of compound mass present).

3.2.3. Effect of dissolved organic carbon on the relative solubility of HOMs

The concentration of natural dissolved organic carbon (DOC), Table 3.1., varies considerably depending on the catchment area of the river. In particular, DOC levels in the Beaulieu are relatively high owing to the forested catchment. The DOC concentration of the sea water samples was within the typical DOC content range of oceanic waters (0.8-1.5 mg L^{-1}; Mantoura & Woodward, 1983). DOC generally behaves conservatively in estuaries (Mantoura & Woodward, 1983) implying that DOC would be expected to behave conservatively in the reaction vessels, *i.e.* not interact with any particles present or adsorb significantly to the glass walls.

Clearly the presence of DOC has an effect on the S_r of HOMs in the various water matrices investigated and discussed earlier (Sections 3.2.1.-3.2.3.) and in turn will

influence the environmental fate and bioavailability of HOMs. Natural DOM, a heterogeneous mixture of organic compounds, of which, approximately 50% is comprised of humic and fulvic acids (Hunchak-Kariouk *et al.*, 1997), will vary in concentration, type and/or polarity, both seasonally and spatially within an estuary and between estuaries depending on the riverine catchment area. Therefore, to examine further the role played by DOC concentration and type, a series of controlled experiments were set up using variable amounts of a commercially produced humic acid (Aldrich, catalogue N° H1,675-2). A 30 mg L^{-1} solution of humic acid (equivalent to a DOC concentration of ~12 mg L^{-1}) in Milli-Q water was prepared, from which a range of dilutions were made using Milli-Q water. The relative solubility of each HOM was then determined over this DOC range for a standard spike of 550 Bq (mass of 0.36 µg) for 2,2',5,5'-TCB, and 925 Bq for DEHP and BaP (masses of 0.83 µg and 0.24 µg, respectively). The pH of these experiments was monitored, using a calibrated Hanna pH meter, and found to be within the range of natural river waters and that of Milli-Q.

From the results (Figure 3.8.) an increase in relative solubility is seen for all compounds with an increase in humic acid concentration. These plots are all defined by a logarithmic function, whose equations are shown on the graphs. The increase in relative solubility is, however, relatively small over the DOC concentrations encountered in the river waters used. Between 1 and 9 mg L^{-1} DOC (which encompasses the range of DOC concentrations encountered in the rivers studied), the increase in the relative solubility of 2,2',5,5'-TCB is 16%. For DEHP, the increase is 29% and for BaP 44%. The non-linear relationship between HOM solubility and humic concentration suggests that DOC concentration has a non-additive effect on HOM solubility. Also shown on the diagrams are the relative solubilities (at an equivalent spike) in each river water sample (as well as for the sea water samples) of each compound studied. For 2,2',5,5'-TCB these points lie close to the solubility line for humic acid. However, it is unlikely that the commercial humic acid used is entirely representative of natural DOM, which comprises of a complex mixture of high molecular weight humic substances (Hunchak-Kariouk *et al.*, 1997). Commercial humic acids often have different molecular characteristics to natural humics, having low carbohydrate and carboxyl contents rendering them less hydrophilic in comparison, and thus, can be up to 40 times more effective in enhancing HOM solubility (Hunchak-Kariouk *et al.*, 1997). Furthermore, the composition, structure, and polarity of natural DOM can vary significantly between aquatic environments depending upon the

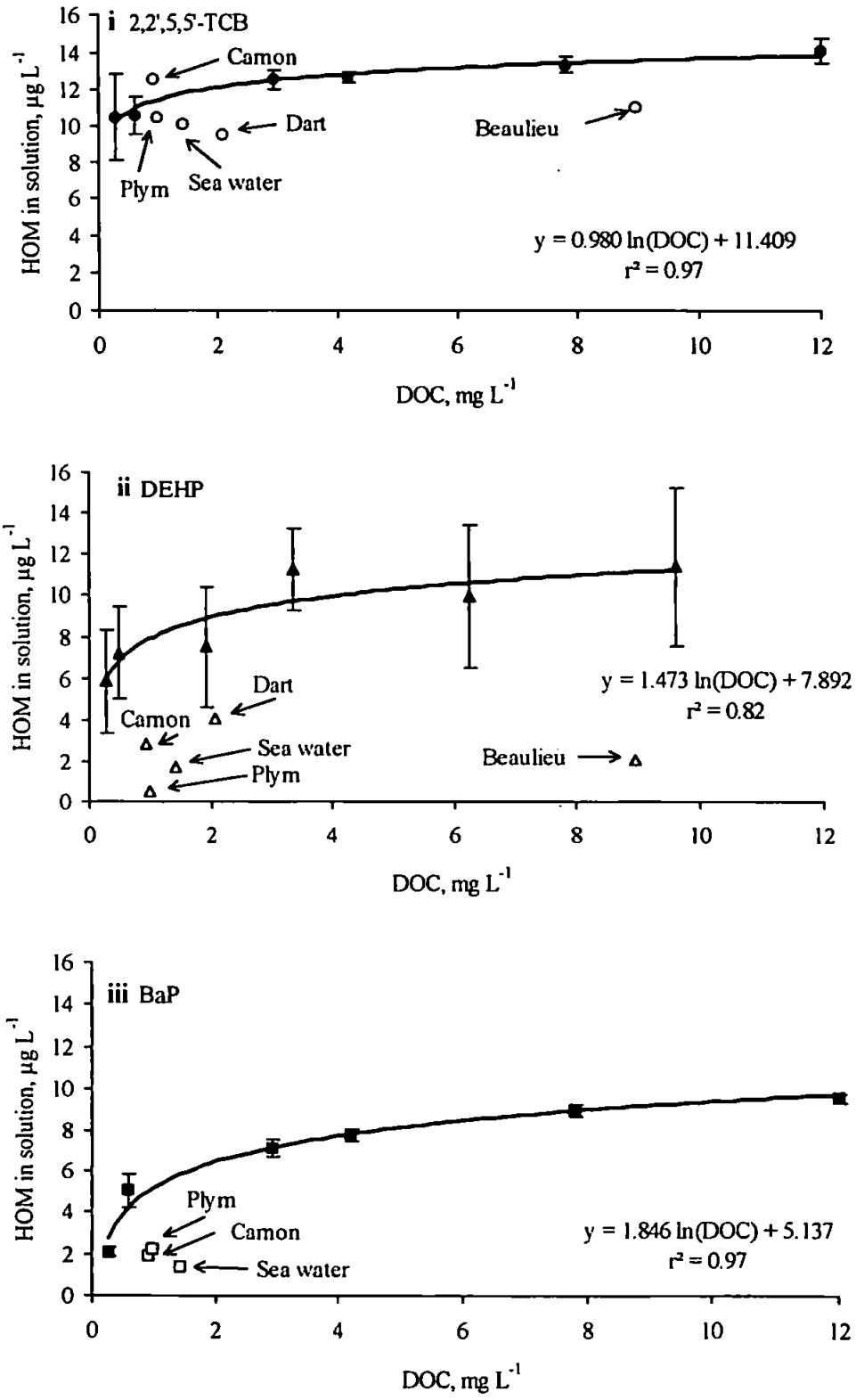

Figure 3.8: Changes in relative solubility (closed symbols) with an increase in dissolved organic carbon (DOC) concentration for the HOMs: (i) 2,2',5,5'-TCB, (ii) DEHP, and (iii) BaP, where the mean value and propagated errors are shown (n=4). Also shown, as open symbols, are the relative solubilities of the compound studied (at an equivalent spike) in each river and sea water samples, for reference.

biological and physicochemical properties of the water (Chiou *et al.*, 1987).

However, the data suggests that 2,2',5,5'-TCB solubility is, in fact, largely independent of DOC type and/or polarity. In contrast, for DEHP and BaP the points are well below the humic acid solubility line suggesting that the relative solubility is strongly influenced by both DOC concentration (Section 3.2.1.2.; Figure 3.4.) and type (Figure 3.8. [i] & [ii]). Thus, it would appear that either the molecular characteristics of commercial humic acids enhance HOM solubility compared to natural DOM (Chiou *et al.*, 1987), or fulvic acids have a much lower affinity for HOMs than humic acids (DePaolis & Kukkonen, 1997). Thus it would be expected that the binding capacity of natural DOM, which comprises a mixture of humic and fulvic acids, is lower than commercial organic compounds.

3.2.4. The effect of salinity on the relative solubility of HOMs

As with DOC, salinity appears to be a controlling factor of the relative solubility of HOMs in estuaries. To demonstrate the effect of increasing salinity on the relative solubility of HOMs an experiment similar to that described in Section 3.2.3. was set up, using UV irradiated sea water (to reduce the concentration of organic matter present) admixed with Milli-Q water to give a range of salinities. Not all of the sea water DOC was removed by UV light, although the DOC concentration decreased from 1.37 mg L^{-1} to 0.65 mg L^{-1}; a concentration comparable to the background DOC levels found in Milli-Q.

Figure 3.9. clearly shows the decrease in relative solubility for all three HOMs as salinity increases. The decrease in relative solubility between Milli-Q and UV irradiated sea water (salinity 33.7×10^{-3}) is 14%, 76%, and 47%, for 2,2',5,5'-TCB, DEHP, and BaP, respectively. This decrease is attributed to the 'salting out' effect. The 2,2',5,5'-TCB and DEHP data are best defined by a linear regression while the BaP data is best defined by a logarithmic plot.

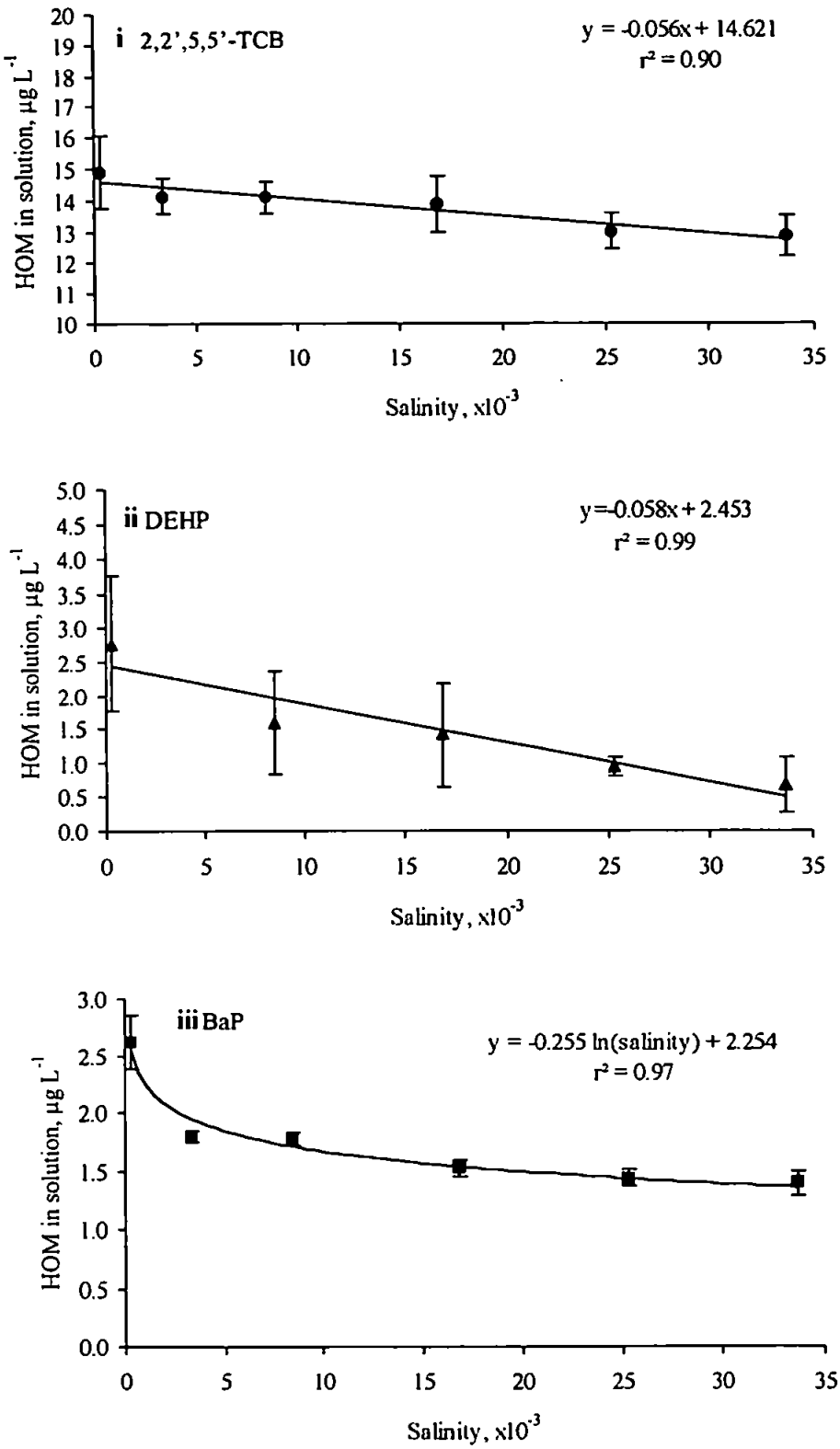

Figure 3.9: Changes in relative solubility with an increase in salinity for the HOMs: (i) 2,2',5,5'-TCB, (ii) DEHP, and (iii) BaP, where the mean value and propagated errors are shown (n=4).

3.2.4.1. The Setschenow constant

The dependency of HOM solubility upon the salt concentration of saline matrices is well established (Xie *et al.*, 1997). Solubility in pure water and higher ionic strength solutions can be related by the Setschenow equation, which empirically describes the magnitude of the 'salting out' effect (May *et al.*, 1978; Rossi & Thomas, 1981):

$$\log\left(\frac{S^{\circ}_{sat}}{S^{s}_{sat}}\right) = \sigma M \qquad (3.5)$$

where S°_{sat} is the compound concentration in pure water at saturation (w/v), S^{s}_{sat} is the compound concentration in sea water at saturation (w/v), σ is the Setschenow constant (L mol^{-1}), and M is the effective molar concentration of the electrolyte.

The linear relationships between the relative solubilities of 2,2',5,5'-TCB and DEHP as a function of salinity, Figure 3.9., can be used to estimate σ, assuming that the ratios of relative solubilities approximate those at saturation. Therefore, Equation 3.5. becomes:

$$\log\left(\frac{S^{\circ}_{r}}{S^{s}_{r}}\right) = \sigma M \qquad (3.6)$$

where S°_{r} is the relative solubility in pure water (w/v), and S^{s}_{r} is the relative solubility in sea water (w/v). Figure 3.10. shows log $\left(S^{\circ}_{r} / S^{s}_{r}\right)$ against the molar water salt concentration (assuming M = 0.5 mol L^{-1} for sea water) for 2,2',5,5'-TCB and DEHP. Setschenow constants are calculated from the gradients of these plots. These values are compared to the published values of Setschenow constants for other compounds derived from solubility studies using mixtures of pure water and natural sea water in Table 3.6. For 2,2',5,5'-TCB, σ is within the same order of magnitude of σ for other PCBs. There are no published σ values for phthalates from which to draw comparison but evidently DEHP is extremely sensitive to salting out, as indicated in Figure 3.3. and by the high σ value compared to other HOMs. A value of σ for BaP was not determined from this data set due to the non-linear relationship existing between its S_r and salinity, a published σ value is shown in Table 3.6. PAH solubilities are known to be sensitive to salt content at low salinities (Whitehouse, 1984) which could explain the S_r decrease for BaP between

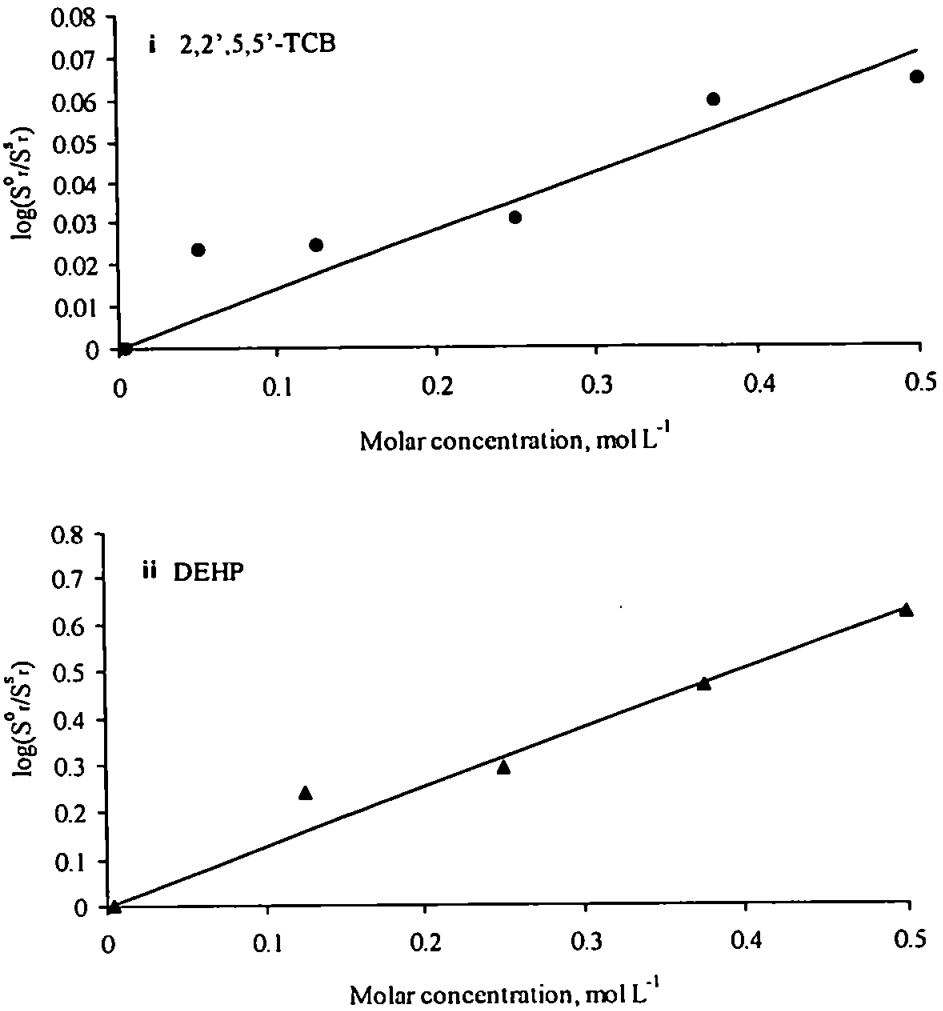

Figure 3.10: Changes in log $\left(S_r^\circ / S_r^s\right)$ with molar sea water salt concentration for (i) 2,2',5,5'-TCB and (ii) DEHP.

Milli-Q and a salinity of about 4, an effect not replicated with further increases in salinity.

An alternative way of deriving σ is by using the published empirical relationship between σ and molar volume, V_H ($cm^3\ mol^{-1}$), for organic compounds (Xie *et al.*, 1997):

$$\sigma = \phi\ V_H \qquad (3.7)$$

where ϕ is a constant. Molar volumes can be calculated from the sum of volumes of the component atoms in the organic compound (Table 3.7.). The molar volumes for 2,2',5,5'-TCB, DEHP, and BaP, calculated in this manner are, 248 $cm^3\ mol^{-1}$, 474 cm^3

Table 3.6: Calculated Setschenow constants for hydrophobic organic micropollutants.

HOM	Setschenow Constant (σ) ($L\ mol^{-1}$)
PCBs	
2,4'-DCB	0.300[a]
2,2',5,5'-TCB	0.140[b]
2,3',4',5-TCB	0.200[a]
2,2',3,4,5'-PCB	0.300[a]
2,2',3,4,4',5-HCB	0.300[a]
Phthalate Ester	
DEHP	1.253[b]
PAHs	
Phenanthrene	0.272[c]-0.330[a]
Pyrene	0.294[c]-0.320[a]
BaP	0.199[d]

Sources: [a] Schwarzenbach *et al.* 1993; [b] This study, 1998; [c] Hashimoto *et al.*, 1984; [d]Means, 1995.

Table 3.7: Molar volumes of organic molecules.

Element	Molar volume ($cm^3\ mol^{-1}$)
C	16.5
H	2.0
O	5.5
Cl	19.5
Aromatic ring	-20.2

Source: Schwarzenbach *et al.*, 1993.

mol^{-1}, and 253 $cm^3\ mol^{-1}$, respectively. The order of this sequence corresponds to the magnitude of σ, confirming that, to some extent, the Setschenow constant is controlled by the molar volume.

3.2.4.2. Relative solubility salting constant

While the Setschenow constant is a useful parameter in its own right, the change in relative solubility of a HOM during estuarine mixing is more important from a geochemical point of view. This change in relative solubility can be described by the relative solubility salting constant, σ_r (which accounts for both salinity and DOC effects),

calculated from the ratio of the linear relative solubility isotherms in river water (S_r^{rw}) and sea water (S_r^{sw}), Tables 3.2. and 3.3., based on the Setschenow concept:

$$\log\left(\frac{S_r^{rw}}{S_r^{sw}}\right) = \sigma_r M \qquad (3.8)$$

The calculated estuarine relative solubility salting constants, assuming M = 0.5 mol L^{-1} for sea water (σ_r; Table 3.8.), indicate that DEHP is generally more sensitive to 'salting out' than 2,2',5,5'-TCB. Therefore, on solubility considerations alone, DEHP would be expected to be retained more in an estuary, as it is less soluble. The exception is the Carnon Estuary, where DOC concentrations are relatively low, and salt levels relatively high (DEHP is more sensitive to salting out compared to 2,2',5,5'-TCB; Figure 3.10.).

Table 3.8: Estuarine relative solubility salting constants (L mol^{-1}) for 2,2',5,5'-TCB and DEHP.

Estuary	Relative solubility salting constant (σ_r)	
	2,2',5,5'-TCB	DEHP
Dart	0.098	0.940
Plym	0.187	0.280
Beaulieu	0.254	1.19
Carnon	0.352	0.051

3.2.5. Summary of HOM relative solubility

Relative solubility isotherms for 2,2',5,5'-TCB, DEHP and BaP (Figures 3.1.-3.3. and 3.5.) were defined for the various water matrices (Tables 3.2.-3.4.).

The influence of natural DOC concentrations on HOM relative solubility was not obvious, suggesting that the role played by DOC type and/or polarity was also of importance. Further investigations employing an Aldrich humic acid (Section 3.2.3.) showed that the relative solubility of 2,2',5,5'-TCB was mainly dependent upon DOC concentration, whilst the relative solubilities of DEHP and BaP were strongly influenced by both DOC type and concentration.

All three HOMs showed a 'salting out' effect in high saline waters (Figure 3.9.) and was discussed in terms of the Setschenow concept (Section 3.2.4.1.). The magnitude

of change in the relative solubilities of 2,2',5,5'-TCB and DEHP during estuarine mixing (due to both DOC and salinity effects) were described by the relative solubility salting constant (Section 3.2.4.2.) for the individual estuaries studied (Table 3.8.).

Now that the role of physicochemical properties of the estuarine waters on the relative solubility of the HOMs has been addressed, the next step is to investigate the role of estuarine particles on the adsorption of HOMs.

CHAPTER 4: PARTICLE-WATER INTERACTIONS OF HOMS

4.1. Introduction

The next stage of the investigation was to quantify the behaviour of the particle-water interaction of hydrophobic organic micropollutants (HOMs) under different reaction conditions. The influence of time (kinetics), salinity, suspended particulate matter (SPM) concentration and particle type were investigated under carefully controlled laboratory conditions (as outlined in Chapter 2). The experimental strategy employed in this chapter is summarised in Scheme 4.1. The results reported in this chapter (summarised in Appendix B3) build on the investigations of the relative solubility of HOMs under estuarine conditions (Chapter 3).

4.1.1. Particle (and solution) characteristics

The geochemical characteristics of the estuarine sediments used are shown in Table 4.1. and show the contrasting particle types from the selected estuaries. Iron and Mn hydroxide coatings are important controlling factors in the adsorption of trace pollutants (both organic and inorganic) onto estuarine sediments (Lion *et al.*, 1982), and the Fe:Mn ratio assesses the relative role played by each metal oxide in adsorption. The Fe rich sediments of the Carnon had the highest specific surface area (SSA), approximately twenty times that of the Plym sediments.

Sorption of uncharged organic compounds onto estuarine sediments is primarily controlled by organic carbon coatings (Karickhoff, 1984). Dart sediments were shown to have the highest organic matter content in terms of particulate organic carbon (POC) and loss on ignition (LOI), although the latter is a rough estimate of the organic carbon content of the particle, with a known error up to 20% (Mook & Hoskin, 1982). LOI was used as a relatively quick and convenient method to assess the organic carbon content of the sediments until the POC could be measured using the Schimadzu TOC-5000 total organic carbon analyser (Section 2.4.2.). Sediments from the Dart and Carnon Rivers have high Ca contents, indicating a high proportion of carbonate material. The role played by both particulate and dissolved Ca in the reduction of the solubility of high molecular weight organic compounds such as humic acids, via flocculation, is well

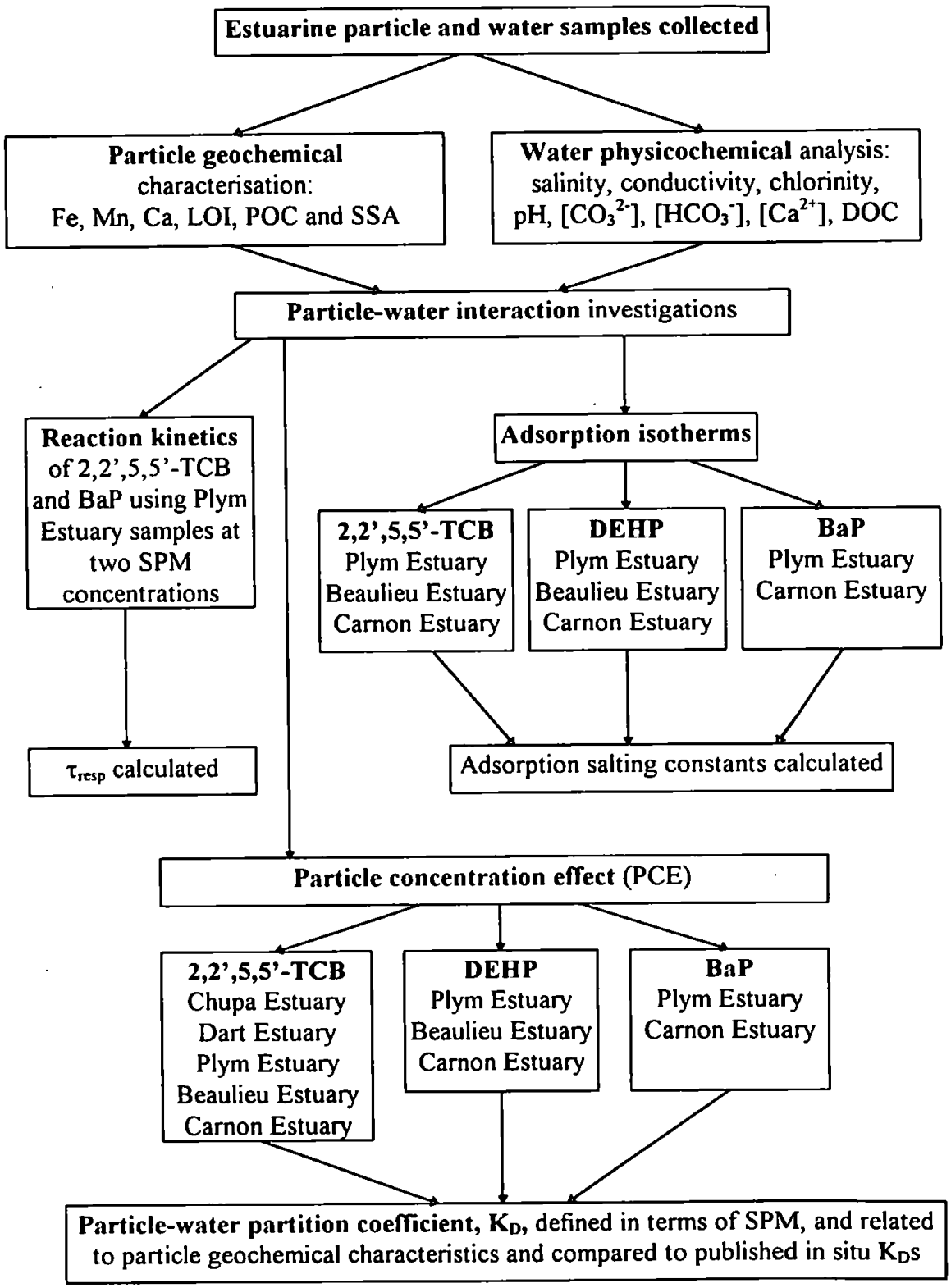

Scheme 4.1: Schematic diagram summarising the experimental strategy for the particle-water interactions of hydrophobic organic micropollutants, where LOI is loss on ignition, POC is particulate organic carbon, SSA is specific surface area, SPM is suspended particulate matter, DOC is dissolved organic carbon, τ_{resp} is the system response time.

Table 4.1: Estuarine sediment geochemical characteristics

Estuary $\bar{x}\pm s_{n-1}$, n=3	Fe (mg g^{-1})	Mn (mg g^{-1})	Fe/Mn	Ca (mg g^{-1})	LOI (%)	Total Carbon (%)	POC (%)	SSA (m^2 g^{-1})
Chupa	10.3±0.43	0.46±0.01	22	3.56±0.34	9.03±0.64	1.28	1.28	13.2
Dart	4.63±0.18	1.09±0.02	4	11.0±0.54	13.2±0.25	5.01	4.98	6.3
Plym	2.48±0.08	0.02±0.001	108	3.30±0.13	9.23±0.06	1.72	1.69	4.0
Beaulieu	8.07±0.30	0.43±0.02	19	3.27±0.12	8.97±0.21	2.35	2.32	6.7
Carnon	53.7±2.39	0.31±0.01	173	9.98±0.38	10.4±0.23	2.67	2.66	61.2

where LOI is loss on ignition, POC is particulate organic carbon, SSA is specific surface area, $\bar{x}$ is the sample mean and s_{n-1} is the sample standard deviation

Table 4.2: Physicochemical properties of sea and river water samples

Sample	Salinity ($x10^{-3}$)	Conductivity (μS)	Chlorinity (mg L^{-1})	pH	$[CO_3^{2-}]$ (mg L^{-1})	$[HCO_3^-]$ (mg L^{-1})	$[Ca^{2+}]$ (mg L^{-1})	DOC (mg L^{-1})
Sea water								
$\bar{x}\pm s_{n-1}$, n=4	30.1±4.81	46±5x10^3	17.4±2.2x10^3	7.96±0.50	3.94±1.53	110±21.3	na	1.41±0.15
R	21.2-33.8	40-53x10^3	15.4-20.4x10^3	7.57-8.96	2.42-6.06	90.0-139		1.30-1.51
River water								
Chupa	<0.3	na	na	9.15	na	na	na	na
Dart	<0.3	64	14±1	5.68-7.79	nd	4.93	2.08±0.10	2.08±0.07
Plym	<0.3	100	13-31	6.59-7.00	nd	7.40-14.8	5.00±0.19	0.98-2.42
Beaulieu	<0.3	210	31±4	7.25	2.42	45.1	20.8±0.74	8.97±0.63
Carnon	<0.3	340	53±5	5.25	nd	3.70	20.0±1.80	0.92±0.07

where $\bar{x}$ is the sample mean, s_{n-1} is the sample standard deviation, n is the number of samples, R is the range, na is not analysed and nd is not detected, a range of data are given for the River Plym, where possible, to incorporate the three water samples collected (Section 2.2.).

established (Kretzschmar & Sticher, 1997; Romkens & Dolfing, 1998) and will, therefore, indirectly influence the adsorption and relative solubility of the HOMs.

The physicochemical properties of the sea and river water samples, outlined in Chapter 3, are summarised in Table 4.2. to give an overview of the estuarine systems studied.

4.2. Reaction Kinetics

A series of kinetic experiments (based on the developed particle-water interaction methodology outlined in Section 2.7.) were undertaken to examine the rate of uptake of HOMs onto estuarine suspended particulate matter (SPM). The objectives of these experiments were to investigate the rates of particle-water interactions, and to assess the time required to attain a quasi-equilibrium and to test the hypothesis that a 16 hour incubation period was a reasonable cut-off for estimates of partition functions (*i.e.* particle-water partition coefficients) relevant to estuarine processes. The particle-water partition coefficient, K_D (mL g^{-1}) (Equations 2.4 & 2.7), was derived for both 2,2',5,5'-TCB and BaP at time intervals of up to 21 days, which represents an upper limit of the flushing time of most small to medium macrotidal estuaries (Morris, 1990). Time-dependent experiments were not carried out for DEHP due to the analytical uncertainties and large variance associated with this data set. However, it should be noted that Al-Omran & Preston (1987) observed that DEHP attained a quasi-equilibrium after 2-3 hours in sea water with an SPM concentration of 1000 mg L^{-1}.

The time-dependent uptake of 2,2',5,5'-TCB and BaP onto Plym estuarine SPM at SPM concentrations of 12 mg L^{-1} and 164 mg L^{-1} are shown in Figure 4.1. and the trends in the reaction profiles are discussed below. In the experiment involving BaP with an SPM concentration of 12 mg L^{-1}, the propagated errors for the first three time intervals were greater than 100% and not shown in Figure 4.1.(ii) for clarity. These large propagated errors were due to large variance in the relatively low counts obtained during the pipette rinse stage of the method. Apart from this experiment, the data in Figure 4.1. exhibits relatively low propagated errors, attesting to the excellent reproducibility of the method when moderate to high particle concentrations are employed.

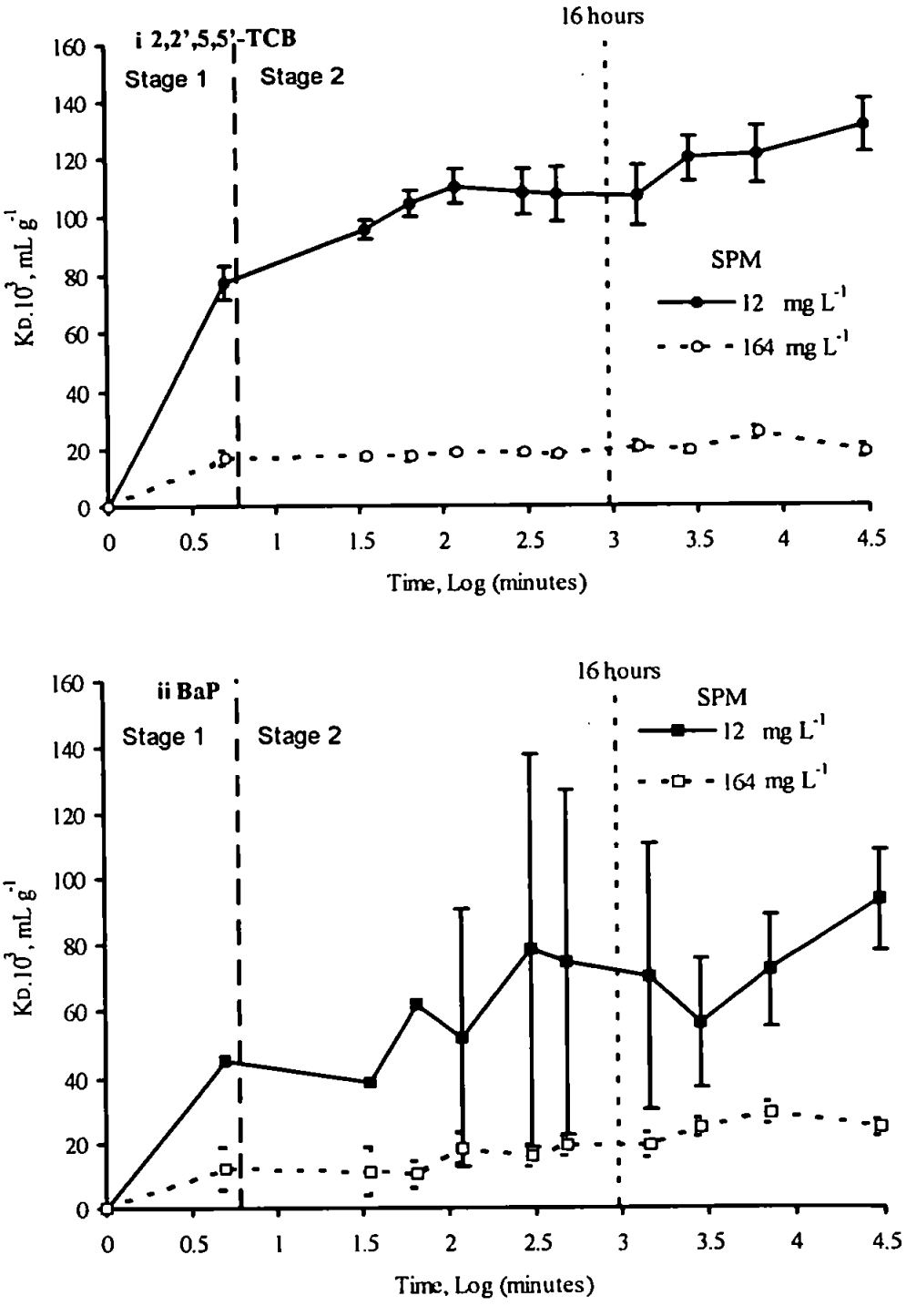

Figure 4.1: Partition coefficients for (i) 2,2',5,5'-TCB and (ii) BaP as a function of time and suspended particulate matter, SPM, concentration in the Plym Estuary. The mean value and error of propagation has been shown (n=4). With the exception of the first three points for BaP at an SPM concentration of 12 mg L^{-1} where the propagated error was greater than 100%.

The particle-water partitioning, Figure 4.1., was not instantaneous, especially at the higher SPM concentration, for both compounds. From the results HOM adsorption appears to be biphasic, with a significant rapid uptake occurring within the first few minutes (Stage 1), due to fast surface reactions, followed by a second slower uptake (Stage 2) over a period of days. Stage 1 uptake accounts for the adsorption of 48% and 74% of the added 2,2',5,5'-TCB and 88% and 66% of the added BaP at SPM concentrations 12 mg L^{-1} and 164 mg L^{-1}, respectively. Stage 2 uptake is considerably less; accounting for 13% and 2.4% of the added 2,2',5,5'-TCB and 5.8% and 14% of the added BaP at SPM concentrations 12 mg L^{-1} and 164 mg L^{-1}, respectively. This second stage could be due to the slow migration of surface adsorbed HOMs into the organic matrix of the particle where stronger binding sites occur (Jannasch *et al.*, 1988). Other controlling factors such as the microbial decay of organic matter or particle-concentration dependent sediment aggregation/disaggregation (Jepsen *et al.*, 1995) may also influence this second adsorption phase over the experimental period. Although an equilibrium is not attained throughout the incubations, the K_Ds at 16 hours were not found to be significantly different to those at 21 days and, therefore, the 16 hour period for equilibrium, on the lateral shaker, has been adopted in all further experiments. Kinetic experiments for the adsorption of hexachlorobenzene onto Detroit River sediments showed that for SPM concentrations of 10-2000 mg L^{-1} equilibrium was not reached until between 50 and 130 days, respectively (Jepsen *et al.*, 1995), whilst Girvin & Scott (1997) found that 2,2',5,5'-TCB adsorption onto montmorillonite soil did not reach equilibrium until after 5 months. Both investigations showed a biphasic adsorption profile as seen in Figure 4.1. However, after these timescales there is no guarantee that the samples have not been chemically or biologically modified.

Such biphasic reaction profiles have been previously observed and quantitatively described for trace metals (Honeyman & Santschi, 1988; Jannasch *et al.*, 1988; Liu, 1996). However, there are no modelled data available for HOMs. The uptake of the HOMs at each SPM concentration was tested using a reversible first-order reaction of the type (Honeyman & Santschi, 1988; Jannasch *et al.*, 1988; Liu, 1996):

$$^{14}C + B \underset{k_{-1}}{\overset{k_1}{\rightleftharpoons}} {}^{14}CB \qquad (4.1)$$

where ^{14}C is the dissolved HOM, B represents an active binding site on the particle, ^{14}CB is the surface adsorbed HOM, k_1 is the forward rate constant and k_{-1} is the reverse rate constant. The differential equation for this process is:

$$\frac{-d[^{14}C]}{dt} = k_1[^{14}C] - k_{-1}[^{14}CB] \qquad (4.2)$$

where k_1 is dependent on the SPM concentration which is assumed to remain constant in each individual experiment, and $[^{14}CB]$ is given by:

$$[^{14}CB] = [^{14}CB]_{ADS} + [^{14}C]_0 - [^{14}C]_t = [^{14}C]_0 - [^{14}C]_t \qquad (4.3)$$

where $[^{14}CB]_{ADS}$ is the pre-existing surface adsorbed HOM on the added estuarine particles, exchangeable with the solution phase, which for the radiotracer experiments is assumed to be zero at t = 0 (Liu, 1996) and $[^{14}C]_0$ and $[^{14}C]_t$ are the dissolved HOM concentrations at t = 0 and at time t, respectively. Integration of Equation 4.2 gives:

$$([^{14}C]_t - [^{14}C]_E) = ([^{14}C]_0 - [^{14}C]_E) \exp[-t(k_1 + k_{-1})] \qquad (4.4)$$

where $[^{14}C]_E$ is the dissolved HOM concentration at equilibrium. The conditional equilibrium constant, K, is given by:

$$K = \frac{k_1}{k_{-1}} = \frac{[^{14}C]_0 - [^{14}C]_E}{[^{14}C]_E} \qquad (4.5)$$

Thus, k_{-1} is defined as:

$$k_{-1} = \frac{k_1[^{14}C]_E}{[^{14}C]_0 - [^{14}C]_E} \qquad (4.6)$$

Equation 4.6 can be substituted into the term $(k_1 + k_{-1})$ from Equation 4.4:

$$(k_1 + k_{-1}) = \left(k_1 + \frac{k_1[^{14}C]_E}{[^{14}C]_0 - [^{14}C]_E}\right) \qquad (4.7)$$

$$= k_1\left(\frac{[^{14}C]_0}{[^{14}C]_0 - [^{14}C]_E}\right) \qquad (4.8)$$

This expression can then be substituted into Equation 4.4 yielding:

$$([^{14}C]_t - [^{14}C]_E) = ([^{14}C]_0 - [^{14}C]_E)\exp\left[-t\left(k_1\frac{[^{14}C]_0}{[^{14}C]_0 - [^{14}C]_E}\right)\right] \qquad (4.9)$$

Rearranging Equation 4.9 yields:

$$\frac{([^{14}C]_t - [^{14}C]_E)}{([^{14}C]_0 - [^{14}C]_E)} = \exp\left[-t\left(k_1\frac{[^{14}C]_0}{[^{14}C]_0 - [^{14}C]_E}\right)\right] \qquad (4.10)$$

$$\ln\left[\frac{([^{14}C]_t - [^{14}C]_E)}{([^{14}C]_0 - [^{14}C]_E)}\right] = -k_1 t\left[\frac{[^{14}C]_0}{[^{14}C]_0 - [^{14}C]_E}\right] \qquad (4.11)$$

which after rearranging becomes:

$$k_1 t = \left[\frac{[^{14}C]_0 - [^{14}C]_E}{[^{14}C]_0}\right]\ln\left[\frac{[^{14}C]_0 - [^{14}C]_E}{[^{14}C]_t - [^{14}C]_E}\right] \qquad (4.12)$$

Equation 4.12 is in the form of a straight line, where the right hand side is plotted as a function of time. The slope of the line yields a value for k_1. Figure 4.2. shows a plot of the integrated function versus time for the uptake data for 2,2',5,5'-TCB with an SPM concentration of 12 mg L^{-1} (Figure 4.1.(i)). A linear relationship is obtained for the first two hours ($r^2 = 0.93$; $n = 5$), although the line does not go through the origin due to the problem of obtaining data immediately after the start of the experiment. The slope of the line yields $k_1 = 1.54\ h^{-1}$ and this together with $[^{14}C]_0 = 100\%$ and $[^{14}C]_E = 43\%$ gives a reverse rate constant $k_{-1} = 1.16\ h^{-1}$ (Equation 4.6). These rate constants were then used in model calculations to predict the uptake of 2,2',5,5'-TCB, with an SPM concentration of 12 mg L^{-1}, as a function of time. These yielded the percentage 2,2',5,5'-TCB

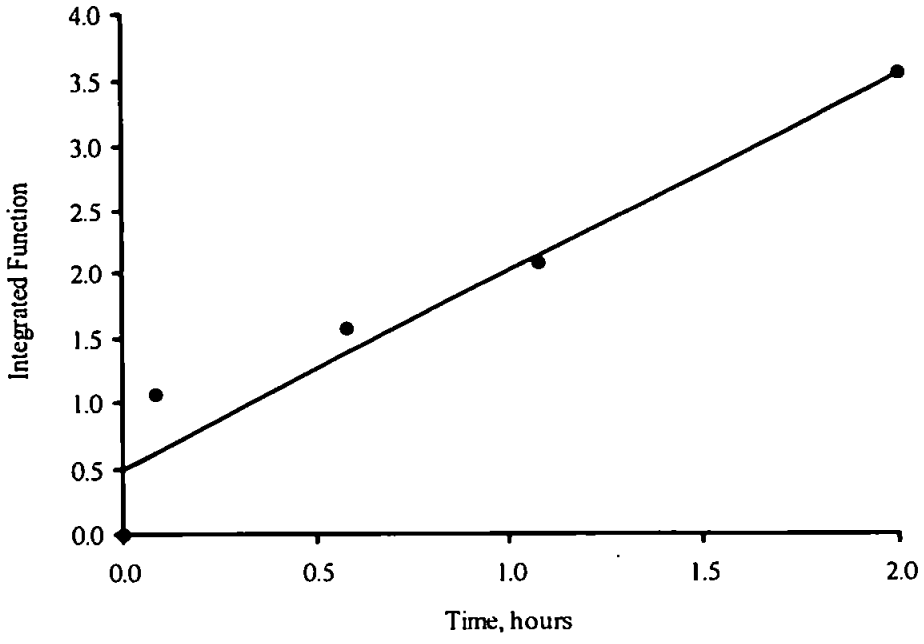

Figure 4.2: Integrated function (see Equation 4.12) versus time for 2,2',5,5'-TCB at a suspended particulate matter concentration of 12 mg L^{-1}.

remaining in solution as a function of time, $[^{14}C]_t$, which was then converted to the K_D via:

$$K_D^t = \frac{(100 - [^{14}C]_t) \cdot 10^6}{[^{14}C]_t \cdot SPM} \qquad (4.13)$$

The predicted and observed values are shown in Figure 4.3. and are in good agreement ($r^2 = 0.76$; n = 11). The forward rate constant obtained at an SPM concentration of 12 mg L^{-1} may also be applicable to higher concentrations of SPM. Thus, the data for 2,2',5,5'-TCB at an SPM concentration of 164 mg L^{-1} was fitted using $k_1 = 1.54\ h^{-1}$ and the results are shown in Figure 4.3. The results are in less good agreement ($r^2 = 0.50$; n = 11) than the results of the previous case, mainly due to the initial rapid uptake within the first 5 minutes. Nevertheless, these results suggest that the forward rate constant is independent of SPM concentration. The particle normalised rate constant, k_1^*, can then be calculated from the forward rate constant:

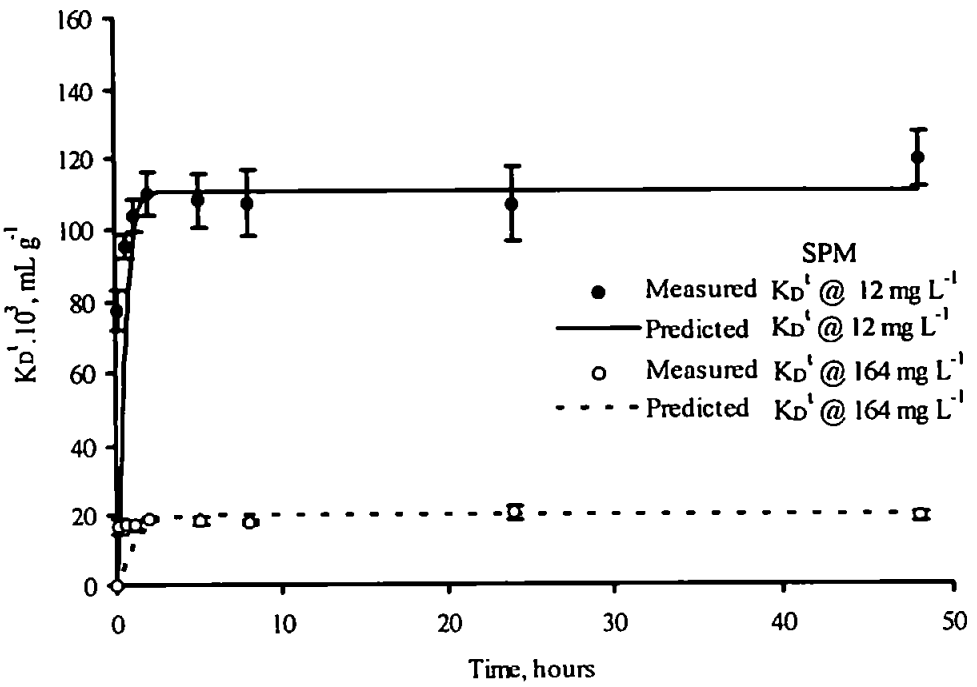

Figure 4.3: Partition coefficients, K_D^t, for 2,2',5,5'-TCB at a suspended particulate matter, SPM, concentration of 12 mg L^{-1} and 164 mg L^{-1} as a function of time for uptake onto Plym Estuary sediments. Both measured K_D^t (where n=4 and the error bars shown are the propagated errors) and predicted K_D^t, based on Equation 4.13 and the forward rate constant obtained at an SPM concentration of 12 mg L^{-1}, are shown.

$$k_1^* = \frac{24\ k_1}{SPM.10^{-6}} \qquad (4.14)$$

The value of k_1^* is 3.1x10^6 mL g^{-1} day^{-1} at 12 mg L^{-1} and 0.2x10^6 mL g^{-1} day^{-1} at 164 mg L^{-1}.

The forward, k_1, and reverse, k_{-1}, rate constants can also be used to estimate the system response time, τ_{resp}, which is defined as the time required to attain 1-(1/2.72) or 63% of the new particle-water partitioning equilibrium after the system has been altered (Honeyman & Santschi, 1988):

$$\tau_{resp} = \frac{1}{k_1 + k_{-1}} \qquad (4.15)$$

For 2,2',5,5'-TCB at 12 mg L^{-1} τ_{resp} was 0.37 hours or approximately 20 minutes.

A similar treatment was made for the BaP data, although reasonable fits could only be obtained for the uptake data (Figure 4.1.(ii)) with an SPM concentration of 12 mg L^{-1}. The forward rate constant was obtained from plotting the uptake data (Figure 4.1.(ii)) according to Equation 4.12 and it was found that $k_1 = 3\ h^{-1}$. Using Equation 4.6 $k_{-1} = 40\ h^{-1}$, $k_1^* = 6x10^6$ mL g^{-1} day^{-1} (Equation 4.14) and $\tau_{resp} = 1$ minute (Equation 4.15). Figure 4.4. shows the observed and predicted K_Ds for BaP, where the fit between the two values is reasonable ($r^2 = 0.66$; n = 11). Thus, the uptake of BaP can be described as kinetically rapid, with the reaction going almost to completion within a few minutes, and equilibrium modelling is appropriate for this compound in estuaries.

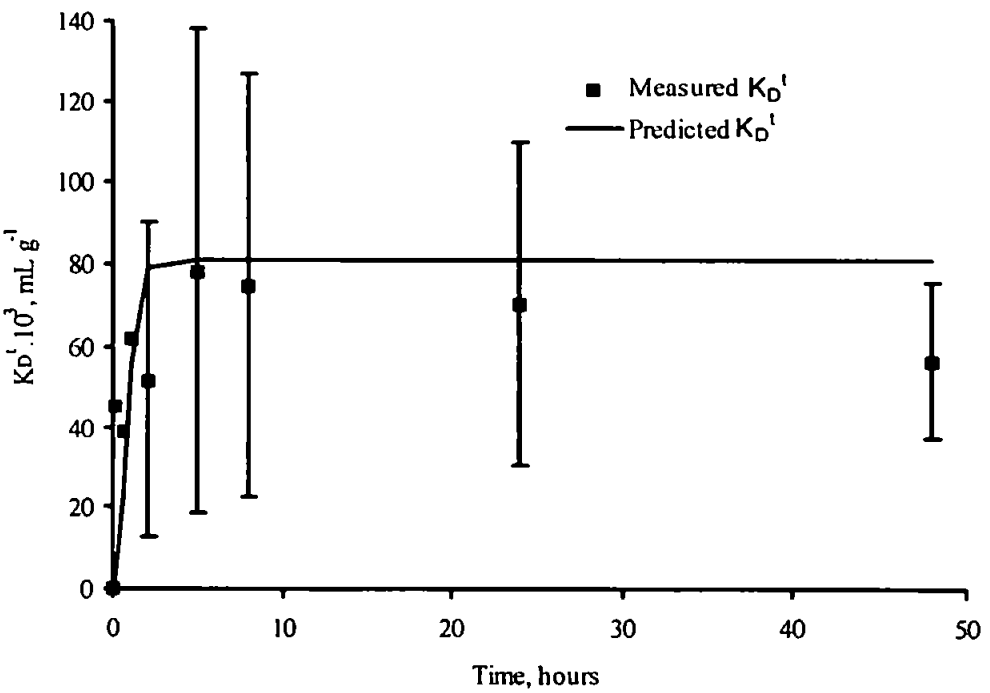

Figure 4.4: Partition coefficients for BaP at a suspended particulate matter concentration of 12 mg L^{-1} as a function of time for uptake on to Plym Estuary sediments. Both measured K_D^t (where n=4 and the error bars shown are the propagated errors) and predicted K_D^t, based on Equation 4.13, are shown.

4.3. Adsorption Isotherms

Adsorption isotherms were determined, from the experimental procedure outlined in Section 2.7., using estuarine water and sediment at end member salinities and an SPM concentration of ~150 mg L^{-1}, typical of macrotidal estuaries (Eisma, 1993), over a 16 hour period (Section 4.2.) for each HOM in order to investigate the nature of the adsorption process.

4.3.1. 2,2',5,5'-Tetrachlorobiphenyl

The adsorption of 2,2',5,5'-TCB to the sediment particles of each of the estuaries under investigation can be described by the Freundlich isotherm (Karickhoff, 1984):

$$P = mC^n \qquad (4.16)$$

where P is the concentration of the compound in the particulate phase (w/w), C is the concentration of the compound in the dissolved phase (w/v), m is the Freundlich constant and n is a measure of the non-linearity of the isotherm or the adsorption process. The adsorption isotherms for 2,2',5,5'-TCB were linear (Figure 4.5.); *i.e.* they pass through the origin, the constant n is equal to unity, and m, the slope of the line, is equivalent to the K_D, *i.e.*:

$$P = K_D C \qquad (4.17)$$

Statistical analysis of the 2,2',5,5'-TCB adsorption isotherms (Figure 4.5.), in the different estuaries is summarised in Table 4.3., and demonstrates the low propagated errors, high correlation coefficients (r^2 >0.99) and low p values. The K_D values determined for the various estuaries were of the same order of magnitude as published K_Ds and are discussed later (Section 4.4.3.3.; Table 4.15.). Linear adsorption isotherms over a given range of aqueous concentrations suggest that adsorption on to the estuarine sediment surface sites remains constant, with no change in availability of binding sites for the 2,2',5,5'-TCB molecules (as assumed for constant B when deriving Equation 4.2, Section 4.2.). The linearity of the results may only apply to the 16 hour incubation

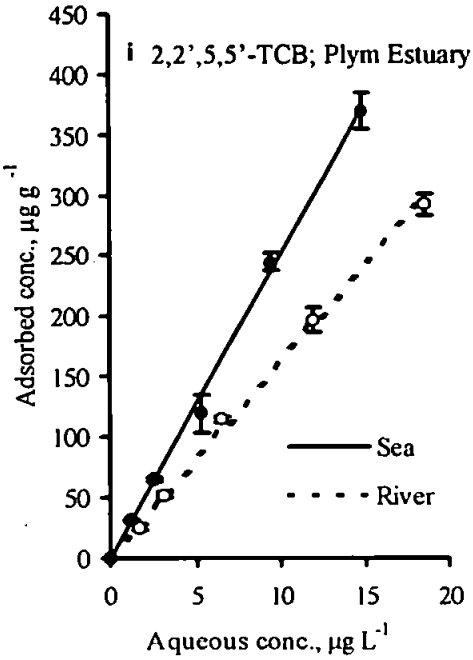

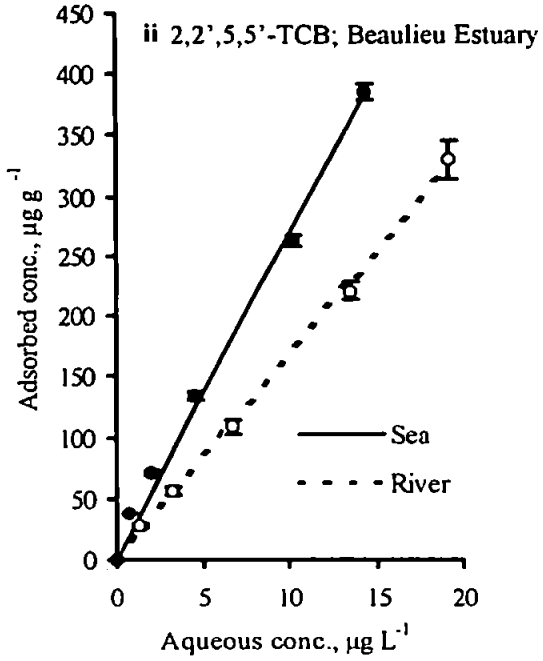

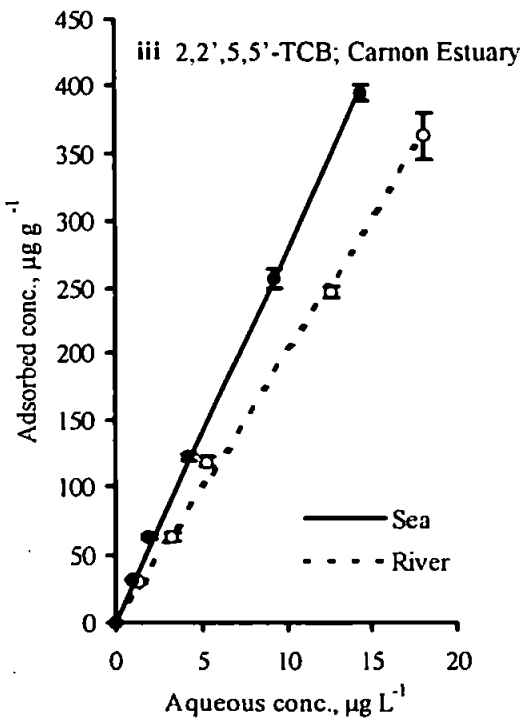

Figure 4.5: Adsorption isotherms for 2,2',5,5'-TCB in the (i) Plym, (ii) Beaulieu, and (iii) Carnon Estuaries, where n=4, and the error bars are the propagated error.

Table 4.3: Freundlich isotherm variables for 2,2',5,5'-TCB in the estuaries studied.

Estuary	n	Linear isotherm K_D (= m) (mL g^{-1})	r^2	p
Plym River	1	16160	0.997	<0.001
Plym Sea	1	25040	0.996	<0.001
Beaulieu River	1	16930	0.998	<0.001
Beaulieu Sea	1	26790	0.990	<0.001
Carnon River	1	20090	0.997	<0.001
Carnon Sea	1	27780	0.998	<0.001

period, reflecting the first stage of the reaction during which physical adsorption predominates. Kinetic data (Section 4.2.) showed a slow, (> 21 days), second phase HOM adsorption onto the particles after an initial rapid uptake. Non-linear effects of adsorption may occur after this timescale, but were not investigated in this study.

The 2,2',5,5'-TCB adsorption isotherms (Figure 4.5.) also indicate an enhanced adsorption in sea water compared with river water. To determine whether this increase in K_D is a result of a change in the relative solubility of the HOMs only (*i.e.* a reduced relative solubility in sea water due to the 'salting out' effect; Section 3.2.4.), or as a result of changes in particulate organic matter as well, the following equation based on the Setschenow concept was applied (Means, 1995):

$$\log\left(\frac{K_D^{sw}}{K_D^{rw}}\right) = \sigma_p M - \log\gamma_p \qquad (4.18)$$

where K_D^{sw} and K_D^{rw} are the partition coefficients (mL g^{-1}) in sea water and river water, respectively (determined from the linear adsorption isotherms), σ_p is an adsorption salting constant, M is the effective molar concentration of sea water, and γ_p is the activity coefficient of the compound in the estuarine sediment particulate organic matter. Assuming that the organic matter of the particles approximates to an ideal reference phase, γ_p will approach unity, and given that M is 0.5 mol L^{-1}, adsorption salting constants were derived and shown in Table 4.4. Values are 2-3 times greater than the estuarine relative solubility salting constant derived previously from relative solubility isotherm data (Section 3.2.4.2.), with the exception of the Carnon Estuary. This suggests

Table 4.4: Calculated salting constants (L mol^{-1}) for 2,2',5,5'-TCB in the estuaries studied.

Estuary	Adsorption salting constant (σ_p)	Relative solubility salting constant (σ_r)
Plym	0.380	0.187
Beaulieu	0.400	0.254
Carnon	0.280	0.352

that, in the case of the Plym and Beaulieu Estuaries, the adsorption increase in sea water is only partially resultant from the decrease in relative solubility caused by the salting out effect (Means, 1995).

It is important to point out that 2,2',5,5'-TCB, as well as DEHP and BaP, are non-ionic molecules, that do not contain hydrogen atoms attached to electronegative atoms. Hence, both hydrogen bonding and electrostatic attraction can be ruled out as binding mechanisms (Sullivan *et al.*, 1982). Hydrophobic interactions and Van der Waals attractions with the particulate surface are more likely to be the main binding processes. Thus, it is suggested that changes in the surface charge of the sediment organic layer occur in sea water, which increases the sorptive capacity of the natural sediments. Hunter & Liss (1979) found a gradual decrease in the negative charge of the organic film around riverine sediments during mixing with high ionic strength sea water, which would allow non-polar HOMs to adsorb more readily to the particulate organic matter, POC, in sea water. Alternatively, changes in the conformation of the organic layer in 3-dimensional space, involving the folding of hydrophobic adsorption sites, may result in the 'trapping' of the HOM in the organic layer of the sediment (Means, 1995). This is represented by the conceptual model shown in Figure 4.6. However, this does not explain the adsorption salting constant being lower than the relative solubility salting constant in the Carnon Estuary. The Carnon River water was relatively acidic until the mixing of fresh water and sea water gave a significant increase in pH, which in turn caused an increase in the negative surface charge of the particle. This is confirmed by the work of Newton & Liss (1987) which describes the change in the surface charge of iron oxide particles from the Carnon estuary. In this case, positively charged river particles at low pH became negatively charged on encountering the high pH sea waters. The reverse charge effect therefore occurs on the Carnon Estuary particles to that occurring for the Plym and

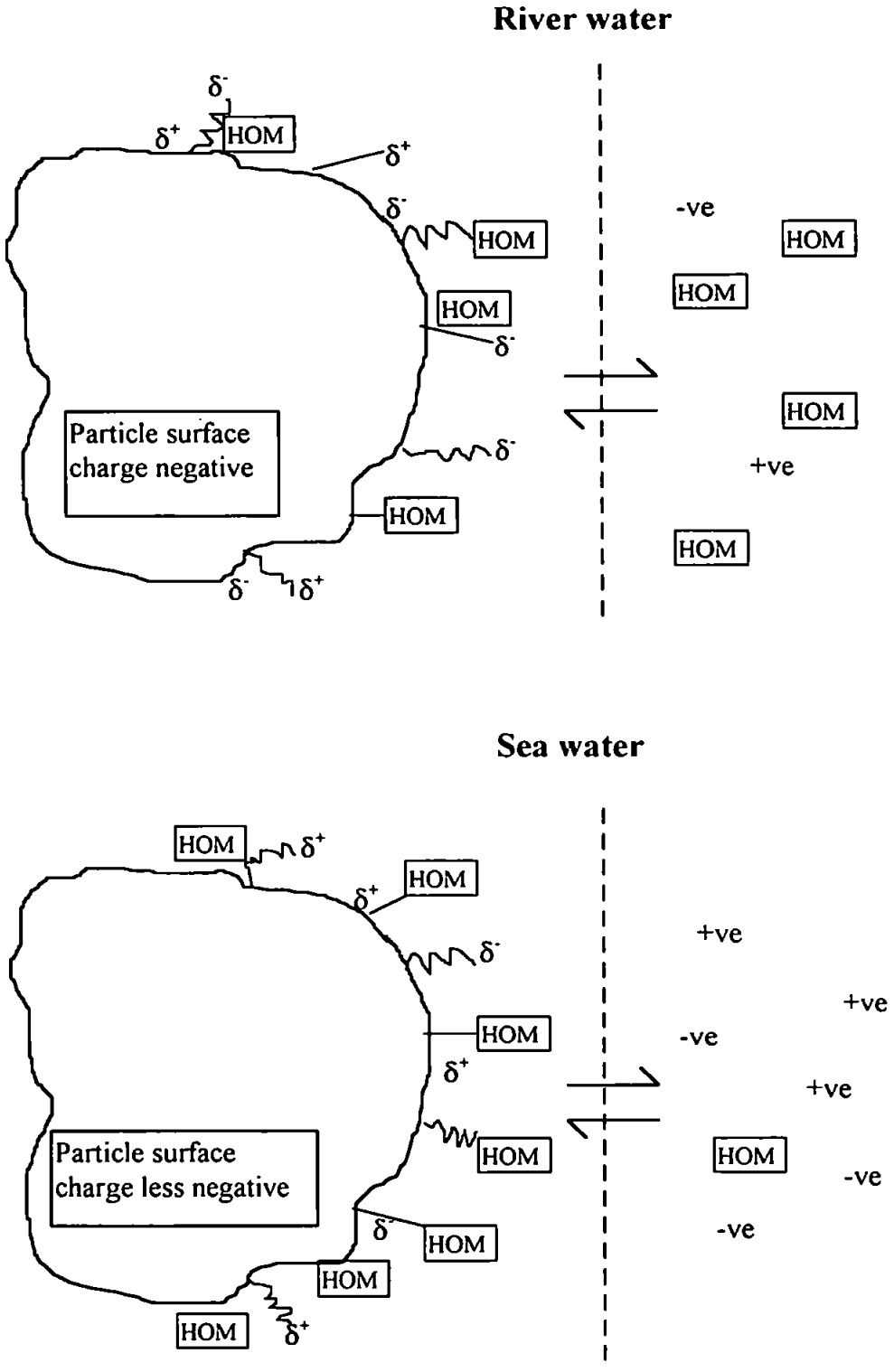

Figure 4.6: Conceptual representation of the adsorption of hydrophobic organic micropollutants, HOMs, on to estuarine particles in river water and sea water, where +ve and -ve represent dissolved ions.

Beaulieu estuarine particles, and therefore, the increase in adsorption with salinity in the Carnon is partly offset by this charge effect.

4.3.2. Bis(2-ethylhexyl)phthalate ester

There is no clear relationship between adsorbed and aqueous DEHP in the three estuaries investigated (Figure 4.7.). Several sea water data points have been omitted from the regressions due to high propagated errors, and have been indicated on the appropriate graphs in Figure 4.7. Such a scatter of data is a common problem for phthalate esters and is seen throughout the literature (Russell & McDuffie, 1986; Al-Omran & Preston, 1987) and may be attributed to the ability of DEHP to form stable homogeneous dispersions in solution (*i.e.* micelles) (Brown *et al.*, 1996), and/or due to the formation of a surface layer of DEHP at the air-water interface, causing analytical errors during extraction of the aqueous phase for analytical counting (Staples *et al.*, 1997). Non-linear adsorption isotherm data for DEHP can be derived by a log-log plot of Equation 4.16:

$$\log P = n \log C + \log m \qquad (4.19)$$

Thus, K_D will vary as a function of the amount of compound present. Data for both linear and non-linear Freundlich isotherms are shown in Table 4.5. Although the r^2 values are better for non-linear Freundlich isotherms, their p values are greater. Thus, linear Freundlich isotherms are statistically more significant for DEHP (Figure 4.7.). One non-linear isotherm has been shown, for the Plym River, for reference.

Non-linear adsorption isotherms ($n < 1$) suggest that preferable adsorption sites for DEHP molecules become occupied and as the phthalate concentration increases, sorption to the particle sites becomes more difficult as remaining sorption sites are less attractive (Schwarzenbach *et al.*, 1993). A study of DEHP sorption to Mississippi River sediments (Williams *et al.*, 1995) found a value of n of about 0.9.

In some cases (*i.e.* Beaulieu river and sea water, Figure 4.7. (ii) a & b) adsorption isotherms may be sigmoid in shape, indicative of a more complex 3-phase adsorption process. At low aqueous concentrations of DEHP, adsorption is preferential (as explained above), followed by a period of non-adsorption, when the particle adsorption sites may be undergoing modification, and then additional adsorption of DEHP at

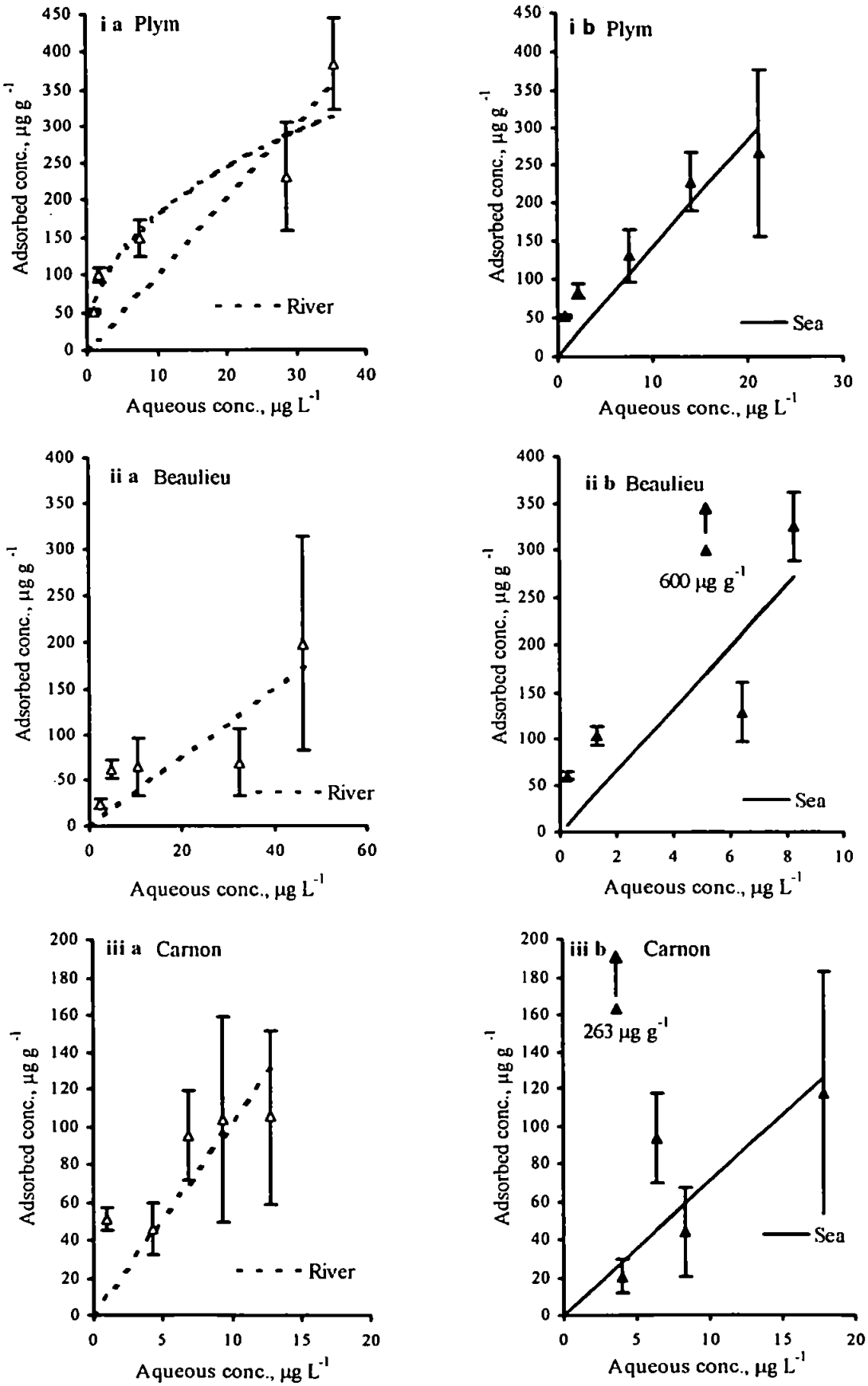

Figure 4.7: Adsorption isotherms for DEHP in the (i) Plym, (ii) Beaulieu, and (iii) Carnon, for a. river water and b. sea water, where n=4 and the error bars are the propagated errors.

high aqueous concentrations. The nature of adsorption of DEHP to estuarine sediments is, however, difficult to evaluate as there is considerable scatter in the data.

Adsorption salting constants (Equation 4.18) calculated from the linear adsorption isotherms for the Plym and Beaulieu Estuaries are shown in Table 4.6., and show an enhanced adsorption to the organic carbon-rich Beaulieu sediments in sea water, similar to that for 2,2',5,5'-TCB, but less enhancement for the relatively organic carbon-poor Plym sediments. Adsorption of DEHP was lowest in the high organic waters of the Beaulieu River. This is possibly due to the compound associating strongly with the soluble humic acids, retaining DEHP in the aqueous phase (Staples *et al.*, 1997). In sea water, soluble humic acids and their associated HOMs, bind with the particles (via salting out). Thus, particle characteristics are changed by the adsorbed humic acid and unassociated DEHP is taken up. This mechanism explains why the adsorption of DEHP on to Beaulieu sediments is enhanced.

A negative adsorption salting constant was calculated for the Carnon Estuary as adsorption was greater in the Carnon river water that in Carnon sea water. Although propagated errors were large, this observation indicates that there is a 'salting in' effect occurring for DEHP. This can be explained by the change in Carnon particulate surface charge from positively charged riverine particles to negatively charged marine particles (Newton & Liss, 1987), which render the particulate organic matter less available for adsorption in sea water by DEHP.

Table 4.5: Freundlich isotherm variables for DEHP in various estuarine systems.

		Linear isotherm			Non-linear isotherm			
Estuary	**n**	**K_D (mL g^{-1})**	**r^2**	**p**	**n**	**m**	**r^2**	**p**
Plym River	1	10050	0.731	0.002	0.45	62.74	0.915	0.011
Plym Sea	1	14180	0.789	0.001	0.49	58.13	0.979	0.001
Beaulieu River	1	3770	0.647	0.006	0.51	19.98	0.749	0.058
Beaulieu Sea	1	33030	0.613	0.018	0.37	99.23	0.765	0.126
Carnon River	1	44580	0.118	0.003	0.32	44.58	0.630	0.109
Carnon Sea	1	7060	0.549	0.015	0.99	7.37	0.620	0.213

Table 4.6: Calculated salting constants (L mol^{-1}) for DEHP.

Estuary	Adsorption salting constant (σ_p)	Relative solubility salting constant (σ_r)
Plym	0.30	0.28
Beaulieu	1.90	1.19
Carnon	-1.60	0.05

4.3.3. Benzo[a]pyrene

Adsorption isotherms for BaP are shown in Figure 4.8. and have been defined by both linear and non-linear Freundlich isotherms in Table 4.7. The linear isotherms are statistically more significant and have been shown in Figure 4.8., along with a non-linear isotherm for the Plym River for comparison. The adsorption salting constant for the Plym Estuary (Table 4.8.) is greater than the published Setschenow constant (a relative solubility salting constant could not be derived from the data in Chapter 3), indicating that enhanced adsorption in sea water to the Plym sediments is not only due to a decrease in the relatively solubility of BaP in sea water, but due to changes in the particulate surface charge and organic matter (as discussed for the 2,2',5,5'-TCB).

As was the case for DEHP a negative adsorption salting constant was calculated for the Carnon data, as adsorption was greater in the Carnon River than in the Carnon sea water, suggesting that a 'salting in' effect, with enhanced BaP adsorption in river water.

Table 4.7: Freundlich isotherm variables for BaP in various estuarine systems.

	Linear isotherm				Non-linear isotherm			
Estuary	n	K_D (mL g^{-1})	r^2	p	n	m	r^2	p
Plym River	1	22980	0.893	<0.001	1.79	17.55	0.960	0.001
Plym Sea	1	36740	0.976	<0.001	0.87	37.65	0.919	0.003
Carnon River	1	81500	0.930	<0.001	0.74	69.88	0.889	0.005
Carnon Sea	1	56270	0.857	<0.001	1.00	58.03	0.853	0.009

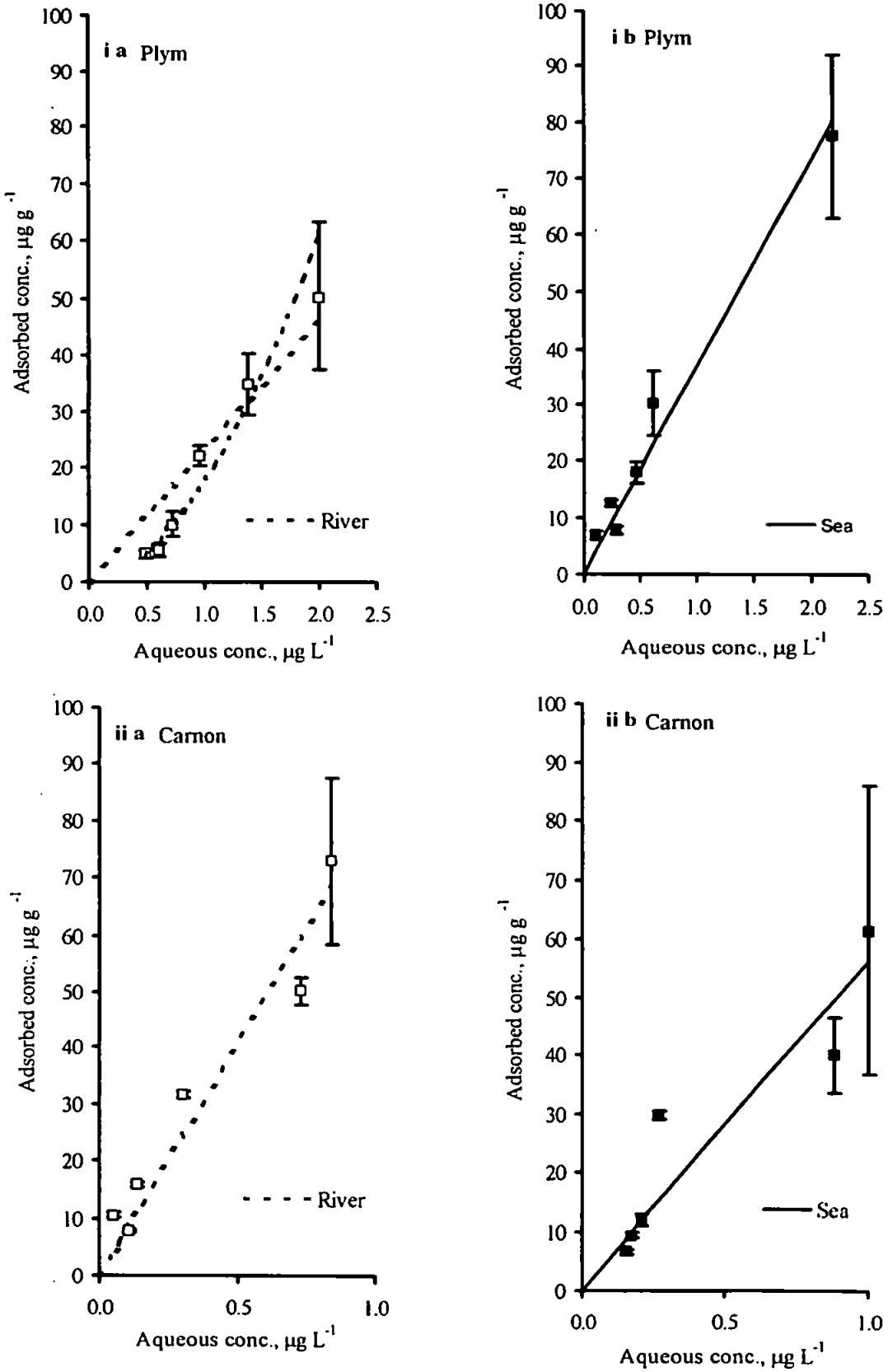

Figure 4.8: Adsorption isotherms for BaP in the (i) Plym and (ii) Carnon estuaries for a. river water and b. sea water, where n=4 and the error bars shown are the propagated errors.

Table 4.8: Calculated adsorption salting constant (L mol^{-1}) and published Setschenow constant (L mol^{-1}) for BaP.

Estuary	Adsorption salting constant (σ_p)	Setschenow constant (σ)
Plym	0.408	
Carnon	-0.322	
		0.199[a]

Source: [a] Means, 1995.

4.4. Particle Concentration Effect

4.4.1. Particle concentration and salinity

Having established that enhanced adsorption of HOMs occurs at high salinities compared to river waters, the next stage was to investigate the role of varying salinity and SPM concentration, throughout the estuarine mixing range, on HOM sorption. An initial experiment involved the adsorption of 2,2',5,5'-TCB over an SPM concentration range of 10-600 mg L^{-1}, to simulate the SPM concentration range normally encountered in macrotidal estuaries, and five different salinities using Dart Estuary samples (Figure 4.9.). The reproducibility of the data was excellent, shown by the low propagated errors. At each SPM concentration a linear equation (Table 4.9.) can be used to describe the effect of salinity on adsorption:

$$K_D = K\,S + K_D^\circ \qquad (4.20)$$

where K is a constant equal to the gradient of the line, S is the salinity ($x10^{-3}$), and K_D° is the partition coefficient (mg L^{-1}) in pure water. Thus, adsorption due to the salting out of the compound (and the particulate organic matter), increases in direct proportion to the concentration of sea water ions, as was found for the relative solubility of 2,2',5,5'-TCB (see Section 3.2.4.). More significantly, however, at each salinity the K_D increased dramatically with a decrease in SPM concentration, suggesting that the particle concentration effect, PCE, was a more important controlling factor of K_D than salinity. For example, K_D increases by no more than 50% over the salinities used, while K_D increases by over ten-fold between SPM concentrations 10 and 600 mg L^{-1}. Magnitudes

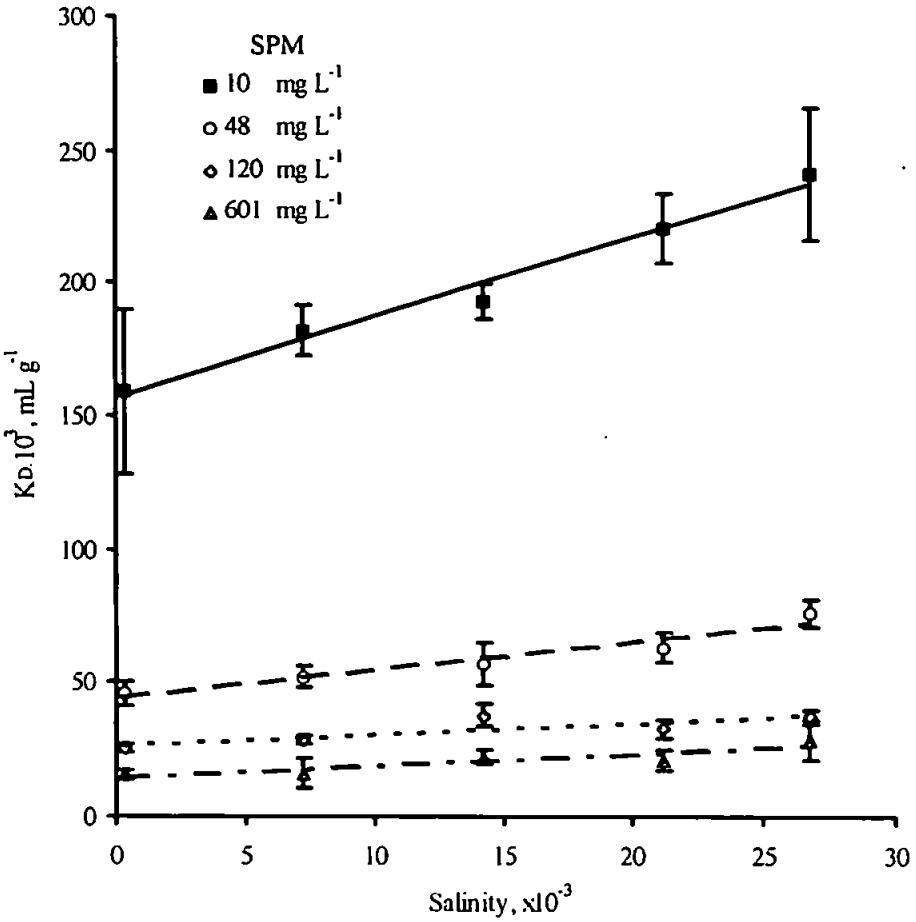

Figure 4.9: Partition coefficients, K_Ds, for 2,2',5,5'-TCB as a function of salinity and suspended particulate matter, SPM, concentration in the Dart Estuary, where n=4 and the error bars are the propagated errors.

Table 4.9: Equations describing the linear relationship between 2,2',5,5'-TCB partition coefficients, K_D, and salinity, $Sx10^{-3}$, at different suspended particulate matter, SPM, concentrations in the River Dart.

SPM ($mg\ L^{-1}$)	**Equation**	**r^2**	**p**
10	$K_D = 3060000S + 156000$	0.982	0.001
48	$K_D = 1080000S + 43700$	0.939	0.007
120	$K_D = 421000S + 26400$	0.674	0.089
600	$K_D = 457000S + 14100$	0.834	0.030

of the constants, K and K_D^o, show that the influence of salting out is greatest at low SPM concentrations, probably because there are less particles per mole of salt present, and salt-induced modification of the particle surface is greatest. Because of the apparent significance of SPM concentration, it was decided to investigate the effect of SPM concentration on K_D for each of the HOMs and estuaries under investigation at end member salinities.

4.4.2. Particle concentration effect

Partition coefficients, K_Ds, for 2,2'5,5'-TCB in the Dart Estuary as a function of SPM concentration (10 mg L^{-1}-1000 mg L^{-1}), and at the extremes of salinity, are shown in Figure 4.10. The inverse relationship between K_D and SPM concentration is well documented in the literature and is referred to as the particle concentration effect, PCE (Gschwend & Wu, 1985; MacKay & Powers, 1987; McKinley & Jenne, 1991). The PCE occurs for all five estuaries, and can be defined by a simple power law, derived from the regression of log K_D against log SPM concentration (Figure 4.11.):

$$\log K_D = \log a - b \log SPM \qquad (4.21)$$

$$K_D = a\, SPM^{-b} \qquad (4.22)$$

where a and b are the constants equivalent to the intercept and gradient of the curve, respectively. Regressions are also shown in terms of K_{oc}, the organic carbon normalised partition coefficient (Gawlik *et al.*, 1997):

$$K_{oc} = \frac{K_D}{POC} \cdot 100 \qquad (4.23)$$

where POC is the particulate organic matter concentration (%). Equation and statistical parameters for each of the estuarine environments are listed in Table 4.10.

The equation obtained for 2,2',5,5'-TCB particle-water partitioning in the Chupa Estuary is distinctly different from those obtained in the British estuaries (Table 4.10) due to the small SPM concentration range over which the Chupa survey was conducted, resulting in only part of the full effect being observed. The effect of salting out of HOMs

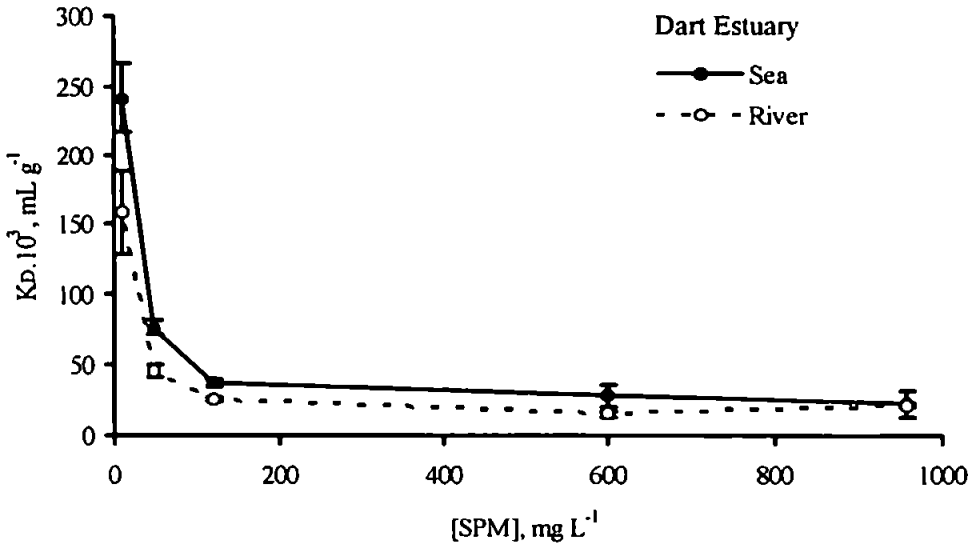

Figure 4.10: Partition coefficients, K_DS, for 2,2',5,5'-TCB as a function of suspended particulate matter, SPM, concentration and salinity in the Dart Estuary, where n=4 and the error bars are the propagated errors.

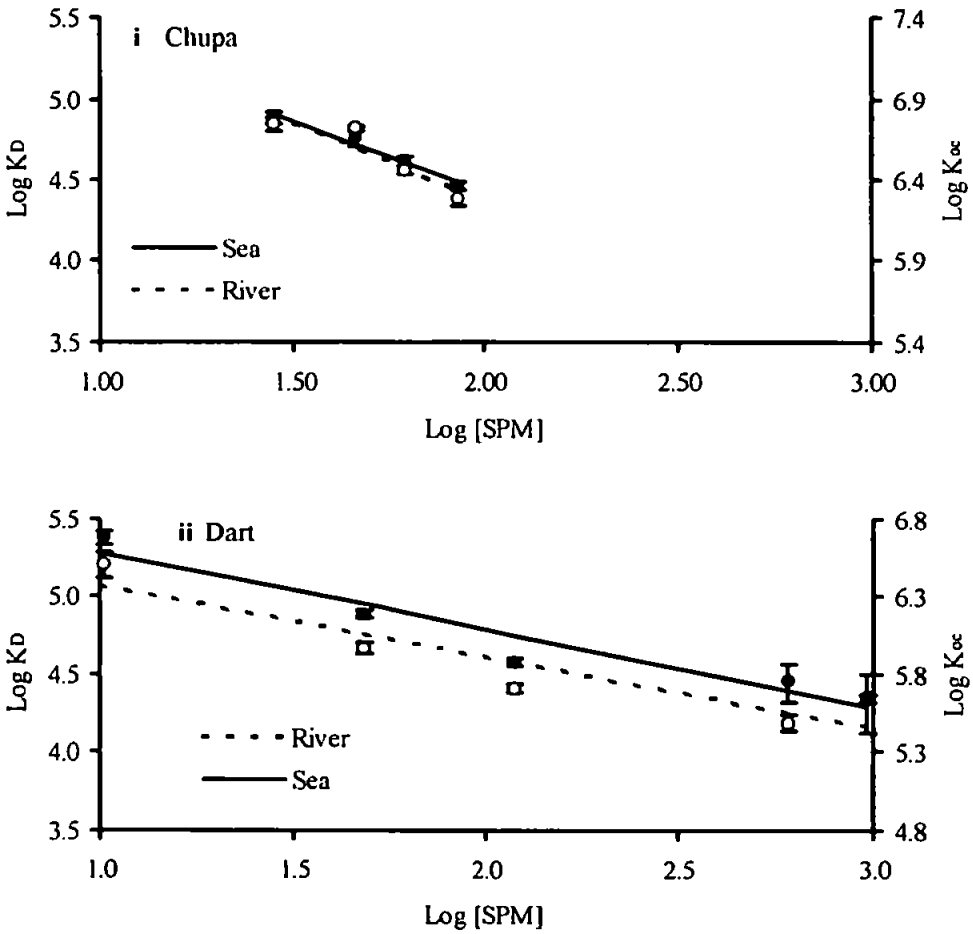

Figure 4.11: Partition coefficients, as log K_D and log K_{oc}, of 2,2',5,5'-TCB as a function of particle concentration, as log [SPM], in river water and sea water for the (i) Chupa, (ii) Dart, (iii) Plym, (iv) Beaulieu, and (v) Carnon Estuaries, where n=4 and the error bars are the propagated errors.

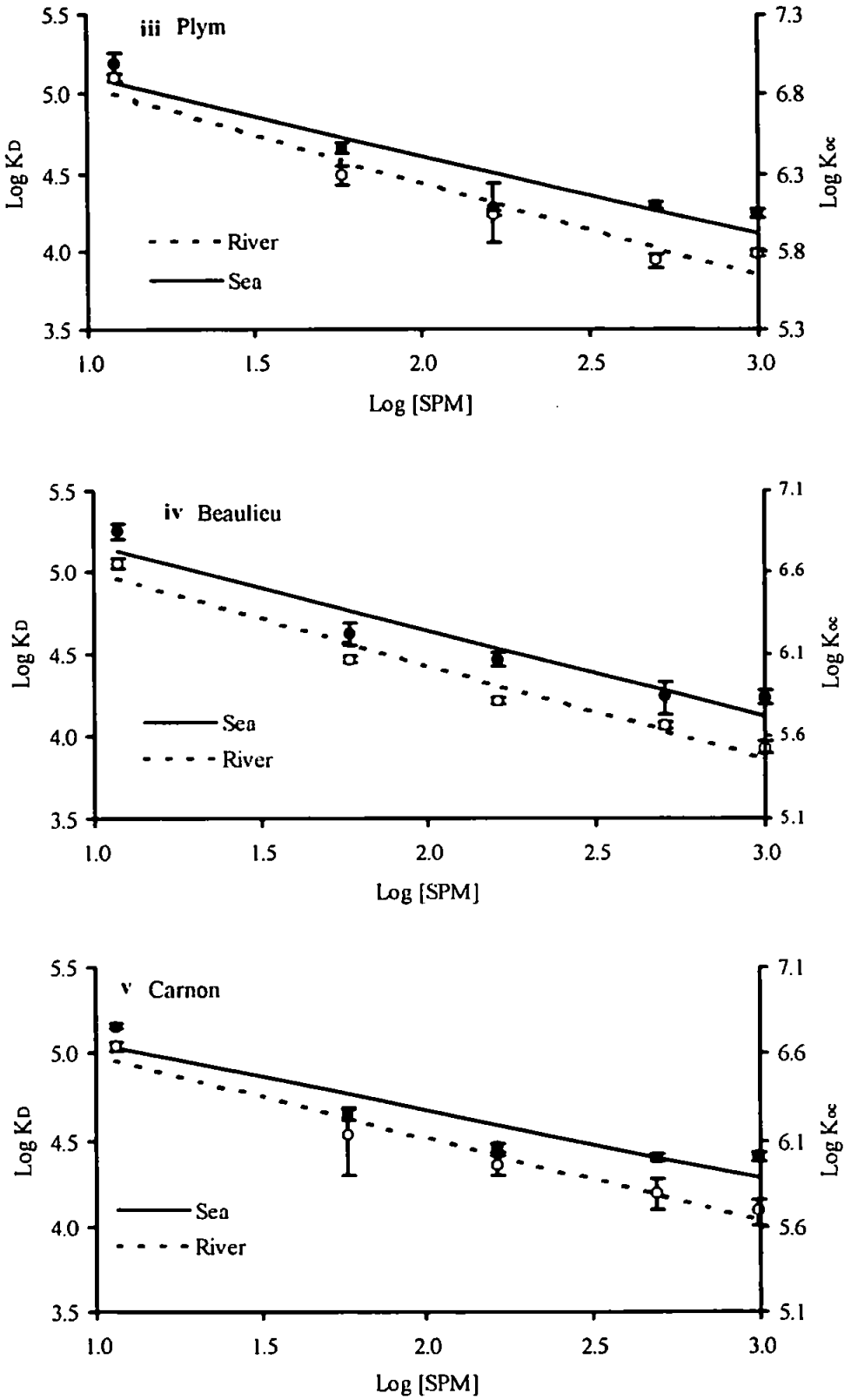

Figure 4.11: Continued.

Table 4.10: Model parameters defined for the particle concentration effect for 2,2',5,5'-TCB partition coefficients in five estuaries.

Estuary	$a.10^5$	b	r^2	p
Chupa River	23.3	1.00	0.855	0.075
Chupa Sea	15.9	0.89	0.966	0.017
Dart River	3.28	0.46	0.853	0.025
Dart Sea	6.01	0.50	0.927	0.009
Plym River	4.53	0.61	0.941	0.006
Plym Sea	3.98	0.50	0.869	0.021
Beaulieu River	3.66	0.57	0.957	0.004
Beaulieu Sea	4.96	0.53	0.922	0.009
Carnon River	2.94	0.48	0.962	0.003
Carnon Sea	2.76	0.38	0.854	0.025

on particle-water interactions is clearly shown in Figure 4.11., with the K_Ds being consistently higher in sea water than river water for all five estuaries over the full range of SPM concentrations. (This is not directly evident in the parameter values listed in Table 4.10., as the effect is sensitive to a combination of both parameters a and b.) The parameters a and b obtained from Equation 4.22 for 2,2',5,5'-TCB were relatively similar for the four British estuaries, compared with the Chupa Estuary parameters, despite the contrasting physicochemical properties of the British estuarine waters and the geochemical characteristics of their sediments. This suggests that changes in particle composition exert relatively little effect on the particle-water partitioning of 2,2',5,5'-TCB compared with particle concentration.

The role of particle geochemistry was investigated further by regressing the intercept (parameter a) from Equation 4.22, or the particle-concentration normalised K_D, against the different particle properties (Table 4.11.). Relationships were not significant at the 95% confidence interval but the r^2 values give some indication of the role of each parameter. Although, there is apparently no correlation with POC in river water (Figure 4.12.), there is a more significant correlation for POC in sea water. This is also reflected in the correlation results for Fe/Mn ratio, suggesting that the presence of salt modifies the particle in some way, causing adsorption to become more dependent upon particle geochemistry. Correlation results for Ca are more significant in river water than sea water, suggesting that the role played by dissolved Ca in HOM adsorption (Section 4.1.1.) is greater at the riverine end of the estuary.

Table 4.11: Results of the correlation of the intercept (parameter a in Equation 4.22) against the geochemical characteristics of the British estuaries sediments, for both river and sea water.

Geochemical characteristics	River water r^2	p	Sea water r^2	p
Fe/Mn ratio	0.008	0.910	0.482	0.306
Ca	0.648	0.195	0.118	0.656
POC	0.082	0.910	0.448	0.331
SSA	0.454	0.326	0.915	0.043

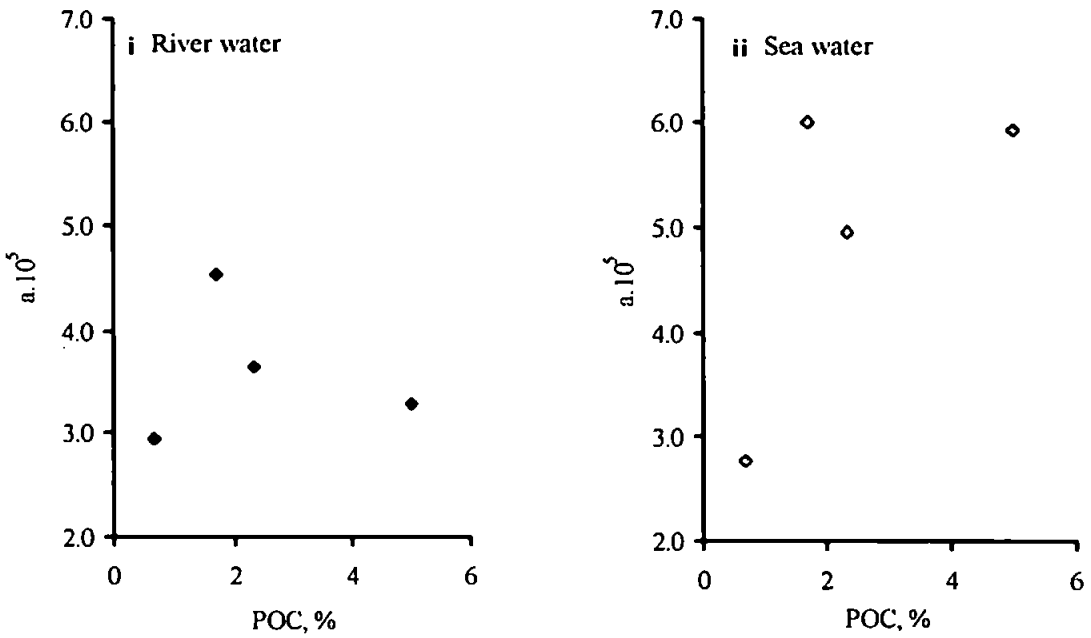

Figure 4.12: Intercept (parameter a in Equation 4.22) as a function of particulate organic carbon, POC, in (i) river water and (ii) sea water.

K_{DS} were similarly defined for DEHP in the Plym, Beaulieu, and Carnon Estuaries (Figure 4.13.), and for BaP in the Plym and Carnon Estuaries (Figure 4.14.). The model parameters are summarised in Table 4.12. The parameters for each compound are of the same order of magnitude suggesting that SPM concentration is a greater controlling factor on the particle-water partitioning than is particle type. The DEHP results, however, are not consistent with the salting in/salting out patterns shown by the corresponding adsorption isotherms, as in the case of the Plym and Carnon Estuaries.

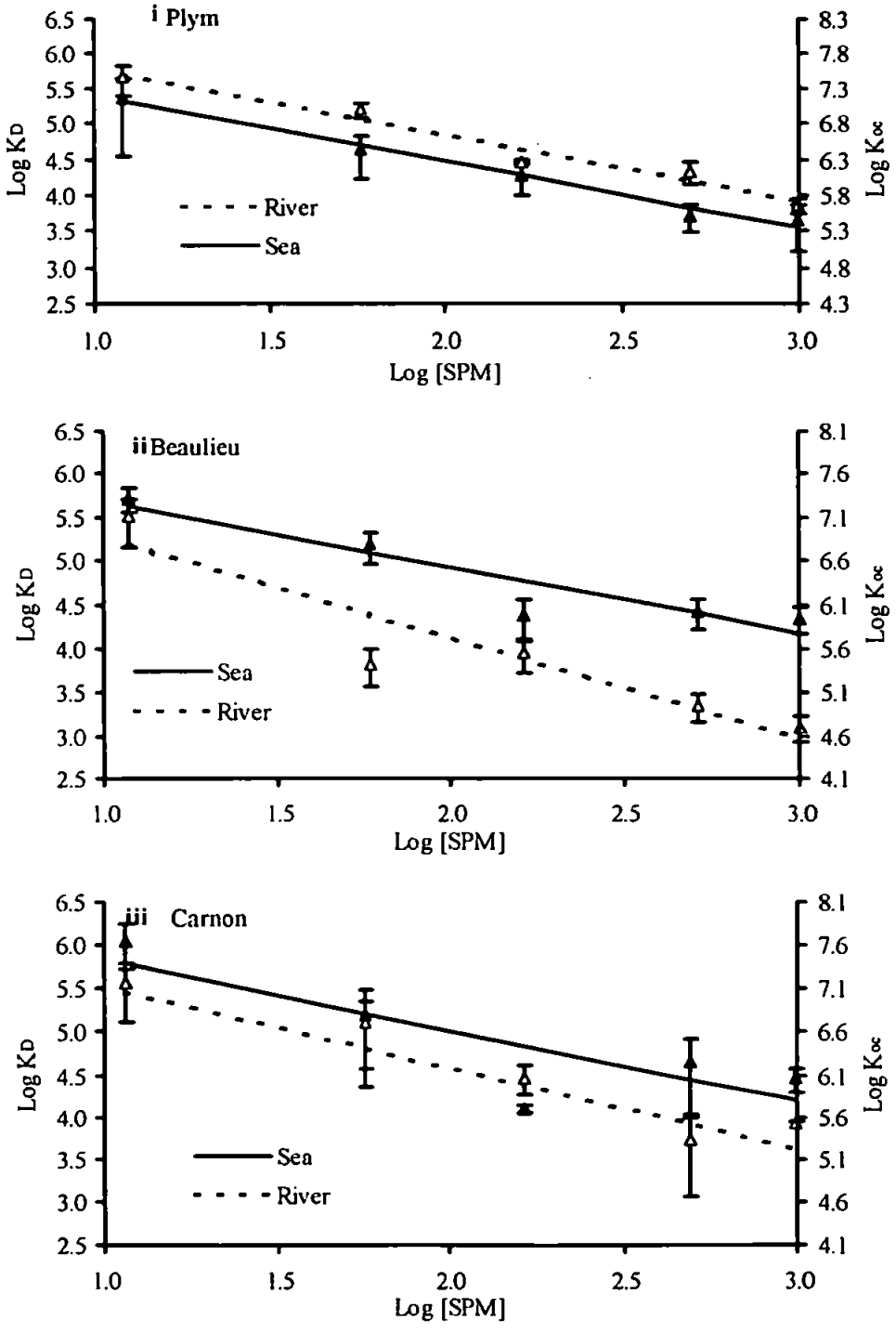

Figure 4.13: Partition coefficients, as log K_D and log K_{oc}, of DEHP as a function of particle concentration, as log [SPM], and salinity in the (i) Plym, (ii) Beaulieu, and (iii) Carnon Estuaries, where n=4 and the error bars are the propagated error.

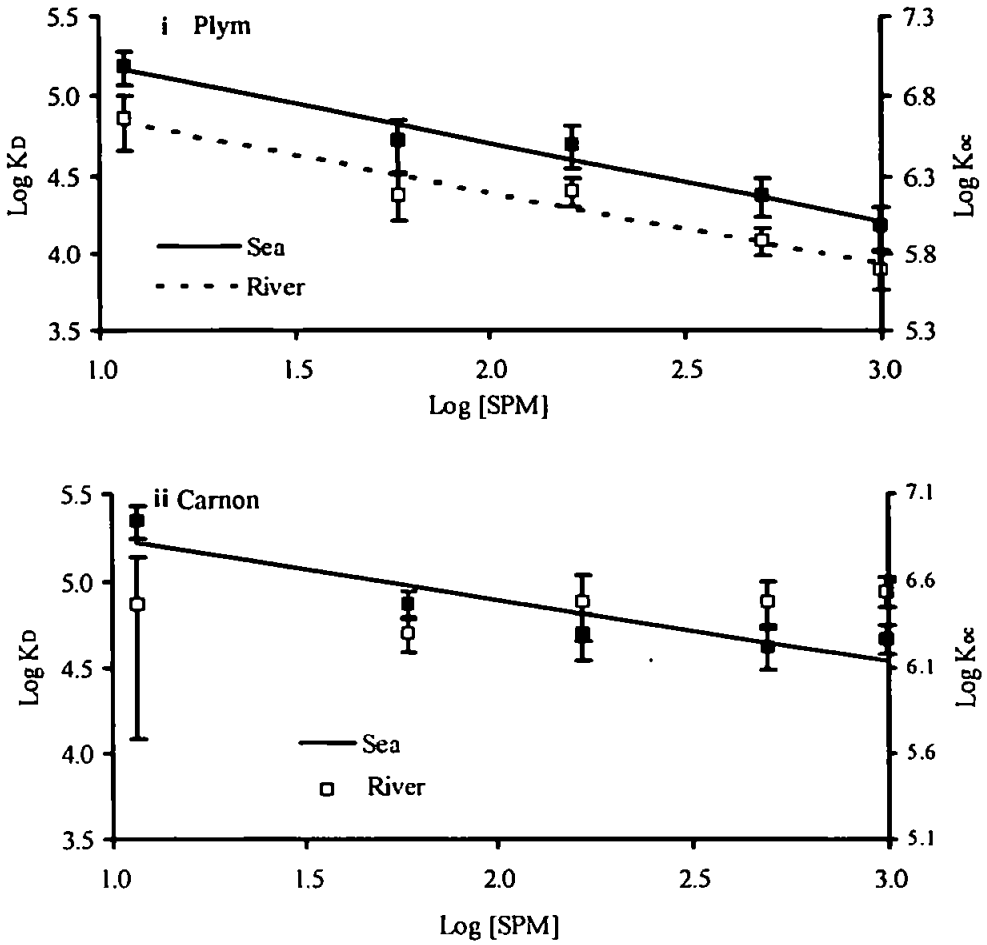

Figure 4.14: Partition coefficients, as log K_D and log K_{oc}, for BaP as a function of particle concentration, as log [SPM], and salinity in the (i) Plym and (ii) Carnon Estuaries, where n=4 and the error bars are the propagated errors.

Table 4.12: Model parameters defining the particle concentration effect for DEHP and BaP partition coefficients in various estuaries

	DEHP				BaP			
Estuary	**a.10^5**	**b**	**r²**	**p**	**a.10^5**	**b**	**r²**	**p**
Plym River	51.8	0.94	0.964	0.003	2.09	0.46	0.949	0.005
Plym Sea	21.2	0.93	0.986	0.001	4.77	0.49	0.963	0.003
Beaulieu River	26.6	1.15	0.876	0.019	ni	ni	ni	ni
Beaulieu Sea	26.6	0.75	0.872	0.020	ni	ni	ni	ni
Carnon River	46.7	0.98	0.934	0.007	ns	ns	ns	ns
Carnon Sea	44.8	0.82	0.684	0.084	4.05	0.36	0.836	0.030

where ni is not investigated and ns is not significant.

This could be due once again to the analytical difficulties associated with this compound (see Section 4.3.2.), which resulted in the large scatter of data points and poor propagated errors for the Carnon Estuary adsorption isotherms. In the case of the Plym Estuary, the 'salting in' of DEHP could be due to the non-linear adsorption isotherm determined for DEHP in the Plym River.

The BaP data for the Carnon Estuary confirms the 'salting in' shown by the corresponding isotherm, and also shows no clear PCE in Carnon river water. This may once again be due to the iron oxide rich particle type found in this acidic river as previously discussed.

4.4.3. Causes of the particle concentration effect

The decrease in K_D with an increase in particle concentration is found throughout the literature for a variety of HOMs (O'Connor & Connolly, 1980; Voice & Weber, 1985; Gschwend & Wu, 1985; MacKay & Powers, 1987; McKinley & Jenne, 1991). The possible causes include both experimental artefacts and environmental processes.

4.4.3.1. Analytical artefacts

Analytical artefacts include the following:

(i) Inadequate separation of the particulate and water phases by centrifugation whereby non-settleable colloidal particles are retained in the aqueous phase, an effect which becomes more pronounced with increasing particle (and colloidal) concentration, thus reducing the K_D value;

(ii) Incomplete extraction of the compound adsorbed on to the glassware leading to an overestimation of HOM associated with the particulate phase, thereby increasing the K_D. This effect becomes less pronounced with increasing SPM concentration;

(iii) Presence of a highly soluble radiochemical impurity which remains in the aqueous phase, causing an overestimation of the phase, hence an underestimation of K_D. This effect increases with increasing SPM concentration;

(iv) Insufficient time for equilibrium to be reached at each SPM concentration, as only the first rapid HOM adsorption has occurred by the 16 hour incubation period (see Section 4.2.).

Analytical artefacts contributing to the PCE were investigated further using 2,2',5,5'-TCB particle-water partitioning in the River Plym (Figure 4.15.). In the experiments there exists a three phase situation due to the incomplete separation of sediment and water phases during centrifugation, whereby non-settling and/or colloidal particles remain in the supernatant causing an underestimation of K_D at high SPM concentration. This effect was investigated by centrifuging a sediment-water suspension, and removing the supernatant containing any colloidal particles, then replacing the supernatant with filtered Plym river water, hence achieving a two phase system with the colloidal particles removed. This situation is conceptualised in Figure 4.16. The relationship between K_D and SPM concentration remained the same in both two and three phase systems, illustrated by almost identical equations for the appropriate K_D-SPM concentration curves shown in Table 4.13.

The second analytical artefact was investigated by recalculating K_Ds assuming a worst-case scenario of 20% loss of compound (irreversibly adsorbed to the glass walls) which was independent of the presence of particles. The K_Ds calculated in this way are shown by the third curve on Figure 4.15. The loss to the glassware is shown to be significant but the inverse relationship between K_D and particle concentration remains. Quantitatively, the intercept value, a, is halved, whilst the gradient value, b, remains the same.

The third analytical artefact regarding solubility impurity can also be discounted. Radio-GC analysis (see Section 2.5.1.) of the radio isotopes both before and after particle-water experiments showed a radiochemical purity in excess of 98% for all three HOMs. Assuming a worst case scenario of 2%, of a soluble contaminant, the K_D has been recalculated, and the results shown on Figure 4.15. Despite a slight increase in K_Ds at high SPM concentrations this does not account for the exponential relationship between K_D and SPM concentration.

Kinetic studies by Jepsen *et al.* (1995) on the adsorption of hexachlorobenzene to Detroit River sediments at SPM concentrations of 10, 100, 500, and 2000 mg L^{-1} continued to show the PCE throughout the 130 day experiment, when equilibrium was reached at all SPM concentrations. Thus kinetic effects are unlikely to contribute to the PCE, at least over timescales involved in estuarine sorption in the water column.

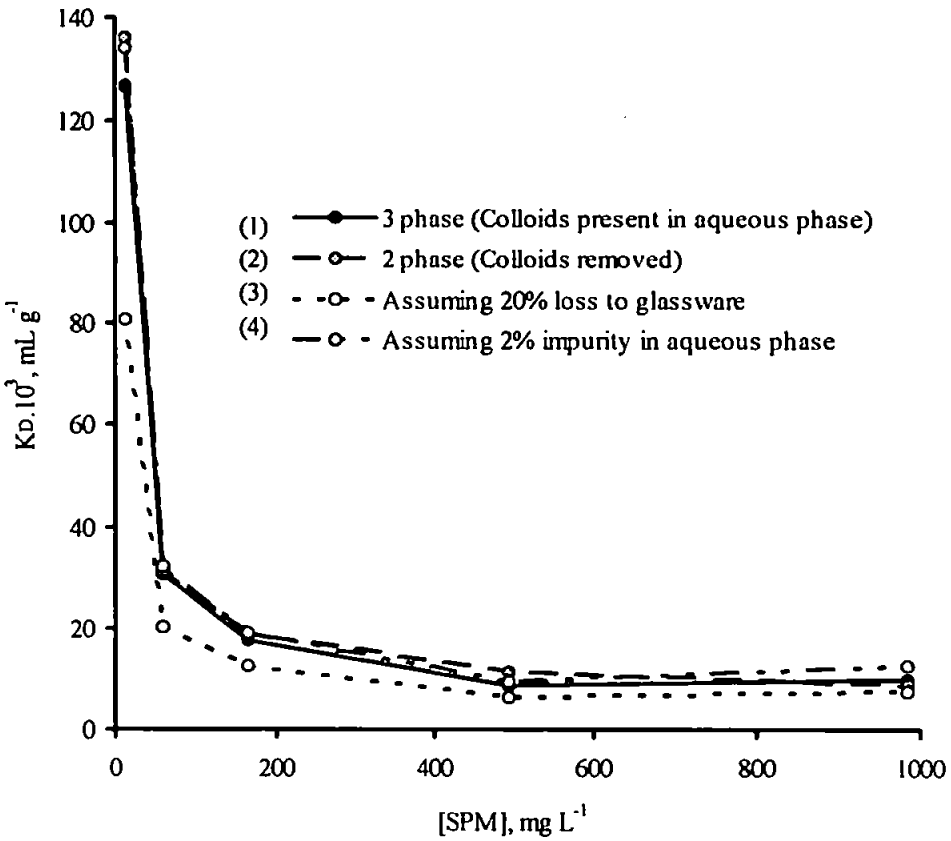

Figure 4.15: Particle concentration effect in the river Plym for 2,2',5,5'-TCB, showing 4 effects investigated.

Table 4.13: Model parameters for 2,2',5,5'-TCB particle concentration effect.

Estuary	$a.10^5$	b	r^2	p
3 phase	4.43	0.60	0.943	0.006
2 phase	4.87	0.61	0.967	0.003
Assuming 20% loss to glassware	2.50	0.56	0.931	0.008
Assuming 2% soluble impurity	4.12	0.57	0.912	0.011

i. Three phase

ii. Two phase

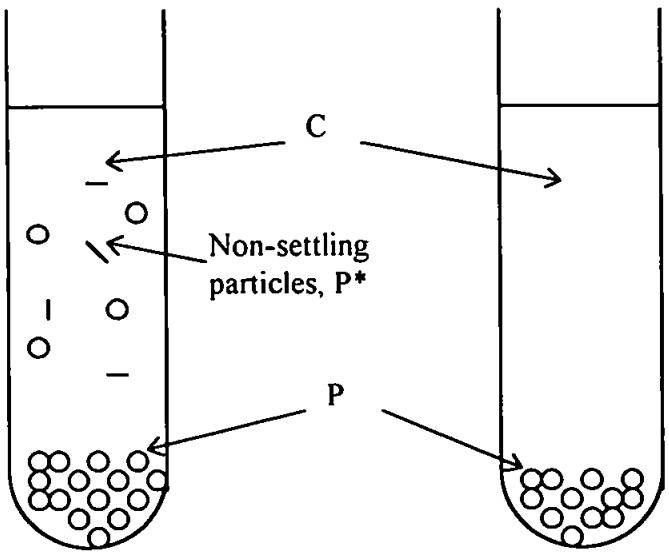

$$K_D = \frac{P}{C + P^*}$$

$$K_D = \frac{P}{C}$$

Figure 4.16: Conceptual representation of (i) the incomplete separation of the sediment and water phases during centrifugation, where the water phase contains colloids or non-settling particles, and (ii) the removal of the colloids or non-settling particles, where K_D is the particle-water partition coefficient, P is the compound concentration in the particulate phase (w/w), P* is the compound associated with the colloids or non-settling particles in the aqueous phase (w/v) and C is the compound concentration in the dissolved phase (w/v).

4.4.3.2. Environmental processes

Environmental processes suggested as causes of the PCE are based on increasing inter-particle collisions and/or particle interactions with increasing SPM concentration. This effect may result in:

(i) Release of solute-binding material (DOC) from sediment at high SPM concentration (through inter-particle collisions) therefore potentially increasing the concentration of HOM in the solution phase at high SPM concentration;

(ii) Increasing particle aggregation, thereby decreasing the available particle surface area per unit mass, with increasing SPM concentration;

(iii) Increasing particle disaggregation, exposing unfavourable adsorption sites with increasing SPM concentration.

Release of DOC and other solute binding material (e.g. colloids) from the sediment at high SPM concentration would result in an increase in aqueous 2,2',5,5'-TCB, hence a reduction in K_D at high SPM concentrations. This effect was further investigated by setting up a series of reactor tubes containing filtered Plym river water and Plym sediments at a concentration of ~ 500 mg L^{-1}. After centrifugation to separate the two phases, the supernatant was removed and placed in spiked reactor tubes, from which a relative solubility isotherm was derived (see Section 3.2.1.1.; Figure 3.2. and repeated in Figure 4.17. for clarity). An increase in DOC and/or colloid material was not accompanied by a significant increase in the gradient of the isotherm compared to the relative solubility isotherm of filtered Plym river water (the gradients were 34 and 32, respectively). Thus any release of DOC is not sufficient to significantly enhance the relative solubility of 2,2',5,5'-TCB, hence cause a significant PCE.

A possible explanation for the PCE is based on particle interactions. The quantities of SPM used in individual incubations were too low to allow determination of any changes in particle size and/or specific surface area. If the PCE is, in fact, due to particle interactions then it is likely that the PCE will be replicated in the field. This hypothesis was investigated further in the next section.

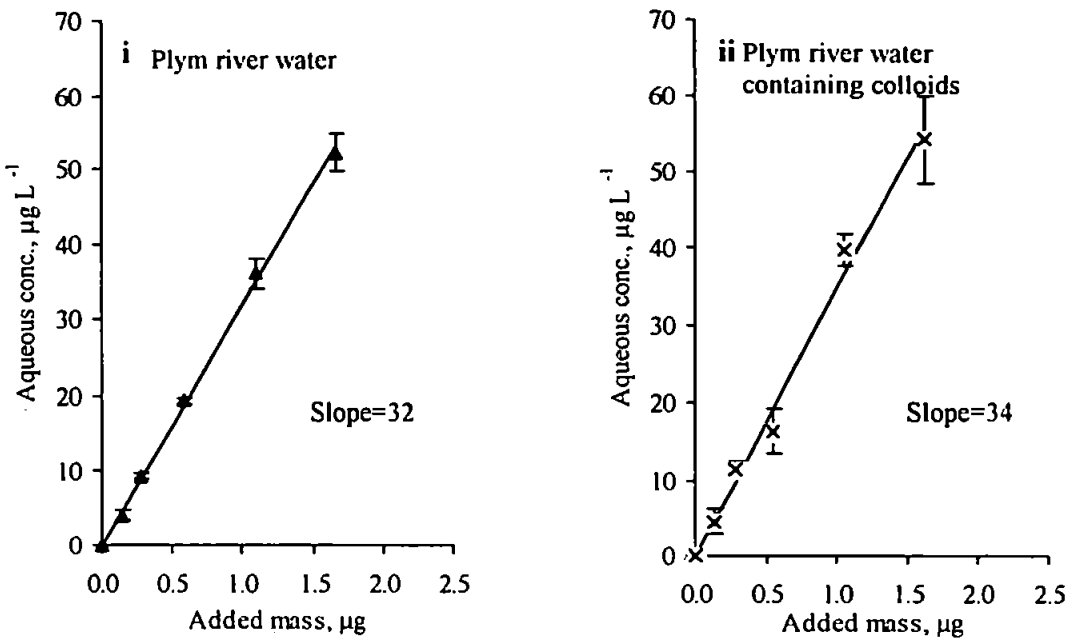

Figure 4.17: Relative solubility isotherms for 2,2',5,5'-TCB in (i) Plym river water and (ii) Plym river water containing colloids or non-settling particles, where the mean value and propagated values are shown (n=4).

4.4.3.3. Comparison of particle concentration effect with field data

Although the cause/s of the PCE remain unresolved, that the effect is observed in the field for many HOMs (Baker *et al.*, 1986; Eadie *et al.*, 1990) suggests it is the result, at least in part, of some natural (probably particle interactive) process which is replicated in the laboratory. This is further confirmed by a comparison of the parameters a and b (Equation 4.22) obtained for 2,2',5,5'-TCB in the five estuaries of this study, with those for published data from *in situ* investigations (Table 4.14.). Despite differences in the method and/or sampling techniques, values are of the same order of magnitude (with the exception of the higher values obtained for the Chupa Estuary), again suggesting that SPM concentration rather than particle type is the dominant control of HOM adsorption on to particles.

K_Ds determined for 2,2',5,5'-TCB in various world river systems over a range of SPM concentrations up to 100 mg L^{-1} are listed in Table 4.15. The pooled data are plotted in Figure 4.18. and conform with a PCE. Also shown in Figure 4.18 is the line representative of the riverine data generated in this study for 2,2',5,5'-TCB where

$a=3.6x10^5$ and b=0.55 (Equation 4.22). Literature data for DEHP particle-water partitioning is given in Table 4.16., and the data are plotted against SPM concentration in Figure 4.19. The line shown is representative of the riverine data generated in this study (*i.e.* $a=50x10^5$ and b=1.00). For BaP a riverine PCE representative of the results generated in this study was derived using the values $a=2.1x10^5$ and b=0.46 and compared to the limited published data available (listed in Table 4.17. and shown in Figure 4.20.). For all three compounds, the *in situ* K_D values, allowing for natural scatter due to particle type, method of analysis and analytical error, fall close to the representative PCE isotherms derived from the results of this study. Equivalent K_{oc} values produced more of a scatter, presumably due to the varying techniques used for determination of POC and have, therefore, not been shown on Figures 4.18.-4.20.

Table 4.14: Model parameters defined for the particle concentration effect for 2,2',5,5'-TCB partition coefficients in different aquatic environments.

Water system	$a.10^5$	b	Reference
Chupa River	23.3	1.00	This study
Chupa Sea	15.9	0.89	
Dart River	3.28	0.46	
Dart Sea	6.01	0.50	
Plym River	4.53	0.61	
Plym Sea	3.98	0.50	
Beaulieu River	3.66	0.27	
Beaulieu Sea	4.96	0.53	
Carnon River	2.94	0.48	
Carnon Sea	2.76	0.38	
Lake Michigan	5.00	0.75	Eadie *et al.* (1990)
Lake Superior	5.30	1.08	Baker *et al.* (1986)
North Sea	6.20	0.94	Duinker (1986)

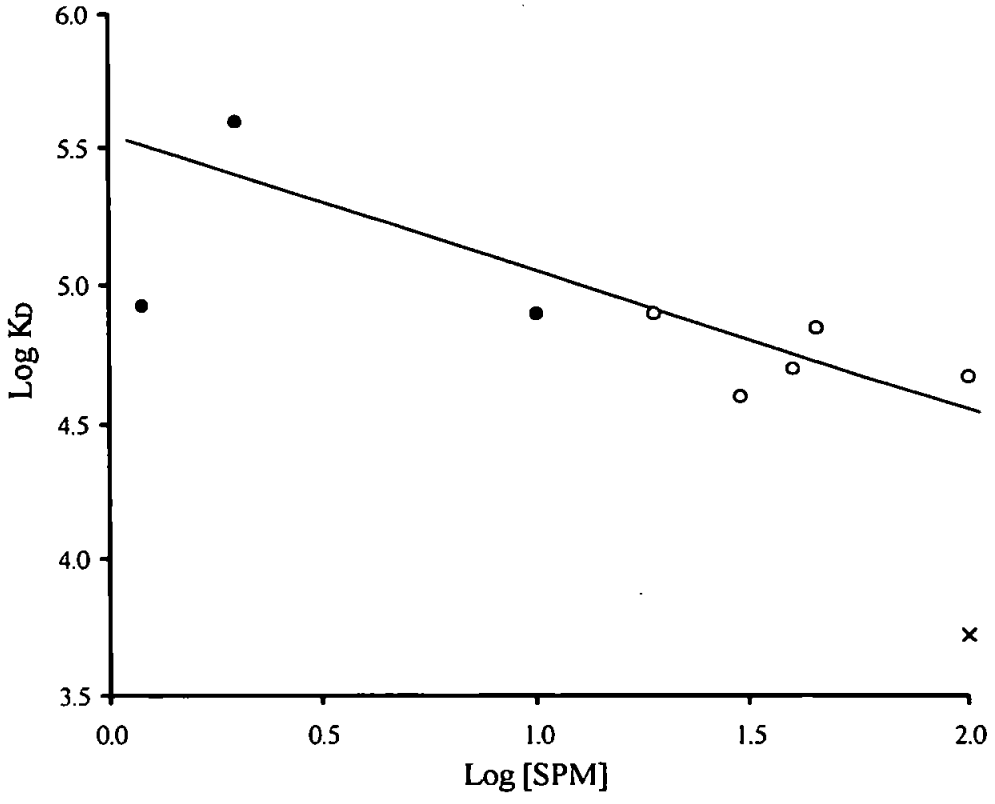

Figure 4.18: Partition coefficients, as log K_D, for 2,2',5,5'-TCB as a function of particle concentration, as log [SPM], in various fresh water systems. Sources of data used are summarised in Table 4.15., soil-water data are represented by a cross, lake water data are represented by closed symbols and river data are represented by open symbols. The particle concentration effect model, using the representative values for $a=3.6 \times 10^5$ and b=0.55 generated in this study, is shown as a solid line.

Table 4.15: Partition coefficients for 2,2',5,5'-TCB in various fresh water systems (salinity < 0.3×10^{-3}).

Water system	**SPM** ($mg\ L^{-1}$)	**POC** (%)	**Log K_D** ($ml\ g^{-1}$)	**Reference**
Soil-water	100	2.2	3.72	Girvin & Scott (1997)
Lake Michigan	1.2	2-42	4.93	Eadie *et al.* (1990)
Lake Superior	2.0	5-40	5.60	Baker *et al.* (1986)
	10		4.90	
Scheldt River	45	-	4.85	Ernst *et al.* (1988)
Rhine River	19	-	4.90	
Weser River	30	-	4.60	
Ems River	40	-	4.70	
Elbe River	100	-	4.67	Duinker *et al.* (1982)

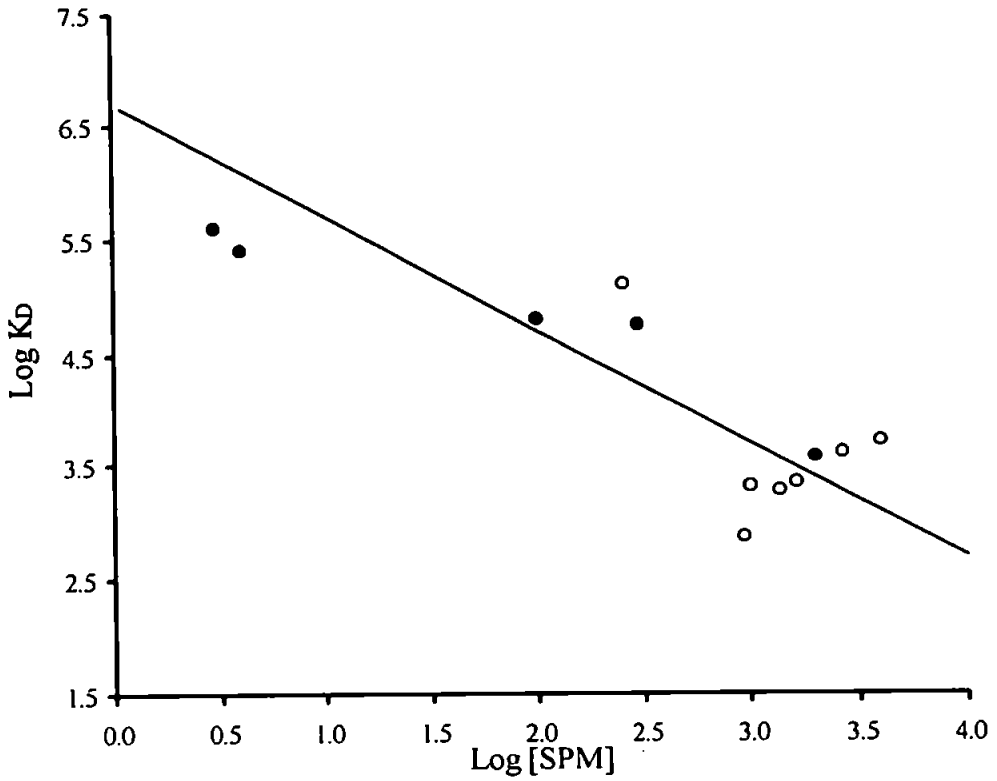

Figure 4.19: Partition coefficients, as log K_D, for DEHP as a function of particle concentration, as log [SPM], in various water systems. Sources of data used are summarised in Table 4.16., riverine data are represented by closed symbols and estuarine data are represented by open symbols. The particle concentration effect model, using the representative values for $a=50x10^5$ and b=1.0 generated in this study, is shown as a solid line.

Table 4.16: Partition coefficients for DEHP in various aquatic environments.

Water system	**Salinity** ($x10^3$)	**SPM** ($mg\ L^{-1}$)	**POC** (%)	**Log K_D** ($ml\ g^{-1}$)	**Reference**
Humber Estuary	0.4	302	5.71	4.75	Zhou & Rowland
Humber Plume	23.8	255	9.81	5.11	(1997)
Mersey Estuary	13.6-28.9	940-2670	1.06	2.88-3.61	Preston & Al-Omran (1989)
Gulf of Mexico	~35.0	920-6900	~1.00	3.71	Sullivan *et al.* (1982)
Mississippi River	1.6	2000-20000	0.15-1.88	2.66-3.77	Williams *et al.* (1995)
St Lawrence River	<0.1	3.0	-	5.60	Staples *et al.* (1997)
Lake Yssel (Rhine)	<0.1	4-100	6.7-45.8	4.80-5.40	Ritsema *et al.* (1989)

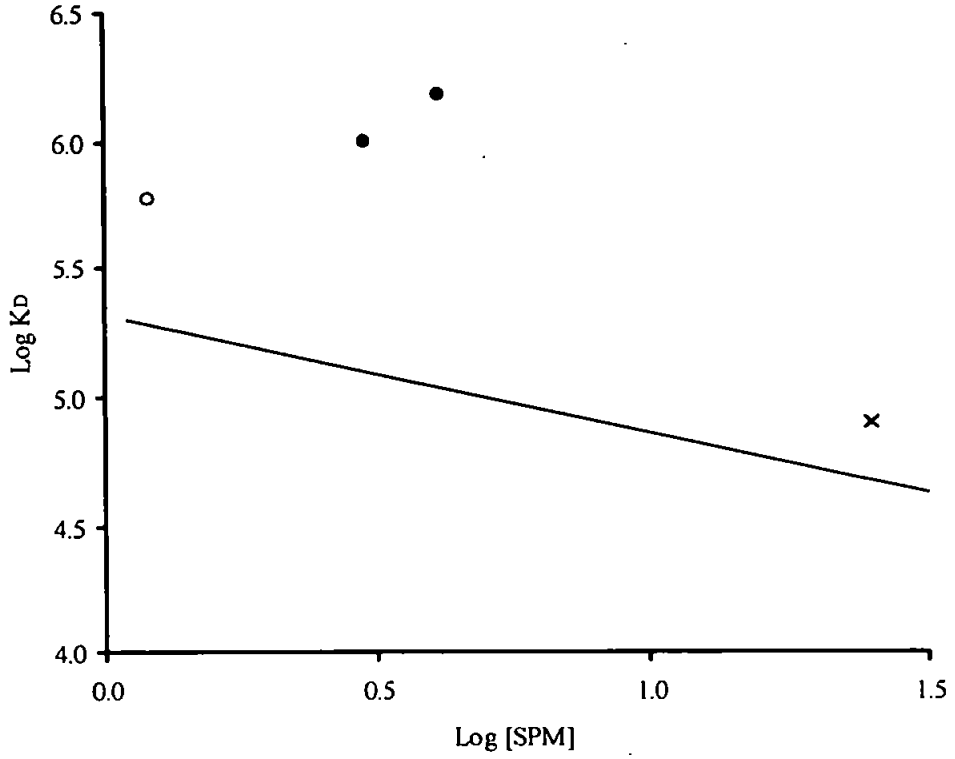

Figure 4.20: Partition coefficients, as log K_D, BaP as a function of particle concentration, as log [SPM], in various water systems. Sources of data used are summarised in Table 4.17., Tamar Estuary data are represented by a cross, Lake Michigan data are represented by open symbols and Chesapeake Bay data are represented by closed symbols. The particle concentration effect model, using the representative values for $a=2.1 \times 10^5$ and b=0.46 generated in this study, is shown as a solid line.

Table 4.17: Partition coefficients for BaP in various aquatic environments.

Water system	**Salinity** ($x10^3$)	**SPM** ($mg\ L^{-1}$)	**POC** (%)	**Log K_D** ($ml\ g^{-1}$)	**Reference**
Lake Michigan	<0.1	1.2	2-42	5.78	Eadie *et al.* (1990)
Tamar Estuary	~30.0	25	-	4.90	Readman *et al.* (1982)
Chesapeake Bay	~35.0	3.0	29	6.19	Ko & Baker (1995)
		4.1	15	6.01	

4.4.4. Summary of particle concentration effect

In conclusion, the PCE appears to be mainly due to an environmental process (most likely as a result of particle interactions; Sections 4.4.3.2. & 4.4.3.3.), rather than an analytical artefact (Section 4.4.3.1.), and should, therefore, be incorporated into any biogeochemical modelling or impact assessment of HOMs in natural waters (See Section 5.4.). The PCE is evidently more important than particle type in controlling the sorption of HOMs to natural particles, but the precise causes remain unresolved and calls for further investigation.

CHAPTER 5: SUMMARY, SIGNIFICANCE AND APPLICATION OF RESULTS

5.1. Introduction

A process-orientated method for the study of the behaviour of HOMs under simulated estuarine conditions has been developed and rigorously tested. The method has been applied to study the relative solubility (Chapter 3) and particle-water partitioning (Chapter 4) of selected hydrophobic organic micropollutants (HOMs) as a function of the estuarine variables salinity, dissolved organic carbon, particulate organic carbon and suspended particulate matter concentration. Relationships have been established between solubility and sorption parameters and estuarine variables. Although these relationships are important in their own right this chapter illustrates how they could be integrated into existing conceptual and numerical transport and distribution models which could then be used to predict the fate of HOMs in estuaries and the coastal zone.

5.2. Relative Solubility

The relative solubility of the three HOMs (2,2',5,5'-TCB, DEHP, and BaP) investigated were shown in Chapter 3 to be dependent upon the concentration and type of dissolved organic carbon (DOC) present, as well as salinity. The cumulative effect of these two estuarine variables on the relative solubility of 2,2',5,5'-TCB and DEHP was assessed by deriving a relative solubility salting constant, σ_r (Section 3.2.4.2.), based on the Setschenow concept, for the four British estuaries studied.

The relationship between the relative solubility of the three HOMs and commercial humic acid have been summarised in Figure 5.1. (See also Section 3.2.3.; Figure 3.8.). Also shown in Figure 5.1. are the relative solubilities of the HOMs in the riverine end-member samples of the British estuaries studied. The change in DOC concentration does not have a clear effect on the relative solubility of the HOMs; for example, an increase of a factor of 10 in the DOC concentration results in only an increase of a factor of 2 in the relative solubility of 2,2',5,5'-TCB. With the possible

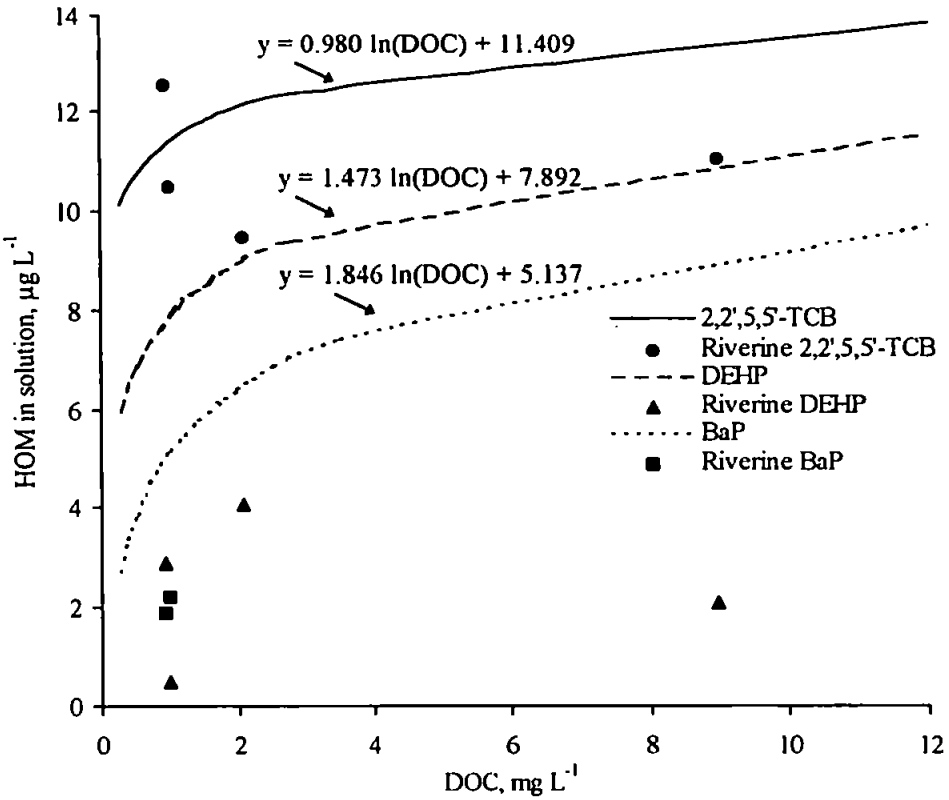

Figure 5.1: Changes in hydrophobic organic micropollutant, HOM, relative solubility as a function of dissolved organic carbon, DOC, concentration, where the best line fits as a function of commercial humic acid are represented as lines and the symbols represent the relative solubility of the HOMs in the riverine end member sample of the British estuaries studied (see also Section 3.2.3.; Figure 3.8.).

exception of 2,2',5,5'-TCB, commercial humic acid is not a suitable analogue for natural DOC. That is, the relative solubility of HOMs is dependent not only on the DOC concentration but also the type of DOC present and the physicochemical properties of the DOC (e.g. specific surface area, polarity, age, degree of mineralisation and aromaticity). Therefore, empirical predictions of relative solubility are not possible for these compounds from these data.

The effects of estuarine variables on the relative solubility are only minor and solubility alone (compared with the particle-water interactions) is not likely to significantly control HOM distribution in estuaries where suspended particles are present.

5.3. Particle-Water Interactions

The particle reactivity of the HOMs was investigated in detail in Chapter 4 and the results are summarised in the next two sections.

5.3.1. Kinetics

The adsorption of these compounds was found to be biphasic, with an initial rapid uptake occurring within minutes (< 5 minutes) followed by a slower second stage occurring over several days (Section 4.2.). Thus, uptake of HOMs is not instantaneous.

System response times, τ_{resp}, (*i.e.* the time required to attain 63% of the new particle-water partitioning equilibrium after the system has been altered; Honeyman & Santschi, 1988) were calculated for both 2,2',5,5'-TCB and BaP (20 minutes and 1 minute, respectively) in Section 4.2. This parameter is a valuable timescale for incorporating into predictive HOM transport models for estuaries. The dissolved and particulate phases are transported in entirely different ways and if the dwell time for constant conditions of the water is not sufficiently long enough, chemical equilibria between the water and particles may not be achieved. In the case of 2,2',5,5'-TCB, about 1% of the original dissolved HOM will remain after 4 system response times have elapsed, hence approximately 80 minutes will be required for sorptive equilibrium to be reached. Thus, when the dwell times are < 80 minutes chemical equilibrium between water and particles will not be achieved and the 2,2',5,5'-TCB is more likely to be transported in the dissolved phase. This may have important implications on the seasonal distribution of HOMs in the low salinity, turbidity maximum zone areas of partially mixed, macrotidal estuaries. For example, flushing times in the upper Tamar Estuary, UK, during winter can be < 1 hour (Millward *et al.*, 1992), conditions under which sorptive equilibrium for 2,2',5,5'-TCB will not be reached. However, flushing times in this region of the Tamar Estuary during the summer, when river flow is lower, are of the order of several hours allowing the sorptive equilibrium of 2,2',5,5'-TCB to be attained. Sorptive equilibrium will be achieved within a few minutes for BaP, and, dwell times are therefore less significant than for 2,2',5,5'-TCB.

5.3.2. Adsorption isotherms and the particle concentration effect

Adsorption isotherms, at constant suspended particulate matter (SPM) concentration, showed that HOM uptake was enhanced in sea water. A hypothesis was proposed that this increase was not only due to a decrease in the relative solubility caused by the salting out effect, but also due to the associated changes in the surface charge and conformation of the sediment organic layer (Section 4.3.). An inverse relationship between the particle-water partition coefficient (K_D) and SPM concentration was observed for all three HOMs, and corresponds with the well documented particle concentration effect (PCE; Section 4.4.2.). This investigation has therefore provided parameterised definitions of K_D in terms of the variables salinity, S ($x10^{-3}$), and SPM concentration (mg L^{-1}):

$$K_D = K\,S + K_D^0 \qquad (5.1)$$

and

$$K_D = a\,SPM^{-b} \qquad (5.2)$$

where K, a, b and K_D^0 (the particle-water partition coefficient in fresh water) are site- and compound-specific constants. Such relationships are clear and simple definitions of the geochemical partitioning of HOMs that can be integrated into a model shell (Figure 5.2.) to provide more site- and compound-specific predictions of HOM transport and distributions.

5.4. Incorporation of Concepts into Existing Transport and Distribution Models

Previous attempts at modelling the fate and behaviour of HOMs, both locally (e.g. Estuarine Contaminant Simulator, ECoS (Harris *et al.*, 1993), and Pollution Information for Contaminants in Estuaries and Seas, PISCES (Ng *et al.*, 1996)) as well as regionally and globally (fugacity-based models; e.g. MacKay & Paterson, 1991) have relied upon the physicochemical properties of the HOM. As well as, empirical formulae relating sediment-water partitioning to their octanol-water partitioning, K_{ow}, and Setschenow

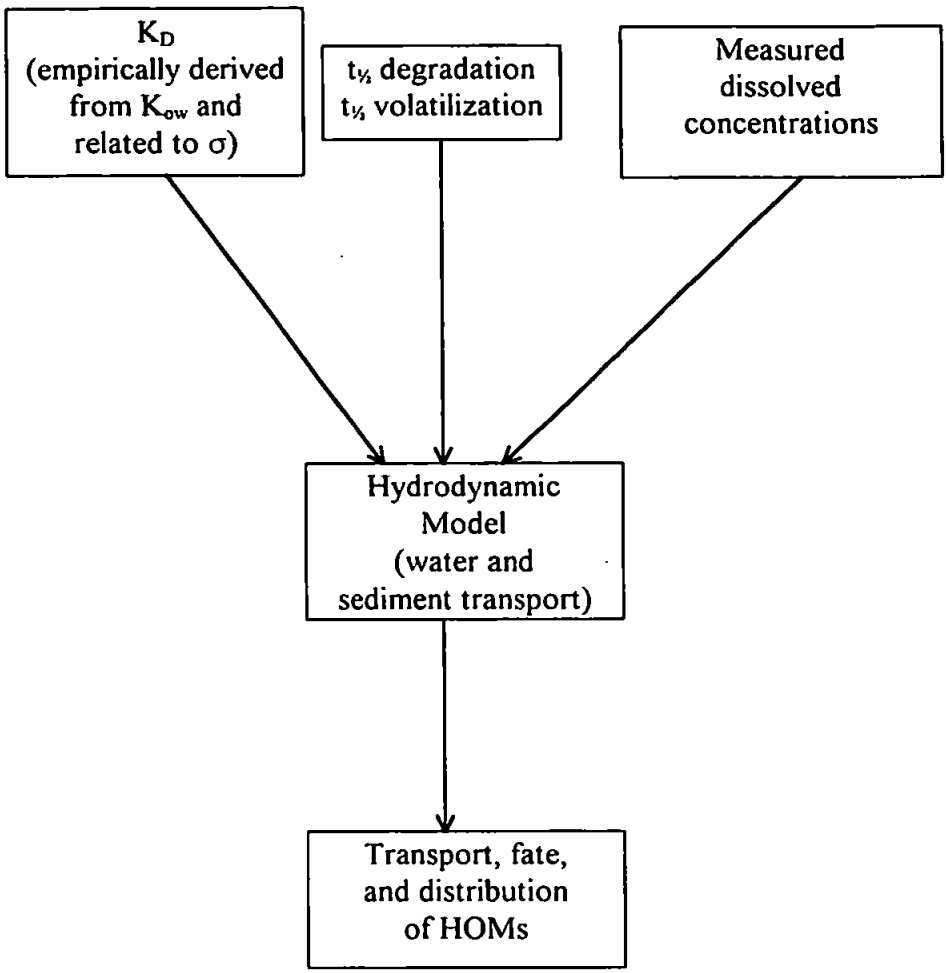

Figure 5.2: General framework (or shell) for modelling HOMs in the aquatic environment. Terms used are defined and described in the text.

constants, σ. The general framework of an aquatic transport model for pollutants is outlined in Figure 5.2.

This may be exemplified by the estuarine simulation shell, ECoS, which assumes that HOM K_Ds increase with increasing salinity, due to the salting out effect (Harris *et al.*, 1993). The extent of increases in K_D are empirically related to the Setschenow constant, σ. The role played by the organic carbon content (f_{oc}) of the suspended particulate matter, SPM, and the K_{ow} of the HOM, are incorporated into an empirical equation (Harris *et al.*, 1993):

$$K_D = 6.2x10^{-4} K_{ow} f_{oc} e^{(0.038 \sigma S)} \qquad (5.3)$$

where S is the salinity. Partition coefficients and end member dissolved concentrations of HOMs are incorporated into a hydrodynamic shell which is configured for the estuary under study in order to predict pollutant distributions. PISCES requires the user to insert a constant K_D (either derived or approximated for the estuary under investigation from K_{ow} values), published values of the degradation and/or volatilisation half life (Howard *et al.*, 1991) and end-member concentrations of the individual HOMs, from which pollutant transport and distributions are predicted.

On a much larger scale, Fugacity models have been developed to provide regional information on the environmental behaviour of organic chemicals between at least four bulk compartments: air, water, soil, and bottom sediment (MacKay & Paterson, 1991). Such models assume chemical equilibrium exists within each bulk compartment, but not between them. This may not be the case in estuaries (a sub-compartment) which are not necessarily at equilibrium. Movements within and between the bulk compartments are then evaluated and expressed in terms of emissions, advective flows, degrading reactions, and interphase transport (such as partitioning, reactivity, and diffusive- and non-diffusive transfer processes). However, the majority of data used to calculate these transport parameters are derived directly or via established trends relating to the physicochemical properties of the HOM, and not from directly measured values from the region of concern. This is primarily due to the lack of extensive HOM partitioning and reactivity databases on a local and regional scale.

It is this shortfall in information that this thesis has attempted to begin to address. Regarding estuaries, as previously mentioned, established distribution models tend to omit the variability of HOM reactivity throughout an estuarine system, and do not address the changes associated with varying the salinity, the DOC, the SPM, and, indirectly, the particulate organic carbon (POC).

As outlined in Sections 5.2. and 5.3. this study has defined these relationships for individual estuaries and representative hydrophobic compounds, for integration into local and regional distribution models. Although these algorithms and the data generated in this work have not been incorporated into a hydrodynamic shell (due to time constraints caused by the extensive method evaluation undertaken at the beginning of this study),

some aspects of how these equations can be applied to environmental problems are exemplified in the following sections.

5.5. Retention of HOMs in Estuaries

5.5.1. Fraction in solution

The most bioavailable fraction of HOM in an aquatic environment is that present in the solution phase (Rubinstein *et al.*, 1990). This fraction is also subject to different hydrodynamic pathways to that fraction adsorbed on to particles. Therefore, it is important for any modelling attempt to predict the fraction of contaminant in the solution phase (F_S, %) and the particulate phase. The F_S can be calculated using the following equation (Turner & Tyler, 1997):

$$F_S = \left[\frac{1}{\left(1 + \frac{K_D \, SPM}{10^6}\right)} \right] . 100\ \% \qquad (5.4)$$

where K_D is in mL g^{-1}, and SPM is in mg L^{-1}. As the K_D for HOMs has been shown to change with SPM concentration (Section 4.4.2.), this must be taken into account when determining F_S, by incorporating Equation 5.2. into Equation 5.4.:

$$F_S = \left[\frac{1}{\left(1 + \frac{a \, SPM^{-(b-1)}}{10^6}\right)} \right] . 100\ \% \qquad (5.5)$$

The fraction in solution for each of the HOMs in river water and sea water were calculated using Equation 5.5. over an SPM concentration range of 0-1000 mg L^{-1} using representative values of a and b (from those generated in Chapter 4) listed in Table 5.1. The results are shown in Figure 5.3. along with those for a constant particle-water partitioning using upper and lower estimates of K_D derived from Equation 5.2. at SPM concentrations of 10 mg L^{-1} and 1000 mg L^{-1}, respectively. Once F_S falls below 50%, (as

Table 5.1: Representative values of parameters a and b (generated in this study; Section 4.4.2.; Equation 4.22), in river and sea water, used for fraction in solution calculations for each hydrophobic organic micropollutant, HOM (Figure 5.3.). The values of b generated in this study and used to determine the estuarine retention of DEHP, (see Section 5.5.2.1 and Figures 5.5.-5.6.), are shown in brackets.

HOM	Matrix	$a.10^5$	b
2,2',5,5'-TCB	River water	3.60	0.55
	Sea water	4.50	0.50
DEHP	River water	50.0	1.00 (0.94-1.15)
	Sea water	44.8	0.82 (0.75-0.93)
BaP	River water	2.10	0.46
	Sea water	4.00	0.40

indicated on Figure 5.3.), then the greatest fraction of HOMs are found adsorbed on the solid phase or sediment. This represents 'significant trapping' of the HOM within the estuary (Brunk *et al.*, 1997), at least over a period comparable with particle residence times, which may be from months to decades (Dyer, 1989).

For all three HOMs, if the upper K_D value predicted at 10 mg L^{-1} were maintained throughout the range of SPM concentrations, F_S approaches 1% as the SPM concentration reaches approximately 100-500 mg L^{-1} in both river water and sea water. If a PCE is included in the calculations then within the SPM concentration range studied F_S does not fall below 11%, 17%, and 10%, in river water for 2,2',5,5'-TCB, DEHP, and BaP, respectively. Adsorption is shown to be enhanced in high salinity waters, therefore, the corresponding values for sea water are 6%, 9%, and 4%, for 2,2',5,5'-TCB, DEHP, and BaP, respectively. Enhanced adsorption at high salinity will reduce the offshore fluxes of HOMs and promote their internal cycling within the estuarine mixing zone. If the K_D value predicted at 1000 mg L^{-1} is used in Equation 5.4 then F_S is overestimated by up to 50% at SPM concentrations below approximately 300 mg L^{-1}. Although these calculations are largely hypothetical they clearly indicate the importance of accounting for a PCE in pollutant flux and retention calculations.

Presuming HOMs are bioavailable predominantly in the solution phase, then only a little of these contaminants will be available for uptake by organisms in highly turbid environments, due to particle scavenging. However, biological uptake from the solution phase could be significant in environments of low particle concentrations, or where the magnitude of b exceeds 1; that is, an increase in particle concentration is more than

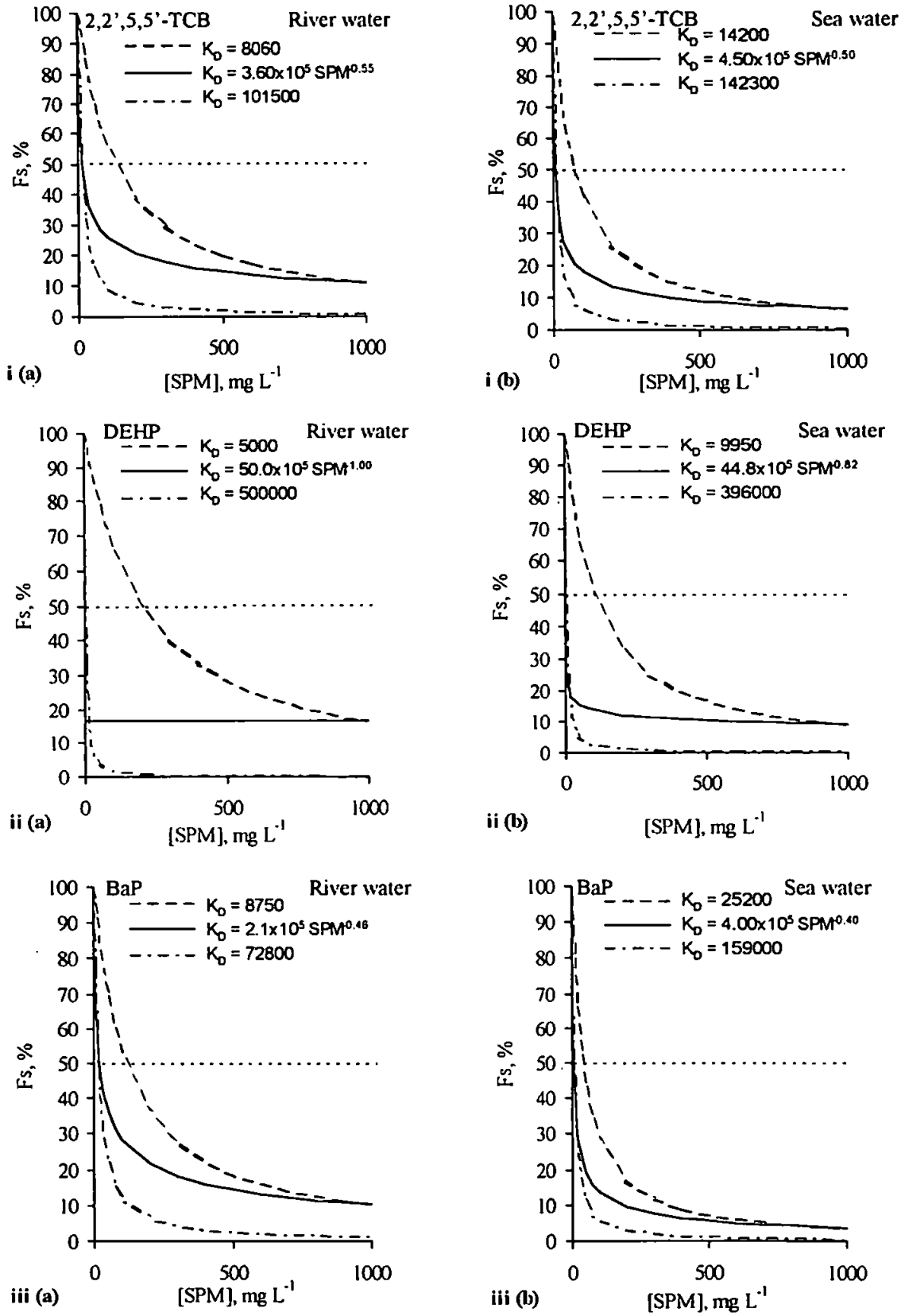

Figure 5.3: Fraction in solution, F_S, as a function of suspended particulate matter, SPM, for (i) 2,2',5,5'-TCB, (ii) DEHP, and (iii) BaP, in (a) river water and (b) sea water, calculated using representative values for the parameters a and b generated in this study and listed in Table 5.1. Constant K_D values shown are derived from the equations given at the SPM concentrations 10 mg L^{-1} and 1000 mg L^{-1}.

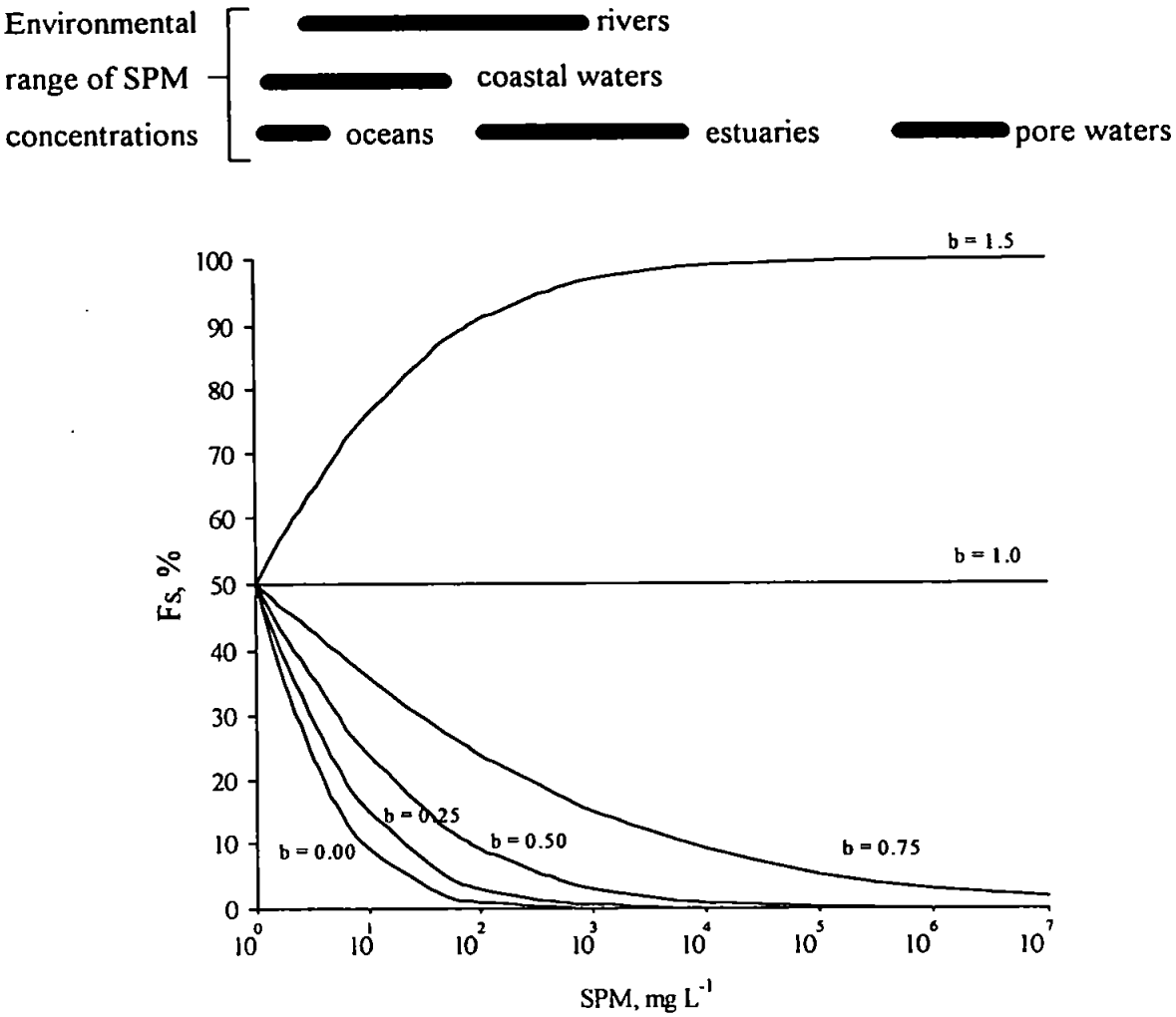

Figure 5.4: Fraction in solution, F_S, calculated using Equation 5.5 as a function of suspended particulate matter, SPM, concentration derived from the particle concentration effect, using a constant value for a ($1x10^6$) and a range of b values between 0.00 and 1.50.

compensated for by the associated reduction in partitioning and an increase in F_S with increasing SPM concentration.

The implications of including the PCE in this model were investigated further by using a representative value of $1x10^6$ for the intercept a (calculated using Equation 4.22), and varying the influence of the PCE. F_S is shown in Figure 5.4. as a function of SPM concentration for different b values between 0.00 and 1.50. The SPM concentration range shown in Figure 5.4. encompasses the various SPM concentrations encountered in the aquatic environment, including oceanic, coastal, estuarine and pore waters.

If a value of b > 1.00 is used then retention of the HOM in an estuary is not significant as the majority of the pollutant is flushed out in accordance with the hydrodynamic flushing time. An increase in F_S is calculated under these conditions as the increase in SPM concentration is more than compensated for by an associated reduction in K_D. Such a situation may exist for DEHP, where b was found to be greater than 1.00 in the Beaulieu River. If b = 1.00 then the reduction in K_D will directly offset the increase in SPM concentration and F_S remains constant at 50% (Figure 5.4.). This is also shown for DEHP in Figure 5.3. ii(a) where F_S remains constant throughout the SPM concentration range. At values of b < 1.00, a reduction in F_S occurs with increasing SPM concentration; *i.e.* the more turbid the environment the greater its retention capacity. When b = 0, there is no SPM concentration dependence of K_D and maximum retention occurs.

5.5.2. Influence of HOM degradation

HOMs are commonly described as persistent in the aquatic environment, with sediments providing a long-term sink for these compounds (Readman *et al.*, 1982; Lang, 1992). Degradation of these compounds in the sediments tends to be negligible in the short-term (*i.e.* compared to estuarine particle residence times) but may be significant in the solution phase. The retention of HOMs in estuaries is, therefore, primarily governed by two competing effects. Firstly, as described in the previous section, by the fraction adsorbed on to suspended particles, which is dependent upon the SPM concentration and K_D. The fraction adsorbed onto the suspended particles, F_P, can be calculated from F_S (Equation 5.5.) as follows:

$$F_P = 100\% - F_S \qquad (5.6)$$

Secondly, the retention of HOMs by estuaries is controlled by the decay rate in the solution phase, which is dependent upon the temperature and several water quality variables (e.g. dissolved oxygen, microbial population, and microbial density). Hence, HOM retention is dependent upon the water quality and transit time of water from the point of discharge to a region of relatively high SPM concentration (such as the turbidity maximum zone, TMZ), and the extent of bed sediment resuspension or suspended

particle trapping in this region. The fraction of total HOM discharged from a point source upriver which is retained in the estuary, F_R, can be calculated as follows:

$$F_R = F_P e^{-kT} \qquad (5.7)$$

assuming first-order degradation of the HOM, where T is the water transit time from source to the TMZ and k is the decay rate constant which is dependent on water quality and temperature. These calculations assume that there is a continual supply of uncontaminated particles into the estuary and its TMZ, from both the riverine discharge and the tidal upestuary transport of marine particles (Eisma, 1993). This model therefore provides upper estimates of the estuarine retention. Empirical modification is required to account for the extent of pre-existing particulate contamination and/or the sorption capacity of the suspended particles for individual HOMs.

5.5.2.1. Bis(2-ethylhexyl)phthalate ester degradation

Published estimates of degradation half-lives for DEHP in natural waters, under realistic conditions of temperature and water quality range from 2-15 days (Staples *et al.*, 1997) which corresponds to a range in first-order decay rate constants of 0.347 to 0.0462 day^{-1}.

Figures 5.5. and 5.6. show the fraction of total DEHP retained in the estuary as a function of SPM concentration for different water transit times and the two DEHP decay constants, using a representative a value and extreme b values generated in this study (Chapter 4; Equation 4.22; summarised in Table 5.1.) and derived from river (Figure 5.5.) and sea (Figure 5.6.) water. These results show how degradation in the water column affects the overall retention in the estuary. For example, for k = 0.347 d^{-1}, the retention may be reduced from about 90% to less than 5% if the transit time is increased from 0 days to 10 days. Thus, in summer, when temperatures are higher and transit times longer, more degradation will occur and the estuary is a less efficient trap for the contaminant.

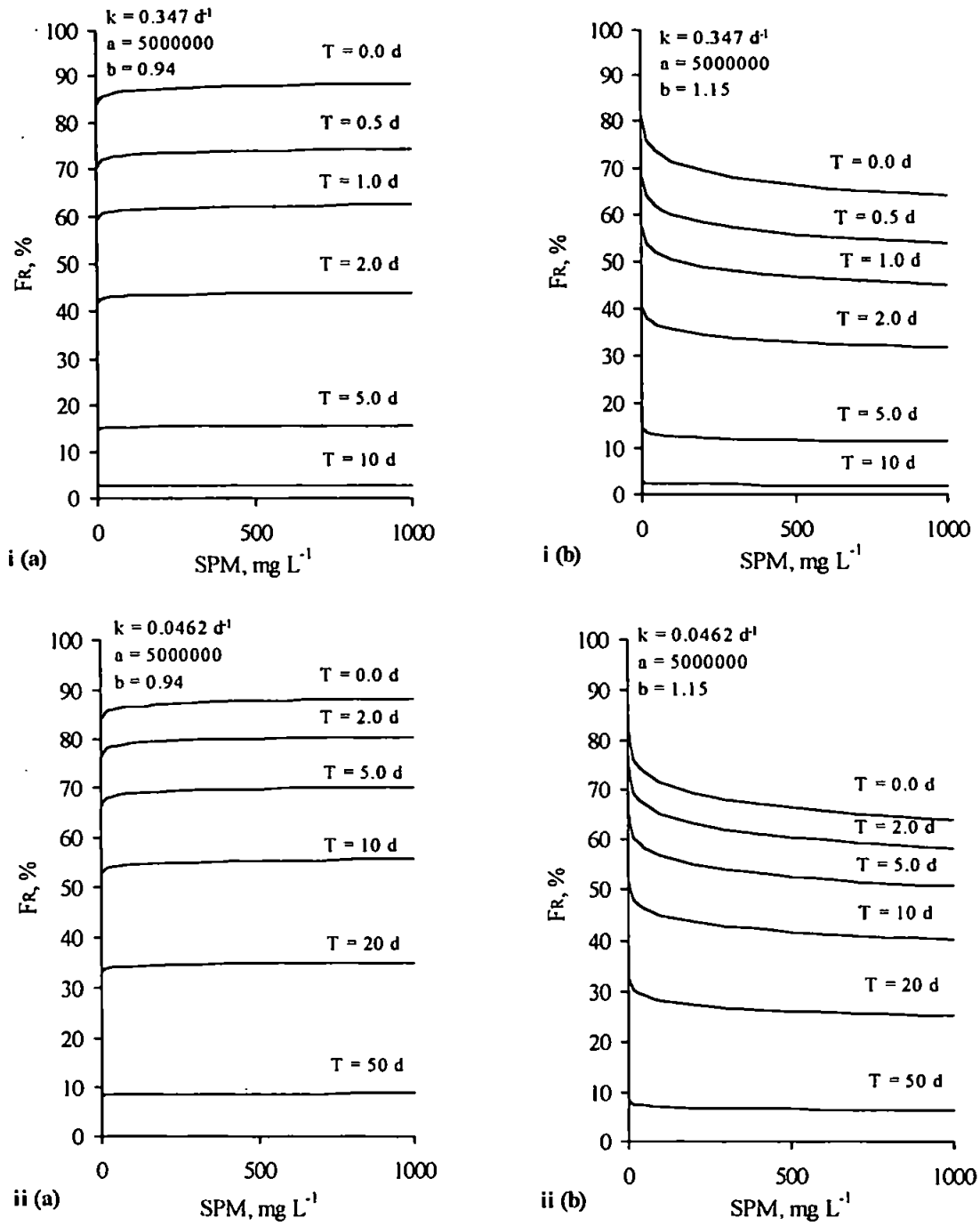

Figure 5.5: Estuarine retention, F_R, of DEHP as a function of suspended particulate matter, SPM, concentration, using a representative a value and extreme b values generated in this study and derived from river water, for different water transit times, T, and for two DEHP degradation constants, k, (i) 0.347 d^{-1} and (ii) 0.0462 d^{-1}.

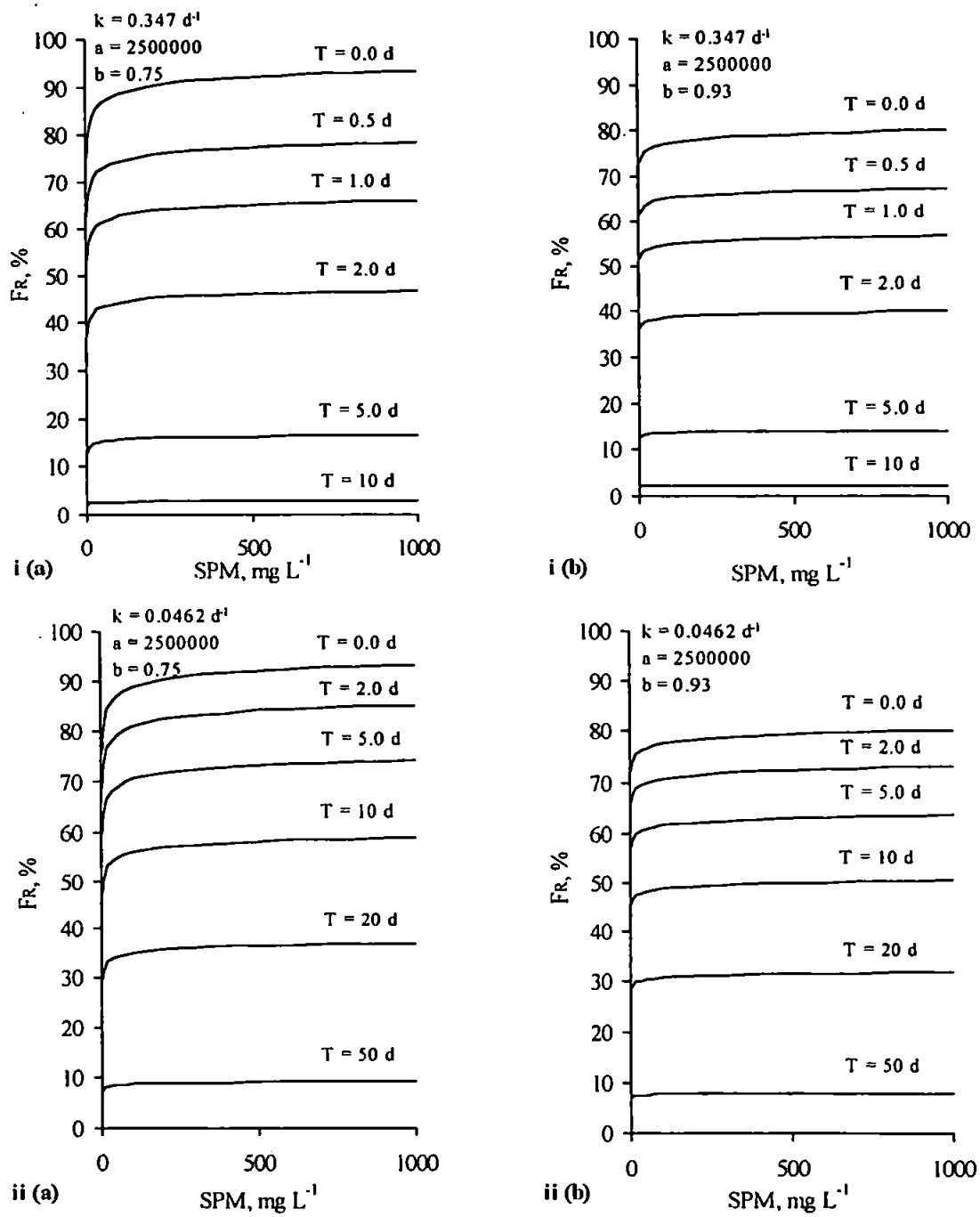

Figure 5.6: Estuarine retention, F_R, of DEHP as a function of suspended particulate matter, SPM, concentration, using a representative a value and extreme b values generated in this study and derived from sea water, for different water transit times, T, and for two DEHP degradation constants, k, (i) 0.347 d^{-1} and (ii) 0.0462 d^{-1}.

5.5.2.2. Benzo[a]pyrene degradation

Direct photolysis half-life values for BaP, under ideal conditions (*i.e.* in particulate free surface waters exposed to light of an environmentally significant wavelength, >290 nm), range from 0.0154 d^{-1} to 0.0458 d^{-1} (Howard *et al.*, 1991), which corresponds to a range in photolysis rate constants (k^0) of 45 d^{-1} to 15 d^{-1}. However, estuarine water column conditions are far from ideal for photolysis to occur at an optimum rate due to the presence of particulates and the depth of the water column. Therefore, k^0 must be converted to a decay constant, k, which approximates that found in the estuarine environment (Schwarzenbach *et al.*, 1993):

$$k = k^0\left(\frac{1 - 10^{-\alpha D z}}{2.303 \alpha D z}\right) \qquad (5.8)$$

where α (m^{-1}) is the diffuse attenuation coefficient, D is a water system constant and z (m) is the depth of the water column. For a turbid macrotidal estuary D = 2.0 (Schwarzenbach *et al.*, 1993); α is dependent upon the SPM concentration, and assuming an SPM concentration of 55 mg L^{-1}, representative of macrotidal estuaries, α = 6 m^{-1} (Campbell & Spinrad, 1987). Assuming an average water column depth of 10 m, k ranges from 0.163 d^{-1} to 0.0543 d^{-1} for BaP. F_R was then calculated for BaP, using representative a and b values generated in this study (Chapter 4) and derived for estuarine end members as listed in Table 5.1. and shown in Figure 5.7. As described for DEHP, these results show the dependence of F_R on decay rate, the PCE and water transit time, and demonstrate the important seasonal changes in the retention capacity of an estuary.

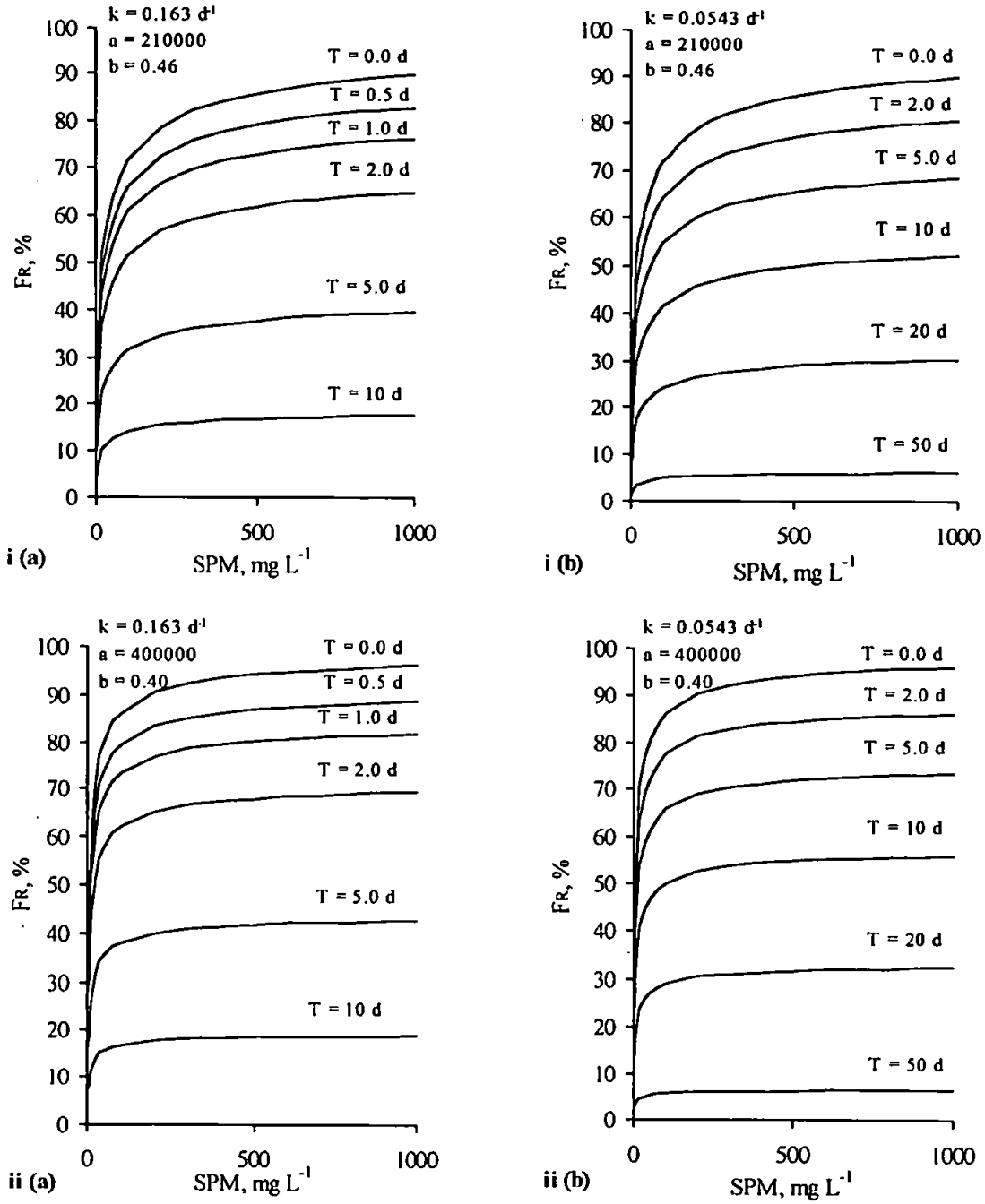

Figure 5.7: Estuarine retention, F_R, of BaP as a function of suspended particulate matter, SPM, concentration, using representative a and b values generated in this study and derived from (i) river water and (ii) sea water, for different transit times, T, and for two BaP photolysis constants, k, (a) 0.163 d^{-1} and (b) 0.0543 d^{-1}.

5.6. Behaviour of HOMs in Estuaries

The overall behaviour of HOMs in estuaries is complex and involves the influence of numerous environmental processes. The general behaviour of HOMs is outlined in Figure 5.8., which summarises the major environmental processes which influence the fate and distribution of HOMs in a partially-mixed, macrotidal estuary. The location of the pollutant discharge, and the form (e.g. dissolved, associated with DOC, and/or particulate) in which the HOM enters the aquatic environment (Readman *et al.*, 1982), will ultimately determine the fate of the HOM.

K_D increases as salinity increases and can be described by Equation 5.1. For a constant SPM concentration, adsorption will be favoured in the seaward reaches of an estuary. However, SPM concentration is not constant throughout the estuarine mixing zone and K_D will vary in accordance with Equation 5.2. In particular SPM concentration varies spatially and temporally in the TMZ. The TMZ is a consequence of several sediment dynamic processes occurring in the estuary (Eisma, 1993). The riverine surface water flow, carrying SPM, diminishes as salinity increases, causing the SPM to settle out and be returned towards the upper part of the estuary with the residual bottom current. SPM then accumulates at the place where the inward bottom flow meets the riverine outward flow (where flow velocities are generally minimal). In addition tidal asymmetry promotes the tidal pumping of sediments towards the TMZ; the flood tide of macrotidal estuaries tend to be stronger, but of shorter duration than the ebb, resulting in more SPM being pumped up estuary during the flood tide than that being carried back during the ebb (Dyer, 1997). The position of the TMZ, is also dependent upon the tidal cycle; more inward during spring tides and low river discharge compared with more outward during neap tides and high river discharge (Eisma, 1993). This movement of the TMZ results in a continual deposition and resuspension of the fine-grained sediment in this region of the estuary. The implications of the TMZ (*i.e.* an increase in SPM concentration) on the distribution of HOMs has been described in terms of a particle concentration effect (PCE, Equation 5.2; Section 4.4.2.) where K_D decreases as SPM concentration increases. The magnitude of b (Equation 4.22), the degradation of the compound from its source to a region of turbidity and the extent of resuspension and particle trapping will determine the overall retention of HOM by an estuary. The influence of individual variables do not act independently upon the HOM and the eventual distribution of these compounds are the result of a cumulative effect, and this must be taken into

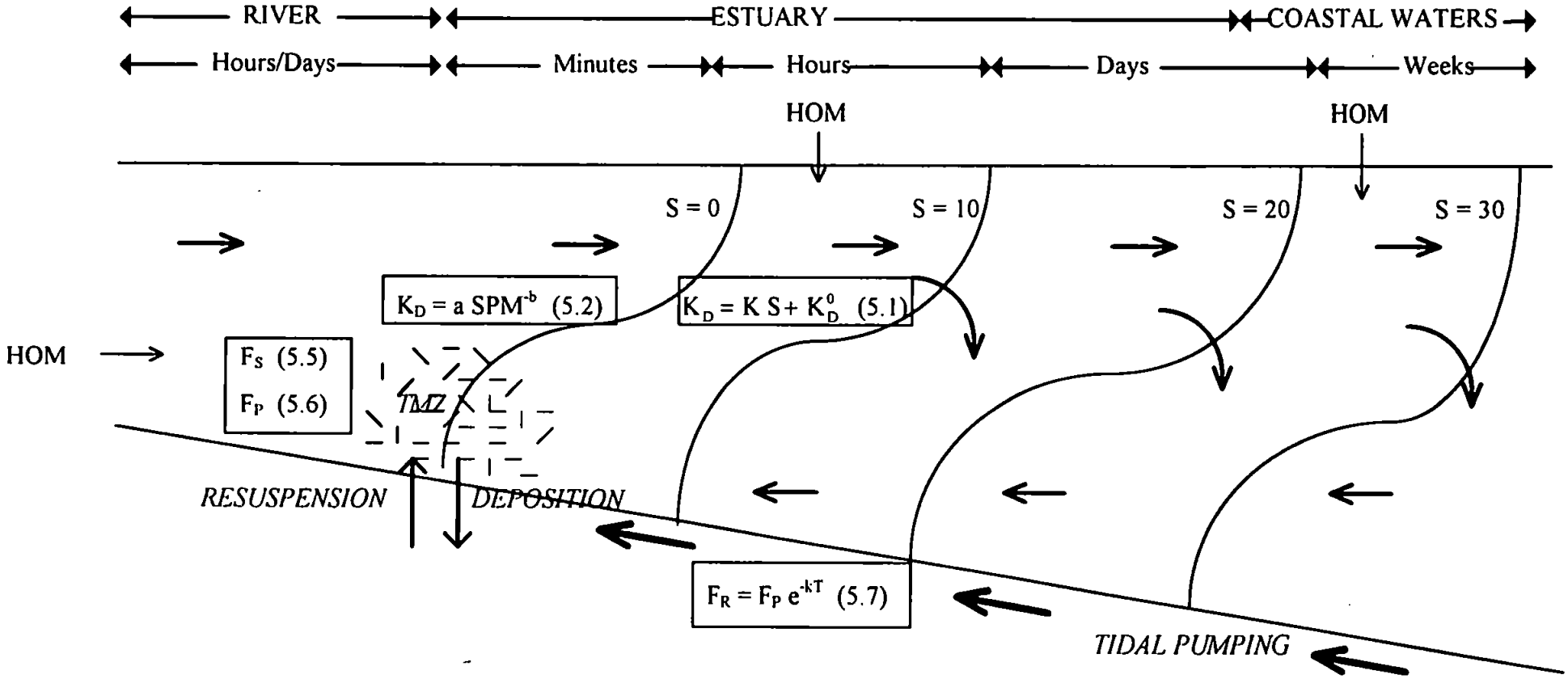

Figure 5.8: Conceptual representation of a partially mixed macrotidal estuary showing the influence of hydrodynamic and sediment dynamic processes on the fate and distribution of a hydrophobic organic micropollutant, HOM, where S is the salinity ($x10^{-3}$), K_D is the particle-water partition coefficient, SPM is the suspended particulate matter concentration, a, b and K are constants, K_D^0 is the partition coefficient in pure water, F_S is the fraction of HOM in solution, F_P is the fraction of HOM adsorbed onto suspended particles, TMZ is the turbidity maximum zone, F_R is the fraction of discharged HOM retained in the estuary, k is the decay rate constant and T is the water transit time. Equations are numbered according to their location in the text.

account when attempting to predict HOM behaviour in estuaries.

5.7. Conclusions

(i) Method Development.

(a) A laboratory based method using ^{14}C-labelled beta-emitting isotopes coupled with liquid scintillation counting has been developed to determine the relative solubility and sorptive behaviour of HOMs under simulated estuarine conditions. The method has been rigorously tested and was successfully applied to selected hydrophobic compounds. The method is generally applicable to any HOM provided sufficient recovery (> 60%) of the compound can be attained.

(ii) Determination of the estuarine physico-chemical conditions controlling HOM solubility and the adsorption of HOMs to estuarine sediments.

(a) Relative solubility isotherms for the three HOMs in the estuaries under investigation showed a 'salting out' effect in high saline waters, the magnitude of which was described by a relative solubility salting constant based on the Setschenow concept.

(b) An increase in relative solubility occurred for all three HOMs as the humic acid concentration was increased, although the dependence on natural DOC concentrations was less obvious. The relative solubilities of DEHP and BaP was shown to be strongly influenced by both DOC type and concentration, whilst the relative solubility of 2,2',5,5'-TCB was mainly dependent upon DOC concentration.

(c) A series of kinetic experiments showed that for both 2,2',5,5'-TCB and BaP the rate of uptake on to estuarine SPM was biphasic, with a significant rapid uptake occurring within minutes followed by a second slower uptake occurring over a period of days. The system response time, τ_{resp}, required for BaP to attain sorptive equilibrium was calculated to be a matter of minutes, whilst the τ_{resp} for 2,2',5,5'-TCB was found to be longer, suggesting that sorptive equilibrium may not always be attained for this HOM when estuarine flushing times are less than the order of an hour.

(d) Adsorption isotherms for all three HOMs were generally linear and could be described by the Freundlich isotherm. Enhanced adsorption in sea water was

shown to be only partially due to a decrease in relative solubility caused by the salting out effect. A hypothesis was proposed that enhanced adsorption at high salinities was also due to changes in the surface charge of the sediment organic layer, and/or changes in the conformation of the organic layer which then trap HOMs. This situation was complicated in the Carnon Estuary where the reverse occurred. Here, on mixing with sea water, the positive surface charge of the riverine SPM becomes negative (Newton & Liss, 1987).

(e) A Particle Concentration Effect, PCE, was demonstrated for all three compounds. That is, the decrease in K_D with an increase in particle concentration. The PCE has long been attributed to experimental artefacts (Voice & Weber, 1985; Gschwend & Wu, 1985). However, investigation of several possible causes including wall adsorption and the presence of non-settleable colloidal particles did not result in the elimination of this effect. A more likely explanation for the PCE is particle-particle interactions that occur in both the environment and the laboratory. This was further emphasised by comparing published in-situ K_D values, over a range of SPM concentrations, to the PCE defined for each HOM in this investigation. The PCE is therefore likely to be an environmental process that must be included in any distribution model.

(iii) Calculation of empirical partitioning codes.

(a) Simple algorithms were defined to describe (1) the increase in K_D with salinity at a constant SPM concentration, and (2) the inverse relationship between K_D and SPM concentration, or the PCE. These algorithms are suitable for incorporation into a hydrodynamic framework to predict the fate and distribution of HOMs in an estuary, and in this thesis they have been incorporated into simple models to show their effects on the transport and retention of HOMs in estuaries.

5.8. Future Work

(1) Although this investigation has provided an extensive database for three compounds in various estuaries, this database must be augmented to provide more detailed and site-specific distribution data and empirical relationships. Not just for these three HOMs but for a larger range of compounds in a larger number of estuaries. Similarly, more detailed investigations into the role played by DOC type and concentration on HOM distribution is required. Such information is required for incorporation into hydrodynamic pollution transport models so that more accurate predictions may be made.

(2) More field data on the distribution of aqueous (both freely dissolved and DOC bound) and particulate (both suspended and deposited sediment) HOM concentrations are urgently required in order that any pollutant transport model predictions can be validated. At present there exists very limited dissolved and particulate HOM data in estuaries.

(3) A feasible extension of this work would be the application of the method to other environments, such as coastal waters and sediment pore waters which are subject to seasonal biogenic variations. As well as to other effects like HOM desorption and repartitioning between particle populations which may influence the fate and distribution of HOMs. Currently, a colleague is modifying the method to investigate the effect of surfactants on the particle-water interactions of HOMs. Dual-labelling (e.g. ^{14}C and ^{3}H) of two HOMs may allow the method to be used to investigate the effect of one HOM upon the aquatic behaviour of another. The method could also be modified to investigate the uptake of HOMs by zoo- and phytoplankton, the ultimate starting point for bioaccumulation and bioconcentration in the aquatic food chain.

REFERENCES

Abramowicz, D. A., Brennan, M. J., Van Dort, H. M. & Gallagher, E. L. (1993) Factors influencing the rate of polychlorinated biphenyl dechlorination in Hudson River sediments. *Environ. Sci. Technol.*, **27**, 1125-1131.

Adriaens, P., Fu, Q. & Grbic-Galic, D. (1995) Bioavailability and transformation of highly chlorinated dibenzo-*p*-dioxins and dibenzofurans in anaerobic soils and sediments. *Environ. Sci. Technol.*, **29**, 2252-2260.

Al-Omran, L. A. & Preston, M. R. (1987) The interactions of phthalate esters with suspended particulate material in fresh and marine waters. *Environ. Pollut.*, **46**, 177-186.

Ayotte, P., Dewailly, E., Ryan, J. J., Bruneau, S. & Lebel, G. (1997) PCBs and dioxin-like compounds in plasma of adult Inuit living in Nunavik (Arctic Quebec). *Chemosphere*, **34**, 1459-1468.

Baker, J. E., Capel, P. A. & Elsenrelch, S. J. (1986) Influence of colloids on sediment-water partitioning coefficients of polychlorobiphenyl congeners in natural waters. *Environ. Sci Technol.*, **20**, 1136-1143.

Barbeau, K. & Wollast, R. (1994) Microautoradiography (with combined liquid scintillation) applied to the study of trace metal uptake by suspended particles: Initial results using ^{63}Ni as a tracer. *Limnol. Oceanogr.*, **39**, 1211-1222.

Beckman Operating Manual (1993) *Beckman LSC6500 Scintillation System Operating Manual*, Beckman Instruments Inc. (Fullerton, USA), pages un-numbered.

Bergen, B. J., Nelson, W. G. & Pruell, R. J. (1993) Partitioning of polychlorinated biphenyl congeners in the sea water of New Bedford Harbour, Massachusetts. *Environ. Sci. Technol.*, **27**, 938-942.

Brannon, J. M., Myers, T. E., Gunnison, D. & Price, C. B. (1991) Nonconstant polychlorinated biphenyl partitioning in New Bedford Harbour sediment during sequential batch leaching. *Environ. Sci. Technol.*, **25**, 1082-1087.

Broman, D., Näf, C., Rolff, C. (1991) Occurrence and dynamics of polychlorinated dibenzo-p-dioxins and dibenzofurans and polycyclic aromatic hydrocarbons in the mixed surface layer of remote coastal and offshore waters of the Baltic. *Environ. Sci. Technol.*, **25**, 1850-1864.

Brooke, D. N., Neilson, I. R., Dobson, S. & Howe, P. D. (1991) *Environmental Hazard Assessment: Di-(2-ethylhexyl)phthalate*. Department of the Environment, Toxic Substances Division (Watford), 52 pp.

Brown, D., Thompson, R. S., Stewart, K. M., Croudace, C. P. & Gillings, E. (1996) The effect of phthalate ester plasticizers on the emergence of the midge (*Chironomus riparius*) from treated sediments. *Chemosphere*, **32**, 2177-2187.

Brownawell, B. J. & Farrington, J. W. (1985) Partitioning of PCBs in marine sediments. In: *Marine and Estuarine Geochemistry*, edited by A. C. Sigleo & A. L. Hattori, Chelsea (Michigan), pp 97-120.

Bruckmeier, B. F. A., Jüttner, I., Schramm, K-W., Winkler, R., Steinberg, C. E. W. & Kettrup, A. (1997) PCBs and PCDD/Fs in the lake sediments of Großer Arbersee, Bavarian Forest, South Germany. *Environ. Pollut.*, **95**, 19-25.

Brunk, B. K., Jirka, G. H. & Lion, L. W. (1997) Effects of salinity changes and the formation of dissolved organic matter coatings on the sorption of phenanthrene: Implications for pollutant trapping in estuaries. *Environ. Sci. Technol.*, **31**, 119-125.

Budzinski, H., Jones, I., Bellocq, J., Piérard, C. & Garrigues, P. (1997) Evaluation of sediment contamination by polycyclic aromatic hydrocarbons in the Gironde Estuary. *Mar. Chem.*, **58**, 85-97.

Campbell, D. E. & Spinrad, R. W. (1987) The relationship between light attenuation and particle characteristics in a turbid estuary. *Estuar. Coast. Shelf Sci.*, **25**, 53-65.

Caron, G., Suffet, I. H., & Belton, T. (1985) Effect of dissolved organic carbon on the environmental distribution of nonpolar organic compounds. *Chemosphere*, **14**, 993-1000.

Caulcutt, R. & Boddy, R. (1983) *Statistics for Analytical Chemists*, Chapman & Hall (London), 253 pp.

Chester, R. (1990) *Marine Geochemistry*, Chapman & Hall (London), 698 pp.

Chester, R. & Hughes, M. J. (1967) A chemical technique for the separation of ferro-manganese minerals, carbonate minerals and adsorbed trace metals from pelagic sediments. *Chem. Geol.*, **2**, 249-262.

Chiou, C. T., Malcolm, R. L., Brinton, T. I. & Kile, D. E. (1986) Water solubility enhancement of some organic pollutants and pesticides by dissolved humic and fulvic acids. *Environ. Sci. Technol.*, **20**, 502-508.

Chiou, C. T., Kile, D. E., Brinton, T. I., Malcolm, R. L., Leenheer, J. A. & MacCarthy, P. (1987) A comparison of water solubility enhancements of organic solutes by aquatic humic materials and commercial humic acids. *Environ. Sci. Technol.*, **21**, 1231-1234.

Crunkilton, R. L. & DeVita, W. M. (1997) Determination of aqueous concentrations of polycyclic aromatic hydrocarbons (PAHs) in an urban stream. *Chemosphere*, **35**, 1447-1463.

D'Adamo, R., Pelosi, S., Trotta, P. & Sansone, G. (1997) Bioaccumulation and biomagnification of polycyclic aromatic hydrocarbons in aquatic organisms. *Mar. Chem.*, **56**, 45-49.

Dachs, J., Bayona, J. M. & Albaigés, J. (1997a) Spatial distribution, vertical profiles and budget of organochlorine compounds in Western Mediterranean Sea water. *Mar. Chem.*, **57**, 313-324.

Dachs, J., Bayona, J. M., Raoux, C. & Albaigés, J. (1997b) Spatial, vertical distribution and budget of polycyclic aromatic hydrocarbons in the Western Mediterranean Sea water. *Environ. Sci. Technol.*, **31**, 682-688.

DeFoe, D. L., Holcombe, G. W., Hammermeister, D. E. & Beisinger, K. E. (1990) Solubility and toxicity of eight phthalate esters to four aquatic organisms. *Environ. Toxicol. Chem.*, **9**, 623-636.

DePaolis, F. & Kukkonen, J. (1997) Binding of organic pollutants to humic and fulvic acids: Influence of pH and the structure of humic material. *Chemosphere*, **34**, 1693-1704.

DeVargas, M. C., DeMedina, H. L. & Araujo K. (1994) Determination of metals in sediments of Sinamaica Lagoon, Venezuela by atomic absorption spectrometry. *Analyst*, **119**, 623-625.

Duinker, J. C. (1986) The role of small, low density particles on the partition of selected PCB congeners between water and suspended matter (North Sea area). *Neth. J. Sea Res.*, **20**, 161-178.

Duinker, J. C., Hillebrand, M. T. J., Nolting, R. F. & Wellershaus, S. (1982) The River Elbe: Processes affecting the behaviour of metals and organochlorines during estuarine mixing. *Neth. J. Sea Res.*, **15**, 141-169.

Duinker, J. C., Hillebrand, M. T. J., Nolting, R. F. & Wellershaus, S. (1985) The River Ems: Processes affecting the behaviour of metals and organochlorines during estuarine mixing. *Neth. J. Sea Res.*, **19**, 19-29.

Dyer, K. R. (1989) Sediment processes in estuaries: Future research requirements. *J. Geophys. Res.*, **94**, 14327-14339.

Dyer, K. R. (1997) *Estuaries: A Physical Introduction*, 2nd Edition. John Wiley & Sons (Chichester), 195 pp.

Dyrssen, D. & Wedborg, M. (1980) Major and minor elements, chemical speciation in estuarine waters. In: *Chemistry and Biogeochemistry of Estuaries*, edited by E. Olausson & I. Cato, John Wiley & Sons (Chichester), pp 71-119.

Eadie, B. J., Morehead, N. R. & Landrum, P. F. (1990) Three-phase partitioning of hydrophobic organic compounds in Great Lakes waters. *Chemosphere*, **1-2**, 161-178.

Eisma, D. (1993) *Suspended Matter in the Aquatic Environment*, Springer-Verlag (Berlin), 315pp.

Ejlertsson, J., Alnervik, M., Jonsson, S. & Svensson, B. H. (1997) Influence of water solubility, side-chain degradability, and side-chain structure on the degradation of phthalic acid esters under methanogenic conditions. *Environ. Sci. Technol.*, **31**, 2761-2764.

Ernst, W, Boon, J. P, & Weber, K. (1988) Occurrence and fate of organic micropollutants in the North Sea. In: *Pollution of the North Sea, an Assessment*, edited by W. Salomoms, B. L. Bayne, Duursma, E. K. & U. Förstner, Springer-Verlag (New York), pp 284-299.

Fatoki, O. S. & Vernon, F. (1990) Phthalate esters in rivers of the Greater Manchester area, UK. *Sci. Total Environ.*, **95**, 227-232.

Fifield, F. W. & Kealey, D. (1995) *Principles and Practice of Analytical Chemistry*, 4th Edition, Blackie Academic and Professional (London), 560 pp.

Futoma, D. J., Smith, S. R., Smith, T. E. & Tanaka, J. (1981) *Polycyclic Aromatic Hydrocarbons in Water Systems*, CRC Press (Florida), 190 pp.

Gawlik, B. M., Sotiriou, N., Feicht, E. A., Schulte-Hostede, S. (1997) Alternatives for the determination of the soil adsorption coefficient, K_{oc}, of non-ionic organic compounds-A review. *Chemosphere*, **34**, 2525-2551.

Giam, C. S., Atlas, E., Powers, Jr., M. A. & Leonard, J. E. (1984) Phthalic acid esters. In: *The Handbook of Environmental Chemistry, Volume 3 Part C, Anthropogenic Compounds*. Edited by O. Hutzinger, Springer-Verlag (Berlin), pp 67-142.

Gibbs, P. E. (1984) The population cycle of the bivalve *Abra tenuis* and its mode of reproduction. *J. Mar. Biol. Assoc. U.K.*, **64**, 791-800.

Girvin, D. C. & Scott, A. J. (1997) Polychlorinated biphenyl sorption by soils: Measurement of soil-water partition coefficients at equilibrium. *Chemosphere*, **35**, 2007-2025.

Gobas, F. A. P. C., McNeill, E. J., Lovett-Doust, L. & Haffner, G. D. (1991) Bioconcentration of chlorinated aromatic hydrocarbons in aquatic macrophytes. *Environ. Sci. Technol.*, **25**, 924-929.

Goulding, K. H. (1986) Radioisotope techniques. In: *A Biologists Guide to Principles and Techniques of Practical Biochemistry*, 3rd Edition, edited by K. Wilson & K. H. Goulding, Edward Arnold (London), pp 314-344.

Gribble, G. W. (1994) The natural production of chlorinated compounds. *Environ. Sci. Technol.*, **28**, 310A-319A.

Gschwend, P. M., & Wu, S-C. (1985) On the constancy of sediment-water partition coefficients of hydrophobic organic pollutants. *Environ. Sci. Technol.*, **19**, 90-96.

Harrad, S. T., Sewart, A. P., Alcock, R., Boumphrey, R., Burnett, V., Duarte-Davidson, R., Halsall, C., Sanders, G., Waterhouse, K., Wild, S. R. & Jones, K. C. (1994) Polychlorinated biphenyls (PCBs) in the British environment: Sinks, sources and trends. *Environ. Pollut.*, **85**, 131-146.

Harris, J. R. W., Gorley, R. N. & Bartlett, C. A. (1993) *ECoS Version 2: An Estuarine Simulation Shell, User Manual*, Plymouth Marine Laboratory, UK, 146 pp.

Hashimoto, Y., Tokura, K., Kishi, H. & Strachan, W. M. J. (1984) Prediction of sea water solubility of aromatic compounds. *Chemosphere*, **13**, 881-888.

Hassett, J. P. & Anderson, M. A. (1978) Association of hydrophobic organic compounds with dissolved organic matter in aquatic systems. *Environ. Sci. Technol.*, **13**, 1526-1529.

Hawker, D. W. & Connell, D. W. (1988) Octanol-water partition coefficients for polychlorinated biphenyl congeners. *Environ. Sci. Technol.*, **22**, 382-387.

Hegeman, W. J. M., Van der Weijden, C. H. & Loch, J. P. G. (1995) Sorption of benzo(*a*)pyrene and phenanthrene on suspended harbour sediment concentration and salinity: A laboratory study using the cosolvent partition coefficient. *Environ. Sci. Technol.*, **29**, 363-371.

Honeyman, B. D., & Santschi, P. H. (1988) Metals in aquatic systems. *Environ. Sci. Technol.*, **22**, 862-871.

Horzempa, L. M. & Di Toro, D. M. (1983) The extent of reversibility of polychlorinated biphenyl adsorption. *Wat. Res.*, **17**, 851-859.

Howard, P. H., Boethling, R. S., Jarvis, W. F., Meylan, W. M. & Michalenko, E. W. (1991) *Handbook of Environmental Degradation Rates*, Lewis publishers (Michigan), 725pp.

Hunchak-Kariouk, K., Schweitzer, L. & Suffet, I. H. (1997) Partitioning of 2,2',4,4'-Tetrachlorobiphenyl by the dissolved organic matter in oxic and anoxic porewaters. *Environ. Sci. Technol.*, **31**, 639-645.

Hunter, K. A. & Liss, P. S. (1979) The surface charge of suspended particles in estuarine and coastal waters. *Nature*, **282**, 823-825.

Hunter, M. A., Kan, A. T. & Tomson, M. B. (1996) Development of a surrogate sediment to study the mechanisms responsible for adsorption/desorption hysteresis. *Environ. Sci. Technol.*, **30**, 2278-2285.

Huthnance, J. M., Allen, J. I., Davies, A. M., Hydes, D. J., James, I. D., Jones, J. E., Millward, G. E., Prandle, D., Proctor, R., Purdie, D. A., Statham, P. J., Tett, P. B., Thomson, S. & Wood, R.G. (1993) Towards water quality models. *Phil. Trans. Roy. Soc. Lond. A*, **343**, 569-584.

Hutzinger, O., Safe, S. & Zitko, V. (1974) *The Chemistry of PCB's*, CRC Press (Cleveland), 269 pp.

Jannasch, H. W., Honeyman, B. D., Balistrieri, L. S. & Murray, J. W. (1988) Kinetics of trace element uptake by marine particles. *Geochim. Cosmochim. Acta.*, **52**, 567-577.

Järnberg, U., Asplund, L., de Wit, C., Grafström, A-K., Haglund, P., Jansson, B., Lexén, K., Strandell, M., Olsson, M. & Jonsson, B. (1993) Polychlorinated biphenyls and polychlorinated naphthalenes in Swedish sediment and biota: Levels, patterns and time trends. *Environ. Sci. Technol.*, **27**, 1364-1374.

Jeffery, G. H., Bassett, J., Mendham, J. & Denney, R. C. (1989) *Vogel's Textbook of Quantitative Chemical Analysis*, 5th Edition, Longman Scientific & Technical (New York), 877 pp.

Jepsen, R., Borglin, S., Lick, W. & Swackhamer, D. L. (1995) Parameters affecting the adsorption of hexachlorobenzene to natural sediments. *Environ. Toxicol. Chem.*, **14**, 1487-1497.

Jobling, S., Reynolds, T., White, R., Parker, M. G. & Stumper, J. P. (1995) A variety of environmentally persistent chemicals, including some phthalate plasticizers, are weakly oestrogenic. *Environ. Health Perspect.*, **103**, 582-587.

Johnson, C. A. & Thornton, I. (1987) Hydrological and chemical factors controlling the concentrations of Fe, Cu, Zn and As in a river system contaminated by acid mine drainage. *Wat. Res.*, **21**, 359-365.

Johnston, P. A., Stringer, R. J. & French, M. C. (1991) Pollution of UK estuaries: Historical and current problems. *Sci. Total Environ.*, **106**, 55-70.

Karcher, W., Fordham, R. J. Dubois, J. J., Glaude, P. G. J. M. & Ligthart, J. A. M. (1983) *Spectral Atlas of Polycyclic Aromatic Compounds*, D. Reidel Publishing Company (Dordrecht), 818 pp.

Karcher, W., Ellison, S., Ewald, M., Garrigues, P., Gevers, E. & Jacob, J. (1988) *Spectral Atlas of Polycyclic Aromatic Compounds*, Volume 2, Kluwer Academic Publishers (Dordrecht), 864 pp.

Karickhoff, S. W. (1984) Organic pollutant sorption in aquatic systems. *J. Hydraul. Eng.*, **110**, 707-735.

Klamer, H. J. C. & Fomsgaard, L. (1993) Geographical distribution of chlorinated biphenyls (CBs) and polycyclic aromatic hydrocarbons (PAHs) in surface sediments from the Humber Plume, North Sea. *Mar. Pollut. Bull.*, **26**, 201-206.

Klamer, H. J. C., Van Zoest, R., Laane, R. W. P. M. & Van Eck, B. T. M. (1994) Estuaries as a filter for organic micropollutants: A case study of PCBs in the Rhine and Scheldt. In: *Changes in Fluxes in Estuaries: Implications from Science to Management*, edited by K. R. Dyer & R. J. Orth, Olsen & Olsen (Fredensborg), pp 121-124.

Ko, F-C. & Baker, J. E. (1995) Partitioning of hydrophobic organic contaminants to resuspended sediments and plankton in the mesohaline Chesapeake Bay. *Mar. Chem.*, **49**, 171-188.

Kretzschmar, R., & Sticher, H. (1997) Transport of humic-coated iron oxide colloids in a sandy soil: Influence of Ca^{2+} and trace metals. *Environ. Sci. Technol.*, **31**, 3497-3504.

Landrum, P. F. (1989) Bioavailability and toxicokinetics of polycyclic aromatic hydrocarbons sorbed to sediments for the amphipod *Pontoporeia hoyi*. *Environ. Sci. Technol.*, **23**, 588-595.

Landrum, P. F., Nihart, S. R., Eadie, B. J. & Gardner, W. S. (1984) Reverse-phase separation method for determining pollutant binding to Aldrich humic acid and dissolved organic carbon of natural waters. *Environ. Sci. Technol.*, **18**, 187-192.

Lang, V. (1992) Review: Polychlorinated biphenyls in the environment. *J. Chromatogr.*, **595**, 1-43.

Law, R. J., Allchin, C. R. & Dixon, A. G. (1991a) Polychlorinated biphenyls in sediments downstream of a contaminated industrial site in North Wales. *Mar. Pollut. Bull.*, **22**, 492-493.

Law, R. J., Fileman, T. W., & Matthiessen, P. (1991b) Phthalate esters and other industrial organic chemicals in the North Sea and Irish Seas. *Wat. Sci. Tech.*, **24**, 127-134.

Li, X-F., Le, X-C., Simpson, C. D., Cullen, W. R. & Reimer, K. J. (1996) Bacterial transformation of pyrene in a marine environment. *Environ. Sci. Technol.*, **30**, 1115-1119.

Lion, L. W., Altmann, R. S. & Leckle, J. O. (1982) Trace-metal adsorption characteristics of estuarine particulate matter: evaluation of contributions of Fe/Mn oxide and organic surface coatings. *Environ. Sci. Technol.*, **16**, 660-666.

Liu, Y. P. (1996) *Modelling Estuarine Chemical Dynamics of Trace Metals*, Ph.D. thesis, University of Plymouth, 239pp.

Long, J. L. A., House, W. A., Parker, A. & Rae, J. E. (1998) Micro-organic compounds associated with sediments in the Humber rivers. *Sci. Total Environ.*, **210/211**, 299-253.

Lotse, E. G., Graetz, D. A., Chesters, G., Lee, G. B., & Newland, L. W., (1968) Lindane adsorption by lake sediments. *Environ Sci. Technol.*, **2**, 353-357.

Lovett, A. A., Foxall, C. D., Creaser, C. S. & Chewe, D. (1997) PCB and PCDD/DF congeners in locally grown fruit and vegetable samples in Wales and England. *Chemosphere*, **34**, 1421-1436.

Maaret, K., Leif, K. & Bjarne, H. (1992) Studies on the behaviour of three organic hydrophobic pollutants in natural humic water. *Chemosphere*, **24**, 919-925.

MacKay, D. & Paterson, S. (1991) Evaluating the multimedia fate of organic chemicals: A level III Fugacity model. *Environ. Sci. Technol.*, **25**, 427-436.

MacKay, D. & Powers, B. (1987) Sorption of hydrophobic chemicals from water: a hypothesis for the mechanism of the particle concentration effect. *Chemosphere*, **16**, 745-757.

Mader, B. T., Uwe-Goss, K. & Eisenreich, S. J. (1997) Sorption of nonionic, hydrophobic organic chemicals to mineral surfaces. *Environ. Sci. Technol.*, **31**, 1079-1086.

MAFF (1995) *Aquatic Environment Monitoring Report Number 45: Radioactivity in Surface and Coastal Waters of the British Isles*, 1994, MAFF (Lowestoft), 111 pp.

Mantoura, R. F. C. & Woodward, E. M. S. (1983) Conservative behaviour of riverine dissolved organic carbon in the Severn Estuary: chemical and geochemical implications. *Geochim. Cosmochim. Acta*, **47**, 1293-1309.

May, W. E., Wasik, S. P. & Freeman, D. H. (1978) Determination of the solubility behaviour of some polycyclic aromatic hydrocarbons in water. *Anal. Chem.*, **51**, 3-16.

McKinley, J. P. & Jenne, E. A. (1991) Experimental investigation and review of the 'solids concentration' effect in adsorption studies. *Environ. Sci. Technol.*, **25**, 2082-2087.

Means, J. C. (1995) Influence of salinity upon sediment-water partitioning of aromatic hydrocarbons. *Mar. Chem.*, **51**, 3-16.

Means, J. C., Wood, S. G., Hassett, J. J. & Banwart, W. J. (1980) Sorption of polynuclear aromatic hydrocarbons by sediment and soils. *Environ. Sci. Technol.*, **14**, 1524-1528.

Millward, G. E., Turner, A., Glasson, D. R. & Glegg, G. A. (1990) Intra- and inter-estuarine variability of particle microstructure. *Sci. Total Environ.*, **97/98**, 289-300.

Millward, G. E., Glegg, G. A. & Morris, A. W. (1992) Zn and Cu removal kinetics in estuarine waters. *Estuar. Coast. Shelf Sci.*, **35**, 37-54.

Mook, D. H. & Hoskin, C. M. (1982) Organic determinations by ignition: caution advised. *Estuar. Coast. Shelf Sci.*, **15**, 697-699.

Morris, A. W. (1990) Kinetic and equilibrium approaches to estuarine chemistry. *Sci. Total Environ.*, **97/98**, 253-266.

Morris, R. J., Law, R. J., Allchin, C. R., Kelly, C. A. & Fileman, C. F. (1989) Metals and organochlorines in dolphins and porpoises of Cardigan Bay, West Wales. *Mar. Pollut. Bull.*, **20**, 512-523.

Morrison, H. A., Gobas, F. A. P. C., Lazar, R. & Haffner, G. D. (1996) Development and verification of a bioaccumulation model for organic contaminants in benthic invertebrates. *Environ. Sci. Technol.*, **30**, 3377-3384.

Mössner, S. & Ballschmiter, K. (1997) Marine mammals as global pollution indicators for organochlorines. *Chemosphere*, **34**, 1285-1296.

Muir, D. C. G., Lawrence, S., Holoka, M., Fairchild, W. L., Segstro, M. D., Webster, G. R. B. & Servos, M. R. (1992) Partitioning of polychlorinated dioxins and furans between water , sediments, and biota in lake mesocosms. *Chemosphere*, **25**, 119-124.

Muller, F. L. L., Burton, J. D. & Statham, P. J. (1991) Long-term changes in the adsorptive properties of FEP separating funnels in a mixed dithiocarbamate-Freon-TF extraction system. *Anal. Chim. Acta*, **245**, 21-25.

Murphy, E. M., Zachara, J. M. & Smith, S. C. (1990) Influence of mineral-bound humic substances on the sorption of hydrophobic organic compounds. *Environ. Sci. Technol.*, **24**, 1507-1516.

Newton, P. P. & Liss, P. S. (1987) Positively charged suspended particles: Studies in an iron-rich river and its estuary. *Limnol. Oceanogr.*, **32**, 1267-1276.

Ng, B., Turner, A., Tyler, A. O., Falconer, R. A. & Millward, G. E. (1996) Modelling contaminant geochemistry in estuaries. *Wat. Res.*, **30**, 63-74.

Niimi, A. J. (1996) Review article: Evaluation of PCBs and PCDD/Fs retention by aquatic organisms. *Sci. Total Environ.*,**192**, 123-150.

O'Connor, D. J. & Connolly, J. P. (1980) The effect of concentration of adsorbing solids on the partition coefficient. *Wat. Res.*, **14**, 1517-1523.

O'Neill, P. (1993) *Environmental Chemistry*, 2nd Edition. Chapman & Hall (London), 268 pp.

Peterson J. C. & Freeman, D. H. (1982) Phthalate ester concentration variations in dated sediment cores from the Chesapeake Bay. *Environ. Sci. Technol.*, **16**, 464-469.

Philips Operating Manual (undated) *Liquid Scintillation Counter PW4700 with Single Board Computer PW4701/01,-/02, Operating Manual*. Philips (UK), 69 pp.

Preston, M. R. & Al-Omran, L. A. (1986) Dissolved and particulate phthalate esters in the River Mersey Estuary. *Mar. Pollut. Bull.*, **17**, 548-553.

Preston, M. R. & Al-Omran, L. A. (1989) Phthalate ester speciation in estuarine water, suspended particulates and sediments. *Environ. Pollut.*, **62**, 183-193.

Rawling, M. C. (1994) *The Hydrography of White Sea Estuaries, Russia.* M.Sc. thesis, University of Plymouth, 162 pp.

Readman, J. W., Mantoura, R. F. C., Rhead, M. M. & Brown, L. (1982) Aquatic distribution and heterotrophic degradation of polycyclic aromatic hydrocarbons (PAH) in the Tamar Estuary. *Estuar. Coast. Shelf Sci.*, **14**, 369-389.

Rhee, G-Y., Sokol, R. C., Bethaney, C. M. & Bush, B. (1993) Dechlorination of polychlorinated biphenyls by Hudson River sediment organisms: Specificity to the chlorination pattern of congeners. *Environ. Sci. Technol.*, **27**, 1190-1192.

Ritsema, R., Cofino, W. P., Frintrop, P. C. M. & Brinkman, U. A. Th. (1989) Trace-level analysis of phthalate esters in surface water and suspended particulate matter by means of capillary gas chromatography with electron-capture and mass-selective detection. *Chemosphere*, **18**, 2161-2175.

Romkens, P. F. A. M. & Dolfing, J. (1998) Effect of Ca on the solubility and molecular size distribution of DOC and Cu binding in soil solution samples. *Environ. Sci. Technol.*, **32**, 363-369.

Rossi, S. S. & Thomas, W. H. (1981) Solubility behaviour of three aromatic hydrocarbons in distilled water and natural sea water. *Environ. Sci. Technol.*, **15**, 715-716.

Rubinstein, N. I., Pruell, R. J., Taplin, B. K., Livolsi, J. A., & Norwood, C. B. (1990) Bioavailability of 2,3,7,8-TCDD, 2,3,7,8-TCDF and PCBs to marine benthos from Passaic River sediments. *Chemosphere*, **20**, 1097-1102.

Russell, D. J. & McDuffie, B. (1986) Chemodynamic properties of phthalate esters: partitioning and soil migration. *Chemosphere*, **15**, 1003-1021.

Rust, M. B., Hardy, R. W. & Stickney, R. R. (1993) A new method for force-feeding larval fish. *Aquaculture*, **116**, 341-352.

Sanders, G., Hamilton-Taylor, J. & Jones, K. C. (1996) PCB and PAH dynamics in a small rural lake. *Environ. Sci. Technol.*, **30**, 2958-2966.

Santodonato, J. (1997) Review of the oestrogenic and antioestrogenic activity of polycyclic aromatic hydrocarbons: Relationship to carcinogenicity. *Chemosphere*, **34**, 835-848.

Schulz-Bull, D. E., Petrick, G. & Duinker, J. C. (1991) Polychlorinated biphenyls in North Sea water. *Mar. Chem.*, **36**, 365-384.

Schwarzenbach, R. P., Gschwend, P. M. & Imboden, D. M. (1993) *Environmental Organic Chemistry*, John Wiley & Sons, Inc. (New York), 681 pp.

Sheu, H-L., Lee, W-J., Lin, S. J., Fang, G-C., Chang, H-C. & You, W-C. (1997) Particle-bound PAH content in ambient air. *Environ. Pollut.*, **96**, 369-382.

Simcik, M. F., Eisenreich, S. J., Golden, K. A., Liu, S-P, Lipiatou, E., Swackhamer, D. L. & Long, D. T. (1996) Atmospheric loading of polycyclic aromatic hydrocarbons to Lake Michigan as recorded in the sediments. *Environ. Sci. Technol.*, **30**, 3039-3046.

Staples, C. A., Peterson, D. R., Parkerton, T. F. & Adams, W. J. (1997) The environmental fate of phthalate esters: A literature review. *Chemosphere*, **35**, 667-749.

Statham, P.J. & Williams, P. J. LeB. (1983) The automatic determination of dissolved organic carbon. In: *Methods of Sea water Analysis*, edited by K. Grasshoff, M. Ehrhardt & K. Kremling, Verlag Chemie (New York), pp 380-393.

Stumm, W. & Morgan, J. J. (1996) *Aquatic Chemistry: Chemical Equilibria and Rates in Natural Waters*, 3rd Edition. J. Wiley & Sons (New York), 1022 pp.

Sullivan, K. F., Atlas, E. L. & Giam, C-S. (1982) Adsorption of phthalic esters from sea water. *Environ. Sci. Technol.*, **16**, 428-432.

Tait, D. & Wiechen, A. (1993) Use of liquid scintillation counting of ^{89}Sr and ^{90}Sr in milk. *Sci. Total Environ.*, **130/131**, 447-457.

Tanabe, S. (1988) PCB problems in the future: Foresight from current knowledge. *Environ. Pollut.*, 50, 5-28.

Tancell, P. J. & Rhead, M. M. (1996) Application of radio-chromatographic techniques to diesel emissions research. *J. Chromatogr. A*, **737**, 181-192.

Turner, A. & Tyler, A. O. (1997) Modelling adsorption and desorption processes in estuaries. In: *Biogeochemistry of Intertidal Sediments*, edited by T. D. Jickells & J. E. Rae, Cambridge University Press (Cambridge), pp 42-58.

Turner, A., Millward, G. E., Bale, A. J. & Morris, A.W. (1993) Application of the K_D concept to the study of trace metal removal and desorption during estuarine mixing. *Estuar. Coast. Shelf Sci.*, **36**, 1-13.

Tyler, A. O. & Millward, G. E. (1996) Distribution and partitioning of polychlorinated dibenzo-*p*-dioxins, polychlorinated dibenzofurans and polychlorinated biphenyls in the Humber Estuary, UK. *Mar. Pollut. Bull.*, **32**, 397-403.

Van Eck, G. T. M., Zwolsman, J. J. G & Saejs, H. L. F. (1997) Influence of compartmentalization on the water quality of reservoirs: Lessons learned from the enclosure of the Haringvliet Estuary. The Netherlands. *Neth. J. Sea Res.*, **40**, 647-669.

Van Metre, P. C., Wilson, J. T., Callender, E. & Fuller, C. C. (1998) Similar rates of decrease of persistent, hydrophobic and particle-reactive contaminants in riverine systems. *Environ. Sci. Technol.*, **32**, 3312-3317.

Van Zoest, R. & Van Eck, G. T. M. (1993) Historical input and behaviour of hexachlorobenzene, polychlorinated biphenyls and polycyclic aromatic hydrocarbons in two dated sediment cores from the Scheldt Estuary, SW Netherlands. *Mar. Chem.*, **44**, 95-103.

Voice, T. C. & Weber, Jr., W. J. (1985) Sorbent concentration effects in liquid/solid partitioning. *Environ. Sci. Technol.*, **19**, 789-796.

Wams, T. J. (1987) Diethylhexylphthalate as an environmental contaminant-A review. *Sci. Total Environ.*, **66**, 1-16.

Wania, F. & MacKay, D. (1996) Tracking the distribution of persistent organic pollutants. *Environ. Sci. Technol.*, **30**, 390A-396A.

Whitehouse, B. G. (1984) The effects of temperature and salinity on the aqueous solubility of polynuclear aromatic hydrocarbons. *Mar. Chem.*, **14**, 319-332.

Wijayaratne, R. D. & Means, J. C. (1984) Sorption of polycyclic aromatic hydrocarbons by natural estuarine colloids. *Mar. Environ. Res.*, **11**, 77-89.

Williams, M. D., Adams, W. J., Parkerton, T. F., Biddinger, G. R. & Robillard, K. A. (1995) Sediment sorption coefficient measurements for four phthalate esters: Experimental results and model theory. *Environ. Toxicol. Chem.*, **14**, 1477-1486.

Williams, P. J. LeB. (1985) Analysis: organic matter. In: *Practical Estuarine Chemistry: A Handbook*, edited by P.C. Head, Cambridge University Press (Cambridge), pp 160-200.

Xie, W-H., Shiu, W-Y., & MacKay, D. (1997) A review of the effect of salts on the solubility of organic compounds in sea water. *Mar. Environ. Res.*, **44**, 429-444.

Ye, D., Siddiqi, M. A., MacCubbin, A. E., Kumar, S. & Sikka, H. C. (1996) Degradation of polynuclear aromatic hydrocarbons by *Sphingomonas pauchimobilis*. *Environ. Sci. Technol.*, **30**, 136-142.

Zhou, J. L. & Rowland, S. J. (1997) Evaluation of the interactions between hydrophobic organic pollutants and suspended particles in estuarine waters. *Wat. Res.*, **31**, 1708-1718.

Zhou, J. L., Rowland, S. & Mantoura, R. F. C. (1995) Partition of synthetic pyrethroid insecticides between dissolved and particulate phases. *Wat. Res.*, **29**, 1023-1031.

Zhou, J. L., Fileman, T. W., Evans, S., Donkin, P., Mantoura, R. F. C., & Rowland, S. J. (1996) Seasonal distribution of dissolved pesticides and polynuclear aromatic hydrocarbons in the Humber Estuary and Humber coastal zone. *Mar. Pollut. Bull.*, **32**, 599-608.

GLOSSARY

BaP: benzo[a]pyrene.

BAF: bioaccumulation factor (Section 1.3.1.3.).

BCF: bioconcentration factor (Section 1.3.1.3.).

Congeners: a series of isomers or compounds (usually PCBs), which have different numbers of chlorine atoms, that originate from the same source.

DEHP: bis(2-ethylhexyl)phthalate ester.

DOC: dissolved organic carbon.

DOM: dissolved organic matter

Electrostriction: reduction in the volume of an aqueous solution caused by the formation of water hydration shells around the ions produced from the dissolution of a salt.

F_R: the fraction of HOM retained in an estuary (Section 5.5.2.).

F_S: the fraction of HOM in solution (Section 5.5.1.).

Fugacity: the potential of a compound to transfer from one environmental compartment to another.

Hydrophobic organic micropollutant, HOM: an organic compound, present in the environment at the sub-micron level, which is 'water-hating' and a possible acute and/or chronic toxin to the local biosphere.

K_D: particle-water partition coefficient (Section 1.3.1.2.)

K_H: Henry's law constant (Section 1.3.1.1.).

K_{oc}: organic carbon normalised partition coefficient (Section 1.3.1.2.).

K_{ow}: *n*-octanol-water partition coefficient (Section 1.2.).

Lipophilicity: 'lipid/fat-liking', a lipophilic compound tends to accumulate in biological tissues.

Loss on ignition, LOI: a measure of the non-refractory organic matter in sediment

LSC: liquid scintillation counting (Section 2.6.).

PAH: polycyclic aromatic hydrocarbons, organic compounds comprising of between two and eight aromatic rings which are naturally occurring and produced during the incomplete combustion of, wood, coal and petroleum products.

Particle concentration effect, PCE: the exponential decrease in the particle-water partition coefficient of an organic compound as the suspended particulate matter concentration increases

PCB: polychlorinated biphenyl, aromatic chlorinated hydrocarbons produced commercially by the direct chlorination of biphenyl (Section 1.2.2.)

PE: phthalate ester, the diesters of phthalic acid (Section 1.2.3.)

POC: particulate organic carbon

Propagation of error: statistical error culminated over the various stages of a multi-staged experimental procedure or calculation (Section 2.7.5; Appendix B).

Quenching: a reduction in the counting efficiency of a scintillation counter caused by interference within a sample affecting the energy transfer from the radiotracer to the photomultiplier tube, reducing the light output of the sample.

Salting out: the reduction in the relative solubility of an organic compound associated with an increase in salinity.

Setschenow constant, σ: a constant describing the magnitude of the 'salting out' effect on a known organic compound (Section 3.2.4.1.).

SPM: suspended particulate matter.

SSA: specific surface area

System response time, τ_{resp}: the time required to attain 63% of the new particle-water partitioning equilibrium after the system has been altered.

Turbidity maximum zone, TMZ: an area of relatively high suspended particulate matter concentration within an estuary.

2,2',5,5'-TCB: 2,2',5,5'-tetrachlorobiphenyl.

APPENDICES

APPENDIX A: GAS-CHROMATOGRAPHY

A1: GC-MS Chromatograms

A2: Radio-GC Chromatograms

APPENDIX B: GENERATED DATA

B1: Method Evaluation Data

B2: Relative Solubility Data

B3: Particle-Water Interaction Data

APPENDIX C: PUBLICATION

M. C. Rawling, A. Turner & A. O. Tyler (1998) Particle-water interactions of 2,2',5,5'-Tetrachlorobiphenyl under simulated estuarine conditions. *Marine Chemistry*, **61**, 115-126.

APPENDIX A: GAS-CHROMATOGRAPHY

A1: GC-MS Chromatograms

Analyst; Dr. J. L. Zhou

A2: Radio-GC Chromatograms

Analysts; M. C. Rawling & T. Hyde

A1: GC-MS Chromatograms

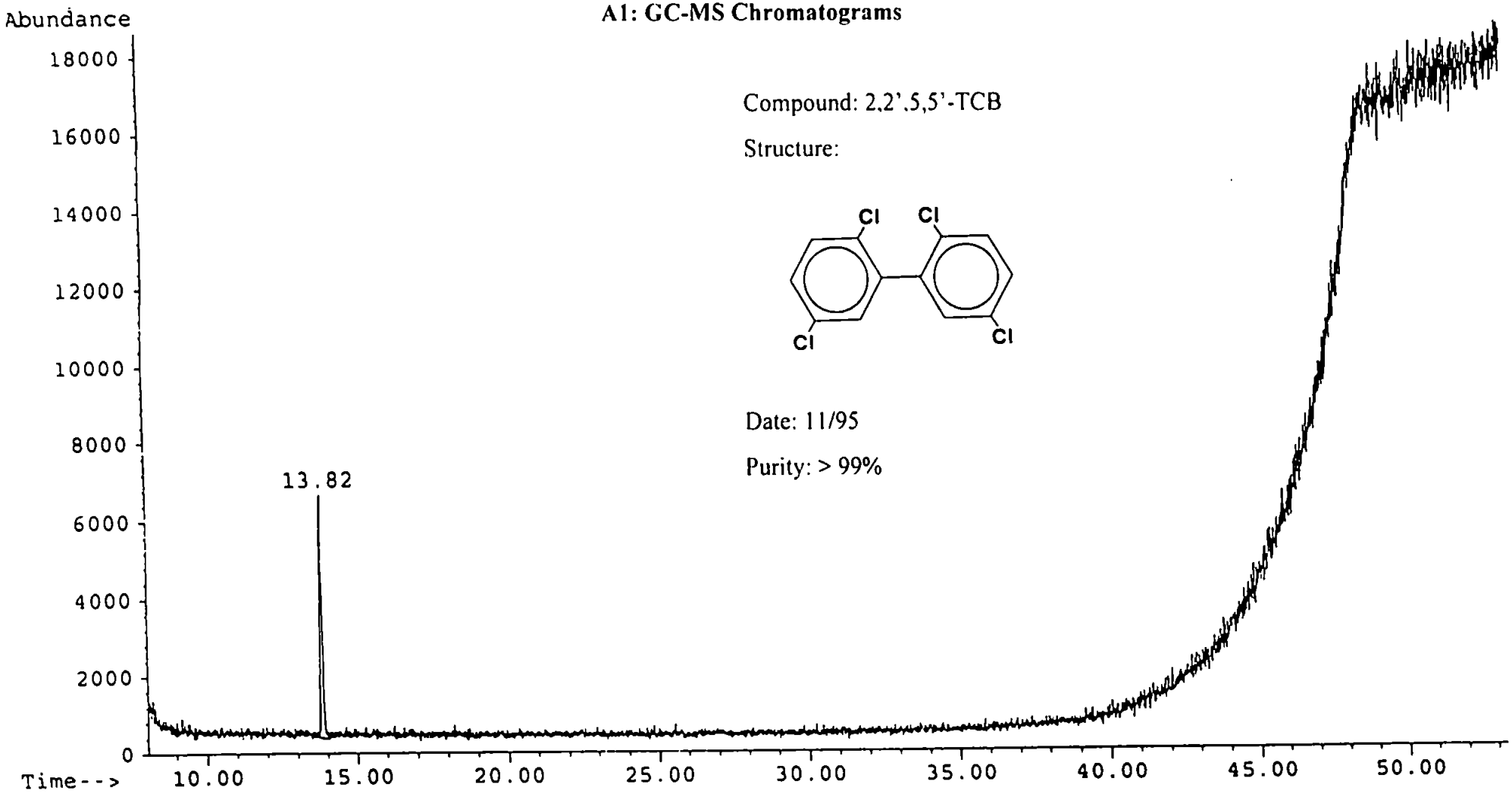

Figure A1.1: Chromatogram showing compound purity of 2,2',5,5'-TCB stock solution.

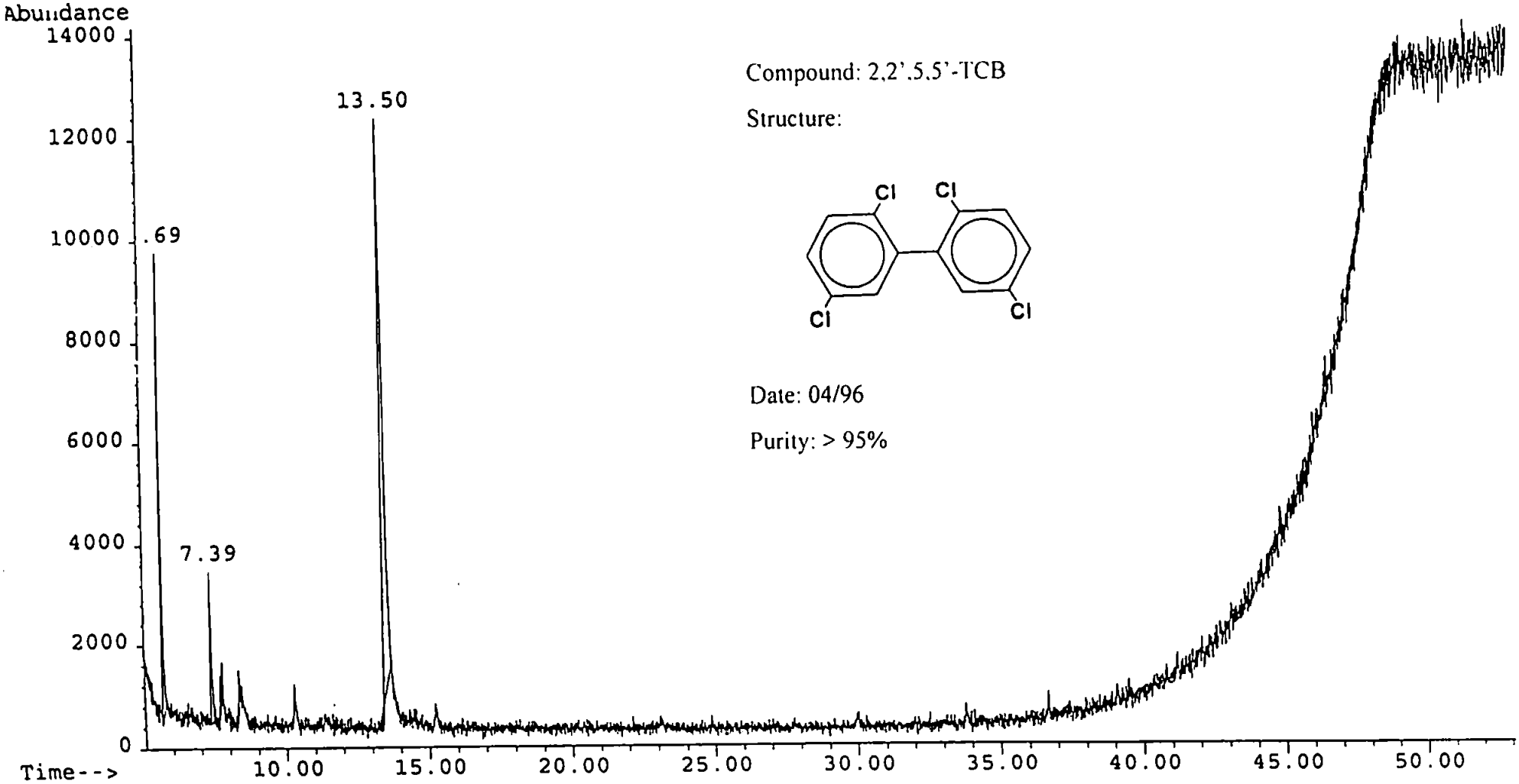

Figure A1.2: Chromatogram showing compound purity of 2,2',5,5'-TCB stock solution.

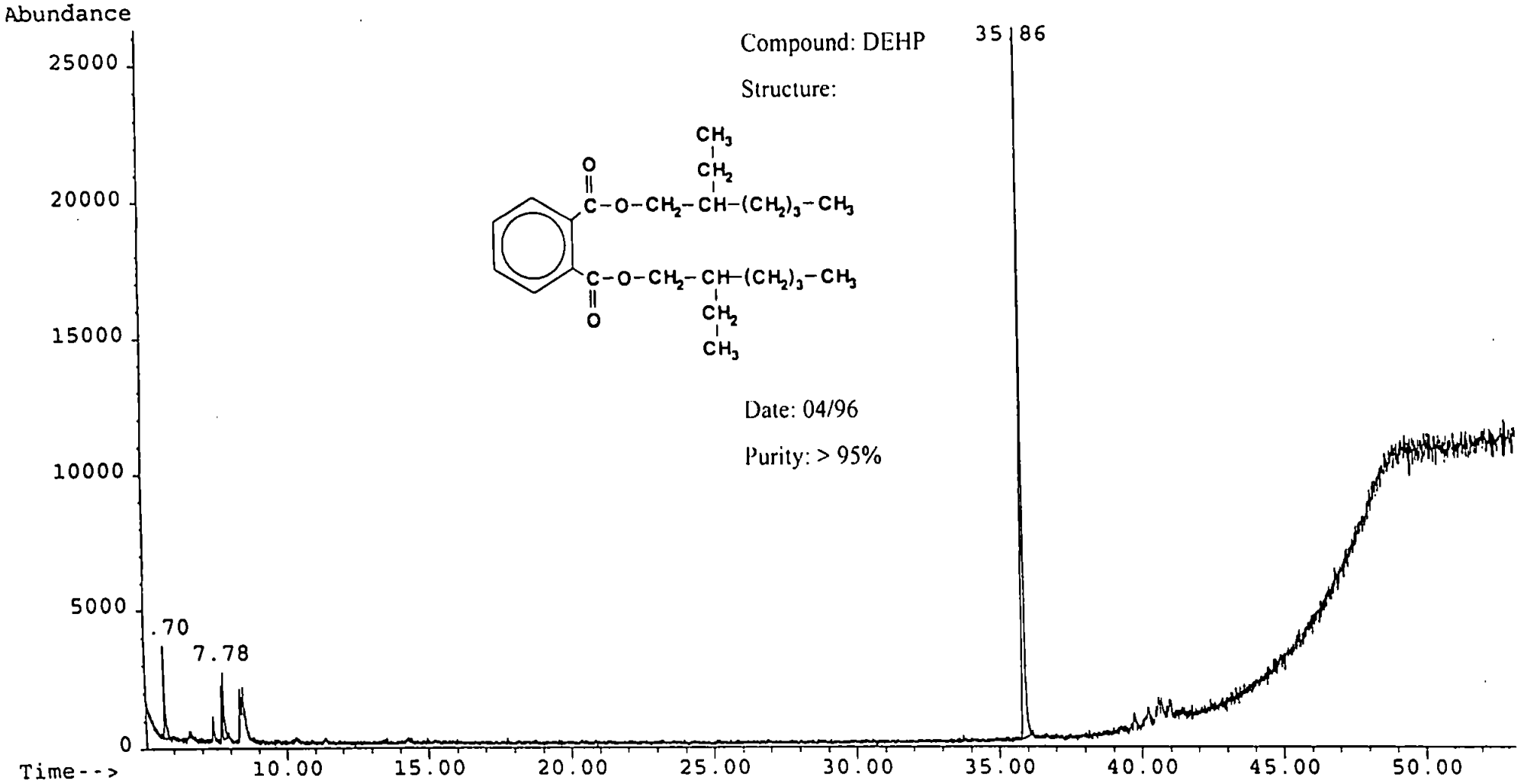

Figure A1.3: Chromatogram showing compound purity of DEHP stock cocktail.

A2: Radio-GC Chromatograms

Compound: 2,2',5,5'-TCB

Structure:

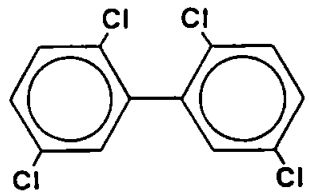

Date: 09/97

Peak number	Height (CPS)	Area (CPS)	Area (%)
1	20.37	171.3	1.88
2	884.7	8929.8	98.12

Figure A2.1: Chromatogram showing radioactive purity of 2,2',5,5'-TCB stock solution prior to an experiment.

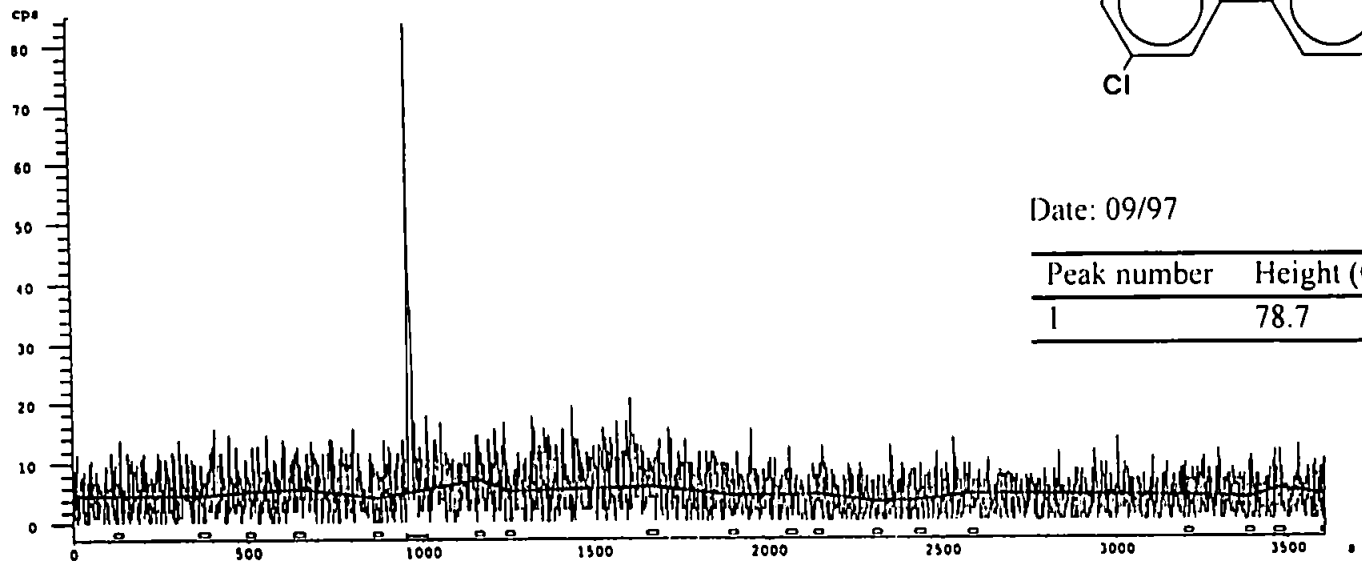

Compound: 2,2',5,5'-TCB

Structure:

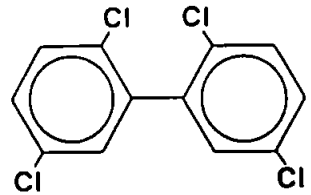

Date: 09/97

Peak number	Height (CPS)	Area (CPS)	Area (%)
1	78.7	570.2	100.00

Figure A2.2: Chromatogram showing radioactive solution of 2.2',5,5'-TCB after an experiment involving Plym river water and sediment samples.

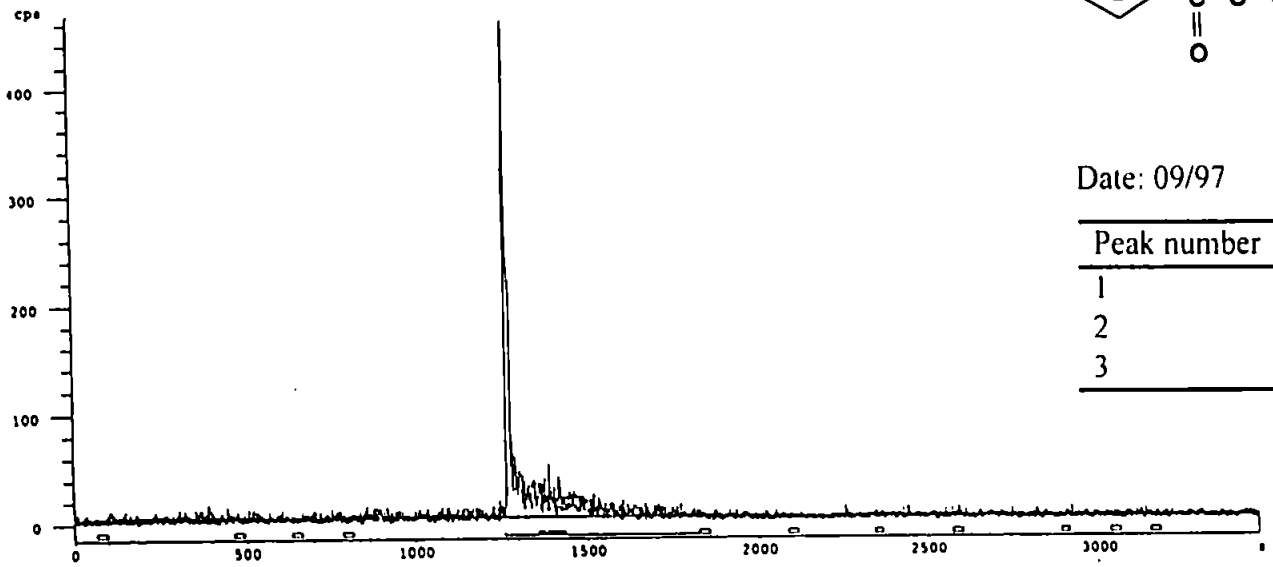

Compound: DEHP

Structure:

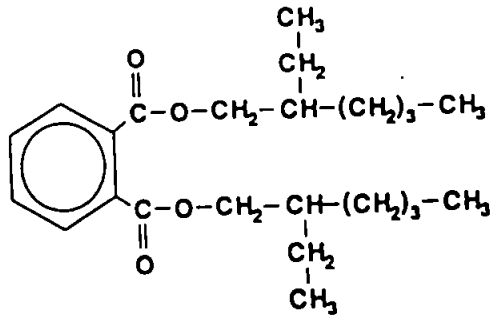

Date: 09/97

Peak number	Height (CPS)	Area (CPS)	Area (%)
1	456.8	8536.2	94.77
2	21.8	74.0	0.82
3	44.8	397.0	4.41

Figure A2.3: Chromatogram showing radioactive purity of DEHP stock solution prior to an experiment.

Compound: DEHP

Structure:

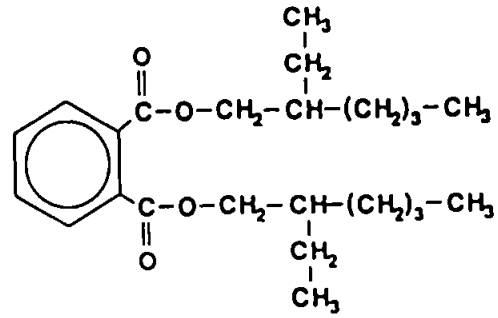

Date: 09/97

Peak number	Height (CPS)	Area (CPS)	Area (%)
1	114	741.4	100.0

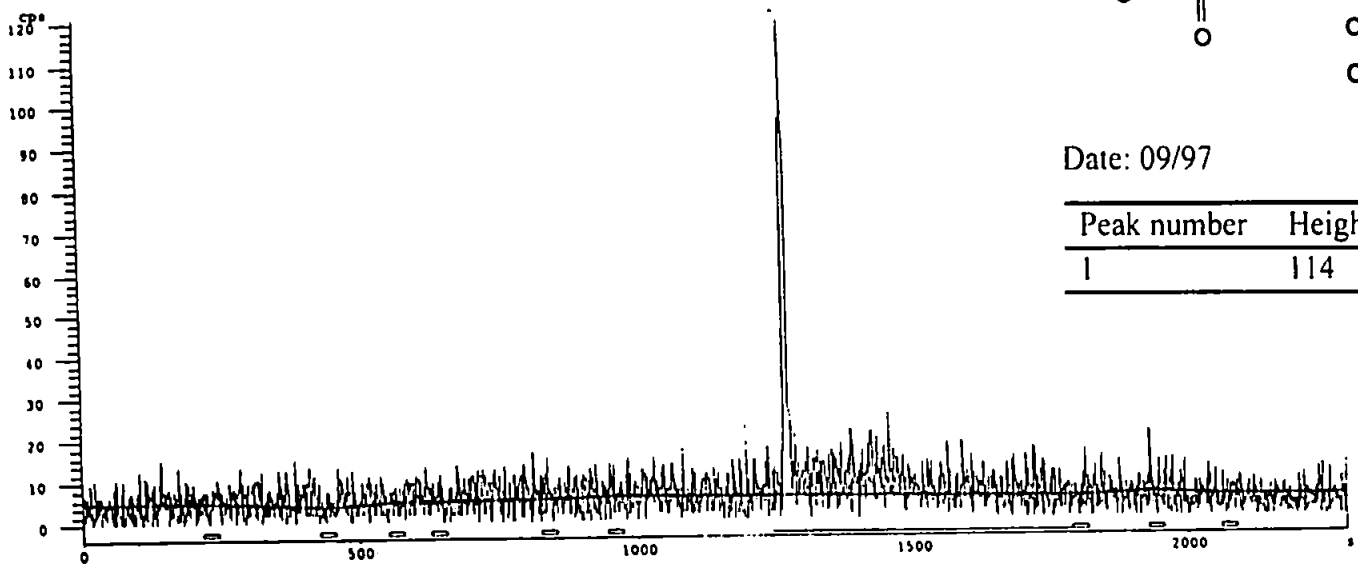

Figure A2.4: Chromatogram showing radioactive purity of DEHP after an experiment involving Plym river water and sediment samples.

Compound: BaP

Structure:

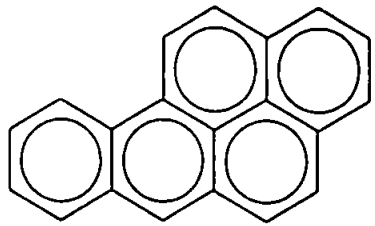

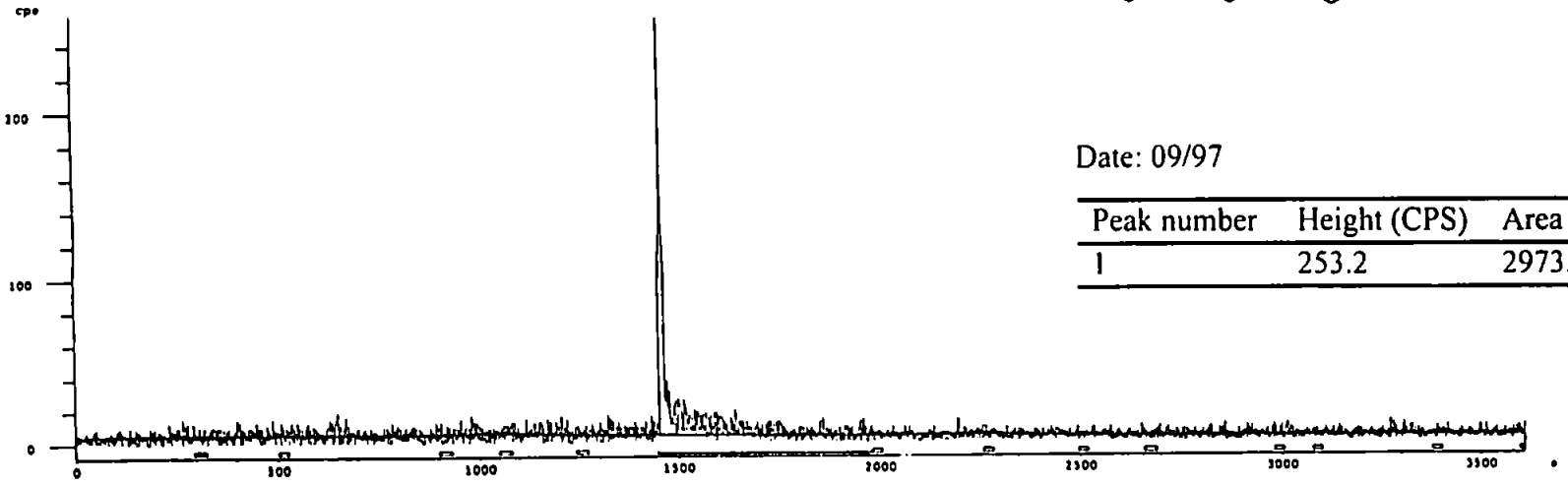

Date: 09/97

Peak number	Height (CPS)	Area (CPS)	Area (%)
1	253.2	2973.5	100.0

Figure A2.5: Chromatogram showing radioactive purity of BaP stock solution prior to an experiment.

Compound: BaP

Structure:

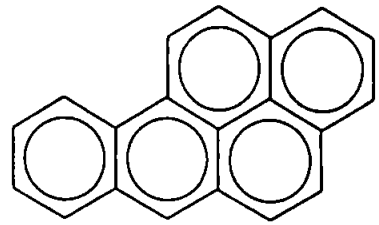

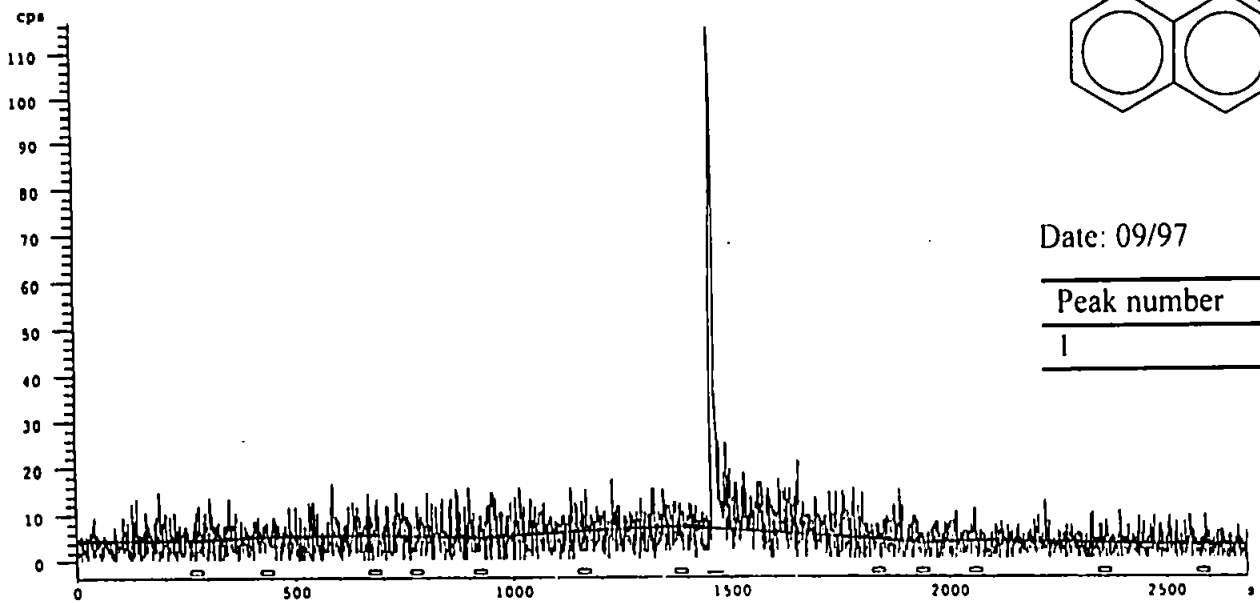

Date: 09/97

Peak number	Height (CPS)	Area (CPS)	Area (%)
1	109	920.6	100.0

Figure A2.6: Chromatogram showing radioactive purity of BaP after an experiment involving Plym river water and sediment samples.

APPENDIX B: GENERATED DATA

B1: Method Evaluation Data

B2: Relative Solubility Data

B3: Particle-Water Interaction Data

Calculation of propagated error, SD, for the particle-water partition coefficient, K_D, (Caulcutt & Boddy, 1983):

$$K_D = \frac{P}{C} \qquad (B.1)$$

$$K_D = \left[\frac{\left(A_o - \left[\left(\left(A_c + A_c^*\right) + \left(A_w + A_w^*\right)\right)\right]\right)}{\left(A_c + A_c^*\right)}\right]\cdot\left[\frac{V}{m}\right] \qquad (B.2)$$

where, P is the compound concentration in the particulate phase (w/w), C is the compound concentration in the dissolved phase (w/v), A_o is the activity of the original spike, A_c is the activity in the aqueous phase, A_c^* is the activity of the pipette rinse, A_w is the activity adsorbed onto the walls of the centrifuge tube, A_w^* is the activity of the repeated extraction of the walls of the centrifuge tube, V is the volume of the water aliquot (mL), and m is the mass of particles (g) in the suspension.

$$SD(P) = \sqrt{(s_{n-1}\text{of } A_o)^2 + (s_{n-1}\text{ of } A_c)^2 + (s_{n-1}\text{ of } A_c^*)^2 + (s_{n-1}\text{ of } A_w)^2 + (s_{n-1}\text{ of } A_w^*)^2} \qquad (B.3)$$

$$CV(P) = \frac{SD(P).100}{\bar{x}\text{ of } P} \qquad (B.4)$$

$$SD(C) = \sqrt{(s_{n-1} \text{ of } A_c)^2 + (s_{n-1} \text{ of } A_c^*)^2} \quad \text{(B.5)}$$

$$CV(C) = \frac{SD(C).100}{\bar{x} \text{ of } C} \quad \text{(B.6)}$$

$$CV(K_D) = \sqrt{CV(P)^2 + CV(C)^2} \quad \text{(B.7)}$$

$$SD(K_D) = \frac{CV(K_D).\bar{x} \text{ of } K_D}{100} \quad \text{(B.8)}$$

where $\bar{x}$ is the sample mean, s_{n-1} is the sample deviation, SD is the propagated error, and CV is the co-variance (n=4).

Appendix B1: Method Evaluation Data

Table B1.1: Quench correction curve data for 2,2',5,5'-TCB.

Sample N°	River water External standard ratio	River water Count efficiency (%)	Sea water External standard ratio	Sea water Count efficiency (%)	*n*-hexane External standard ratio	*n*-hexane Count efficiency (%)
1	1.07	101.2	1.13	98.2	1.07	99.5
2	1.31	97.7	1.30	94.3	1.25	98.9
3	1.42	93.7	1.44	87.1	1.37	96.0
4	1.55	90.6	1.51	85.0	1.47	92.6
5	1.57	82.4	1.64	74.9	1.57	89.0
6	1.72	74.6	1.70	68.8	1.68	80.4
7	1.84	62.9	1.85	50.8	1.76	71.9
8	1.94	46.5	1.95	39.2	1.90	55.4
9	1.96	46.2	1.99	27.5	1.96	45.6
10	2.00	28.4	2.00	19.7	1.98	38.6

Table B1.2: Determination of photon quenching and phospholuminescnence.

Volume Sea water (mL)	Photon quenching 2,2',5,5'-TCB Count efficiency (%) $\bar{x}\pm s_{n-1}$	BaP Count efficiency (%) $\bar{x}\pm s_{n-1}$	Phospholuminescence Time days	BKG (DPM) $\bar{x}\pm s_{n-1}$
0.1	102±3	101±1	1	44.2±4.5
0.2	101±2	102±2	2	40.4±3.2
0.4	105±1	101±1	3	39.9±2.7
0.7	101±2	99±1	6	36.3±2.5
1.0	101±1	101±1	13	33.5±2.4

Table B1.3: Recovery of compounds after volatilisation and change of solvent type

Time (mins)	2,2',5,5'-TCB Recovered compound (%) $\bar{x}\pm s_{n-1}$	DEHP Recovered compound (%) $\bar{x}\pm s_{n-1}$	BaP Recovered compound (%) $\bar{x}\pm s_{n-1}$	Volume of solvent (mL)	2,2',5,5'-TCB *n*-hexane (%) $\bar{x}\pm$SD	DCM (%) $\bar{x}\pm$SD
0	100±2	100±1	100±2	4	75±5	78±7
1	101±1	100±1	96±2	6	78±14	
3	101±1	96±2	93±1	8	76±5	67±4
5	100±1	96±1	87±1	10	73±3	
10	99±1	97±2	54±2	12	73±6	74±9
20	99±1	99±3	43±1			
30	86±11	93±3	36±3			

where DCM is dichloromethane.

Table B1.4: Recovery of compound as a function of original activity.

2,2',5,5'-TCB		DEHP		BaP	
DPM.10^3	Recovered compound $\bar{x}$±SD (%)	DPM.10^3	Recovered compound $\bar{x}$±SD (%)	DPM.10^3	Recovered compound $\bar{x}$±SD (%)
17.09	78±8.4	12.70	52±8.6	7.14	94±5.1
20.66	73±3.2	25.39	67±5.9	9.28	103±5.0
41.32	79±7.7	50.79	81±12	28.31	85±11
82.64	66±18	114.3	84±9.0	54.25	89±5.0
165.3	68±8.8	165.1	86±9.7	110.9	79±15
				165.1	79±19

Appendix B2: Relative Solubility Data

Table B2.1: Relative solubility data for 2,2',5,5'-TCB.

Milli-Q		Sea water		Dart	
Added mass (µg)	Aqueous conc. (µg L^{-1}) $\bar{x}$±SD	Added mass (µg)	Aqueous conc. (µg L^{-1}) $\bar{x}$±SD	Added mass (µg)	Aqueous conc. (µg L^{-1}) $\bar{x}$±SD
0.17	4.68±0.43	0.17	4.45±0.87	0.17	4.52±0.79
0.21	6.59±0.31	0.28	7.93±0.79	0.21	6.75±0.75
0.41	13.35±1.45	0.57	16.66±0.31	0.41	12.17±1.25
0.82	23.35±6.47	1.13	27.93±4.52	0.82	26.50±0.63
1.65	37.06±4.08	2.27	44.47±4.36	1.65	46.11±12.79
2.27	58.27±4.98				
2.92	72.55±2.14				
3.40	86.82±9.10				

Plym		Plym colloidal		Beaulieu		Carnon	
Added mass (µg)	Aqueous conc. (µg L^{-1}) $\bar{x}$±SD	Added mass (µg)	Aqueous conc. (µg L^{-1}) $\bar{x}$±SD	Added mass (µg)	Aqueous conc. (µg L^{-1}) $\bar{x}$±SD	Added mass (µg)	Aqueous conc. (µg L^{-1}) $\bar{x}$±SD
0.14	4.07±0.69	0.14	4.54±1.62	0.13	3.36±0.15	0.12	3.35±1.12
0.28	9.38±0.47	0.28	11.46±1.10	0.28	9.31±0.35	0.28	10.17±0.51
0.58	19.30±0.49	0.55	16.46±2.92	0.54	18.97±0.80	0.54	20.92±1.05
1.10	36.09±2.01	1.06	39.89±2.09	1.10	37.85±1.10	1.08	40.55±2.56
1.66	52.21±2.49	1.62	54.28±5.82	1.64	54.58±3.42	1.63	62.99±2.72

Table B2.2: Relative solubility data for DEHP.

Milli-Q		Sea water		Dart	
Added mass (µg)	Aqueous conc. (µg L^{-1}) $\bar{x}$±SD	Added mass (µg)	Aqueous conc. (µg L^{-1}) $\bar{x}$±SD	Added mass (µg)	Aqueous conc. (µg L^{-1}) $\bar{x}$±SD
0.21	1.64±0.70	0.22	0.36±0.25	0.21	0.73±0.63
0.42	4.89±0.45	0.48	0.54±0.32	0.42	3.39±0.46
0.84	7.76±1.95	0.90	1.31±0.32	0.84	4.03±3.96
1.89	12.91±3.54	1.79	4.03±2.87	1.89	7.66±3.40
2.74	23.51±4.81	2.68	5.69±3.52	2.74	19.93±9.46
Plym		Beaulieu		Carnon	
Added mass (µg)	Aqueous conc. (µg L^{-1}) $\bar{x}$±SD	Added mass (µg)	Aqueous conc. (µg L^{-1}) $\bar{x}$±SD	Added mass (µg)	Aqueous conc. (µg L^{-1}) $\bar{x}$±SD
0.21	0.12±0.06	0.24	0.44±0.17	0.24	0.56±0.13
0.42	0.44±0.11	0.44	0.71±0.24	0.49	1.78±1.17
0.89	1.13±0.51	0.92	2.07±0.91	0.98	2.86±1.30
1.83	4.04±1.38	1.81	8.00±3.28	1.90	1.90±1.36
2.72	9.27±8.58	2.73	28.58±4.78	2.83	2.83±2.47

Table B2.3: Relative solubility data for BaP.

Milli-Q		Sea water		Plym		Carnon	
Added mass (µg)	Aqueous conc. (µg L^{-1}) $\bar{x}$±SD	Added mass (µg)	Aqueous conc. (µg L^{-1}) $\bar{x}$±SD	Added mass (µg)	Aqueous conc. (µg L^{-1}) $\bar{x}$±SD	Added mass (µg)	Aqueous conc. (µg L^{-1}) $\bar{x}$±SD
0.03	1.03±0.06	0.03	0.79±0.07	0.03	0.80±0.03	0.03	1.02±0.11
0.04	1.29±0.06	0.04	0.93±0.08	0.04	0.94±0.04	0.04	1.07±0.09
0.06	1.47±0.06	0.06	1.04±0.13	0.06	1.38±0.05	0.06	1.37±0.012
0.12	1.83±0.13	0.12	1.16±0.09	0.11	2.02±0.05	0.11	1.57±0.09
0.23	2.07±0.21	0.23	1.30±0.06	0.24	2.20±0.22	0.24	1.85±0.20
0.48	2.56±0.33	0.48	1.55±0.09	0.48	2.45±0.19	0.46	2.14±0.22

Table B2.4: Glass-water partitioning data for 2,2',5,5'-TCB.

Milli-Q			Sea water		
Aqueous conc. (ng mL^{-1})	Solvent extracted glasswall conc. (ng cm^{-2}) $\bar{x}$±SD	Mass balance glasswall conc. (ng cm^{-2}) $\bar{x}$±SD	Aqueous conc. (ng mL^{-1})	Solvent extracted glasswall conc. (ng cm^{-2}) $\bar{x}$±SD	Mass balance glasswall conc. (ng cm^{-2}) $\bar{x}$±SD
4.68	1.03±0.31	2.04±0.23	4.45	0.80±0.24	1.88±0.46
6.59	0.50±0.05	1.97±0.17	7.93	1.86±0.59	3.33±0.42
13.35	1.52±0.33	3.85±0.77	16.66	2.55±0.73	6.24±0.16
23.35	2.09±1.20	9.49±1.07	27.93	9.64±3.10	15.34±2.41
37.06	10.09±3.20	24.11±2.17	44.47	24.83±4.56	36.75±2.32
86.82	25.59±2.19	44.41±4.84	74.07	31.93±7.79	51.20±4.15

Table B2.4: Continued.

	Dart			Plym	
Aqueous conc. (ng mL^{-1})	Solvent extracted glasswall conc. (ng cm^{-2}) $\bar{x}$±SD	Mass balance glasswall conc. (ng cm^{-2}) $\bar{x}$±SD	Aqueous conc. (ng mL^{-1})	Solvent extracted glasswall conc. (ng cm^{-2}) $\bar{x}$±SD	Mass balance glasswall conc. (ng cm^{-2}) $\bar{x}$±SD
4.52	0.96±0.32	2.13±0.55	4.07	0.50±0.18	1.60±0.36
6.75	0.57±0.15	1.89±0.34	9.38	0.75±0.07	2.53±0.25
12.17	2.18±0.77	4.48±0.58	19.30	1.37±0.25	4.35±0.26
26.50	3.65±1.04	7.81±0.29	36.09	5.09±0.32	10.04±1.07
46.11	14.86±2.67	19.29±6.51	52.21	8.01±1.08	16.50±1.33
78.60	26.92±2.64	48.78±1.72			
	Beaulieu			Carnon	
Aqueous conc. (ng mL^{-1})	Solvent extracted glasswall conc. (ng cm^{-2}) $\bar{x}$±SD	Mass balance glasswall conc. (ng cm^{-2}) $\bar{x}$±SD	Aqueous conc. (ng mL^{-1})	Solvent extracted glasswall conc. (ng cm^{-2}) $\bar{x}$±SD	Mass balance glasswall conc. (ng cm^{-2}) $\bar{x}$±SD
3.36	0.25±0.05	1.73±0.08	3.35	0.55±0.22	1.43±0.60
9.31	0.74±0.18	2.44±0.12	10.17	0.85±0.17	1.96±0.31
18.97	1.59±0.28	4.33±0.45	20.92	1.64±0.25	3.30±0.62
37.85	4.38±0.59	9.06±0.59	40.55	4.51±1.80	7.29±1.38
54.58	7.65±2.34	14.58±1.95	62.99	3.94±0.49	9.78±1.64

Table B2.5: Glass-water partitioning data for DEHP.

	Milli-Q			Plym	
Aqueous conc. (ng mL^{-1})	Solvent extracted glasswall conc. (ng cm^{-2}) $\bar{x}$±SD	Mass balance glasswall conc. (ng cm^{-2}) $\bar{x}$±SD	Aqueous conc. (ng mL^{-1})	Solvent extracted glasswall conc. (ng cm^{-2}) $\bar{x}$±SD	Mass balance glasswall conc. (ng cm^{-2}) $\bar{x}$±SD
1.64	2.07±0.31	4.73±0.37	0.12	2.16±0.41	5.58±0.03
4.89	4.94±0.61	8.60±0.24	0.44	5.36±0.77	11.07±0.06
7.76	13.94±2.40	18.28±1.04	1.13	15.74±1.27	23.25±0.09
12.91	34.13±4.08	43.54±1.91	4.04	31.07±4.55	46.43±0.73
23.51	51.42±6.60	60.31±2.56	9.27	43.55±7.18	64.38±4.57

Table B2.5: Continued.

Aqueous conc. (ng mL^{-1})	Carnon Solvent extracted glasswall conc. (ng cm^{-2}) $\bar{x}$±SD	Mass balance glasswall conc. (ng cm^{-2}) $\bar{x}$±SD
0.56	2.85±0.28	6.19±0.08
1.78	7.95±0.93	11.78±0.61
5.86	20.20±1.03	24.34±0.56
2.95	42.40±1.24	49.26±0.69
6.73	64.58±2.60	72.42±1.91

Table B2.6: Effect of dissolved organic carbon, DOC, on relative solubility data.

2,2',5,5'-TCB		DEHP		BaP	
DOC (mg L^{-1})	Aqueous conc. (µg L^{-1}) $\bar{x}$±SD	DOC (mg L^{-1})	Aqueous conc. (µg L^{-1}) $\bar{x}$±SD	DOC (mg L^{-1})	Aqueous conc. (µg L^{-1}) $\bar{x}$±SD
0.27	10.46±2.42	0.27	5.85±2.47	0.27	2.07±0.21
0.60	10.54±1.05	0.48	7.22±2.21	0.60	5.04±0.81
2.94	12.50±0.53	1.93	7.50±2.88	2.94	7.07±0.43
4.20	12.64±0.26	3.37	11.25±2.00	4.20	7.78±0.31
7.79	13.34±0.43	6.26	9.93±3.46	7.79	8.95±0.28
11.99	14.09±0.66	9.63	11.39±3.84	11.99	9.57±0.22

Table B2.7: Effect of salinity on relative solubility data.

Salinity (x10^{-3})	2,2',5,5'-TCB Aqueous conc. (µg L^{-1}) $\bar{x}$±SD	DEHP Aqueous conc. (µg L^{-1}) $\bar{x}$±SD	BaP Aqueous conc. (µg L^{-1}) $\bar{x}$±SD
0.30	14.90±1.16	2.77±1.00	2.62±0.24
3.37	14.12±0.57		1.79±0.05
8.43	14.08±0.49	1.60±0.77	1.77±0.06
16.85	13.88±0.91	1.41±0.76	1.52±0.07
25.28	13.00±0.55	0.95±0.14	1.44±0.08
33.70	12.86±0.65	0.67±0.40	1.39±0.10

Appendix B3: Particle-Water Interaction Data

Table B3.1: Kinetic data for 2,2',5,5'-TCB and BaP at two suspended particulate matter concentrations.

	2,2',5,5'-TCB		BaP	
	164 mg L^{-1}	12 mg L^{-1}	164 mg L^{-1}	12 mg L^{-1}
Time (mins)	K_D (mL g^{-1}) $\bar{x}$±SD	K_D (mL g^{-1}) $\bar{x}$±SD	K_D (mL g^{-1}) $\bar{x}$±SD	K_D (mL g^{-1}) $\bar{x}$±SD
5	16900±2350	77400±5680	12000±6500	45100±82400
35	17300±1150	95300±3300	11300±7690	38600±61100
65	17300±1360	103900±4360	10200±4180	62000±94200
120	18900±680	110000±6050	18300±4760	51600±38700
300	18600±1080	108100±7750	16000±3260	78300±59600
480	17900±700	107400±9240	19100±3260	74700±52000
1440	20600±1870	106900±10400	19400±3950	70200±40000
2880	19600±1440	119700±8000	24900±2740	56400±19200
7200	25500±2400	121100±10100	29400±3190	72100±16900
30240	19100±2370	131100±9690	24800±2450	93100±15200

Table B3.2: Adsorption data for 2,2',5,5'-TCB.

Plym River water		Plym Sea water		Beaulieu River water	
Aqueous conc. (µg L^{-1})	Adsorbed conc. (µg g^{-1}) $\bar{x}$±SD	Aqueous conc. (µg L^{-1})	Adsorbed conc. (µg g^{-1}) $\bar{x}$±SD	Aqueous conc. (µg L^{-1})	Adsorbed conc. (µg g^{-1}) $\bar{x}$±SD
1.65	25.24±2.19	1.22	31.05±1.32	1.27	28.23±1.25
3.12	52.24±2.30	2.49	64.92±1.88	3.28	56.12±3.47
6.49	113.9±1.97	5.35	119.3±15.9	6.69	108.4±5.46
11.90	195.9±10.4	9.40	244.4±7.42	13.45	220.8±6.84
18.49	293.1±8.82	14.83	370.4±15.0	19.17	330.5±15.6
Beaulieu Sea water		Carnon River water		Carnon Sea water	
Aqueous conc. (µg L^{-1})	Adsorbed conc. (µg g^{-1}) $\bar{x}$±SD	Aqueous conc. (µg L^{-1})	Adsorbed conc. (µg g^{-1}) $\bar{x}$±SD	Aqueous conc. (µg L^{-1})	Adsorbed conc. (µg g^{-1}) $\bar{x}$±SD
0.70	37.90±0.66	1.28	29.85±0.99	0.95	31.50±0.52
2.04	71.08±1.00	3.27	62.56±2.99	1.95	62.69±1.02
4.63	134.3±3.00	5.21	118.8±4.04	4.24	121.9±2.01
10.23	263.0±4.95	12.56	247.2±4.46	9.17	257.1±6.89
14.34	385.3±6.03	18.07	362.9±17.4	14.36	394.6±5.55

Table B3.3: Adsorption data for DEHP.

Plym River water		Plym Sea water		Beaulieu River water	
Aqueous conc. ($\mu g\ L^{-1}$)	Adsorbed conc. ($\mu g\ g^{-1}$) $\bar{x}$±SD	Aqueous conc. ($\mu g\ L^{-1}$)	Adsorbed conc. ($\mu g\ g^{-1}$) $\bar{x}$±SD	Aqueous conc. ($\mu g\ L^{-1}$)	Adsorbed conc. ($\mu g\ g^{-1}$) $\bar{x}$±SD
1.01	51.52±2.45	0.75	52.56±2.14	2.16	23.88±4.87
1.54	99.76±9.22	2.14	84.08±8.74	4.69	62.80±10.2
7.49	148.3±24.7	7.54	130.8±34.3	10.31	65.22±32.0
28.73	230.7±73.5	14.11	228.0±38.2	32.20	69.51±36.9
35.43	382.9±60.9	21.19	266.6±110.6	46.17	199.0±115.5
Beaulieu Sea water		Carnon River water		Carnon Sea water	
Aqueous conc. ($\mu g\ L^{-1}$)	Adsorbed conc. ($\mu g\ g^{-1}$) $\bar{x}$±SD	Aqueous conc. ($\mu g\ L^{-1}$)	Adsorbed conc. ($\mu g\ g^{-1}$) $\bar{x}$±SD	Aqueous conc. ($\mu g\ L^{-1}$)	Adsorbed conc. ($\mu g\ g^{-1}$) $\bar{x}$±SD
0.22	60.11±2.44	0.99	51.09±6.13	3.98	20.70±9.11
1.29	102.7±8.03	4.26	46.02±13.7	8.34	44.05±23.2
6.40	129.3±28.0	6.81	95.31±23.9	6.41	93.41±23.9
8.23	324.8±45.9	9.34	104.2±54.6	17.88	117.6±65.5
5.15	603.3±65.0	12.73	105.2±46.6	3.61	263.5±42.21

Table B3.4: Adsorption data for BaP.

Plym River water		Plym Sea water	
Aqueous conc. ($\mu g\ L^{-1}$)	Adsorbed conc. ($\mu g\ g^{-1}$) $\bar{x}$±SD	Aqueous conc. ($\mu g\ L^{-1}$)	Adsorbed conc. ($\mu g\ g^{-1}$) $\bar{x}$±SD
0.48	4.79±0.65	0.11	6.99±0.73
0.60	5.52±1.11	0.28	7.81±0.69
0.73	9.96±2.12	0.24	12.43±0.58
0.96	22.04±1.77	0.46	17.94±1.85
1.39	34.84±5.47	0.63	30.36±5.89
2.00	50.23±12.9	2.18	77.63±14.6
Carnon River water		Carnon Sea water	
Aqueous conc. ($\mu g\ L^{-1}$)	Adsorbed conc. ($\mu g\ g^{-1}$) $\bar{x}$±SD	Aqueous conc. ($\mu g\ L^{-1}$)	Adsorbed conc. ($\mu g\ g^{-1}$) $\bar{x}$±SD
0.10	7.76±0.28	0.16	6.66±0.36
0.05	10.49±0.41	0.18	9.39±0.44
0.13	15.85±0.54	0.21	12.03±0.91
0.30	31.66±0.64	0.27	29.68±0.73
0.73	50.16±2.55	0.88	40.02±6.41
0.84	73.00±14.5	1.00	61.28±24.7

Table B3.5: Partition coefficients, K_Ds, for 2,2',5,5'-TCB over a range of salinities in the Dart Estuary at four suspended particulate matter concentrations.

Salinity ($x10^{-3}$)	601 mg L^{-1} K_D (mL g^{-1}) $\bar{x}$±SD	120 mg L^{-1} K_D (mL g^{-1}) $\bar{x}$±SD	48 mg L^{-1} K_D (mL g^{-1}) $\bar{x}$±SD	10 mg L^{-1} K_D (mL g^{-1}) $\bar{x}$±SD
0.3	15400±1800	25300±1500	45600±4210	158600±30500
7.0	15800±5630	28300±1650	51900±3920	181300±9500
14.0	22000±2480	37700±3990	56700±8070	192400±6600
21.0	20800±3700	32700±3530	63200±5390	220700±13700
27.0	28300±7720	37100±2360	76400±5420	241500±25000

Table B3.6: Partition coefficients, K_Ds, for 2,2',5,5'-TCB over a range of suspended particulate [SPM] concentrations.

	Chupa			Dart	
[SPM] mg L^{-1}	River water K_D (mL g^{-1}) $\bar{x}$±SD	Sea water K_D (mL g^{-1}) $\bar{x}$±SD	[SPM] mg L^{-1}	River water K_D (mL g^{-1}) $\bar{x}$±SD	Sea water K_D (mL g^{-1}) $\bar{x}$±SD
28	70900±6890	76300±6490	10	158500±30500	241500±25000
46	66300±3010	58000±8140	48	45600±4210	76400±5400
62	35900±2100	40900±3320	120	25300±1500	37100±2360
85	24200±2900	28400±1590	601	15300±1800	28300±7720
			958	21800±1290	22200±8850
	Plym			Beaulieu	
[SPM] mg L^{-1}	River water K_D (mL g^{-1}) $\bar{x}$±SD	Sea water K_D (mL g^{-1}) $\bar{x}$±SD	[SPM] mg L^{-1}	River water K_D (mL g^{-1}) $\bar{x}$±SD	Sea water K_D (mL g^{-1}) $\bar{x}$±SD
12	126800±7930	155800±24200	12	113000±8220	179800±21600
58	31200±4110	45800±3010	59	29100±1320	41700±6870
164	17600±640	19300±8050	163	16200±945	29300±2920
493	8600±890	19700±820	508	11500±430	17300±3970
985	9700±540	17600±910	1015	8500±730	17100±1580
	Carnon			Plym (Colloidless)	
[SPM] mg L^{-1}	River water K_D (mL g^{-1}) $\bar{x}$±SD	Sea water K_D (mL g^{-1}) $\bar{x}$±SD	[SPM] mg L^{-1}	River water K_D (mL g^{-1}) $\bar{x}$±SD	
12	110400±6510	143800±5660	12	132000±7900	
58	34100±14000	44900±3630	58	31500±4000	
164	23200±3000	28900±1830	164	18700±1200	
492	15900±3460	25400±1100	493	11100±1400	
983	12400±2160	25700±1700	985	8600±1300	

Table B3.7: Partition coefficients, K_Ds, for DEHP over a range of suspended particulate matter [SPM] concentrations.

	Plym			Beaulieu	
[SPM] mg L^{-1}	River water K_D (mL g^{-1}) $\bar{x}$±SD	Sea water K_D (mL g^{-1}) $\bar{x}$±SD	[SPM] mg L^{-1}	River water K_D (mL g^{-1}) $\bar{x}$±SD	Sea water K_D (mL g^{-1}) $\bar{x}$±SD
12	470000±222000	238000±205000	12	329000±185000	520000±154000
58	159000±39900	42600±25400	59	6800±3100	154000±60500
164	28400±1540	18700±8570	163	8800±3650	24100±12100
493	21300±7020	5300±2250	508	2200±750	26300±9700
985	7300±1750	4500±2850	1015	1300±440	22000±6990

	Carnon	
[SPM] mg L^{-1}	River water K_D (mL g^{-1}) $\bar{x}$±SD	Sea water K_D (mL g^{-1}) $\bar{x}$±SD
12	366000±237000	1120000±586000
58	132000±93500	160000±138000
164	29800±11300	12700±1340
492	5400±4230	46500±35500
983	8300±690	28700±9000

Table B3.8: Partition coefficients, K_Ds, for BaP over a range of suspended particulate matter [SPM] concentrations.

	Plym			Carnon	
[SPM] mg L^{-1}	River K_D (mL g^{-1}) $\bar{x}$±SD	Sea water K_D (mL g^{-1}) $\bar{x}$±SD	[SPM] mg L^{-1}	River K_D (mL g^{-1}) $\bar{x}$±SD	Sea water K_D (mL g^{-1}) $\bar{x}$±SD
12	72600±27800	152500±37000	12	75700±63700	223000±45400
58	24300±8090	52100±18700	58	50500±12100	74400±13700
165	25100±5120	49700±14500	165	77000±31300	50000±15300
493	12200±2530	23700±6400	493	78200±22400	41900±11800
987	8100±2190	15400±4670	987	89200±17900	47100±9010

APPENDIX C: PUBLICATION

M. C. Rawling, A. Turner & A. O. Tyler (1998) Particle-water interactions of 2,2',5,5'-Tetrachlorobiphenyl under simulated estuarine conditions. *Marine Chemistry*, **61**, 115-126.

ELSEVIER

Marine Chemistry 61 (1998) 115–126

MARINE CHEMISTRY

Particle–water interactions of 2,2′,5,5′-tetrachlorobiphenyl under simulated estuarine conditions

M. Carl Rawling, Andrew Turner *, Andrew O. Tyler [1]

Department of Environmental Sciences, University of Plymouth, Drake Circus, Plymouth PL4 8AA, UK

Received 12 September 1997; revised 21 January 1998; accepted 6 February 1998

Abstract

A batch sorption technique for the determination of particle–water interactions of hydrophobic organic micropollutants under simulated estuarine conditions is described. Results are presented for the behaviour of 2,2′,5,5′-tetrachlorobiphenyl (2,2′,5,5′-TCB) in river and sea waters, both in the presence and absence of estuarine suspended particles. Adsorption onto particles in sea water was enhanced compared with adsorption in river water owing to salting out of the compound, and possibly of the particulate organic matter, in the presence of high concentrations of dissolved ions. The particle–water distribution coefficient, K_D, decreased from about 120×10^3 to 10×10^3 ml g^{-1}, and from about 150×10^3 to 20×10^3 ml g^{-1}, in river water and sea water, respectively, over a particle concentration range of 10–1000 mg l^{-1}. Incomplete recovery of compound from the reactor walls is partly responsible for a particle concentration effect, while artefacts relating to inadequate sediment and water phase separation were ruled out following further experiments. The particle concentration effect, which is replicated in many field studies of hydrophobic organic micropollutants, including 2,2′,5,5′-TCB, is incorporated into a simple partitioning model and is discussed in the context of the likely estuarine behaviour of such compounds.

Keywords: hydrophobic organic micropollutants; solubility; adsorption; particles; estuaries

1. Introduction

Many hydrophobic organic micropollutants (HOMs) such as polychlorinated biphenyls, phthalic acid esters and polycyclic aromatic hydrocarbons are of concern to water quality managers because of their toxicity, lipophilicity and resistance to degradation. The latter characteristics ensure that the dominant short-term and long-term receptacle of HOMs in the aqueous environment is organic-rich sediment, encompassing bed sediment, suspended particles and biogenic matter. It is essential, therefore, to understand the mechanisms by and extent to which HOMs adsorb onto, desorb from and repartition amongst heterogeneous particle populations in order that their fate may be predicted and the design and siting of effluent pipelines improved (Ng et al., 1996).

Sorption-controlling parameters are highly variable, both spatially and temporally, in estuaries, where mixing of fresh and saline waters and fluvial

* Corresponding author.

[1] BMT Marine Information Systems, Grove House, Meridians Cross, 7 Ocean Way, Ocean Village, Southampton SO14 3TJ, UK.

0304-4203/98/$19.00
PII S0304-4203(98)00027-9

and marine particles occurs, and a diversity of plankton communities are generated in situ. Consequently, theoretical and empirical approaches have failed to result in accurate, comprehensive definitions of estuarine sorption processes for HOMs which are suitable for predictive modelling purposes. Field measurements of sediment and water column distributions have enabled pollution inventories to be calculated and in situ chemical reactivity to be diagnosed (Bergen et al., 1993; Tyler et al., 1994; Axelman et al., 1997), but data generation may be time consuming and expensive and does not necessarily resolve the specific controlling biogeochemical mechanisms. Alternatively, empirical relationships between HOM sorption constants and octanol–water partitioning have been sought (Wijayaratne and Means, 1984; Maruya et al., 1996). Although the octanol–water partition coefficient is regarded as a key parameter for evaluating the environmental fate of lipophilic compounds, simple partitioning between two immiscible phases is not compatible with some observations on the adsorption of HOMs to natural particles, including its dependence on the concentration of suspended particulate matter, SPM (Mackay and Powers, 1987; Zhao and Lang, 1996), and quality, as well as quantity, of particulate organic matter (Zhou et al., 1995; Xing, 1997).

Most estuarine sorption constants for HOMs have been derived from batch sorption studies. Here, particle–water interactions are empirically defined in terms of environmental variables which can be readily controlled in the laboratory. Methods for the generation of empirical data based on tracing radiolabelled analogues of HOMs have been described (Jepsen et al., 1995; Girvin and Scott, 1997; Hunchak-Kariouk et al., 1997), but few studies have employed natural sediments suspended in their native waters under realistic estuarine conditions (Means, 1995; Hegeman et al., 1995). To this end, we have rigorously tested a routine, process-orientated batch sorption approach which involves tracing ^{14}C-labelled HOMs under simulated, yet realistic estuarine conditions using natural samples. In this paper, we describe the experimental procedure and present preliminary results for 2,2',5,5'-tetrachlorobiphenyl (2,2',5,5'-TCB), a relatively abundant polychlorinated biphenyl congener (IUPAC 52) of suitable stability and hydrophobicity. The results are parameterised in the form of geochemical algorithms which may be incorporated into estuarine transport models, and are discussed in the context of the likely behaviour of such compounds in estuaries.

2. Methods

2.1. Sample collection and characterisation

Shore-based sampling of river water and intertidal mud was undertaken in the Plym (Devon, UK; Fig. 1), a small, macrotidal estuary whose upper catchment comprises granitic moorland and lower catchment is industrialised. Samples of 6 l river water (from above the tidal limit) and English Channel sea

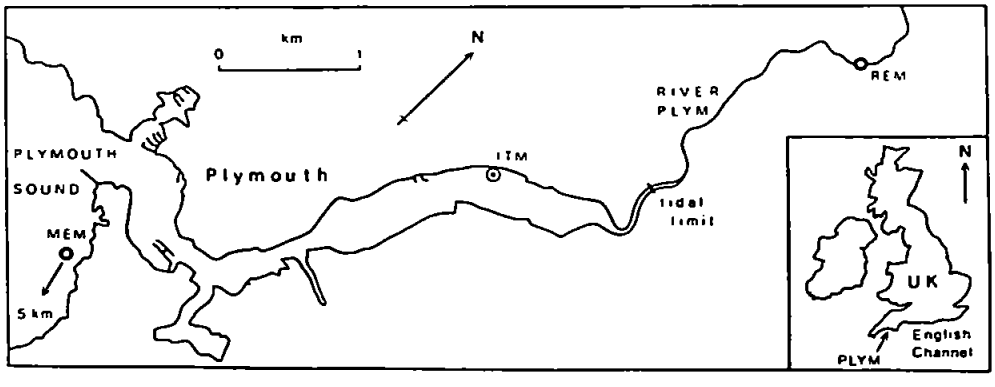

Fig. 1. The Plym Estuary and sample locations. REM and MEM are river and marine end-member water samples, respectively, and ITM is the intertidal estuarine mud sample.

Table 1
Geochemical characteristic of the water and sediment samples used in the experiments

	River water	Sea water
Salinity, $\times 10^{-3}$	< 0.3	30.1
Conductivity, μS	100	46000
pH	6.80	7.96
Organic carbon, mg l^{-1}	1.70	1.41
Cl^-, mg l^{-1}	22	–
Alkalinity, mg l^{-1}	11	–
Ca^{2+}, mg l^{-1}	5.0	–
	Estuarine sediment (ϕ < 63 μm) @ SPM = 12–985 mg l^{-1}	
Fe, mg g^{-1}	2.48 ± 0.08	
Ca, mg g^{-1}	3.30 ± 0.13	
Mn, μg g^{-1}	20 ± 1.0	
Organic carbon, %	1.69	
Surface area, m^2 g^{-1}	4.0	

Concentrations of particulate Fe, Ca and Mn represent those available to an acetic acid extraction and are reported as the mean and standard deviation of three replicate digests.

water (from 5 km to the south of the estuary) were collected in ashed pyrex bottles and filtered through Whatman GF/F (ϕ = 0.7 μm) filters on return to the laboratory. The filtrate was stored in ashed pyrex bottles at 4°C in the dark until further use (within a few days of collection). To an aliquot of about 50 ml, 50 μl phosphoric acid was added and the dissolved organic carbon concentration was determined using a Schimadzu-5000 total organic carbon analyser. Conductivity, salinity and pH were determined in situ after calibration of the appropriate instruments, while selected ions were measured on return to the laboratory using established methods (Jeffery et al., 1989). Surface sediment from the intertidal estuarine mudflats was collected in a 500 ml glass jar. The sample was wet sieved through a 63 μm nylon mesh using filtered river water, and a slurry of particle concentration ~ 20 g l^{-1} was then prepared by appropriate dilution in river water. This was stored in the dark at 4°C with occasional agitation, and regularly calibrated for sediment concentration by subsample filtration. Freeze-dried aliquots of the slurry were analysed for organic C as above after digestion in phosphoric acid, specific surface area using a BET nitrogen adsorption technique, and Fe, Mn and Ca by flame atomic absorption spectrometry following extraction with acetic acid–hydroxylamine hydrochloride (Millward et al., 1990). Characteristics of the water and sediment samples are shown in Table 1.

2.2. Sample incubation and counting

The following protocol, based on that of Means et al. (1980) and Zhou et al. (1995), was adopted for the incubation of the radiolabelled compound under simulated estuarine conditions and subsequent sediment–water phase separation. This approach eliminates the carrier solvent from the experiments, minimises adsorption of the compound onto glassware during phase separation, and avoids chemical interferences associated with scintillation counting of particles or extracts thereof.

^{14}C-labelled 2,2′,5,5′-TCB (Sigma Chemicals), whose chemical and radiochemical properties are listed in Table 2, was employed as the tracer in this study. Because of its toxicity and radioactivity all experiments were undertaken with extreme caution by trained personnel working in specially designated laboratories. An accurate spike of between 200 and 3000 Bq in *n*-hexane (@ 37 Bq μl^{-1}) was placed on the wall of a hexane washed glass centrifuge tube using a glass microsyringe. The hexane was then evaporated in a fume cupboard and 20 ml filtered water added using a glass pipette. For sorption studies an accurate volume of the sediment slurry or appropriate dilution thereof was pipetted into the water such that the resulting turbidities (in the range 10–1000 mg l^{-1}) were typical of those encountered in macrotidal estuaries. The sample was incubated at

Table 2
Chemical properties of 2,2′,5,5′-TCB and the ^{14}C-labelled analogue employed in the experiments

Molecular formula	$C_{12}H_6Cl_4$
Molecular mass, g mol^{-1}	292
Solubility, C_{sl}, @ 25°C, μg l^{-1}	25.4[a]
Octanol–water partition coefficient, log K_{ow}, @ 25°C	6.09[b]
Specific activity, SA, Bq $mmol^{-1}$	4.9×10^8
Radiochemical purity, %	≥ 98

[a]Mackay et al. (1980).
[b]Rapaport and Eisenreich (1984).

20°C in the dark on a lateral shaker for 16 h whereafter the sediment and water phases were separated by centrifugation at 3000 rpm for 30 min. Ensuring no disturbance of particles at the bottom of the centrifuge tube, a 1 ml aliquot of supernatant was pipetted into 4 ml Ultima Gold liquid scintillation cocktail (LSC; Canberra-Packard). The remaining contents of the tube were discarded and residual compound adsorbed to the glass walls was extracted using 4 ml hexane for 16 h on a lateral shaker, and a 1 ml aliquot of the extract was pipetted into 4 ml LSC. The dissolved and extract activities were then counted on a Beckman LS6500 scintillation counter with factory installed internal quench curves. For saline samples addition of cocktail produced a white precipitate, but photon quenching was found to be minimal when checked against equal activities in the presence of 4 ml LSC and variable amounts (100–1000 μl) of sea water.

The relative solubility of the compound, C_r ($\mu g\ l^{-1}$), which is dependent on the amount of compound added, the temperature (20°C) and the sample type is calculated as follows:

$$C_r = \frac{A_s \text{rmm} 10^6}{\text{SA}} \quad (1)$$

where A_s is the activity of the supernatant (Bq ml^{-1}), rmm is the molecular mass of 2,2',5,5'-TCB (g mol^{-1}) and SA is its specific activity (Bq $mmol^{-1}$; Table 2). The sediment–water distribution coefficient, K_D (ml g^{-1}), is calculated as follows:

$$K_D = \frac{A_0 - A_w - (A_s V)}{A_s m} \quad (2)$$

where A_0 and A_w are the activities (Bq) of the original spike and the tube extract, respectively, V is the volume of water (ml) and m is the mass of particles (g) in the sample. All experiments were undertaken in quadruplicate, and error bars presented for relative solubilities and sediment–water partitioning are calculated from the propagation of errors resulting from each step of the experiment (Caulcutt and Boddy, 1983).

2.3. Compound recovery

Because sediment–water partitioning data are derived from mass balance an evaluation of the recovery of the original spike is required. For non-turbidised, distilled–deionised Milli-Q water this procedure retrieved 70 ± 5.3% ($n = 6$) of the original activity and ways of improving the recovery were, therefore, investigated. Recovery was found to be independent of original compound activity, centrifuge tube age (new vs. ~ 1000 h usage), polarity of extractant solvent and time interval (up to 20 min) between carrier solvent evaporation and sample introduction. However, recovery was increased to about 80% and found to be independent of sample matrix, by raising extractant volume to 6 ml (further volume increases had negligible effect), solvent rinsing of glass pipettes and repeat extraction of the centrifuge tube. Typical activities in each phase for a range in simulated estuarine conditions are given in Table 3.

Presumably, compound loss occurs through strong (irreversible) adsorption to the glassware. By nature of the experimental design, it is not possible to quantify loss in the presence of particles, although it is reasonable to assume that the effect of increasing particle concentration is to reduce loss to glassware through a reduction in the ratio of glass to sediment surface area. For the range in particle concentrations used in the experiments, the ratio of sediment surface area, derived from BET analysis, to surface area of centrifuge tube filled to 20 ml, derived geometrically, varied between about 20 and 0.2. Potential

Table 3
Typical percentage activities, as mean ± propagated error ($n = 4$), of 2,2',5,5'-TCB in each phase under different simulated estuarine conditions

Phase	Derivation (Eq. (2))	Milli-Q water	River water	Sea water	River water + 12 mg l^{-1} SPM	River water + 985 mg l^{-1} SPM
Water	$(A_s V)/A_0$	65 ± 7.1	70 ± 1.8	59 ± 1.1	36 ± 1.7	8.9 ± 0.5
Glass	A_w/A_0	14 ± 2.7	9.4 ± 2.9	17 ± 4.8	12 ± 1.1	5.8 ± 0.9
Particles	$(A_0 - A_w - (A_s V))/A_0$	–	–	–	52 ± 2.1	85 ± 1.0

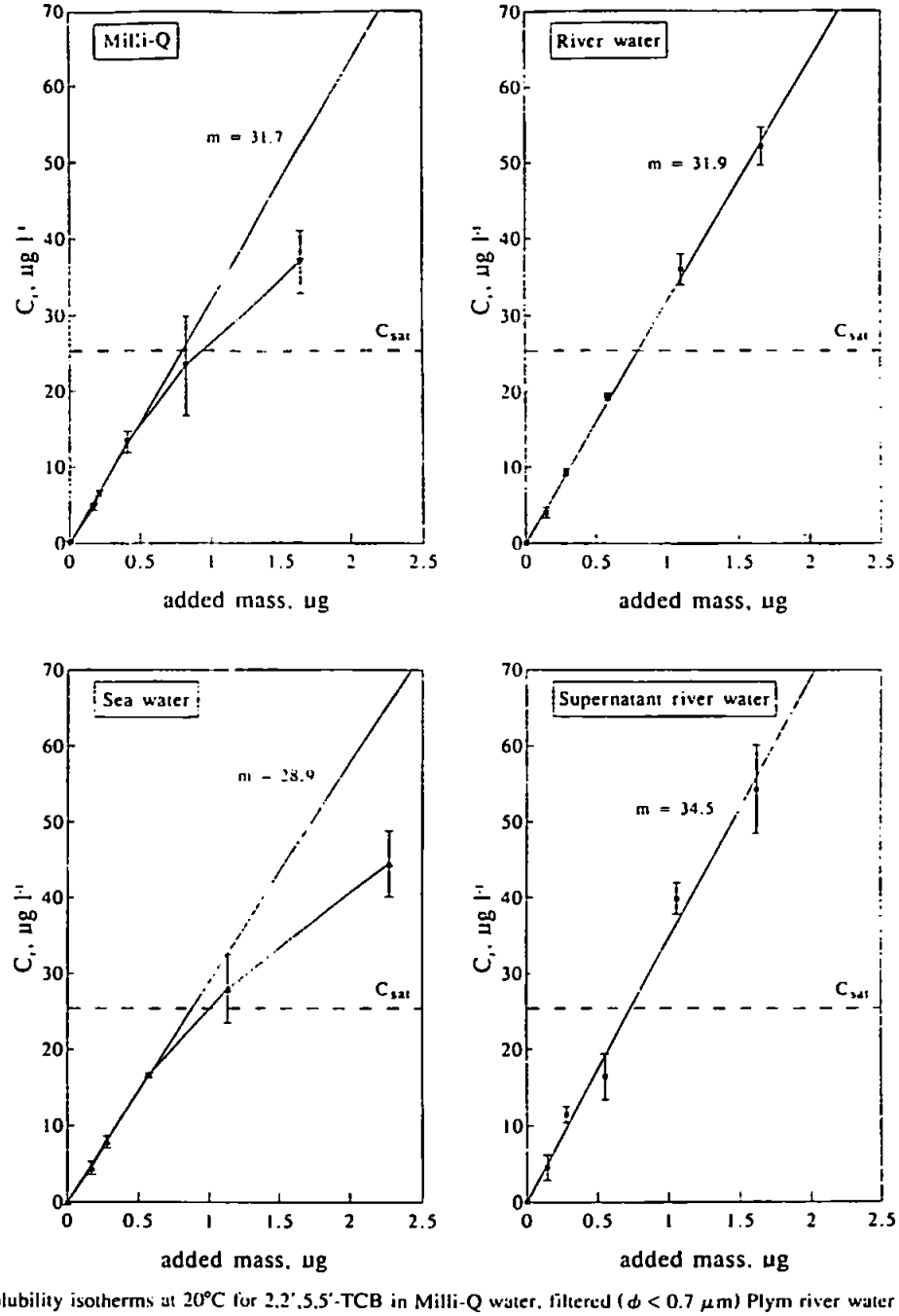

Fig. 2. Relative solubility isotherms at 20°C for 2,2',5,5'-TCB in Milli-Q water, filtered ($\phi < 0.7$ µm) Plym river water and sea water, and supernatant water derived from centrifugation of turbidised (SPM ~ 500 mg l^{-1}) river water. Gradients are for the best fit lines through all filtered and supernatant river water data, and through the linear portions of the plots (first three data points only) for Milli-Q and filtered sea water. C_{sat} is the published solubility at saturation at 25°C (Mackay et al., 1980).

artefacts arising from compound loss to glassware are discussed in the context of the results.

The radiochemical composition of solvent extracts derived from experiments employing river water and estuarine particles was examined by radio-gas chromatography (Tancell and Rhead, 1996). Only the peak of 2,2',5,5'-TCB was present, and its radiochemical purity was found to exceed 98%, indicating no significant compound degradation or radiochemical contamination during experiments.

3. Results and discussion

3.1. Relative solubility

The effects of varying amounts of added 2,2',5,5'-TCB on its concentration in solution, C_r, are shown in Fig. 2 for Milli-Q water, filtered River Plym water and sea water, and supernatant river Plym water (see later discussion for explanation). We have called these plots relative solubility isotherms, where the activity in the supernatant is a measure of the solubility, or partitioning between water and glass, relative to the total amount of compound present. The objective of this approach is to compare relative solubilities in different water matrices over dissolved compound concentration ranges typically encountered in the estuarine water column (Duinker et al., 1985) and pore waters (Brownawell and Farrington, 1985). Also shown on the diagram is a measure of the saturated solubility, C_{sat}, of 2,2',5,5'-TCB in pure water (Table 2). For Milli-Q water the isotherm is linear to about 15 $\mu g\ l^{-1}$ and then becomes convex as the saturated solubility is approached. Further additions of compound, not shown on the diagram, led to a dramatic increase in relative solubility and highly variable results, suggesting the onset of micelle formation. As a result of these observations, it was ensured that adsorption experiments were undertaken such that the concentration in solution did not exceed that range encompassed by the linear portion of the relevant isotherm. The shape of the isotherm for sea water was similar but relative solubilities were slightly lower than in Milli-Q water due to the salting out effect, i.e., the reduction in volume of water available for dissolution through electrostriction.

The relative solubility isotherm in Plym river water is linear throughout the range of compound mass studied. Relative solubility is similar to that in Milli-Q water up to an aqueous concentration of about 15 $\mu g\ l^{-1}$, with further additions of compound leading to an increasing difference in relative solubilities. Enhanced solubility of hydrophobic organic compounds in the presence of dissolved organic matter is well documented (Landrum et al., 1984; Chiou et al., 1987) and can be understood from the surfactant characteristics of the natural dissolved organic matter; i.e., the HOM binds to hydrophobic regions of dissolved organic matter (DOM), such as alkyl chains, while the entire complex is held in solution or colloidal dispersion by hydrophilic sites of the DOM, such as carboxylic acids.

The ratio of the gradient of the isotherm in river water to the gradient of the linear portion of the isotherm in sea water gives a measure of the sensitivity of the compound to salting out by sea water, with possible additional and/or competing effects from riverine and marine organic matter and microorganisms. This effect can be expressed in terms of a salting constant, σ_r, as follows (Hashimoto et al., 1984):

$$\log\left(C_r^{rw}/C_r^{sw}\right) = \sigma_r M \qquad (3)$$

where C_r^{rw} and C_r^{sw} are the relative solubilities in river water and saline water, respectively, and M is the total molar salt concentration. Thus, a typical sea water salt concentration of 0.5 mol l^{-1} yields a salting constant, defining the change in solubility of 2,2',5,5'-TCB on estuarine mixing, of about 0.1 l mol^{-1}.

3.2. Sediment–water partitioning

Isotherms for 2,2',5,5'-TCB adsorption to Plym estuarine particles (@ 150 mg l^{-1}) suspended in end-member waters are shown in Fig. 3, and conform with the Freundlich equation:

$$P = K_D C^n \qquad (4)$$

where P is the compound concentration adsorbed to particles (w/w), C is the aqueous compound concentration (w/v) in the presence of particles, K_D is the distribution coefficient (ml g^{-1}), and n is a constant related to the sorption capacity of the parti-

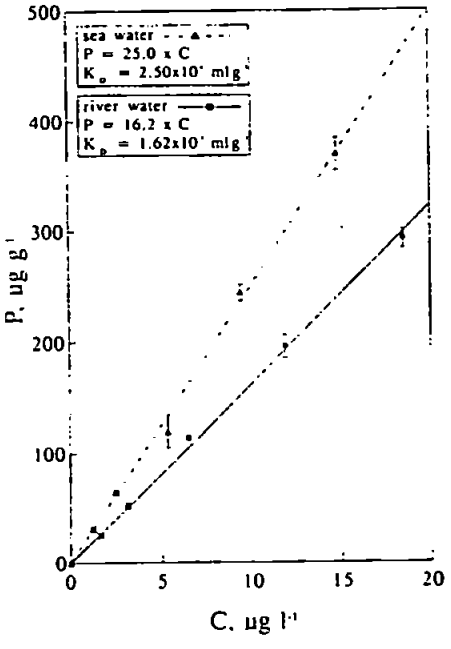

Fig. 3. Adsorption isotherms at 20°C for 2,2',5,5'-TCB on Plym estuary particles (@ 150 mg l^{-1}) suspended in Plym river water and sea water.

cle surface. The apparent linearity of the isotherms indicates a value of n close to unity and that equilibrium partitioning is largely independent of compound concentration. The ratio of the gradients of the isotherms, or K_Ds, in the marine and river end-members may be used to calculate an adsorption salting constant, σ_{ads}, as follows (Means, 1995):

$$\log\left(K_D^{sw}/K_D^{rw}\right) = \sigma_{ads} M. \quad (5)$$

A value of about 0.4 l mol^{-1} is obtained for a molar salt concentration of 0.5, which considerably exceeds the corresponding value derived from the ratio of relative solubilities. The effects of ionic strength on aqueous solubility alone cannot, therefore, account for enhanced adsorption in saline waters. In addition, there is likely some form of interaction between sea water ions and the sorbent phase, such as salting out of particulate organic matter (improving its solvent characteristics), or conformational changes to hydrophobic regions of the particulate organic matter surrounding adsorbed HOM molecules (Means, 1995).

The effect of increasing particle concentration on the particle–water partitioning, shown also in terms of K_{oc}, the organic carbon-normalised partitioning, is presented in Fig. 4. The characteristic inverse relationship is well documented and has been termed the 'particle concentration effect' (PCE) (McKinley

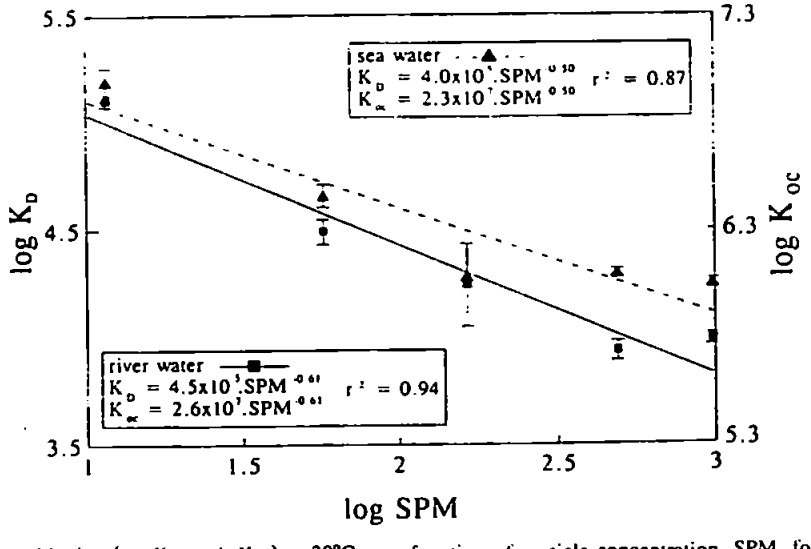

Fig. 4. Sediment–water partitioning (as K_D and K_{oc}) at 20°C as a function of particle concentration, SPM, for 2,2',5,5'-TCB on Plym estuary particles suspended in Plym river water and sea water.

Table 4
Values of a and b for 2,2',5,5'-TCB derived from regressions of log K_D vs. log SPM (Eq. (6))

Sample	Derivation of K_D	a ($\times 10^5$)	b	r^2
Filtered River Plym water turbidised with Plym Estuary sediment	Mass balance	4.5	0.61	0.943
	NSP removed, mass balance	4.8	0.61	0.967
	Mass balance after 20% loss correction	2.5	0.56	0.931
Filtered English Channel seawater turbidised with Plym Estuary sediment	Mass balance	4.0	0.50	0.869

and Jenne, 1991). The effect may be defined by the following algorithm:

$$K_D = a\mathrm{SPM}^{-b} \quad (6)$$

where SPM is the suspended particle concentration (mg l^{-1}), and a and b are constants which are salinity-dependent, and site- and compound-specific. Values of a and b for 2,2',5,5'-TCB derived from River Plym and sea water data are shown in Table 4, while empirical equations defining the effect observed in different aquatic environments (both laboratory- and field-based) are given in Table 5.

3.3. Causes of a particle concentration effect

Possible causes of the PCE include artefacts resulting from the experimental design, and real effects (e.g., particle interactions) which may be extrapolated to the environment. By nature of the way in which K_Ds are derived (Eq. (2)), loss of compound to the glassware results in an overestimation of the K_D, an effect which increases with decreasing particle:glass surface area ratio or particle concentration. The potential magnitude of this effect was investigated by recalculating K_Ds assuming a 20% loss of added compound (as determined from original mass balance experiments) that was independent of particle concentration. The effect of this worst case scenario, exemplified in Table 4 for River Plym experiments, is to reduce K_Ds by an amount that is inversely proportional to the particle concentration yet insufficient to eliminate a clear PCE. Quantitatively, the intercept of the regression is reduced by about 50% while the gradient of about −0.6 is maintained. Moreover, that PCEs have been observed when particles and water, separated by filtration, have been counted directly (Table 5; Eadie et al., 1990), is further evidence that the effect is not wholly related to the way in which K_Ds are derived from mass balance.

Many explanations for the PCE have been based on the presence of colloidal matter (Servos and Muir,

Table 5
Empirical equations defining the particle concentration effect observed for 2,2',5,5'-TCB in different environments

Sample	Derivation of K_D	SPM, mg l^{-1}	Equation	Reference
Unfiltered New Bedford Harbour water	Sample filtered in situ; filter and filtrate extracts analyzed by EC-GC[a]	~1–30	$\log K_D = -0.027\ \mathrm{SPM} + 5.36$	Bergen et al. (1993)
			$\log K_D = -b \log \mathrm{SPM} + a$ (Eq. (6))	
Unfiltered Lake Michigan water	Innoculated sample filtered; filter and filtrate counted	0.3–1.9	$a = 5.00 \times 10^5$; $b = 0.75$	Eadie et al. (1990)
Unfiltered Lake Superior water	Sample filtered in situ; filter and filtrate extracts analyzed by EC-GC[a]	0.2–8	$a = 5.30 \times 10^5$; $b = 1.08$	Baker et al. (1986)
Unfiltered North Sea coastal water	Sample filtered in situ; filter and filtrate extracts analyzed by EC-GC[a]	1–150	$a = 6.20 \times 10^5$; $b = -0.94$	Duinker (1986)

[a]Electron capture-gas chromatography.

1989; Pankow and McKenzie, 1991), comprising organic macromolecules and submicron particles, and/or larger, non-settling particles (NSP). It is becoming increasingly evident that such material is highly significant for the transport and fate of pollutants in estuaries, having a large surface area per unit mass for the adsorption and complexation of contaminants (Benoit et al., 1994), being able to act as reducing agents or modify photochemical reactions in the water column (Sigleo and Means, 1990), and possessing no settling velocity, thereby ensuring relatively rapid, quasi-conservative transport across biogeochemical gradients (Turner and Millward, 1994). Ideally, therefore, three phase partitioning should be considered for any geochemical and ecotoxicological study, yet conventional methods of phase separation such as centrifugation do not allow discrimination of this fraction. In this study, pollutant-binding colloidal material, derived from interparticle collisions, and NSP, preexisting in the original slurry, are retained by the supernatant and, therefore, operationally encompassed by the dissolved pool. Association of HOMs with this material, whose abundance (w/v) is a function of sediment concentration, would therefore result in an apparent PCE.

The significance of colloids and NSP, released from particles comprising the sediment slurry, to the binding of 2,2',5,5'-TCB was evaluated by repeating a particle concentration isotherm for the Plym Estuary after having centrifuged each reactor plus turbidised sample and removed the supernatant. The relative solubility of 2,2',5,5'-TCB was determined in the supernatant derived from a sample turbidised to ~ 500 mg l^{-1}, as described above. Filtered ($\phi <$ 0.7 μm) river water was then added to each reactor, plus remaining sediment, for the adsorption studies. The results indicate that any release of material from the sediment caused neither significant enhancement of solubility in river water (Fig. 2) nor change in the gradient and intercept of the regression of the particle concentration isotherm (Table 4). These observations suggest that, while preexisting, filterable colloidal material may enhance pollutant solubility at relatively high aqueous concentrations through complexation and adsorption, material released to the estuarine water column in situ via suspended particle interactions is generally of limited importance to the behaviour of HOMs.

The foregoing discussion would appear to be in conflict with the release of particulate organic matter and NSP observed in other laboratory studies of HOM sorption along a particle concentration gradient (Gschwend and Wu, 1985; Servos and Muir, 1989; Koelmans and Lijklema, 1992; Zhao and Lang, 1996). However, release of organic matter and fine particles to the aqueous phase may have been promoted in these studies where sediment filtration or dilution (as a slurry) was not undertaken to eliminate or reduce the concentration of pore-water colloids and NSP, and/or the aqueous phase employed was distilled water which is not at equilibrium with the sediment. Although a PCE was largely removed in one study after pre-washing the sediment (Gschwend and Wu, 1985), the experiments did not focus on the range of particle concentrations (< 100 mg l^{-1}) where the PCE is most pronounced.

3.4. Implications for the behaviour of hydrophobic organic micropollutants in estuaries

Although the cause/s of the PCE remain unresolved, that the effect is observed in the field for many HOMs, including 2,2',5,5'-TCB (Baker et al., 1986; Duinker, 1986; Bergen et al., 1993), suggests it is the result, at least in part, of some natural process (possibly related to interparticle collisions) which is replicated in the laboratory. As such, the effect should be incorporated into contaminant transport models or environmental impact evaluations concerning hydrophobic compounds. An important parameter relating to the mobility and bioavailability of HOMs is that fraction of the total compound in the water column which occurs in the dissolved phase. This fraction, f_c, is calculated from the sediment–water partitioning as follows:

$$f_c = \frac{1}{1 + \left[K_D \mathrm{SPM}/10^6\right]} \tag{7}$$

or, incorporating a PCE (Eq. (6)):

$$f_c = \frac{1}{1 + \left[a\mathrm{SPM}^{-(b-1)}/10^6\right]} \tag{8}$$

The fraction of 2,2',5,5'-TCB in solution in river and sea waters, calculated using values of a and b derived from the regressions of Plym data, is shown as

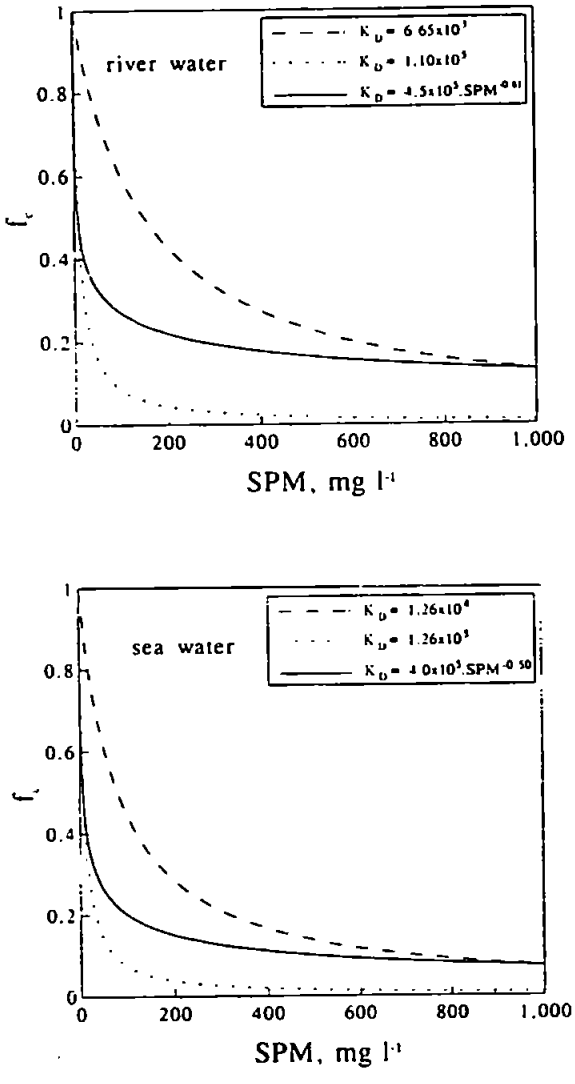

Fig. 5. The fraction in solution, f_s, as a function of particle concentration, SPM, calculated for extreme, invariant K_Ds, and a particle concentration dependence of K_D, for 2,2',5,5'-TCB in Plym river water and sea water.

a function of suspended particle concentration in Fig. 5. Also shown are the fractions in solution calculated for a constant partitioning (Eq. (7)) using K_Ds extrapolated from the regressions at suspended particle concentrations of 10 and 1000 mg l^{-1}. If the K_D value predicted at 10 mg l^{-1} were maintained at all particle concentrations, then the fraction in solution would fall below 1% at turbidities in excess of 1 g l^{-1}. However, a PCE ensures that, within the particle concentration range studied, the fraction in solution does not fall below about 13 and 7% in river water and sea water, respectively. Conversely, if the K_D value predicted at 1000 mg l^{-1} were maintained throughout, then the fraction in solution would be overestimated by at least 50% within a particle concentration range of about 2–400 mg l^{-1}.

The likely effects of enhanced adsorption in saline water are to reduce the offshore fluxes of HOMs and promote their internal cycling within the estuarine mixing zone, as hypothesized below. Thus, marine particles, relatively enriched in HOMs, are driven upstream as bedload by asymmetrical tidal currents to the estuarine null zone (Bale et al., 1985). Here, at reduced salinities, the resuspension of particles forming the turbidity maximum is accompanied by the desorption of HOMs back into the water column (an effect not defined by the present study). Although release of solute-binding colloids and NSP via inter-particle collisions is likely to be insufficient to assist desorption, the injection of specific HOM-binding colloids from tidally disturbed, organic-rich pore waters may be locally significant. Such colloids, although poorly characterised, appear to be lipid-rich and more abundant in contaminated environments (Chin and Gschwend, 1992). Dissolved HOMs, including those entering the water column from organic-rich pore waters, are then transported seawards, some escaping to the coastal zone, and the remainder undergoing adsorption onto marine particles suspended in the water column before being returned upestuary to the null zone. The retention of such contaminants in estuaries is therefore dependent on (i) the difference in adsorption characteristics in river and sea waters, (ii) the magnitude of HOM desorption from resuspending particles of the turbidity maximum, and (iii) the degree of internal cycling of fine sediments in the system. Clearly this hypothesis requires validation by field studies of dissolved and particulate HOMs in estuaries, while inter-compound and inter-estuarine variability of HOM sorption requires further laboratory studies under a greater variety of simulated conditions.

4. Conclusions

The method developed and tested in this paper is suitable for the empirical study of the particle–water

interactions of HOMs using natural estuarine samples, provided that irreversible adsorption of the compound under study to reactor walls is not too great. Preliminary experiments using 2,2′,5,5′-TCB and samples from a small, macrotidal estuary showed that, compared with pure water, solubility is enhanced in river water, presumably through complexation with dissolved and colloidal organic material, and reduced slightly in sea water, through salting out of the compound. Adsorption onto fine estuarine sediment is enhanced in sea water over river water due to salting out of the compound and, perhaps, the particulate organic matter.

A reduction in the sediment–water partitioning with increasing suspended particle concentration, SPM, was defined by the algorithm: $K_D = a\mathrm{SPM}^{-b}$, where a and b in river water and sea water were 4.5×10^5 and 0.61, and 4.0×10^5 and 0.50, respectively. The extent of irreversible compound adsorption to the glassware was not sufficient to account for a particle concentration effect, while artefacts relating to inadequate particle–water phase separation during centrifugation were ruled out following further experiments in which supernatant river water was replaced by filtered river water. That the effect is observed in the field for many HOMs, including 2,2′,5,5′-TCB, suggests it is caused by some environmental (e.g., particle interactive) process which is replicated under laboratory conditions.

Regarding the estuarine behaviour of HOMs, enhanced adsorption at high salinities is likely to reduce their export to shelf seas and promote their internal cycling within the estuarine mixing zone, while a particle concentration effect ensures that a significant fraction of HOMs will remain in solution, even at the elevated particle concentrations typically encountered in turbidity maxima.

Acknowledgements

The authors gratefully acknowledge Dr. J. Zhou (University of Bangor), and Drs. M. Rhead and G. Millward (UoP) for helpful discussions about the work. MCR was supported by an NERC (CASE) studentship.

References

Axelman, J., Broman, D., Naf, C., 1997. Field measurements of PCB partitioning between water and planktonic organisms: influence of growth, particle size, and solute–solvent interactions. Environ. Sci. Technol. 31, 665–669.

Baker, J.E., Capel, P.D., Eisenreich, S.J., 1986. Influence of colloids on sediment–water partition coefficients of polychlorobiphenyl congeners in natural waters. Environ. Sci. Technol. 20, 1136–1143.

Bale, A.J., Morris, A.W., Howland, R.J.M., 1985. Seasonal sediment movement in the Tamar Estuary. Oceanol. Acta 8, 1–6.

Benoit, G., Oktay-Marshall, S.D., Cantu II, A., Hood, E.M., Coleman, C.H., Corapcioglu, M.O., Santschi, P.H., 1994. Partitioning of Cu, Pb, Ag, Zn, Fe, Al, and Mn between filter-retained particles, colloids, and solution in six Texas estuaries. Mar. Chem. 45, 307–336.

Bergen, B.J., Nelson, W.G., Pruell, R.J., 1993. Partitioning of polychlorinated biphenyl congeners in the seawater of New Bedford Harbor, MA. Environ. Sci. Technol. 27, 938–942.

Brownawell, B.J., Farrington, J.W., 1985. Partitioning of PCBs in marine sediments. In: Sigleo, A.C., Hattori, A. (Eds.), Marine and Estuarine Geochemistry. Lewis, Chelsea, MI, pp. 97–120.

Caulcutt, R., Boddy, R., 1983. Statistics for Analytical Chemists. Chapman & Hall, London, 253 pp.

Chin, Y.-P., Gschwend, P.M., 1992. Partitioning of polycyclic aromatic hydrocarbons to marine porewater organic colloids. Environ. Sci. Technol. 26, 1621–1626.

Chiou, C.T., Kile, D.E., Brinton, T.I., Malcolm, R.L., Leenheer, J.A., MacCarthy, P., 1987. A comparison of water solubility enhancements of organic solutes by aquatic humic materials and commercial humic acids. Environ. Sci. Technol. 21, 1231–1234.

Duinker, J.C., 1986. The role of small, low density particles on the partition of selected PCB congeners between water and suspended matter (North Sea area). Neth. J. Sea Res. 20, 229–238.

Duinker, J.C., Hillebrand, M.T.J., Nolting, R.F., 1985. The River Ems: processes affecting the behaviour of metals and organochlorines during estuarine mixing. Neth. J. Sea Res. 19, 19–29.

Eadie, B.J., Morehead, N.R., Landrum, P.F., 1990. Three-phase partitioning of hydrophobic organic compounds in Great Lakes waters. Chemosphere 20, 161–178.

Girvin, D.C., Scott, A.J., 1997. Polychlorinated biphenyl sorption by soils: measurement of soil–water partition coefficients at equilibrium. Chemosphere 35, 2007–2025.

Gschwend, P.M., Wu, S.-C., 1985. On the constancy of sediment–water partition coefficients of hydrophobic organic pollutants. Environ. Sci. Technol. 19, 90–96.

Hashimoto, Y., Tokura, K., Kishi, H., Strachan, W.M.J., 1984. Prediction of seawater solubility of aromatic compounds. Chemosphere 13, 881–888.

Hegeman, W.J.M., van der Weijden, C.H., Loch, J.P.G., 1995. Sorption of benzo(*a*)pyrene and phenanthrene on suspended harbor sediment as a function of suspended sediment concen-

tration and salinity: a laboratory study using the cosolvent partition coefficient. Environ. Sci. Technol. 29, 363–371.

Hunchak-Kariouk, K., Schweitzer, L., Suffet, I.H., 1997. Partitioning of 2,2',4,4'-tetrachlorobiphenyl by the dissolved organic matter in oxic and anoxic porewaters. Environ. Sci. Technol. 31, 639–645.

Jeffery, G.H., Bassett, J., Mendham, J. Denney, R.C., 1989. Vogel's Textbook of Quantitative Chemical Analysis, 5th edn. Longman, New York, 877 pp.

Jepsen, R., Borglin, S., Lick, W., Swackhamer, D.L., 1995. Parameters affecting the adsorption of hexachlorobenzene to natural sediments. Environ. Toxicol. Chem. 14, 1487–1497.

Koelmans, A.A., Lijklema, L., 1992. Sorption of 1,2,3,4-tetrachlorobenzene to sediments: the application of a simple three phase model. Chemosphere 25, 313–325.

Landrum, P.F., Nihart, S.R., Eadie, B.J., Gardner, W.S., 1984. Reverse-phase separation method for determining pollutant binding to Aldrich humic acid and dissolved organic carbon of natural waters. Environ. Sci. Technol. 18, 187–192.

Mackay, D., Powers, B., 1987. Sorption of hydrophobic chemicals from water: a hypothesis for the mechanism of the particle concentration effect. Chemosphere 16, 745–757.

Mackay, D., Mascarenhas, R., Shiu, W.Y., 1980. Aqueous solubility of polychlorinated biphenyls. Chemosphere 9, 257–264.

McKinley, J.P., Jenne, E.A., 1991. Experimental investigation and review of the solids concentration effect in adsorption studies. Environ. Sci. Technol. 25, 2082–2087.

Maruya, K.A., Risebrough, R.W., Horne, A.J., 1996. Partitioning of polynuclear aromatic hydrocarbons between sediments from San Francisco Bay and their porewaters. Environ. Sci. Technol. 30, 2942–2947.

Means, J.C., 1995. Influence of salinity upon sediment–water partitioning of aromatic hydrocarbons. Mar. Chem. 51, 3–16.

Means, J.C., Wood, S.G., Hassett, J.J., Banwart, W.L., 1980. Sorption of polynuclear aromatic hydrocarbons by sediments and soils. Environ. Sci. Technol. 14, 1524–1528.

Millward, G.E., Turner, A., Glegg, G.A., Glasson, D.R., 1990. Intra- and inter-estuarine variability of particle microstructure. Sci. Total Environ. 97/98, 289–300.

Ng, B., Turner, A., Tyler, A.O., Falconer, R.A., Millward, G.E., 1996. Modelling contaminant geochemistry in estuaries. Water Res. 30, 63–74.

Pankow, J.F., McKenzie, S.W., 1991. Parameterizing the equilibrium distribution of chemicals between the dissolved, solid particulate matter, and colloidal matter compartments in aqueous systems. Environ. Sci. Technol. 25, 2046–2053.

Rapaport, R.A., Eisenreich, S.J., 1984. Chromatographic determination of octanol–water partition coefficients for 58 polychlorinated biphenyl congeners. Environ. Sci. Technol. 18, 163–170.

Servos, M.R., Muir, D.C.G., 1989. Effect of suspended sediment concentration on the sediment to water partition coefficient for 1,3,6,8-tetrachlorodibenzo-*p*-dioxin. Environ. Sci. Technol. 23, 1302–1306.

Sigleo, A.C., Means, J.C., 1990. Organic and inorganic components in estuarine colloids: implications for sorption and transport of pollutants. Rev. Environ. Contam. Toxicol. 112, 123–147.

Tancell, P.J., Rhead, M.M., 1996. Application of radio-chromatographic techniques to diesel emissions research. J. Chromatogr. A 737, 181–192.

Turner, A., Millward, G.E., 1994. The partitioning of trace metals in a macrotidal estuary: Implications for contaminant transport models. Estuar. Coastal Shelf Sci. 39, 45–58.

Tyler, A.O., Millward, G.E., Jones, P.H., Turner, A., 1994. Polychlorinated dibenzo-*para*-dioxins and polychlorinated dibenzofurans in sediments from UK estuaries. Estuar. Coastal Shelf Sci. 39, 1–13.

Wijayaratne, R.D., Means, J.C., 1984. Sorption of polycyclic aromatic hydrocarbons by natural estuarine colloids. Mar. Environ. Res. 11, 77–89.

Xing, B., 1997. The effect of the quality of soil organic matter on sorption of naphthalene. Chemosphere 35, 633–642.

Zhao, Y.-H., Lang, P.-Z., 1996. Evaluation of the partitioning of hydrophobic pollutants between aquatic and solid phases in natural systems. Sci. Total Environ. 177, 1–7.

Zhou, J.L., Rowland, S., Mantoura, R.F.C., 1995. Partition of synthetic pyrethroid insecticides between dissolved and particulate phases. Water Res. 29, 1023–1031.